The opportunities of supplementary damping systems in Dutch high-rise buildings

Rens van Lierop

August 2021

IMd Raadgevende Ingenieurs

TU Delft

The opportunities of supplementary damping systems in Dutch high-rise buildings

by

R. van Lierop

to obtain the degree of Master of Science
at the Delft University of Technology,
Faculty of Civil Engineering and Geosciences

Student number:	4462858	
Project duration:	October 9, 2020 – August 27, 2021	
Thesis committee:	Dr. ir. K.C. (Karel) Terwel,	TU Delft (chair)
	Dr. A. (Alice) Cicirello,	TU Delft
	Ir. R. (Roy) Crielaard,	TU Delft
	Ir. R.H. (Remko) Wiltjer,	IMd
	Ir. R. (Rob) Treels,	IMd

An electronic version of this thesis is available at `http://repository.tudelft.nl/`.

Cover Image: Edited render of the Baantoren. Original render adopted from The Powerhouse Company.

TU Delft

IMd Raadgevende Ingenieurs

Preface

This report presents my master thesis research about the opportunities of supplementary damping in Dutch high-rise buildings. It is part of the finalisation of the Master Civil Engineering at the Delft University of Technology. The research has been performed in collaboration with IMd, an engineering company from Rotterdam.

The process of this thesis started more than one year ago, when I had a meeting at IMd, to discuss possible research topics. During this meeting, Remko mentioned the interesting topic of dampers in high-rise building. As a building engineering student, I have always been focused on static loads rather than dynamic loads. Therefore, it seemed interesting and challenging to broaden my knowledge on this new subject.

At the start of this thesis, I was not very familiar with structural dynamics and I barely knew anything about supplemental dampers. Now, after one year of doing research, this is totally different. Terms like eigenfrequency, random vibrations, modal analysis and tuned mass dampers became part of my structural toolkit, which hopefully will be useful in my future career.

This report marks the end of a special year. During the process of writing this thesis, there were times in which the progress seemed to be very slow and the road ahead seemed to be very long. However, looking back, I am very proud of the final result and I am happy with all the things I have learned.

Hopefully, my research will encourage Dutch structural engineers to consider the application of supplemental dampers in their design of slender high-rise buildings. Because as my research proves, dampers can provide new opportunities, or in Dutch '*Dempers zijn geen dompers*'.

Rens van Lierop
August 20, 2021

Acknowledgements

I would like to thank the following people for their support during the writing of this report:

Rob Treels (IMd)
Dear Rob, your experience with the Baantoren and your knowledge on dynamic calculation procedure were a big help to me. I would like to thank you for all our online and offline meetings throughout this year, these meetings were very valuable to me. Dankjewel!

Remko Wiltjer (IMd)
Dear Remko, I would like to thank you for providing me the opportunity to graduate in collaboration with IMd and for introducing me to the topic of dampers in high-rise buildings. I really appreciate your enthusiasm and interest in my research throughout this year!

Roy Crielaard (TU Delft)
Dear Roy, I am very grateful for your feedback throughout this year. All your suggestions really helped to shape my research and improve my work! I appreciated that you gave me feedback during your summer holiday, this feedback really helped me in improving the essential parts of my report.

Alice Cicirello (TU Delft)
Dear Alice, I would like to thank you for challenging me during this research and helping me to understand the fundamentals of random vibrations. Without your explanations, I would not have been able to analytically model the effects of a tuned mass dampers. Hopefully, we can meet offline in the future.

Karel Terwel (TU Delft & IMd)
Dear Karel, first of all I would like to thank you for putting me in contact with IMd. Furthermore, I would like to thank you for the useful feedback during the progress meetings. Your feedback really helped me in defining the scope and objectives of this research.

IMd
I am very grateful that IMd provided me the opportunity to graduate in collaboration with their engineering company. I very much appreciated the days at the office. I would like to thank Matthij and Ikram in particularly for their help during some parts of this process.

Experts from the field
Firstly, I would like to thank Melissa Burton from Arup for the very interesting meeting on the topic of accelerations in high-rise buildings. Secondly, I would like to thank Christian Meinhardt for the meeting about tuned mass dampers, it was very insightful.

Proof-readers
Dear Miranda, Marleen, Gina, and Karin thank you for proofreading some of the most essential parts of my report, this was very helpful.

Literature
I would like to thank the authors of the books *Wind loads on structures* (Dyrbye & Hansen 1997), *Dynamic of Structures* (Chopra 1995) and the *lecture notes on random vibrations* (Vrouwenvelder 2004). These books helped me in understanding the challenging subject of dynamics, wind and random vibrations. I can recommend these books to all students and engineers that are interested in these topics.

Friends
Dear friends, thank you all for the amazing time in Delft. When I came to Delft 6 years ago, I could not have imagined how much I was going to enjoy my student days. I have a lot of good memories, for example *borrelen* at Sint Jansbrug, the Equistudiesessies, the coffee breaks, 21-diners, random vacations, chilling on my balcony, and eating TJC-burgers.

Robin Mak
Dear Robin, I am very glad that after years of friendship we somehow managed to graduate on the same day. Although I was not always fully invested in your stories on compliant differential mechanisms, studying with you (and Willem) definitely improved my staycation in the University Library this summer.

Roommates
Dear roommates, it was always nice to have a chat with you in our house as a distraction from my work, especially in these corona times. Hopefully, all my stories about the beautiful subject of supplemental dampers were interesting enough to compensate for all my complaints about the amount of work.

Parents
Dear parents, I would like to thank you for the support throughout all these years at the TU Delft. I am always very happy to come back to Nuenen during the weekends, it still feels like home (partly because of the bath and the *soepstengels*). Furthermore, I would like to thank my dad for helping me with creating the physical dynamic model.

Summary

In Dutch cities, the number of high-rise buildings with a height of more than 70 meters has increased rapidly over the last decade. Although the Dutch high-rise buildings can not be considered as very tall, these buildings are in general relatively slender.

The structural design of high-rise buildings comes with three main design objectives: Satisfying strength requirements, deflection requirements, and acceleration requirements. For increasingly tall and slender buildings, the acceleration requirements regarding wind-induced dynamic response can become the governing design criterion. If the accelerations become too high, occupants can perceive these motions and experience discomfort.

Excessive accelerations in buildings can be prevented by different design strategies. The two most straightforward approaches are to increase the lateral stiffness or the mass of a building. However, the drawback of these approaches is that additional material is required, which is not necessary for the strength requirements. This is undesirable when taking other design aspects such as climate impact and construction costs. Another, potentially more efficient solution can be the application of supplementary damping systems. These systems consist of devices that mitigate the wind-induced response of a structure. The application of supplemental dampers could possibly benefit climate impact, comfort, the amount of foundation piles, cost and design uncertainties.

Nevertheless, dampers have never been applied in Dutch buildings. This report investigates the application of supplemental dampers as an opportunity for the design of high-rise buildings. In this research, it is investigated when and how the use of dampers could benefit conventional buildings. Furthermore, the effect of dampers on more lightweight and flexible buildings, like timber structures, is investigated.

Firstly, a parameter study on the interplay of the main dynamic parameters: mass, stiffness, and damping, was performed to obtain insight into their relations. This study was based on the Eurocode along-wind acceleration calculation procedure, torsional and across-wind accelerations were not taken into account. By varying the individual parameters, the effects on the dynamic response were investigated.

From this analysis, it was concluded that the highest along-wind accelerations occur for lightweight and flexible buildings. Hence, these buildings can be considered as dynamically sensitive. The effect of an increased damping ratio by supplemental dampers has also been investigated in this study. It follows that a small increase of the damping ratio to only a few percent of the critical damping, can already result in a significant mitigation of the accelerations.

In the second phase of the research, a variant study on the dynamic behaviour of high-rise structures has been performed. The objective of this study was to identify ranges of design parameters for which the application of dampers can be effective.

Firstly, a 2D parametric model of a structural building geometry was created in Rhino Grasshopper. Based on the findings of the parameter study, more than 6500 variants of a dynamically sensitive lightweight steel structure were investigated. This structure consists of a square floor plan (21m x 21m) and a braced steel core (7m x 7m). In this model, the following input parameters were varied: the building height (60m-130m), the floor mass (300-1000 kg/m^2), the top deflection limit (1/200-1/800), the total damping ratio (1.0%-4.0%) and the application of an outrigger (yes/no).

For all building variants, the dynamic response had to be determined to identify opportunities for the use of dampers. To determine the dynamic building properties, realistic structural systems had to be generated for these variants. As there were a lot of variants, this process was automated with a Grasshopper finite element analysis plug-in, named Karamba. This plug-in can automatically determine the required cross sections in a structure, to comply with the strength and deformation requirements for the inputted load cases.

Firstly, the minimal steel cross sections were determined for each variant, so that they complied with the strength requirements. This output can be considered the ultimate limit state (ULS) structural geometry. Secondly, it was verified whether the deflections of these ULS systems complied with the deflection requirements for the serviceability limit state (SLS) load cases. If not, the relevant cross sections were automatically increased in size, until the deflection limits were fulfilled as well. Furthermore, for these resulting structural systems, the dynamic modal properties were determined with Karamba. These properties were used to compute the maximum along-wind accelerations for each variant according to the Eurocode procedure.

For each combination of building parameters, it was determined which of the design criteria was governing: strength, deformations, and accelerations. These relations were visualised in *governing-design-criteria charts*, in which building variants governed by acceleration design can be identified. For the said buildings, the application of supplemental dampers can provide opportunities. The developed charts can be used to make more informed decisions in the early design phases for dynamically sensitive buildings.

Taking into account the specific assumptions from this research, it turns out that applying dampers to obtain a target damping ratio of maximum 4.0%, can solve most dynamic issues. The application of supplemental dampers proves to provide opportunities for the following building types, with a height range of 60 to 130 meters. Firstly, for steel buildings with a lightweight floor system around 300 kg/m^2 and a regular top deflection limit of height/800. Such a system can represent a building with CLT (Cross laminated timber) floors and a regular deflection limit. Secondly, for steel buildings with a relatively lightweight floor system, around 500 kg/m^2 and a reduced top deflection limit height/500. This can be considered as a building with a steel-composite floors and a reduced deflection limit. Furthermore, opportunities arise for new types of lightweight and flexible structures, such as timber high-rise buildings.

Finally, it was investigated how a target damping ratio can be realised in practice by applying a tuned mass damper (TMD). The effect of a TMD on the along-wind response of a building variant was investigated in an analytical manner with a Python script. In this script, the TMD properties like mass ratio, TMD stiffness, TMD damping ratio and TMD location could be varied. The theory of random vibrations was applied to model the fluctuating wind in the frequency domain. The building response was determined by a modal analysis. The required dynamic building properties were obtained from the Grasshopper model.

From this analysis, it turns out that A TMD with a mass in the order of 0.5% to 1% of the modal mass, is effective in reducing wind-induced responses to an acceptable level. A TMD turns out to be most effective when installed at a building's upper floor. Other practical design aspects, such as the tuning range, the maximum allowed TMD motions, building functions, and the cost, play a role as well.

Furthermore, dampers can also reduce the building deformations caused by fluctuating wind loads. This may be taken into account in the SLS by a reduced dynamic amplification factor for the equivalent static wind load. From a safety perspective, the mitigating effects of a TMD should only be taken into account for SLS load cases to guarantee the structural integrity. For buildings in which the SLS criteria are

governing, this can result in a reduction of the total deflection of up to 15%, which reduces the required structural material.

A case study was performed on the design of the Baantoren, a 153 meter tall slender tower in Rotterdam. In the original design of this building, accelerations were governing. Therefore, additional reinforcement was added to increase the building stiffness and overcome dynamic issues. It was concluded that up to 170,000 kilograms of this additional reinforcement steel could have been saved by the application of a TMD with a mass ratio of 1%. This could result in a reduction of the total building costs of approximately 300,000 euros. Moreover, 80 tons of CO_2 emissions would be prevented.

In conclusion, with the application of supplemental dampers, structural materials can be saved in dynamically sensitive Dutch high-rise buildings. Furthermore, opportunities arise for new lightweight and relatively flexible structural systems. Therefore, dampers can be considered as a valuable contribution to the toolbox of Dutch structural engineers.

Contents

Nomenclature

Latin symbols

$[C]$	Damping Matrix
$[K]$	Stiffness matrix
$[M]$	Mass matrix
$\hat{F}$	Force amplitude
$\overline{m}$	TMD mass ratio
A_{cr}	Beam area
A_{ref}	Reference area for the wind load
B	Background factor
c	Damping
c_0	Orography factor
C_f	Force coefficient
C_n	Euler bernouli factor
c_{prob1}	Probability factor
C_sC_d	Structural factor
C_z	Decay factor
Coh_{ij}	Coherence between point i and j
EI	Stiffness
f	Frequency [hz]
f_0	Fundamental frequency
F_w	Wind force
H	Transfer function
h	Height
I_v	Turbulence factor
k	Stiffness
k_p	Peak factor
k_r	Terrain factor
L_t	Reference length scale
m	Mass
M_e	Equivalent distributed mass
n	Storey number
Nx	Fundamental eigenfrequency
q_1	Mode 1
q_b	Basic velocity pressure
q_p	Peak velocity pressure
R	Resonance factor
S	Spectrum
S_{FF}	Force spectrum
$S_{u_ju_j}$	Displacement Response spectrum of DOF j
S_u	Spectrum
T	Averaging time mean wind velocity
u	Displacement
v_{b0}	Fundamental basic wind velocity
$V_{b_{sls}}$	SLS basic wind velocity
$V_{b_{uls}}$	ULS basic wind velocity
v_d	Relative TMD displacement
$v_{fluc}(z)$	Fluctuating wind velocity
V_i	Wind velocity at height i
$v_{mean}(z)$	Mean wind velocity
V_{ref}	Reference velocity

$v_{total}(z)$ Total wind velocity

x Displacement

z_0 Roughness length

z_e, z_t, z_s Reference height

z_i Height at location i

Greek symbols

$\underline{\phi}$ ith modal eigenvector

χ Aerodynamic admittance

δ_a Aerodynamic damping

δ_d Supplemental damping

δ_s Intrinsic damping

μ_1 TMD mass ratio of first modal mass

ν Up-crossing frequency

ω Angular frequency [rad/sec]

ρ Air density

σ Standard deviation

σ_v Standard deviation of the turbulence

ξ Intrinsic damping ratio

ζ Damping ratio

ζ_e Effective damping ratio

ζ_i Intrinsic damping ratio

Mathematical symbols

$[X]$ Matrix

$[X]^T$ Transpose of matrix

$[X^*]$ Modal matrix

$\underline{x}$ Vector x

$\underline{x}_{k,1}$ First item of vector k

$\ddot{x}$ Acceleration of x

$\dot{x}$ Velocity of x

$\phi_{r,c}$ Component of row r and column c

x^* Modal value of x

Used abbreviations

CLT Cross Laminated Timber

DOF Degree Of Freedom

IDR Inter-Storey Drift Ratio

SLS Serviceability Limit State

TMD Tuned Mass Damper

UC Unity Check

ULS Ultimate Limit State

Chapter 1

Introduction

1.1 Background

In Dutch cities, the number of high-rise buildings with a height of more than 70 meters has increased rapidly over the last decade. This trend is driven by the popularity of living in the densely populated *Randstad*, a big housing shortage, and an ambitious high-rise vision of the municipality of Rotterdam (Rotterdam 2019).

Although Dutch high-rise buildings, with a current maximum of around 200 meters, cannot be considered as super tall, are generally relatively slender. This means that the height-to-width ratio is large. The slenderness of Dutch towers is guided by strict daylight regulations and small building plots. The latter is a result of the densification of Dutch cities. Moreover, it is important to decrease the climate impact of high-rise buildings, and to create economically efficient towers and pile foundations, particularly regarding the Dutch soft soil conditions. For this, it is of importance to save structural materials and minimise the total building mass.

The structural design of high-rise buildings comes with three main design objectives: satisfying strength requirements, deflection requirements, and acceleration requirements. The strength requirements guarantee the structural integrity and safety of a building. The other requirements, based on deflections and accelerations, guarantee the serviceability of a building. For increasingly tall and slender buildings in particular, these serviceability requirements start to play a significant role and often even become the governing design factor.

Both high slenderness and low building mass are factors that increase the dynamic sensitivity of a building. Therefore, in combination with the previously described trends, it is expected that in the near future the structural design of high-rise buildings will be more frequently governed by wind-induced acceleration requirements. If the building accelerations become too high, inhabitants can perceive these motions, which may result in discomfort, fear or even motion sickness in extreme cases (Burton et al. 2015). It is therefore important to be aware of these issues and prevent excessive accelerations.

In general, three design strategies can be adopted to reduce the dynamic vibrations of a building: increasing the building mass, increasing the stiffness, or the application of supplemental damping systems (see the definition box). From the perspective of a structural engineer, the first two options are in general the least complex. For the first two strategies, the building properties are altered in such a way that the building becomes less dynamically sensitive, which ensures that the accelerations are reduced. However, these design strategies are in direct contradiction with the earlier described Dutch high-rise trends with increasing slenderness and the desire for lightweight buildings. The last strategy, the application of supplemental dampers, reduces the effect of dynamic loads on buildings, rather than altering building properties. These dampers dissipate the energy that causes the vibrations, resulting in lower building accelerations. This strategy has not been applied in Dutch high-rise buildings yet.

Definition supplementary damping system
A supplementary damping system increases a structure's inherent ability to control motion by providing additional damping, generated by damping devices. Fundamentally, a damping system absorbs dynamic energy from a structure and reduces the effects of excessive motions (RDWI n.d.).

The question arises why supplemental dampers are not applied in the Dutch building industry yet. Considering the lack of experience with dynamically sensitive structures, it is possible that the application of dampers is considered too complex. This would mean that opportunities are missed. In this report, these possible opportunities will be investigated with the focus on the application of a tuned mass damper (TMD).

1.2 Motivation and relevance

The topic of this research is relevant from different points of views, which are shortly introduced in this paragraph.

Opportunities for the application of supplemental dampers occur in two areas: Firstly, it can be beneficial to investigate whether or not the current types of Dutch high-rise buildings can be designed more efficiently by applying dampers. The possible material savings are beneficial to reduce the climate impact of high-rise buildings, save on the amount of costly foundation piles, and reduce construction costs. Buildings for which the application of dampers could have been beneficial, are the Baantoren (Treels 2019*a*) in Rotterdam and the European Patent Office in Rijswijk (Robbemont 2019), see Figure 1.1a. For these buildings the design based on the deflection limits resulted in too high accelerations. In these cases this has been solved by increasing the building stiffness by additional structural material. This material possibly could have been saved if a damper was applied.

Secondly, the application of dampers could result in new opportunities for new types of structural systems, with low mass and low stiffness, such as timber high-rise buildings. Without the application of supplemental dampers, it turns out to be difficult to design feasible structures that inherit these properties and still fulfill the structural acceleration requirements. This was for example the case for Mjostarnet, a Timber high-rise tower in Norway, for which the acceleration limits of the top floor are barely met due to the lack of stiffness (Abrahamsen & As 2016), see Figure 1.1b.

(a) *European patent office, Rijswijk*
Adopted from EPO.org

(b) *Mjostarnet, Norway*
Adopted from Woodify AS / Vjus AS

In addition, the application of supplemental dampers could allow for more slender buildings in the future, as the feasibility of these slender buildings can increase. This means that also the smaller building plots in inner

cities can become available for high-rise buildings. Furthermore, two major drawbacks to the surrounding environment of a high-rise building are reduced for buildings with a higher slenderness ratio: shadows on neighbouring plots are diminished and horizon pollution is decreased.

Moreover, the use of dampers offers an opportunity in reducing design risks. The intrinsic damping ratio of a structure is hard to determine precisely, which introduces uncertainties in the dynamic behaviour of a building (Gomez 2019). Therefore the prediction of accurate building accelerations turns out to be a challenge as well. These kind of uncertainties can be reduced by making conservative design choices, such as increasing the mass and stiffness of a building. Since these properties can not be altered after construction, this conservative adjustments have to be made already during the design phase of a building, so before the actual dynamic behaviour can be established. For the majority of the buildings, in hindsight, this conservative approach turns out to be unnecessary.

In contrast, the properties of a tuned mass damper can be adjusted relatively easily after construction. This means that the actual dynamic behaviour can be measured and determined accurately, which reduces the amount of uncertainties. Therefore, by the application of supplemental dampers, the conservative tendency in design can be reduced, which saves material and cost.

1.3 Research questions

In this section the research objective is introduced and the main research question is defined. Sub-questions are defined as well, which will help in answering the main research question.

1.3.1 Research objective

The main objective of this research is to introduce internationally gathered knowledge on dynamic high-rise behaviour in the Dutch construction sector and explore and investigate the opportunities of supplementary damping in the Dutch context. The chances and challenges of dynamical behaviour and how to deal with this will be researched. This master thesis should provide structural engineers with knowledge on when the application of supplemental damping could be beneficial in the design of high-rise structures, with the focus on the preliminary design phase.

1.3.2 Main research question

The main research question that will be answered in this thesis report is as follows:

In what way can supplementary damping be applied in Dutch, slender, tall buildings to efficiently meet the structural design requirements?

1.3.3 Sub-questions

The main research question is answered with the help of sub-question, which are listed below. These sub-questions are categorised in three parts, which correspond with the structure of the report. In these sub-questions the term 'high-rise buildings' refers to buildings within the scope as defined in Section 1.4.

Part I: Theory

This part presents the relevant background theory and investigates the following sub-questions:

1. How are the governing design criteria defined?
2. What are the fundamentals of wind engineering for high-rise buildings?
3. Which aspects play a role in the design of dynamically sensitive high-rise buildings?
4. How can supplemental dampers be applied to mitigate wind-induced vibrations?

Part II: Opportunities for dampers

This part defines opportunities for supplemental dampers and investigates the following sub-questions:

1. How do the dynamic building properties affect the dynamic behaviour of high-rise buildings?
2. Which of the design criteria is governing for different high-rise buildings?
3. For which building properties can the application of supplemental dampers be beneficial?
4. What is the required damping ratio to limit the wind-induced accelerations for high-rise buildings?

Part III: The application of tuned mass dampers

This part is about the application of tuned mass dampers and investigates the following sub-questions:

1. What are the practical implications of the utilisation of a tuned mass damper in a high-rise building?
2. How can a theoretically required damping ratio be obtained in practice, by the application of a tuned mass damper?

1.4 Scope limitations

The scope of the project is limited in the following manner:

- This research is performed from the perspective of the current Dutch building context. This implies: soft soil conditions, relatively slender buildings, no seismic loads, a current building maximum of 200 meters and relatively low land cost, and concrete as main material.
- Only dynamic effects caused by wind loads are included. Seismic dynamic effects are out of the scope of this research.
- The Dutch acceleration regulations are adapted in this research. Some comments on this scope limitation can be found in Chapter 2.
- The height of the investigated tall buildings is limited to a range between 60 meters and 150 meters.
- The research is performed for buildings with a symmetric square floor plan. In this way, torsional induced accelerations are prevented as much as possible.
- All the calculated building variants are assumed to use steel as the structural material for cross sections, as these types of building are more sensitive to dynamic behaviour than heavy concrete buildings, see Chapter 6.
- From the three main types of accelerations: along wind, across wind and torsional accelerations, only the along-wind component is considered during the different analyses, as explained in Chapter 3.
- The influence of the rotational and transnational stiffness of the foundation is neglected. In all cases, a fully clamped foundation is assumed.
- The influence of surrounding buildings on the wind loads, the so called interference effect, is not considered in this research.
- The values of the intrinsic and aerodynamic damping ratio will not be studied in detail. Assumptions will be made to account for these types of damping, as explained in Chapter 4.
- The research to the practical aspects of dampers is limited to the application of conventional tuned mass dampers, see Chapter 5.
- The focus of this research is on passive conventional tuned mass dampers. Active systems are not taken into account.
- Applying a more aerodynamic building shape could be an efficient method to reduce the dynamic loads on buildings as well. However, in this research the focus is on the application of supplemental dampers only.
- The application of supplemental dampers can be interesting for timber high-rise buildings. However, no structural calculations for timber will be performed. Therefore, the possibilities for timber are only highlighted in a general manner in this report.

1.5 Methodology

Different research methods are applied in this research. For each part, the set-up of the research is shortly described. The structure of the report is based on this methodology.

Part I: Theory
In this part the theoretical sub-questions are answered. To define an answer to these questions, a literature study is performed. This research investigates the governing design criteria in Chapter 2. The fundamentals of wind-engineering and the origin of wind loads are covered in Chapter 3. Next, relevant aspects for the design of dynamically sensitive high-rise buildings are introduced in Chapter 4. Lastly, the concept of supplemental dampers is introduced in Chapter 5.

The fundamental theoretical questions are answered with the help of books on relevant topics. The questions related to the application of the theory in practice were mainly answered on the basis of scientific papers. Moreover, two online interviews have been conducted with experts in the field. One with Melissa Burton, from Arup, about comfort criteria. One with Christian Meinhardt, from Gerb, about the application of supplemental dampers.

Part II: Opportunities for dampers
This part forms the core of this research. In this part ranges of building parameters are defined for which the application of supplementary damping could provide design opportunities. Firstly, the effects of the dynamic building properties on the dynamic response are investigated by a parameter study in Chapter 6. This parameter study is based on the dynamic procedures from the Eurocode. The insights in these relations, together with the theory from part I, are used as the starting point for a variant study.

This variant study is performed to investigate the relations between the governing design criteria for different high-rise buildings. For this variant study a 2D structural parametric model of a slender steel building is defined, as explained in Chapter 7. The geometry and the structural properties of this building model are determined based on the parameter study and the theoretical research. With the defined model, the static and dynamic responses to different design loads are determined for varying buildings. With the data of this variant study it can be investigated which of the design criteria is governing for different building properties, this is described in Chapter 8. These results can be used to define parameter ranges in which supplemental dampers can prove to be an opportunity.

Part III: The application of tuned mass dampers
This part focuses, in contrast to part II, on the more practical aspects of the application of a tuned mass damper (TMD). Firstly, additional literature research has been performed to investigate the design aspects of a tuned mass damper. Design formulas have been found with which the main design properties of a TMD can be determined, these are introduced in Chapter 9.

Secondly, the effects of a TMD on the structural dynamic response are determined analytically by a developed Python model, which is defined in Chapter 10. This model applies the theory of random vibrations and a modal analysis. With this script, it is possible to investigate the mitigation effects of a TMD on the

wind-induced accelerations. Moreover, the effect of different TMD properties are investigated by varying the input TMD parameters in the model.

Finally, in Chapter 11 an illustrative case study is performed on the benefits of supplementary damping. In this case study, it is determined how much structural material, money, and CO_2 could have been saved by the application of a TMD in an actual building design.

1.6 Report structure

The structure of the report is divided in four parts. The first three parts correspond to a set of sub-questions, as defined in Section 1.3.3. The last part, Part IV defines an answer to the main research question. This last part of the report contains a discussion and a conclusion. Furthermore, recommendations and suggestions for further research are made. An overview of the structure of the report is provided in Figure 1.2. In this figure the connections between the different parts are visualised by arrows.

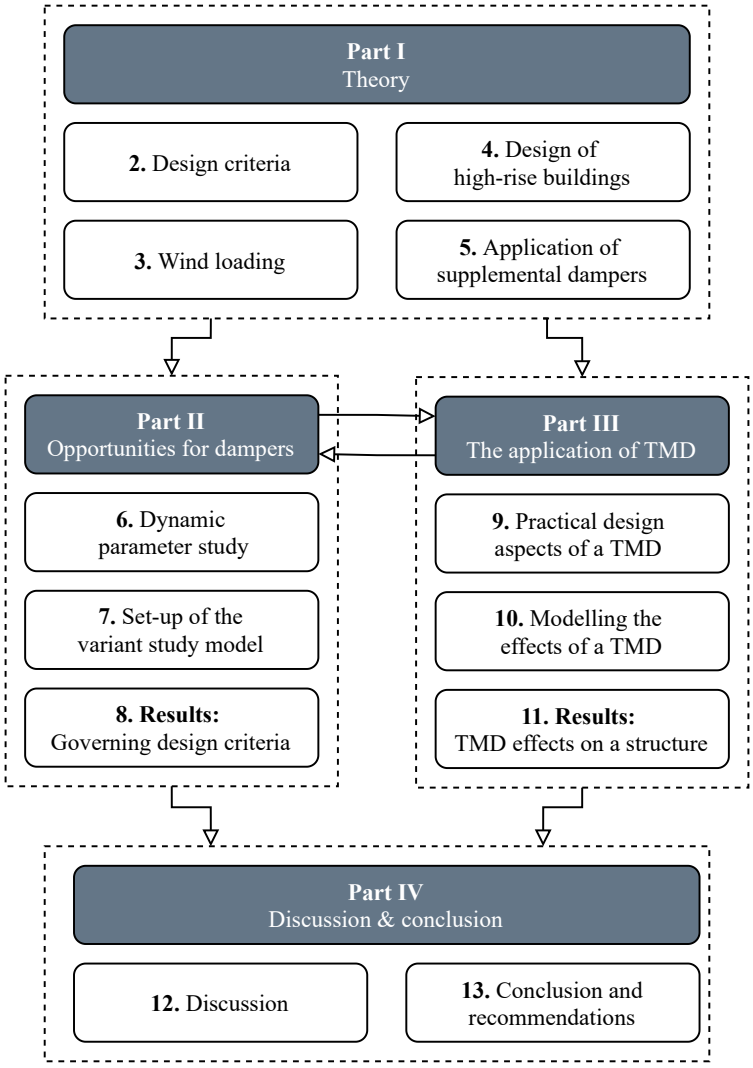

Figure 1.2: *Overview of the report structure*

Part I

Theory

Chapter 2

Design criteria

This chapter investigates the relations between the three main design requirements: strength, deformations and accelerations. The underlying concepts behind these criteria are explained in Section 2.1 and design strategies are provided. Subsequently, the regulations as prescribed by building codes are covered. The focus is on the acceleration governed design (Section 2.4), because these requirements are specific for dynamically sensitive structures, as is the topic of this thesis.

2.1 Governing design

By far the most important design aspect for a structural design of a building is the safety, a building may not collapse. Therefore a building should inherit enough strength. The design on strength is referred to as the ultimate limit state design (ULS). Whatever happens, a building should be able to withstand loads that could be reasonably expected. For low-rise buildings the ULS design is often governing.

However, for high-rise buildings, other design aspects begin to play a role as well, especially regarding lateral loads. These aspects have to do with the serviceability: can a building be used as intended? This type of design aspects are covered by the serviceability limit state design (SLS). The SLS design has to do with factors that do not influence the buildings safety, but that do affect the user comfort of the building occupants, in other words a building should be habitable. The SLS requirements can be divided in two main design factors: limiting the maximum deflections and limiting the maximum accelerations.

A high-rise building should be designed according to these requirements. A structure must inherit the required strength and comply with the maximum allowed deflections and maximum allowed accelerations limits. These design aspects have their own predefined corresponding load cases and different return periods. These three design criteria all need to be fulfilled separately. If one requirement is not met, the design has to be adapted. This requirement is referred to as the governing design criterion, as explained in the definition box. The design of a structure is governed by the weakest design link. This means that the amount of material that is required to fulfil the governing design criterion determines the minimum required amount of material. Hence, it does not make sense to optimise the strength design if the deflection design is governing. This concept is visualised in Figure 2.1.

Definition governing design criterion
The governing design criterion refers to the design factor that determines the minimum required structural design of a building. The design factors are: strength, deflections, and accelerations.

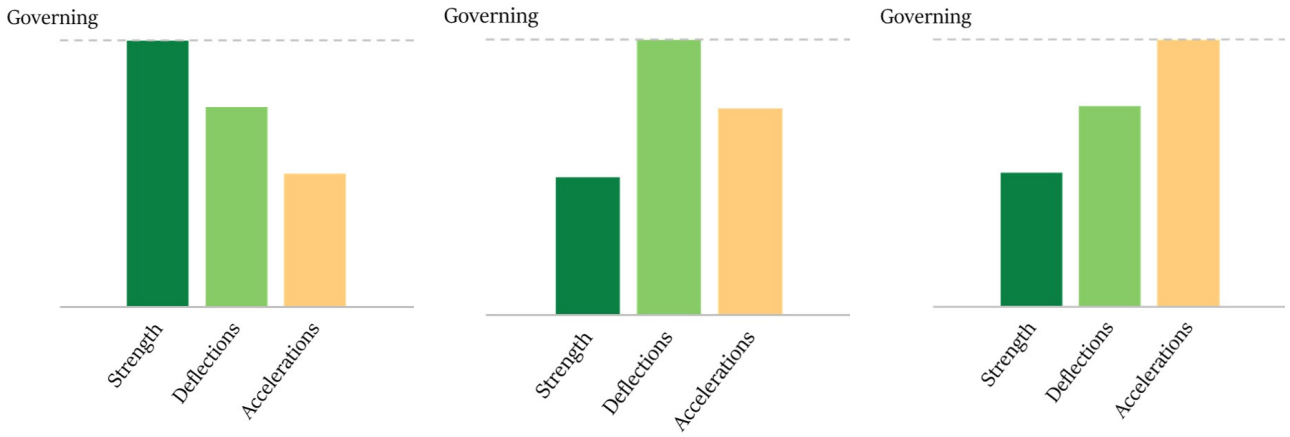

(a) *Strength* (b) *Deflections* (c) *Accelerations*

Figure 2.1: *The governing design criteria*

Fundamental differences exist between the governing design criteria. Design on strength is about safety, which is a binary concept: a structure may not collapse. During the lifetime of a building, the ULS design limits may never be exceeded, as this would result in irreversible damage. Loads and strength are both stochastic concepts, it is therefore not possible to design a building 'on the edge', as the risk of the occurrence of an structurally unfavourable event is too high. To reduce the risks to an acceptable level, safety factors are applied (De Vries et al. 2013). Typically high return periods are applied for the design on strength.

The design based on deflections and accelerations is fundamentally different because it is about serviceability and comfort. Exceeding these limits does not result in any serious danger. It can only result in minor non-structural damage or in discomfort for the occupants. Therefore, it is not disastrous if the SLS limits are exceeded, this may even be acceptable. This means that risk reduction is less of an issue for SLS design. Therefore, safety factors do not have to be applied. In addition, the defined limits are more ambiguous and open for interpretation. If the consequences of the design choices are understood well, it is not be a problem to apply less strict design limitations.

Insights in the governing design criteria can be used to save material in the structural design. Figure 2.2 illustrates this concept. In this figure, it can be observed that the SLS design based on limiting deflections and acceleration are both governing over the ULS design based on strength. This implies that the building is stronger than strictly required from a safety perspective. If the deflection and acceleration design can be designed more efficiently, structural material can be saved. There are three different ways to decrease the *gap* from Figure 2.2 between ULS and SLS design, as listed below. The individual design criteria are explained in more detail in the following sections.

Option 1| Apply more lenient SLS design limits: The SLS design requirements could be decreased, since these requirements are not about safety. For example higher accelerations can be allowed (Abrahamsen & As 2016). The advantages and disadvantages of this option must be carefully examined and the implications on the buildings serviceability should be extensively investigated and discussed with the stakeholders. .

Option 2| Deal with the impact of loading: Different, more clever, design solutions could be considered. Normally, the SLS requirements are fulfilled by increasing the amount of structural material to

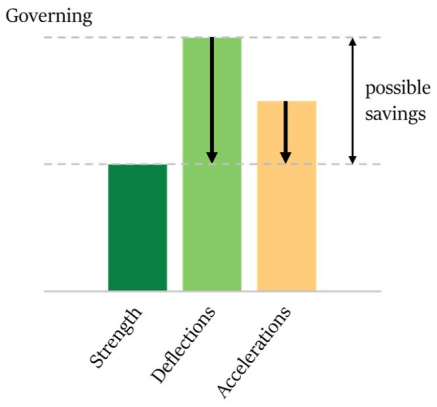

Figure 2.2: *Possible savings by decreasing the gap*

increase the structural stiffness or the building's inertia. Different solutions could be considered as well. Regarding deflections the component tolerances could be increased, to allow for the additional deflections in the non-structural elements. To reduce accelerations, the application of supplemental dampers could be considered. In this way, the governing design is shifted more into the direction of the ULS design. The structural designer should examine and compare the effect of these different design solutions on efficiency, sustainability, cost, amount of material, etc.

Option 3| Reduce the loads on the structure: Regarding lateral wind loads, a third design approach exists. The amount of load on a building is does not only depends on the wind around the structure, but also on the structure itself. By adjusting the design to a more aerodynamic shape, the wind pressures on a structure can be reduced significantly (Advisory Committee on Technical Recommendations for Construction 2008). This design strategy does not reduce the gap from Figure 2.2, but it reduces the material usage for all three design factors, as the loads are reduced. The influence of the building shape on the structural response is not within in the scope of this thesis. However, it is good to be aware of this design strategy, since it can be a very effective method in reducing wind-induced problems.

2.2 Strength governed design (ULS)

If the tower design is governed by strength this means that the minimum amount of required material for the structural design is determined by safety requirements, including safety factors. In this case, the deflection limit and comfort requirements are automatically fulfilled. The strength-based design inherits enough stiffness and inertia to fulfill these requirements. The maximum expected deflections and accelerations are thus smaller than allowed.

The design on strength is about preventing the failure of individual structural elements and the stability of the whole structure. Moreover, the strength requirements should ensure enough structural redundancy and robustness. These aspects are included by the application of safety factors, which ensure that enough redundancy and safety is inherited to guarantee the structural integrity. For buildings in which a failure could have major consequences, additional safety factors are applied, taken into account by consequence classes.

Not only static loads can result in failure. Dynamic loads will also play a role in the ULS design, see Chapter 3. Firstly, the fluctuating load component will result in additional loads on a structure, which should be taken into account in the ULS as well. Secondly, if resonance occurs, for example induced by vortex shedding, the dynamic loads can be heavily amplified. This may lead to failure.

2.3 Deformations governed design (SLS)

If the structural design of a high-rise building is governed by the deformations, generally this means that the building's lateral stiffness is the governing design factor. For these cases, the minimum ULS design, based on strength, results in too high deflections. Hence, the structure should contain more material than is strictly necessary from a safety point of view. Deflection requirements are often the governing design factor for high-rise buildings (Hoenderkamp 2011).

2.3.1 Deflection limits

To ensure that a building can be used as intended, a building has to comply with certain deflection limits. The determination of these requirements for the serviceability limit state, is not as straightforward as the determination of the requirements regarding the ultimate limit state. Different deflection limitations may play a role, two common used limits in building codes are explained here:

Top deflection limit

In the Netherlands, during the early design phases, often the top deflection limit is applied. This limit is about the maximum deflection of the upper floor, relative to the building's height. This limit in fact is an indirect way of taking into account the inter-storey shear drift ratios. The top deflection limit is often used in preliminary design phases, as it is easier to apply. In general, for the top deflection a limitation of $h/500\cdot$ is used if the rotational capacity of the foundation is included. If the design is assumed clamped at the bottom floor, a limit of $h/750\cdot$ is considered (Eurocode 2005a)(Ham & Terwel 2017). Throughout this report, the top deflection limit is applied.

Inter-storey drift ratio limit

Another commonly used deflection limit is the inter-storey drift ratio (IDR) limit. This limit is defined as the difference in horizontal displacement over one floor divided by the storey height (Smith 2011). Internationally this limits varies from $h_{st}/300$ to $h_{st}/500$ (Smith 2011). Steel allows for higher IDR deformations than reinforced concrete. In contrast to the top deflection limit, the IDR is a direct measure of the relevant deformations. Too high peak inter-storey drifts will result in damage in partition walls. The occurrence of damage depends on the applied material. For brick walls, the IDR limits have to be more strict than for more ductile materials.

These two limits are not fixed, because an exceedance of the deflection limit normally does not result in danger. Limiting the deflections is however important for the following reasons as described by Smith (Smith 2011):

- **Cladding and facade**: Facade elements should be designed in such a way that they can accommodate the movements imposed upon them. This is important to maintain the functionality of weather

tightness, acoustic and thermal insulation, and structural integrity. For these functions the local deformations are of importance.
- **Partition walls and architectural finishes**: Due to differences in local deformations, cracks and damage may occur to these internal elements. This has to be prevented.
- **Lifts**: If a building deforms, the lift shaft will deform with a certain slope as well. For the operation of the lifts it is important to ensure that enough clearance is provided between the lift cables and the lift shaft.
- **Visible deformations**: In extreme cases, the slope of a building may be visible and perceivable for occupants when the building floor becomes non-horizontal.

The previously described aspects and problems all require a limitation of the building deformation. However, decreasing the building deformations is not the only option. To a certain extent, all these deformation-induced problems could be solved by adapting a performance based design approach. This allows for greater freedom in choosing the deflection limits (Smith 2011). For example, it could be decided to apply facade elements with smaller panel sizes or with higher tolerances in the connections to allow for larger movements in the facade. Problems with lift cables can be prevented by increasing the dimensions of the lift shaft. Furthermore, an engineer could anticipate on issues with cracks in partition walls by applying more ductile materials. If such design measures are applied, more lenient deflection limits can be adapted.

In this report, such a performance-based design approach is assumed, in which no set value for the deflection limits is applied. All the results of the analyses in Chapter 8 are presented for top deflection limits. It is up to the reader to determine which deflection limits should be used for their specific design.

2.4 Accelerations governed design (SLS)

Fluctuating wind gusts results in building accelerations, as explained in chapter 3. These accelerations do not impact the ULS design of a tower. However,if these accelerations become excessive this can result in discomfort and fear for the users of a building (Burton et al. 2015). To prevent this from happening building codes limit the maximum allowed accelerations. Especially for high-rise buildings this limitation can turn out to become the governing design criterion. If this is the case, this means that the strength and deflection governed designs do not fulfill the acceleration criteria. This section explains and discusses the acceleration requirements.

2.4.1 Theory behind acceleration limits

Strength and deformation requirements exist to prevent damage to structures. In contrast, acceleration requirements are implemented to prevent discomfort to human beings. As all humans are different, the human response to motion is highly variable from person to person. This complicates the determination of proper acceleration limits. Two concepts can be used as a basis for the acceleration regulations: the perception threshold and the tolerance threshold (Kwok et al. 2015).

2.4.1.1 Perception threshold

The first concept in the determination of acceleration criteria is the perception threshold. The perception of acceleration by human beings is a complex subject, which depends on different factors. This is described

by Burton, Kwok and Abdelrazaq in the book 'Wind-induced motion of tall buildings' (Kwok et al. 2015).

The perception of motion depends, among other factors, on the intensity and frequency of motion, the individual sensitivity to motion, the presence of visual and acoustic cues, and body orientation. There is a wide variety in the individual ability to detect motion. Some people can be very sensitive to certain levels of motion, while others do barely perceive these motions. Moreover, the acceleration perception limits are not set in stone, the perception of acceleration can be triggered by visual and acoustic cues. For example, by the movement of blinds, swinging of lights, and creaking structural noises. Perception can also be triggered by communication with other human beings that spread their observations regarding building motions.

Because the perception of acceleration differs highly from person to person, it is not possible to define one value as 'the acceleration limit'. Therefore, perception limits are defined in a probabilistic format, see Figure 2.3. Each line corresponds to a certain percentage of occupants that will perceive the accelerations for a certain limit.

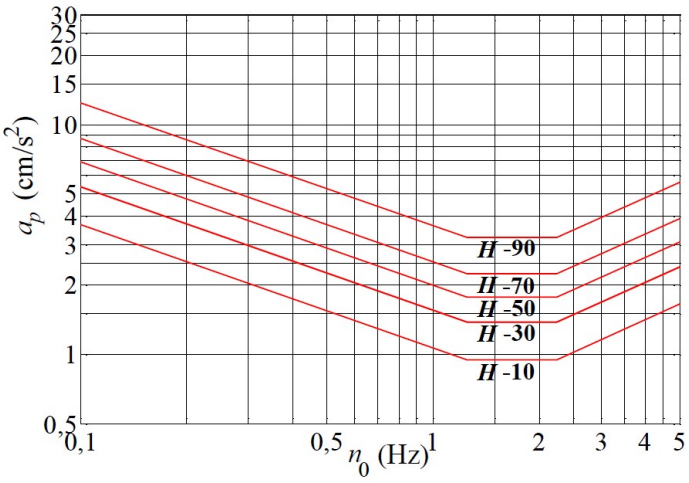

Figure 2.3: *Perception limits for different eigenfrequencies. Adopted from: (Advisory Committee on Technical Recommendations for Construction 2008)*

2.4.1.2 Tolerance threshold

Ideally, occupants of buildings do not perceive any building motion. However, preventing all perceivable building motions is not a sustainable and cost-efficient design approach. In general, the perception of small accelerations by occupants can be accepted, especially if this does not occur too often. This is possible since the acceleration limits are only dictated by comfort criteria and not by safety criteria. Nevertheless, very bothering accelerations should be prevented as they can cause fear, motion sickness, and balance issues for occupants. From this, it can be understood that in addition to the perception threshold, a tolerance threshold can be defined as well.

There have been very few motion simulator investigations with the focus on the tolerance criteria (Kwok et al. 2015). Research on tolerance thresholds is more difficult than research on perception thresholds, due to the more ambiguous character of the former one. It is, for example, difficult to simulate the relevant aspects, like return period and fear, in a research set-up. Moreover, the tolerance threshold varies from person to person as well.

Tolerance to acceleration can be increased by education and experience. If occupants are made aware of the possibility of accelerations, this can minimise the fear-component (Kwok et al. 2015). In the Mjøstårnet timber tower in Norway, this concept has been adapted (Abrahamsen & As 2016). In which the top floors of this tower do not fully comply with the ISO requirements. However, motion sickness and other serious physical discomfort should be avoided at all times.

2.4.1.3 Definition of the acceleration criteria

Ideally, the acceleration requirements are defined somewhere between the perception limit and the tolerance limit. However, as mentioned in the previous paragraph, due to the uncertainties, it is difficult to define proper tolerance limits. In general this results in relatively conservative building codes, often guided by the perception thresholds. Several building codes have been visualised in Figure 2.4. The ISO code, as defined by the International Organization for Standardization, is based on the acceleration level that approximately 2% of the occupants in the upper part of a building may find objectionable, defined for a 1 year return-period (Kwok et al. 2015).

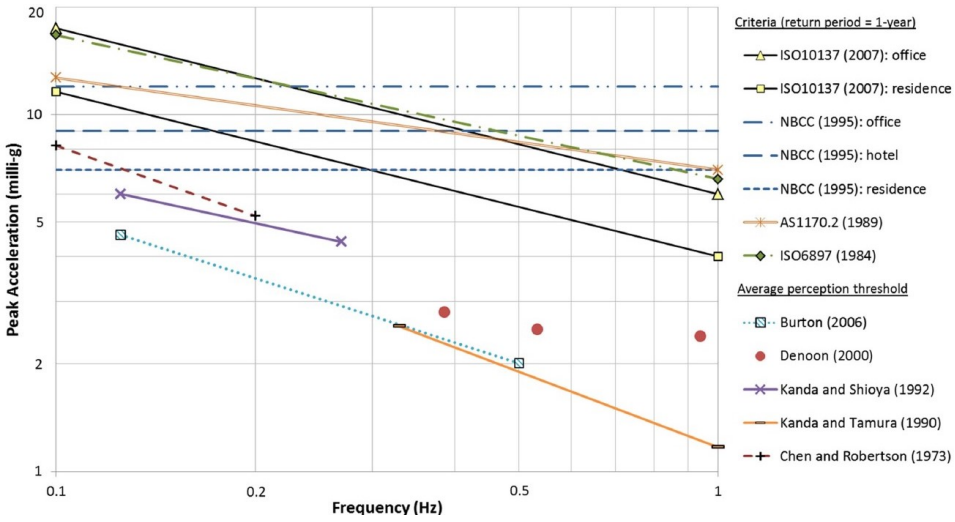

Figure 2.4: *Internationally used acceleration requirements*
Adopted from (Burton et al. 2015)

2.4.2 Acceleration limits

The Dutch acceleration limits are defined in Figure 2.5a. Internationally used acceleration limits are illustrated in Figure 2.5b and Figure 2.4. A distinction is made between the acceleration limits for office and resident towers. In contrast to ULS requirements the design return period regarding to maximum accelerations is set to 1 year in the Eurocode (Advisory Committee on Technical Recommendations for Construction 2008). In general, three different types of acceleration can be distinguished: along-wind, across-wind and torsional acceleration. Combination rules exist to determine the combined effect of these accelerations on building occupants. However, this report solely focuses on the along-wind accelerations. Throughout this research the current Dutch acceleration standards are applied.

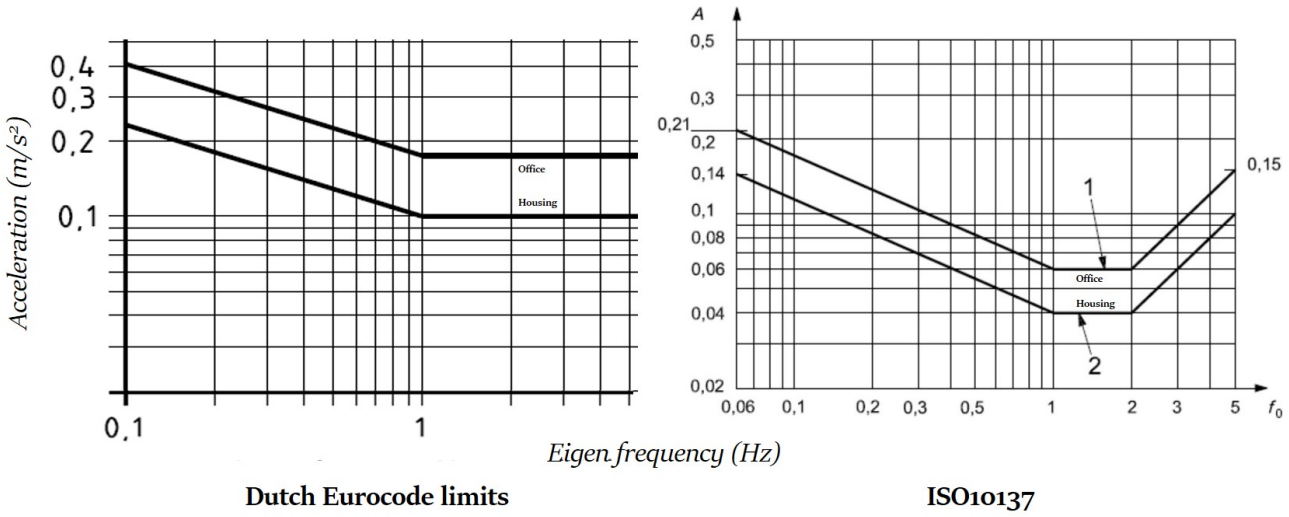

Figure 2.5: *Comparison of the maximum allowed along-wind accelerations for a 1 year return period for the Dutch Eurocode (left) and ISO code (right).*
Both Figures have been scaled to the same size, to allow for easy comparison.

2.4.3 Dutch limits versus international limits

Internationally, ISO10137 is the most common standard for acceleration limits (Meinhardt 2021) Burton (2021). From Figure 2.5 it can be observed that international acceleration limits defined much stricter than the Dutch standard. For motions in residential buildings with a frequency of 0.10 Hz, the Dutch standard allows a maximum acceleration of 0.23 m/s^2. For the same building properties the ISO standard would allow only 0.14 m/s^2, which should be considered as a very large difference. Also in comparison with other International codes, as illustrated in Figure 2.4, the Dutch acceleration requirements are very lenient (Burton et al. 2015).

Taking into consideration the little experience with wind engineering in the Netherlands compared to the international practice, serious doubts are raised on the reliability of the Dutch limits. The question can be raised if the Dutch acceleration regulations would not result in uncomfortably high accelerations. To interpreted and understand these regulations, some additional research has been performed. From this research, it is concluded that the difference with the international limits are inexplicably large. Even if the international codes can considered as conservative, the extremes of the Dutch limits appear to large. No background literature on the topic of acceleration regulations has been discovered that supports the Dutch limits. Moreover, on the basis of expert interviews, the doubts were not removed, but strengthened (Meinhardt 2021) (Burton 2021).

In normal buildings the Dutch limits will not induce problems, as the accelerations will simply not reach the extreme values of the limits. However, for future very dynamically sensitive buildings, this could be an issue. Therefore, it is recommended to perform research on the validity of the Dutch acceleration limits. Until then, it is recommended to be careful with the application of the Dutch acceleration limits.

2.5 Conclusions

- Three main design criteria are applied in the design of high-rise structures: strength, deformations, and accelerations. Only the strength criterion is about safety, the other two are respectively about the serviceability requirements and occupant comfort.
- In general a top deflection limit of $h/500$ is applied for high-rise buildings or $h/750$ if the foundation effects are excluded from the design phase.
- The inter-storey shear drift directly relates storey deflections to damage in partition walls. In general a limit between $h_{st}/300$ and $h_{st}/500$ is applied.
- A performance base design approach can be applied regarding the deflection limits. In this way more lenient deflection limits could be applied.
- Acceleration comfort requirements are based on occupant perception and tolerance limits. Both these aspects are ambiguous, which makes it difficult to define proper acceleration regulations. In general the limits are frequency and function dependent.
- The Dutch acceleration limits seem to be too lenient, compared to international building codes. Additional research is recommended on this topic.

Chapter 3

Wind loading

To be able to determine and understand the wind-induced dynamic behaviour of buildings, it is of importance to understand the underlying concepts first. Therefore, this chapter covers the fundamental aspects of wind-engineering. Firstly, the origin of wind loads will be discussed (Section 3.1). Secondly, modeling approaches for wind on buildings are introduced (Section 3.2). In the last section the possible occurring wind-induced dynamic responses are explained. The modelling of wind-induced loads is covered more in depth in Chapter 10.

3.1 Origin of wind loads

Simiu and Yeo describe the physical origin of wind in the following manner: "Wind, or the motion of air with respect to the surface of the Earth, is fundamentally caused by variable solar heating of the Earth's atmosphere. It is initiated, in a more immediate sense, by differences of pressure between points of equal elevation. Such differences may be brought about by thermodynamic and mechanical phenomena that occur in the atmosphere both in time and space." (Emil Simiu 2019). This constant motion of the air can be perceived by humans and is called 'wind'. The surface of the earth can be considered as the boundary layer of this wind flow, a concept well-known from fluid mechanics. Due to friction between the wind and the surface, the wind-flow over the earth surface is slowed down, just like the velocity of the water flow is lower at the bottom of a river. If the surface would be perfectly flat, the wind flow would be laminar. The velocity profile would in that case be described by a perfect logarithmic curve. However, due to irregularities in the landscape such as mountains, forests, and man-made structures, the flow around the earth's surface is turbulent. Therefore, the wind flow in the boundary layer is turbulent, see Figure 3.1. This turbulence is an import source of dynamic loads on high-rise buildings .

3.1.1 Wind velocity profile

The wind pressure on a structure is directly related to the wind velocity profile (Emil Simiu 2019). Therefore, to determine the wind loads on a structure, the wind velocity profile has to be obtained first. This wind velocity profile can mathematically be described by two components: the mean wind velocity and the fluctuating wind velocity, see Equation 3.1. The mean wind velocity is defined as the average 10 minute wind speed, it defines the wind speed as a result of the laminar flow component from the Earth's boundary layer, this component is indicated by the 'V_{mean}' label in Figure 3.1. The fluctuating wind velocity component describes the variation in velocity relative to the average laminar velocity profile, caused by the wind turbulence, labeled as '$V_{fluctuating}$' in Figure 3.1. The wind profile in a city with a lot of high-rise buildings will be more turbulent than the wind profile in a rural area, see Figure 3.1. As can be observed from Figure 3.1 the turbulence component causes deviations in the velocity profile from the original laminar mean flow, over the height. The more turbulent the wind flow, the bigger the scatter in the wind fluctuations.

$$v_{total}(z) = v_{mean}(z) + v_{fluctuating}(z) \tag{3.1}$$

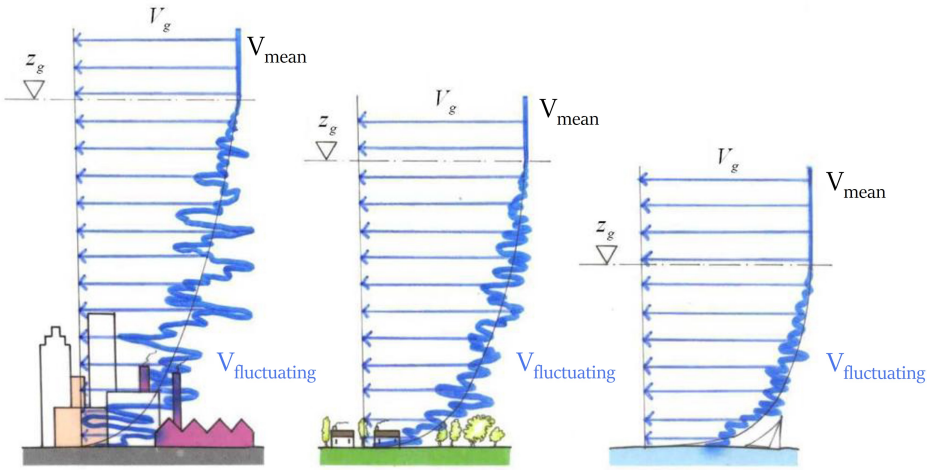

Figure 3.1: *Wind velocity profile, varying over height and location, including turbulence. Edited Figure, Figure adopted from (Advisory Committee on Technical Recommendations for Construction 2008).*

3.1.2 Wind pressure

The frequency of the 10 minute mean velocity component is too low to initiate a dynamic response of a building. Therefore, the mean velocity component is considered as the 'static' wind component that determines the main static behaviour of a building. The static wind load can be determined by Bernoulli's equation, that defines the relation between wind velocity and the wind pressure, see Equation 3.2.

$$q_p(t) = \frac{1}{2} * \rho * (v_{mean}(t))^2 \tag{3.2}$$

On the other hand, the fluctuating wind velocity component initiates the dynamic behaviour of a building (Dyrbye & Hansen 1997). The fluctuating wind component results in wind gusts that result in osculating forces on the building. The occurrence of these osculating wind gusts happens with a certain frequency. When the gust frequency is close to one of the buildings eigenfrequencies, this can result in resonance of the structure. In the case of resonance building motions are amplified, which may result in excessive accelerations and deformations.

3.1.3 Stochastic wind model

For design purposes, the extreme values of the wind velocity for a certain return period have to be determined. For the acceleration design criteria this return period is 1 year, for ULS calculations this period is normally 50 years. The wind velocity fluctuations are a random process (Strømmen 2010). From this it followes that the fluctuating wind loads can only be described by stochastic probability density functions, rather than by discrete values (Vrouwenvelder 2004). It can be understood from stochastic theory that for longer design return periods, the probability that rare strong wind events will occur during the buildings lifetime increases. This distribution can be described by a Weibull or Rayleigh function, see Figure 3.3a (Strømmen 2010).

The wind velocity is specific for a certain country or region. The peak values of the mean component and

the fluctuating component depend on the climate zone in which the structure of interest is located (Advisory Committee on Technical Recommendations for Construction 2008). The values of the average wind velocities are based on long term statistics. Throughout this report the properties of the Dutch wind zone II, as defined in the Eurocode, are applied.
The mean velocity is not constant over time, in most codes the mean wind velocity is defined for a period of 10 minutes. For this period the mean wind is considered homogeneous (Strømmen 2010), see Figure 3.2. The characteristic mean wind velocity in the Eurocode is defined at 10 meters height and is independent of the wind direction and the time of the year (Eurocode 2005*b*).

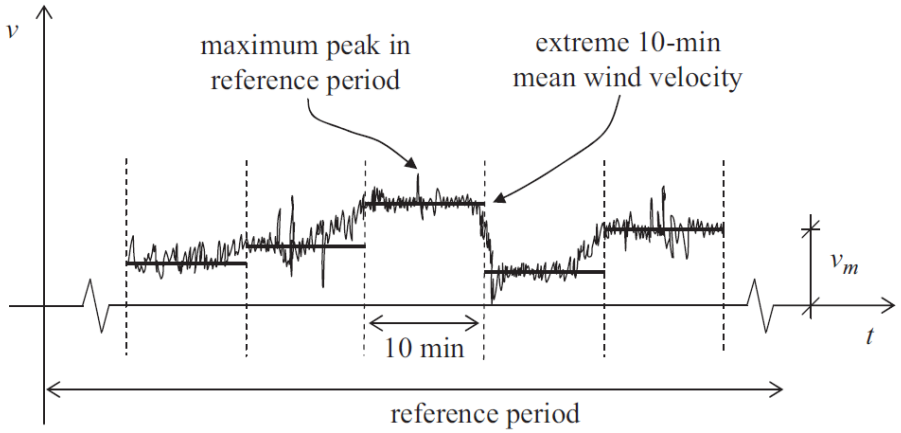

Figure 3.2: *Fluctuations off the mean wind velocity profile. Adopted from (Steenbergen et al. 2012)*

In this 10 minute time frame, the wind load is not actually constant. As a result of the turbulence the wind speed is varying in time and space (all 3 dimensions: x, y, z) in a random manner. The fluctuations can be modelled as a variation of the mean velocity and are considered to be constant for only very short time intervals of a few seconds. These fluctuations can be modelled by a Gaussian probability distribution with the mean wind velocity as the mean value of this distribution, see Figure 3.3b. The time dependence of the mean wind component and the fluctuating wind component are illustrated in Figure 3.2 and 3.3b. The distribution of the wind profile in space (z-axis) is illustrated in Figure 3.1. The intensity and the occurrence of peak values of the fluctuating component can be described by a Gaussian distribution around the mean wind velocity value. It can be shown that if a stochastic process with zero mean value is stationary and Gaussian distributed, its extreme values are proportional to its standard deviation. Therefore the maximum wind peak is proportional to the standard deviation of the fluctuating wind velocity. This relation is described by a peak factor (Strømmen 2010), see Figure 3.3b

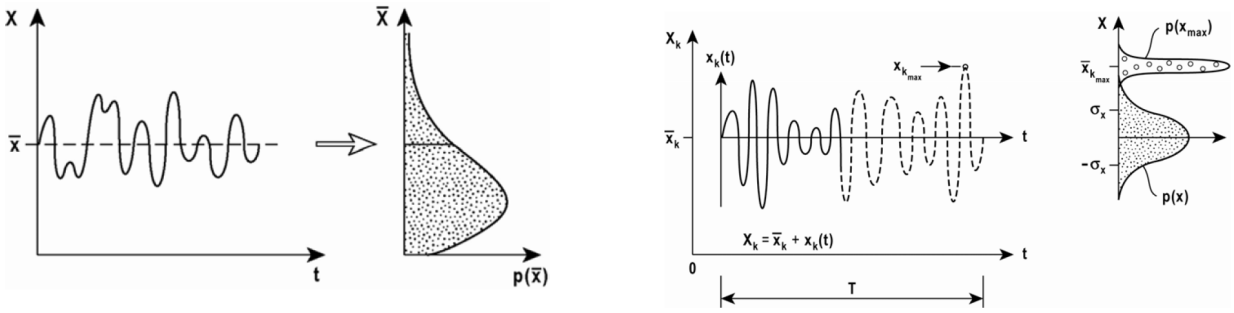

(a) *Mean wind load probability*

(b) *Peak load probability*

Figure 3.3: *Wind load statistics, Adopted from (Strømmen 2010)*

3.1.4 Wind load frequencies

A typical wind spectrum is visualised in Figure 3.4. From this figure it can be observed that in general, the fundamental eigenfrequencies of low-rise buildings are relatively high. In this region of the wind spectrum the magnitude of the spectral density is low. For tall buildings, the fundamental eigenfrequencies are lower and hence closer to the center of the wind spectrum. This explains why tall buildings are more prone to wind induced dynamic behaviour. The ASCE Standard classifies a building as dynamically sensitive if the first modal eigenfrequency of vibration f_0 is smaller than 1 Hz (Boggs & Dragovich 2006). For higher order modes, the natural frequencies are higher than the value of the fundamental frequency. As can be observed, these frequencies are less close to the relevant wind spectrum frequencies, hence their contribution to the response is minimal. This is why higher order modes are less relevant for the structural dynamic response and can in general be ignored in wind-engineering (Lu & Chen 2011*a*).

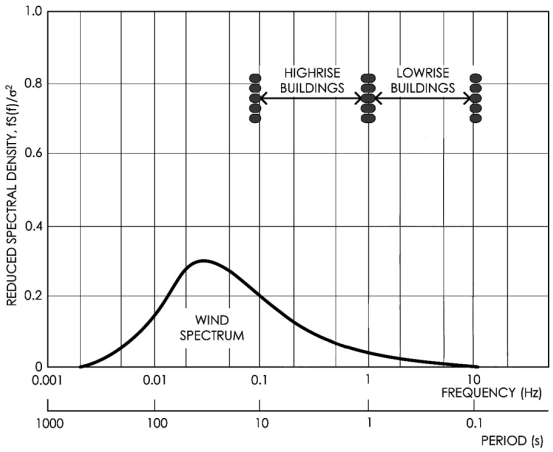

Figure 3.4: *A typical wind spectrum: Wind-gust frequencies compared to building frequencies. Edited figure, originally Adopted from: (Boggs & Dragovich 2006)*

3.2 Modelling of wind

Different methods exist to determine the wind-induced behaviour of tall buildings. Each method has its own accuracy, computational complexity, and cost in terms of money and time.

3.2.1 Modelling methods

The following modelling methods can be distinguished:

- Equivalent static wind forces
- Random vibrations theory
- Wind tunnel tests
- Computational fluid dynamics (CFD)

3.2.1.1 Equivalent static wind forces

In building codes like the Eurocode the dynamic contributions of the turbulent flow are taken into account by converting the dynamic load to an equivalent static load. To do so, the wind pressure q_p from Equation 3.2 is multiplied by the structural factor CsCd which takes into account the dynamic contributions and the gust factor, see Equation 3.3. The calculation procedure to determine the equivalent static wind forces is, in fact, an application of the theory of random vibrations. In addition, the wind force is multiplied by a static force coefficient Cf that represents the drag coefficient and is dependent on the building shape. This results in the total equivalent static load as defined by Equation 3.3 (Eurocode 2005*b*).

$$F_w = C_s C_d * C_f * q_p(z_i) * A_{ref} \tag{3.3}$$

In this equation F_d defines the total wind force on a reference area A_{ref}. q_p is the peak distributed velocity pressure defined by Equation 3.2. C_f represents the drag coefficient, $C_s C_d$ is called the structural factor and consists of the shape factor and the dynamic gust factor.

3.2.1.2 Random vibrations theory

It can be understood that taking into account the dynamic behaviour by an equivalent static force is a simplification. Making use of an equivalent force, rather than a dynamic force, is sufficient for the calculation of buildings that are not sensitive to dynamic behaviour. However, for dynamic sensitive buildings, more sophisticated, detailed, methods may be required. Especially for the application of supplementary damping the dynamic behaviour must be investigated properly. For these types of buildings a dynamic response analysis can be performed with the help of random vibration theory (Advisory Committee on Technical Recommendations for Construction 2008).

The random wind signal can be considered as an infinite summation of sine functions with different frequencies. The stochastic properties of this signal can be represented by a spectrum, which is a measure of the variance associated with the fluctuating wind velocity. With the theory of random vibrations, the total dynamic response of a building can be defined as a summation of dynamic responses to the individual sine loads. The theory of random vibrations is covered in more detail in Chapter 10.

3.2.1.3 Wind tunnel tests

The most accurate wind profile can be obtained by a wind tunnel test. During a wind tunnel test, realistic wind loads are measured on a scaled building model. The conditions in the wind tunnel are in such a way that the test represents the local wind climate. With a wind tunnel test it is possible to investigate the influence of surrounding buildings, on the structure of interest. This is an important difference with the previously discussed methods. The use of wind tunnel testing is recommended for all dynamically sensitive buildings, but it is essential for cases in which the building has a irregular shape, or for cases in which the

surroundings of the building may have a large influence on the wind profile.

3.2.1.4 Computational fluid dynamics

Computational fluid dynamics (CFD) is the analysis of fluid flows using numerical solution methods (*An introduction to CFD: what, why and how* n.d.). A CFD analysis can be considered as a numerical wind tunnel test, in which the dynamic response is determined by a computer rather than by an actual model. Nowadays, CFD analyses are still very computational intensive and are not widely applied in the design of buildings yet (Kalkman et al. 2013), it is however expected that CFD analyses will play a major role in the future of dynamic response calculations.

3.2.2 Modelling domain

As mentioned, wind load can be considered as a random process. Wind can be modelled in two different two different domains: The time domain and the frequency domain (moon Kim Ki-pyo You Jang-youl You 2014). These domains are visualised in Figure 3.5. It is important to note that these two different domains contain the same information, they are only visualised in a different domain. With the use of for example a Fourier transformations, the original signal can be converted from the time to the frequency domain and vice versa.

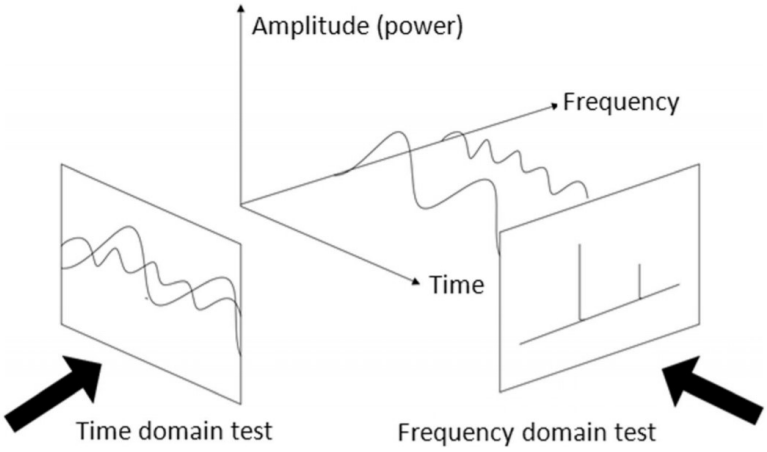

Figure 3.5: *Relation between time and frequency domain. Adopted from (Sun 2019)*

Modelling in the time domain is the most intuitive way of wind modelling, as this way of modelling represents the wind in the same way as human beings perceive the wind load. The wind is modelled as a varying load in time and space. This signal could be simply determined by measuring the wind velocity at a certain location over a longer period of time. As the wind profile is randomly distributed in time and space, generating a corresponding load pattern for a building in the time domain is time demanding and complex (Strømmen 2010). The challenge in modelling the wind in the time domain is two-fold: First, it is difficult to determine the wind properties for a time period that has enough statistical significance to produce reliable results. Second, modelling in the time domain is computationally very intensive.

In general, it is more convenient to model the wind in the frequency domain rather than in the time domain. In this case, use is made of the general theory that every signal can be described by an infinite set of harmonic functions. In the frequency domain the time-dependent wind signal is analysed and transformed

to a set of individual harmonic vibrations, all with different frequencies and amplitude. Such a transformation may for example be performed by the Fourier transform. The advantage of this approach is that the dynamic response can be calculated separately for each of these individual signals. Mathematically this is more efficient. Subsequently, all these responses are combined to one combined response. To create a mathematical description in the frequency domain the wind field must be considered as a stochastic process. As mentioned, the wind signal can be represented by a spectrum, this spectrum contains the information on the stochastic properties of the wind field (Vrouwenvelder 2004). In Chapter 10 the theory of random vibrations will be applied, in the frequency domain.

3.3 Wind-induced response

Wind loads causes in stresses in structural members, this results (horizontal) deflections in a building. These stresses and deflections are mainly caused by the static wind load component of Equation 3.1. For dynamically sensitive buildings, the fluctuating wind component can play a role as well in the deformations and stresses. For these dynamic loads, the largest contribution to the total response comes from fluctuating components with a frequency close to one of the eigenfrequencies, since these loads are dynamically amplified by resonance.

In addition, for dynamically sensitive buildings, wind-induced accelerations can become a significant design factor. As described in chapter 2 excessive building accelerations can result in discomfort for building occupants and should hence be prevented. Three different types of building accelerations, as listed below, play a factor in the design of tall buildings:

- Along-wind accelerations
- Across-wind accelerations
- Torsional accelerations

The different wind responses are illustrated in Figure 3.6. Along wind accelerations can be described well by theoretical models. The calculation procedures for along wind acceleration are hence quite consistent throughout different building codes. This contrasts with the calculation procedures for across wind and torsional responses, these effects turn out to be more difficult to model accurately (Kwon & Kareem 2013). In the following paragraphs the three different types of accelerations are shortly introduced.

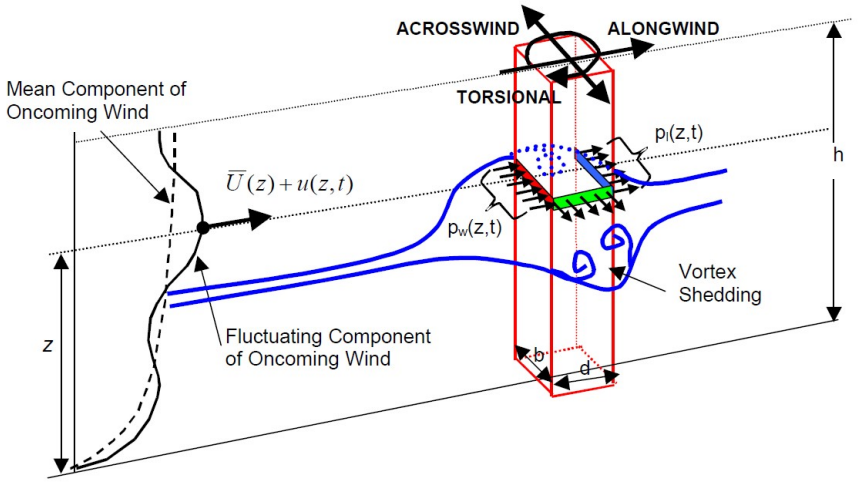

Figure 3.6: *Wind actions on a building. Adopted from (Tracy Kijewski 2000)*

3.3.1 Along-wind response

For non-slender buildings, the understanding of the dynamic behaviour of a structure is quite intuitive: the dynamic response will occur mainly in the along wind direction as a result of wind buffeting. The fluctuating wind gusts, that are an effect of the turbulence in the wind velocity profile, initiate wind-induced accelerations in the along wind direction. In the case that the frequencies of these gusts are close to one of the building's modal frequencies, resonance can occur. The more in-depth calculations of the along wind response are discussed and applied in Chapter 6, 7, and 10.

The Eurocode (NEN-EN1991-1-4) offers two methods to calculate the along-wind accelerations: procedure 1 described in annex B and procedure 2 described in annex C. Especially for slender structures, procedure 2 is preferred over procedure 1, as this one provides more reliable results (Steenbergen et al. 2012). Therefore, throughout this report Eurocode method 2 will be used for calculations. In this Eurocode method an application of the theory of random wind vibrations, as developed by Davenport, and further developed by Solari, is adapted (Dyrbye & Hansen 1997). The exact formulas to determine the maximum acceleration are not presented here, but can be found in Annex B and C of NEN-EN 1991-1-4 (Eurocode 2005*b*). Please note, a new Eurocode regarding wind-loads and accelerations is in development, in which the equations will be slightly updated.

3.3.2 Across-wind response

For higher and more slender buildings, the across wind dynamic response becomes significant. This response is the result of vortex shedding. Due to vortex shedding, oscillations of the building occur in the direction perpendicular to the wind, which results in vibrations. This across wind response can be governing for tall and slender buildings (Dyrbye & Hansen 1997).

The concept of vortex shedding can be explained by taking a look at the wind flow. When a laminar wind flow is interrupted by a building, a boundary layer will occur around the buildings surface due to friction. Bernoulli's principle states that the acceleration of the wind flow result in pressure differences (Advisory Committee on Technical Recommendations for Construction 2008). Due to these pressure differences, The

incoming wind flow will separate at the buildings across wind sides, resulting in an unstable turbulent wake. In this turbulent wake vortexes are generated (Sockel 1994). The pressure differences that occur due to the alternating vortex shedding results in alternating lift forces on the structure perpendicular to the wind flow (Dyrbye & Hansen 1997). Vortex-induced vibrations occur when vortices are shed alternately from the two opposite sides of the structure in a harmonic manner. This happens a specific range of intermediate Reynolds numbers and relatively low velocities. If the frequency of this shedding corresponds to one of the structure's natural frequencies, problematic resonance occurs, slender buildings are more sensitive to this phenomenon (Emil Simiu 2019). The shedding of vortexes is visualised in Figure 3.7.

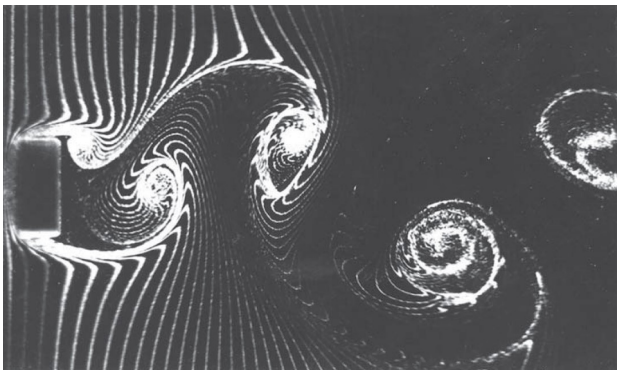

Figure 3.7: *Vortex shedding clearly visible. Adopted from (Nakamura 1993)*

Interference effects can play a major role in the occurrence of problematic vortex shedding. The highest risks occur for slender buildings that are constructed closely in line together and for a slender structure that are hit by the shedding vortices of nearby large structures (Dyrbye & Hansen 1997). Both these risk factors are highly depends on the environment of a building. Hence, it is difficult to analytically predict potential vibrations caused by vortex shedding. The developed analytical models are therefore still rather approximate and can only be used in preliminary design(Dyrbye & Hansen 1997). For buildings that inherit a risk on the occurrence of problematic vortex shedding, wind tunnel test has to be performed. For aeroelastic phenomena like vortex shedding a return period of 10 years is recommended instead of the 1 year return period for along wind accelerations (Advisory Committee on Technical Recommendations for Construction 2008).

3.3.3 Torsional-wind response

Moreover torsional accelerations can arise, in which the building rotates and accelerates around its z-axis. Torsional accelerations are caused by eccentric fluctuating wind loads. Eccentric loads can occur in two situations: 1) If a uniform wind load act on a non-symmetrical building, the resulting wind force will be eccentric. 2) If a non-uniform wind load acts on a building, this causes in an eccentric resulting wind force. This results in a non-uniform load, see Figure 3.8. In both cases, the fluctuating wind components generate fluctuating torsional moments on the building. These moments induce torsional dynamic actions on a structure. Reason number 2 especially occurs for buildings with a large facade area. The larger the facade area, the less coherent the flow will be, due to the limited size of wind vortices (Vrouwenvelder 2004). This concept was considered an issue in the design of the European patent office in Rijswijk, due to the large facade area of this building. (Robbemont 2019).

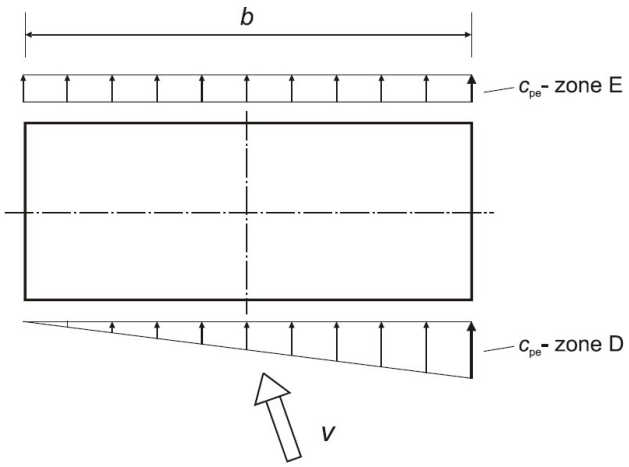

Figure 3.8: *The effect of non symmetric wind (Eurocode 2005b)*

3.4 Conclusion

- The wind velocity profile can be considered as consisting of two separate components: the mean and the fluctuating wind component. The former results in static loading. The latter initiates the dynamic response of a structure.
- Wind loading is a random process, which can only be modelled by statistical methods.
- Wind results in three types of accelerations on structures: along-wind, across-wind and torsional accelerations. Only along-wind accelerations can be accurately modelled in an analytical manner. Therefore, across-wind and torsional responses are not taken into account in this research.

Chapter 4

Design of high-rise buildings

To understand the dynamic response of tall buildings, first of all it is important to understand the design aspects of 'standard' high-rise buildings, prone to static loads. Therefore, in Section 4.1 the design considerations for static loads are covered. The focus in this report is on dynamically sensitive buildings, for these building dynamic aspects become a factor in the design. The relevant dynamic properties are explained in Section 4.2. In the final section, non-structural design aspects are shortly introduced.

4.1 Static structural design aspects

The construction of high-rise buildings introduces problems that do not exist for low-rise buildings. A high-rise building is designed as a unique combinations of functions, local circumstances, and requirements (Hoenderkamp 2011). To cover all those aspects, different types of stability systems and structural materials can be applied, all with their own properties. In this section, some design aspects for the design of high-rise structures are introduced.

4.1.1 Stability systems

For high-rise buildings, the deflection requirements are often the governing design criterion, which result in different design challenges, especially regarding the stability system. The structural design of high-rise buildings is highly focused on providing stability and stiffness for lateral wind-loads. Therefore, the design of the stability system becomes a very decisive part of the structural design of tall buildings. The most common systems are illustrated in Figure 4.1. The application of a certain stability system depends, among other aspects, on the height, the slenderness ratio, architectural requirements, the applied structural materials, and the function of the building. The most common types of stability systems are listed below (Hoenderkamp 2011):

A) Shear wall system
B) Coupling wall system
C) Central core system
D) Outrigger system
E) Tube system
F) Rigid frame system
G) Braced frame system
H) Megaframe system

These systems have been schematically visualised in Figure 4.1. A description of each system is attached in Appendix A. Please note that the different systems can also be combined into a hybrid system. Moreover, it is possible to apply different systems in the longitudinal and the transverse direction, this can be efficient for rectangular floor plans, for example.

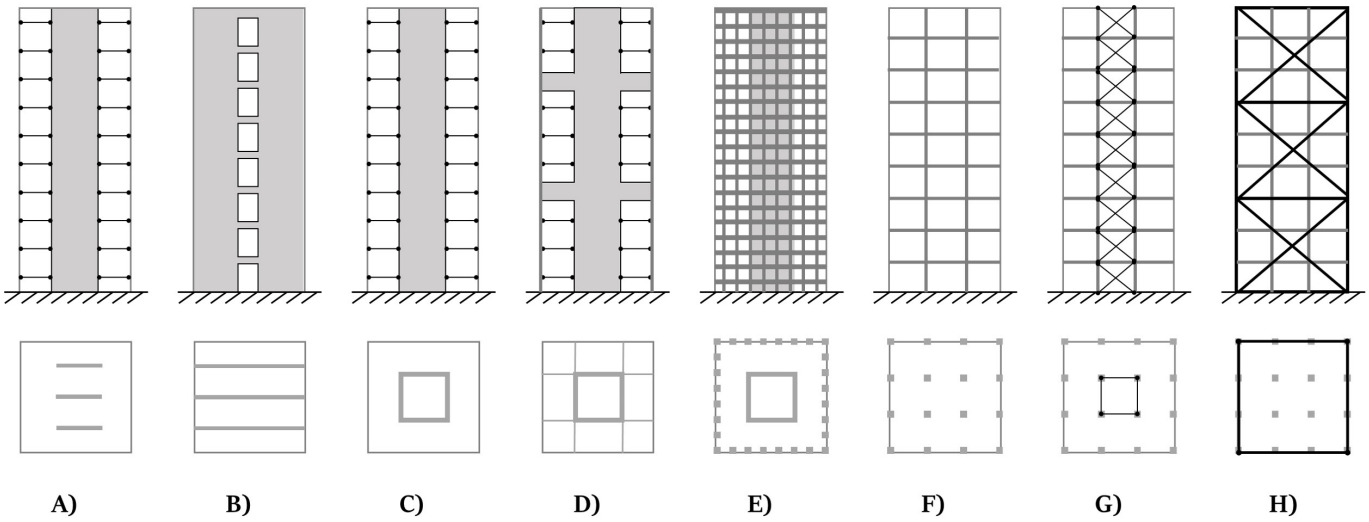

Figure 4.1: *Most common types of stability systems*

4.1.2 The second-order effect

Another aspect that has to be considered for the design of high-rise buildings is the influence of the second-order effect. In a tall building, as a result of structural imperfections and load deformations, eccentricities occur. These eccentricities, in combination with the high vertical column forces, result in additional bending moments on the structure, as visualised in Figure 4.2.

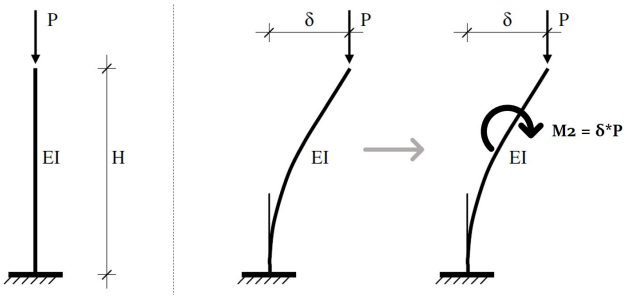

Figure 4.2: *Left: No second-order effect. Right: Additional bending moment due to the second-order effect. Modified Figure, Adopted from: (Hoenderkamp 2011).*

These additional bending moments can increase the loads on a building significantly, and thus should be taken into account for the design of high-rise structures. As a rule of thumb the lateral design loads should be multiplied by a factor of 1.2 to account for the second-order effect. The Eurocode provides design formulas for a more precise determination of the second-order effect, this method is applied in Chapter 7.

The larger the deformations get, the more significant the second-order effect becomes. This must be kept in mind if a performance-based deformation design approach is applied, as introduced in Chapter 2. The second-order effect affects both the ULS and the SLS design loads. Nevertheless, the contribution of the second-order effect will be significantly smaller for SLS design due to different starting points: For SLS the initial imperfections do not have to be taken into account, the horizontal deformations are less, and the vertical reaction force is smaller.

4.2 Dynamic structural design aspects

The structural dynamic behaviour depends on different building properties than the static structural behaviour. The following properties determine the dynamic behaviour:

- Eigenfrequencies
- Total building Mass
- Stiffness
- Damping ratio
- Height
- Mode shapes

If these parameters are adjusted, the dynamic properties of a building will change. In this way, a structural designer can alter the dynamic behaviour of a structure, for example to fulfil the structural requirements regarding accelerations and vibrations. Interesting aspects of these properties are discussed in this section. Actually, the eigenfrequencies and the modal shape can not be distinguished as dynamic building properties, as they are dependent on the mass, stiffness, height and damping ratio. Nevertheless, they are discussed separately because of their major influence on the dynamic behaviour. The relations of the dynamic parameters are discussed in more detail in Chapter 6.

4.2.1 Eigenfrequencies

The modal-eigenfrequencies, also referred to as the natural frequencies or simply 'the eigenfrequency' are tan important building property in dynamic design. The eigenfrequencies define the oscillation frequency of a building during free vibrations. Eigenfrequencies highly influence the dynamic response of a building: the closer the loading frequency is to one of the modal eigenfrequencies, the bigger the structural dynamic response will be.

The eigenfrequencies are a building property, independent of the load. The value of the eigenfrequency depends on the stiffness, the building mass, and the height of the structure. The value of the damping ratio also slightly affects the value of the eigenfrequency, but this is often neglected for low-damped structures, like tall buildings.

The eigenfrequency is in general not constant over the lifetime of a building. Changes in the structure like the cracking of concrete can reduce the stiffness, which influences the eigenfrequency. This will directly affect the dynamic behaviour of a structure. Therefore, a sensitivity analysis on the eigenfrequency is recommended during the design stage (Boggs & Dragovich 2006).

For single degree-of-freedom systems the angular eigenfrequency is defined by Equation 4.1. The value depends on the stiffness and mass of the system. The eigenfrequency can be expressed in two different ways. The angular frequency can be converted to the standard natural frequency in Hz [cycles per second], as described in Equation 4.2.

$$\omega = \sqrt{\frac{k}{m}}\ [rad/sec] \qquad (4.1) \qquad\qquad f = \frac{\omega}{2\pi}\ [Hz] \qquad (4.2)$$

For multiple degree-of-freedoms systems (MDOF) the eigenfrequencies can be determined by performing a modal analysis. Standard mathematical software or finite element programs can be used for this purpose.

Rule of thumbs are described in literature to estimate the eigenfrequency of a structure, based on empiric research. The Eurocode has adopted Equation 4.3 to calculate the eigenfrequency of a tall building (> 70m) (Eurocode 2005*b*). This equation is based on empirical research by Ellis and Bre (Ellis & Bre 1980). Care must be taken when using this equation. Especially for light-weight and flexible buildings, this equation will not provide an accurate estimation of the actual eigenfrequency, since the mass and stiffness are not explicitly taken into account.

$$\eta_1 = \frac{46}{h} \tag{4.3}$$

Another estimation of the eigenfrequency can be calculated by the Equations for a continuous Euler-Bernoulli cantilever beam, as described in Equation 4.4. For a clamped beam the Cn value will be equal to 3.52 for the first mode. In this case ρ represents the beam density, and hence takes into account the influence of the building mass. The advantage of this equation is its dependence on stiffness and mass, which allow for better insights in preliminary design choices. It should be noted that the Euler-Bernoulli beam theory does not include shear deformations, which decreases the accuracy of this formula (Rossmann et al. n.d.).

$$\omega_n = \frac{Cn}{h^2} * \sqrt{\frac{EI}{\rho * A_{cr}}} \tag{4.4}$$

4.2.2 Total building Mass

The mass of a building generates inertia. The inertia influences the dynamic behaviour of a structure: buildings with a high inertia are more difficult to bring into motion, than buildings with a low inertia. Moreover, the mass of a building affects the eigenfrequency of a structures.

Regarding the mass, all the mass that is brought into motion during dynamic excitation should be considered in dynamic calculations. This means that not only the structural mass should be considered, but also, among others, the mass of facades and partition walls. In general, the mass of a structure is mainly determined by the mass of the floor system (Alexander 2010). It is important to note that the relation between the structural mass per unit length and the structural height can not be considered linear: If the height of a building doubles, the mass will increase by a factor larger than 2, see Figure 4.3. Due to the fact that loads in the top of the structure act on all subsequent structural members. Therefore, the contribution of the structural system will become more important in the determination of the overall mass for taller buildings.

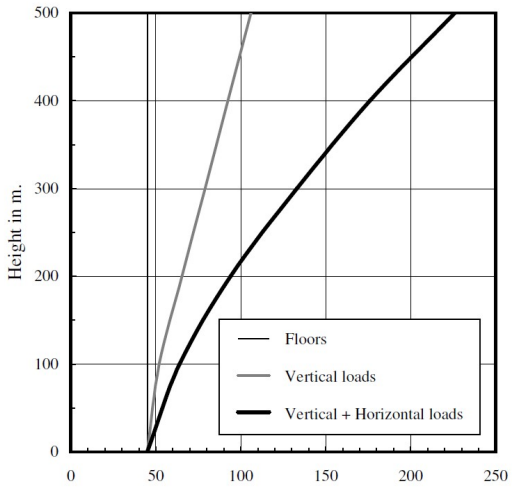

Figure 4.3: *Relation between the mass per unit length and the height of a building. Adopted from: (Hoenderkamp 2011)*

4.2.3 Stiffness

The stiffness of a structure mainly depends on the building height, the stability system and the applied structural materials. The higher the stiffness the smaller the absolute top displacement of a structure will be. Although, this does not mean that an increase in stiffness is always positive, as the stiffness is positively related to the eigenfrequency: the higher the stiffness, the higher the eigenfrequency. If the eigenfrequency is close to the loading frequency, resonance can occur. For wind loads, which have a relatively low frequency, an increase in stiffness, however, leads to a favourable reduction in the dynamic response, see Figure 3.4 (Smith & Willford 2007).

4.2.4 Damping ratio

Damping is a structural parameter that is of importance in the prevention of excessive vibrations. The value of the damping parameter defines the amount of energy dissipation within a structural system . This dissipation of energy within an oscillating structure determines if and at which rate, the amplitude of vibration is reduced for a system in motion. The damping ratio is a dimensionless measure of the damping, as defined in Chapter 10.

As mentioned, damping is about the dissipation of energy from the system to its environment. This dissipation is caused by the conversion of kinetic and potential energy to heat, which is subsequently dissipated from the structural system to the environment. The higher the damping ratio, the faster this dissipation of energy occurs. Due to the presence of damping, the vibrations of a structure in motion are reduced. A theoretically undamped structure, which is equivalent to a structure with a damping ratio of zero, would after excitation keep in motion forever. This behaviour is never seen in nature, as every natural system inherits some damping. For structures with a damping ratio higher than zero, energy will be dissipated during motion. When the energy is finally dissipated, the structure returns to its equilibrium position. The higher the damping ratio, the more energy is dissipated per excitation, which results in a faster decrement of motion.

Three different sources of damping can be distinguished: intrinsic damping (δ_s), aerodynamic damping (δ_a), and supplemental damping (δ_d) (Lago et al. 2019). The sum of these components determines the total

damping ratio of the structure, see Equation 4.5 which is also used in the Eurocode (Eurocode 2005*b*).

$$\delta = \delta_s + \delta_a + \delta_d \tag{4.5}$$

Intrinsic damping

Intrinsic damping is the type of damping that is inherited in the structural system anyhow, without taking explicit measures. The intrinsic damping is the result of different sources of damping within a structure, for example (Lago et al. 2019) and (Smith & Willford 2008):

- Material damping
- Friction in connections
- Foundation and soil types
- Non-structural components (cladding, interior partitions, etc.)

The amount of intrinsic damping is difficult to estimate and depends on the structural system and structural material. The intrinsic damping ratio will be in the order of 1% (Eurocode 2005*b*), however some research suggests that the intrinsic damping ratio for tall buildings in the Netherlands may be higher, up to 2%, due to the soft soil conditions (Gomez 2019). On the other hand, international research suggests that for tall buildings the damping ratio should be reduced (Smith & Willford 2007). Throughout this report, the intrinsic damping is assumed to be 1%.

Aerodynamic damping

Aerodynamic damping occurs when the oscillation of the structure is such that the building motion starts to bring the surrounding air in motion. In that case, energy is transferred from the structure to the air. The higher the building's velocity, the higher the aerodynamic motion. Often the aerodynamic damping is neglected in design calculations. Therefore, the aerodynamic damping is out of the scope of this report as well.

Supplemental damping

If the dynamic response of a structure does not fulfill the requirements as defined in Chapter 2, it can be to artificially increase the damping of the system. This additional damping is called supplementary damping and can be generated with the help of dynamic modification devices, called supplemental dampers. Those supplementary damping systems are designed to counteract the structural motion. Applying dampers increases the damping ratio and therefore helps to decrease the motion and accelerations of a structure. Examples of supplemental dampers are viscous dampers, viscoelastic dampers, and tuned mass dampers (TMD). This topic is extensively discussed in Chapter 5.

4.2.5 Mode shapes

A mode shape is the deformation that a structure would show when vibrating at the corresponding natural frequency (Dlubal 2019). The motion of a multiple-degree-of-freedom system can be considered as a summation of different mode shapes, see Figure 4.4. The modes are mathematically described as orthogonal. Each possible building motion can be described as a superposition of the weighted mode shapes. Each mode has its own corresponding modal frequency. When a building is brought into motion by one of the exact modal frequencies, only the corresponding mode will contribute to the motion (Clough & Penzien 1995).

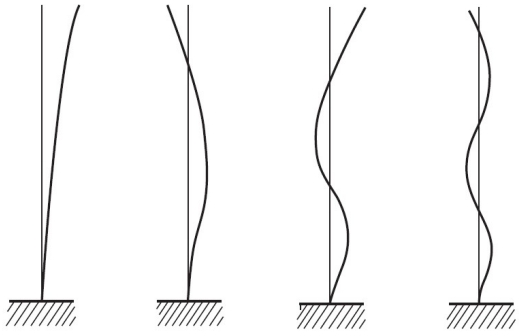

Figure 4.4: *The first four modal shapes of a cantilever structure. Adopted from (Emil Simiu 2019)*

The higher the mode number, the higher the corresponding modal eigenfrequency. Regarding wind-induced vibrations it is normally only necessary to take into account the first dynamic mode in each direction (along, across, torsion) as these modes can account for 90% of the overall motion (Ellis & Bre 1980). This is due to the fact that the frequency of wind-gust is relatively low and that the positive-negative shape of higher modes result in an out-balancing of dynamic effects for these modes (Boggs & Dragovich 2006).

4.2.6 Mitigation of wind-induced responses: design strategies

As described in Chapter 2, the accelerations of a high-rise building are restricted. These limits are defined by building code regulations, as discussed in Chapter 2. If the dynamic responses of a designed structure exceed these limits, design measures should be taken. In general, three possible design approaches exist to reduce the dynamic vibrations:

- Modify the dynamic building parameters
- Modify the building geometry
- Apply supplementary damping

These general design strategies have been visualised in a flowchart in Figure 4.5.

By modifying the dynamic parameters of a building, the behaviour of a structure can be altered. For example, by increasing the building mass or by increasing the building stiffness. Additional material is required for these solutions.
Another option is to modify the building geometry into a more aerodynamic building shape. This option adjusts the magnitude of the wind loads, rather than the behaviour of the building. The last option is to apply supplemental dampers in the building. The supplemental dampers increase the damping ratio of the structure, which reduces the dynamic building response.

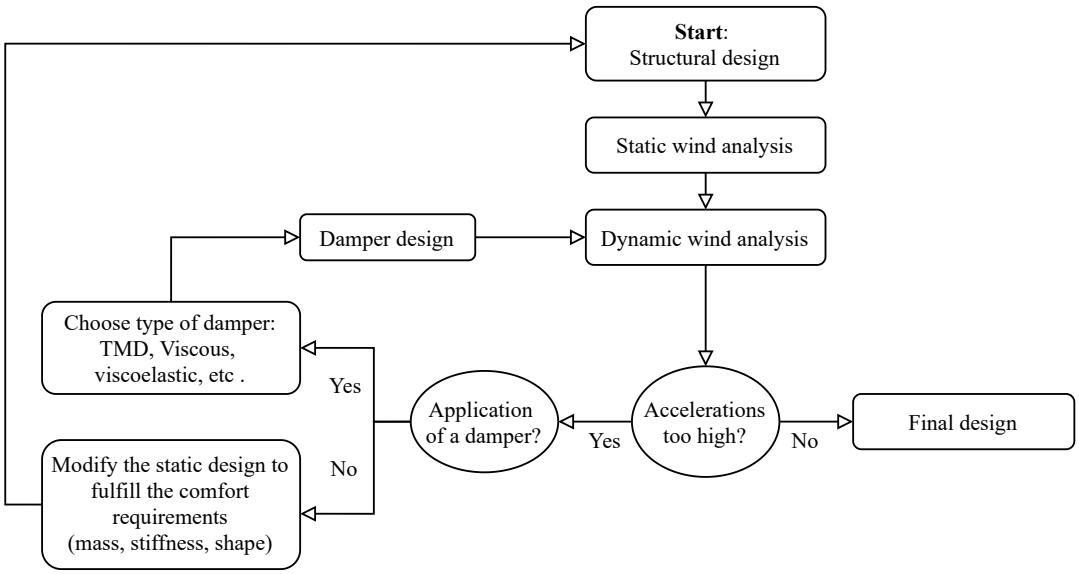

Figure 4.5: *Flowchart for the design of dynamically sensitive structures*

4.3 Structural materials

A design factor with major influence on all kinds of building properties is the structural material. The choice of the used materials affects, among others, the structural design, the building physics, construction process, and architectural appearance. conventional tall buildings are constructed in steel, reinforced concrete or a combination of these materials. The application of timber in the design of high-rise buildings is an ongoing topic of research. Only few timber high-rise structures have been built over the world. So far, timber is mainly applied in combination with steel or concrete. For example, by applying cross laminated timber floor slabs (CLT).

In this research the material properties that influence the dynamic building behaviour are of main interest: mass, stiffness, and damping. The application of steel and timber results in more lightweight structures, due to the more favourable relation of mass and stiffness. For most design criteria, a relatively low building mass is considered beneficial. However, regarding dynamic behaviour, lightweight buildings are more prone to dynamic vibrations, as is explained in Chapter 6.

Moreover, the intrinsic stiffness of timber is lower than for concrete and steel. This makes it harder to fulfill the deflection limits if timber is applied as the structural material. Such a lower stiffness is disadvantageous for the dynamic behaviour of a structure, see Chapter 6.

Finally, the dynamic behaviour is influenced by the intrinsic damping ratio. This property varies slightly for the different structural materials. In general, The intrinsic damping ratio of steel structures is expected to be a bit lower than that of concrete structures (Geurts & van Bentum 2015) (Eurocode 2005*b*). For timber towers on the other hand, a little higher intrinsic damping ratio is expected (Feldmann et al. 2016), which could be beneficial in the design of slender timber towers, more research is needed on this subject.

4.4 Non-structural design aspects

The design of a high-rise building is a complicated task that involves different design fields. These different fields affect each other and result in boundary conditions for other design aspects. Therefore, the different fields have to collaborate to create the best possible integrated design. An optimal structural design does not necessarily result in an optimal overall design of a high-rise building. In this report, the focus is solely on the structural design of high-rise buildings. However, it should be kept in mind that the following aspects are of relevance for the structural design of a high-rise building as well:

- **Day-light regulations**: enough day-light must penetrate into the floors of a tower, this introduces limitations to the maximum building dimensions.

- **Core dimensions**: The size of a structural core size should be limited to create an economical feasible structure, with enough rentable floor area. If the core is too big, too much valuable space is lost. On the other hand, the core should provide enough space to allocate the required services like lifts, staircases, and MEP installations.

- **Facade**: Building occupants prefer a good and open view. A dense structural grid, located in the facade, should thus be prevented.

- **Flexibility**: Especially for office towers, the floor plan should be as flexible as possible to allow for flexibility in function. Therefore, the amount of structural walls and columns in the floor plan should be minimised.

- **Fire safety**: A tall building should be fire safe for at least 120 minutes. This has implications for the choice of the structural system and the structural material.

- **Acoustics**: Especially in residential towers, a building has to comply to strict sound regulations. Lightweight materials are unfavourable regarding acoustics.

- **Storey height**: From a cost point of view, in particular regarding the facade cost, it is beneficial to keep the storey height as low as possible. As the minimum clear heights are defined in regulations, savings can only be made in limiting the floor system thickness.

4.5 Conclusions

- Different dynamic aspects are of importance for the structural response, namely: Eigenfrequencies, stiffness, total building mass, damping ratio, height, and mode shapes.
- Three strategies exist to mitigate the wind-induced motion of a building: an increase of mass, stiffness, or the damping ratio. It is also possible to modify the building shape, but this option is excluded from the scope of this research.
- The total damping ratio is made up out of three components: intrinsic, aerodynamic, and supplemental damping. In this report, the first two are assumed to result in a combined damping ratio of 0.01. The damping ratio can be increased by the application of supplemental dampers.
- Non-structural aspects play a role in the design of high-rise structures as well. These aspects can impact the structural design considerations.

Chapter 5

Application of supplemental dampers

As explained in Chapter 4 a theoretical increase of the total damping ratio reduces the dynamic response. Such a theoretical increase in the damping can be achieved in practice by applying supplementary damping systems. Different types of supplemental dampers systems exist. Several common systems are introduced in Section 5.1 and 5.2. Practical design aspects and uncertainties introduced by the application of dampers are covered in Section 5.3.

5.1 Categorisation of supplementary dampers

A lot of different types of damping systems have been developed, each with their own properties. These systems can be categorized in different groups, dependent on their properties (Lago et al. 2019):

- Displacement-dependent dampers
- Motion-dependent dampers
- Velocity-dependent dampers
- Force-dependent dampers

The behaviour of displacement-dependent dampers depends on the absolute displacement of the damping device, the motion frequency does not play a role. In contrast, the reaction force of motion-dependent dampers depends on both the displacement and the frequency of the motion. On the other hand, the functioning of velocity-dependent dampers is based on the relative velocity between the two damper-ends. The amount of damping generated by a force-dependent damper is a function of the structural force on a damper. Some damping system can fall into more than one category. Viscoelastic dampers are for example a combination of velocity-dependent and displacement-dependent dampers (Lago et al. 2019).

5.1.1 Passive and active systems

Moreover, a distinction between passive dampers and active dampers can be defined. The scope of this thesis will be limited to passive damping systems. Nevertheless, both concepts will be shortly introduced in this section.

Passive systems are fully mechanical and do not require an external power source, the damping mechanism of passive dampers is directly based on the building motion. This building motion results in forces on the damper, which result in a reaction force from the damper. Energy is dissipated in the damper to generate this reaction force. The damping force is thus generated without the intervention of human beings or computer systems,

An active system is controlled by a computer. This computer determines the required control force to counteract the occurring dynamic motions. The required response is only indirectly based on the motions of the building. Such a system requires an external energy source. In general, active dampers can work more efficiently than passive dampers. However, reliability concerns are introduced by the application of active dampers. For example, blackouts can occur during a storm, which can cause failure of the damping system.

In addition, the maintenance cost and operational cost of active dampers are relatively high (El-Khoury & Adeli 2013). The application of active dampers is in general considered as more complex and risky than the application of passive dampers.

5.2 Types of damping systems

Several types of supplemental dampers have been developed and are used in all types of high-rise buildings to reduce vibrations. The most common types of dampers are listed below:

- Tuned mass dampers (TMD) (motion-dependent)
- Viscous dampers (velocity-dependent)
- Viscoelastic dampers (displacement- and velocity-dependent)
- Friction dampers (force-dependent)
- Metallic dampers (displacement-dependent)

These types of dampers are able to effectively reduce the dynamic loading effects on buildings. In general, a damping ratio of 8% to 10 % is the maximum required damping ratio to eliminate resonant responses of wind load (Smith & Willford 2007). For the heights of Dutch high-rise buildings even less damping is required, this is discussed more in detail in Chapter 6.

In the following paragraphs, Tuned mass dampers, viscous dampers and viscoelastic dampers are introduced. The advantages and disadvantages of the application of these types of dampers are described in more detail in appendix B. Metallic and friction dampers are not discussed in this report, as these dampers are mainly used to mitigate seismic-induced building responses, rather than wind-induced responses.

5.2.1 Tuned mass dampers

Tuned mass dampers transfer the motion energy in a building to a secondary oscillating system that is connected to the main structure by springs and dampers. The secondary system, the actual TMD, is a device that consists of a large mass, see Figure 5.1b. This mass is usually on the order of a few percent of the total mass of the primary structure (Montgomery n.d.). See Chapter 9 for a more detailed description of TMD's. A simplified model of a tuned mass damper system is illustrated in Figure 5.1a. In this figure $M_1{}^*$ represents the fundamental modal building mass, m_d represents the mass of the TMD. The secondary mass is 'tuned' in such a way that the eigenfrequency of the secondary system is almost equal to the fundamental modal eigenfrequency of the structure. In this way the building motions close to the eigenfrequency, which would normally raise resonance problems, are transferred to the secondary mass with a phase shift (Kwok & Samali 1995).

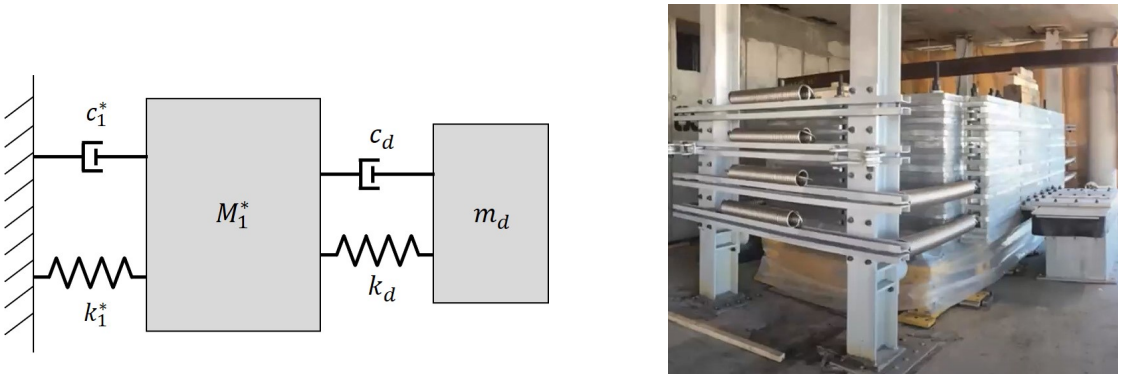

(a) *Schematic overview* (b) *TMD in practice*

Figure 5.1: *Tuned mass damper*
(b) adopted from Gerb (Meinhardt 2021)

Different types of tuned mass dampers exist. Convential TMD's consist of a mass that is able to move in the horizontal direction. Other commonly applied types are tuned liquid column dampers and pendulum tuned mass dampers, as famous from the Tapei 101 (Gutierrez Soto & Adeli 2013). This report focusses on the conventional type of TMD's.

The application of a tuned secondary mass in itself, is not a damping mechanism. The transfer of motion from the building to a secondary mass does not directly result in a dissipation of energy. Therefore, 'real' dampers have to be connected in between the main structure and the tuned mass, like viscous dampers. These dampers actually dissipate the energy of the secondary mass. Without these additional dampers the energy would only be temporarily stored in the secondary system. Eventually, this energy would be transferred back to the main structure, which would again result in vibrations.

The larger the lateral displacement of the primary structure, the more effective a TMD will be. Therefore, a tuned mass damper is typically installed at the top floor of a building. This is the location with the largest lateral displacement in the first mode, which is the fundamental mode in the case of wind-induced motions (Montgomery n.d.). Separate TMD's can be applied in each wind direction, but combined bidirectional systems can be applied as well.

5.2.2 Viscous fluid dampers

Fluid viscous dampers, or simply 'viscous dampers', are a type of velocity-dependent dampers. A resisting force is generated as a function of the relative velocity between the two ends of the damper. This restraining force is out of phase with the maximum load, which makes it an efficient system. If motion is applied to this type of damper, a piston is moved through a chamber filled with a silicone oil fluid, see Figure 5.2a and 5.2b. When this piston is in motion, pressure differences occur that make the oil flow through an orifice in the piston. During this process, kinetic energy is converted to heat, which dissipates in the atmosphere. This dissipating of energy is the actual damping (Philippe 2011).

Viscous dampers are most effective at locations where the relative velocity between the damper ends is the highest. The higher the relative velocity difference between the two damper ends, the bigger the restraining force. Dampers installed at positions with a lower velocity will also be activated, but they will generate a

lower resisting force. In contrast to TMD's, viscous dampers are normally distributed over the height of the structure. A disadvantage of the application of viscous dampers is that they do not inherit any stiffness. This means that a viscous damper can not be located in between the stiffening elements of a structure, as the dampers only provide a resisting force in dynamic conditions and do not resist any static loads.
The functioning of a viscous damper is not dependent on the frequency of motion. Therefore, in contrast to a TMD, a viscous damper can be effective for loads in every dynamic mode, providing the dampers are located in a smart way (Lago et al. 2019).

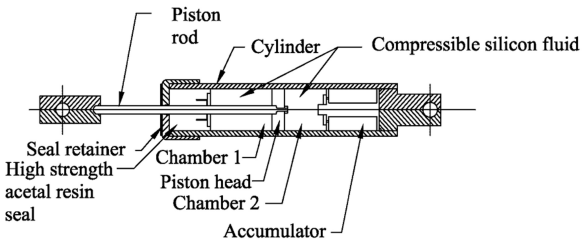

(a) *Schematic overview*

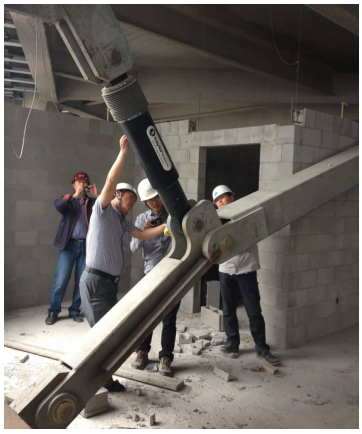

(b) *Viscous damper in practice*

Figure 5.2: *Viscous damper*
(a) adopted from (Patil & Jangid 2011) (b) adopted from www.taylordevices.com

5.2.3 Viscoelastic dampers

The last type of dampers that are discussed in this report are viscoelastic dampers (VE). The damper restraining force of a viscoelastic damper is both velocity-dependent and displacement-dependent . This means that, in contrast to viscous dampers, viscoelastic dampers provide some stiffness against static loads. In fact a viscoelastic damper combines the properties of a viscous damper and a spring. This behaviour is established by connecting rigid steel elements by a layer of viscoelastic material, like rubber, see Figure 5.3a. This viscoelastic material generates stiffness and damping under shear deformations. The magnitude of the restraining force depends on the displacement and the relative velocity between the elements ends (Lago et al. 2019).

Since viscous dampers do inherit some stiffness, they can be applied as a substitution for stiffening members. For example, as a substitution for coupling beams in shear walls, or as a part of an outrigger-column connection, as as proposed by Montgomery and Christopoulos, see Figure 5.3b (Christopoulos & Montgomery 2013). In this way a viscoelastic damper does not take up any additional space in the structure. It should however be mentioned that the static stiffness of a viscoelastic damper can be up to 6 times lower than for dynamic loading (Christopoulos & Montgomery 2013).

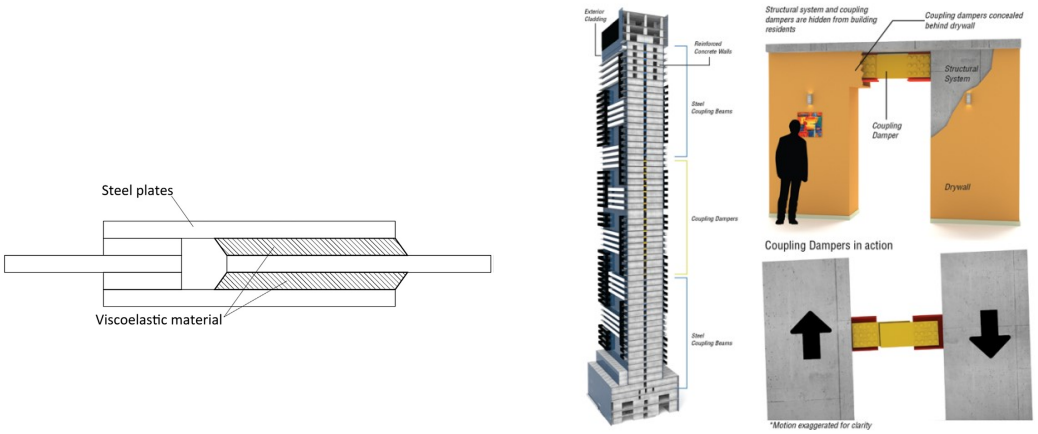

(a) *Schematic overview* (b) *Viscoelastic damper in practice*

Figure 5.3: *Viscoelastic damper. (a) adopted from (Lago et al. 2019) (b) adopted from ww.kineticadynamics.com*

5.3 Practical aspects and uncertainties

The use of supplementary dampers introduces additional design complexity. In this section different aspects that have be taken into account when applying supplementary damping systems are shortly introduced.

5.3.1 Practical aspects

If it is decided to include supplemental dampers in the design, the aspects as listed below should be taken into account. This list is adopted from (Lago et al. 2019). Chapter 9 covers these aspects more in detail.

- Source of external dynamic excitation
- Intrinsic damping ratio
- Dynamic building properties
- Performance level
- Damper - structure interaction
- Load at the damper
- Available space
- Construction material
- Lifting capabilities at the site during installation
- Maintenance and inspection requirements

5.3.2 Design uncertainties

The effectiveness of a supplementary damping system does not only depend on the damping system itself, but also on other local circumstances that may influence the damping behaviour. Neglecting these aspects could lead to unconservative results (Lago et al. 2019). Examples of such aspects are:

- Construction tolerances
- Temperature influence
- Possible friction
- Additional stiffness
- Fatigue issues
- Required maintenance
- Service lifetime

Other important boundary conditions that determine the effectiveness of a damping system and thus should be taken into account in the design of a damping system are: soil-structure interaction effects, time dependent building stiffness (for example due to concrete cracking), and the value of the intrinsic damping. Moreover, the amount of damping can be slightly dependent on the amplitude of motion, this is called aeroelastic damping (Smith & Willford 2007). These properties can be highly uncertain during design, while their influence on the total structural response can be major.

All these factors and uncertainties should be considered during the design of a supplementary damping system, otherwise the resulting amount of damping could be overestimated. To take care of all these uncertainties, an iterative design process is required. Moreover, it is important to perform sensitivity analyses on the important parameters during the design process. Finally, structural designers should be aware of the risks that are introduced by applying dampers to meet the strength (ULS) requirements, this subject is covered in the next section.

5.3.3 The application of dampers in the ULS design

As described in Chapter 4.2.4 supplemental dampers can help to reduce accelerations and deformations, which are both serviceability requirements. As discussed in Chapter 2 the serviceability criteria are about the quality of a building, not about safety. This means that if a damper works less well as expected, due to the uncertainties as discussed in the previous section, no major problems occur. Moreover, for a TMD, the damping properties can relatively easily be adjusted and updated.

In theory, it is possible to apply supplemental dampers in the ULS design as well to help fulfill the strength requirements of a building, since the fluctuating wind load contributions are reduced by the application of supplementary damping. However, in practice, the use of damping devices in the ULS design raises a number of reliability concerns, regarding the safety of a structure. If dampers are applied in the ULS and thus help to guarantee the structural integrity, they should be very reliable. Especially for tuned mass dampers the required level of reliability is difficult to achieve, due to the following factors:

- Design uncertainties: A tuned mass damper only provides the calculated amount of damping if the damper is closely tuned to the eigenfrequencies of the building. Determination of the eigenfrequency during the design gives an estimation, but no exact prediction. In practice, the actual eigenfrequencies can deviate quite significantly, which may reduce the expected effectiveness of a TMD. Moreover, the eigenfrequencies can also be amplitude dependent, which results in the same issues.

- Time: The eigenfrequency of a structure might change over time, for example due to concrete cracking. Again, this could result in a 'detuned' damper, which is less effective (Aly 2012).

- ULS vs SLS: Most dampers are designed for SLS requirements. The properties of a structure like the eigenfrequency and stiffness can differ in ULS and SLS. From this it follows that if a damper is tuned to the SLS properties, it does not automatically mean that it is tuned to the ULS properties as well. Ignoring these differences could lead to unconservative results.

- Redundancy: If one element of a building fails, this may never result in failure of the whole structure. This also holds for a supplementary damping system. If only one TMD is applied, as is often the case,

a designer can not simply rely on the functioning of a damper for the structural integrity. Applying more than one TMD could overcome this problem, but will have an impact on various other design aspects like cost and space (Smith & Willford 2008).

- Maintenance: the design life time of a damper device does not necessarily have to be equal to the design life of the building in which it is applied. Damper devices must be maintained regularly, which is not desirable for a device that is important for the safety of the structure in ULS. This issue also holds for viscous damping devices.

In conclusion, it is not recommended to use a TMD as part of the ULS design. However, it is not impossible if a proper safety strategy is applied. The issues as described in the previous paragraph are specific for tuned mass dampers. In contrast, viscous and viscoelastic dampers, can be used in the ULS design. First of all, these damping systems are distributed over the structure and consist of multiple dampers, this increases the redundancy and hence the safety. Moreover, the working of these dampers is does not depend on the frequency of the load, they are simply part of the load path and will react with a damping force for every motion. Therefore design uncertainties are less significant. However, care should still be taken during design as the tolerances in construction can have a major effect and maintenance is still an issue.

The favourable effect of a TMD can only be taken into account for SLS load cases. In general for high-rise buildings the deformation or the acceleration criteria are the governing design factor (SLS), see Chapter 8. In theses cases, the application of a TMD can be beneficial, as the governing load cases may be reduced by the mitigating effect of the TMD. In situations for which the ULS load case is governing, the positive effects of a TMD can not be taken into account in the governing load case. In these situations it may be more effective to apply viscous or viscoelastic dampers.

5.4 Conclusions

- Tuned mass dampers, viscous fluid dampers and viscoelastic dampers are suitable to mitigate wind-induced dynamic response. All have their advantages and disadvantages.
- Neglecting the uncertainties that are inherited in the design of supplemental damping systems can result in unconservative outcomes and unexpected building responses.
- It is not recommended to apply a TMD as part of the ULS design, due to reliability concerns.
- For SLS load cases a TMD can be beneficial if the design is governed by the deformations or accelerations criteria.

Part II

Opportunities for dampers

Chapter 6

Dynamic parameter study

In this chapter the influence of the dynamic parameters, as introduced in Chapter 4, on the dynamic response is investigated by a parameter analysis. The design formulas from the Eurocode have been modelled with the help of a Python script to perform a parameter study on the parameters of interest like: mass, stiffness, height and damping ratio. The results of this part of this research will be used as a starting point to define a dynamically sensitive variant study model, which can be used in Chapter 7.

6.1 Parameter study

During this parameter study the different main dynamic properties have been varied one by one, to investigate the influence on the dynamic behaviour. The resulting charts show the sensitivity of each parameter according to the NEN-EN 1991-1-4 Eurocode (Eurocode 2005*b*). Procedure 2 (EC. annex C) is used to compute the along-wind accelerations. A Python script has been created to calculate these accelerations, this script is attached in Appendix E.

6.1.1 The model

A relatively slender building, comparable to the Baantoren, has been used as the starting point, to create a dynamically sensitive structure. This building has a square floor plan of 21m x 21m. The intrinsic damping ratio is set to 1%. The distributed mass is set to 100,000 kg/m, which can be considered as a relatively light-weight building. The assumed building properties in this parameter study will influence the quantitative outcomes of the study. This is not considered as a problem, Because the goal of this parameter study is to obtain insight in the qualitative relations rather than on the exact values.

The eigenfrequencies have been calculated by an adjusted form of the estimation equation from the Eurocode, Equation 4.3, as proposed by (Ellis & Bre 1980), namely: 46/height. Since the mass and the stiffness can not be taken into account in this formula, Equation had to be adjusted. Therefore the relations from Equation 4.4 are applied, to ensure that an increase of the stiffness by a factor 2 results in an increase of the eigenfrequency by a factor $\sqrt{2}$.

6.2 Along-wind versus across-wind accelerations

As mentioned in Chapter 3 both the along-wind and the across-wind accelerations are of importance for the design of a high-rise tower. It is interesting to check which of these two is governing for the design. Procedure 2 of the Eurocode has been used to calculate the along-wind response. The Eurocode does not provide a procedure to determine the across-wind response. Therefore, the formulas for the across-wind accelerations have been obtained from the Italian report (Advisory Committee on Technical Recommendations for Construction 2008). For buildings with a square floor plan, these equations are only valid if the slenderness ratio is lower than 6. For the 21m x 21m floor plan, this would mean that the results are valid for

a 120 meter tall tower. For higher buildings a more detailed analysis is required to obtain reliable results. Nevertheless, these formulas give some insight into the relation between the along-wind and across-wind accelerations. In Figure 6.1 the maximum accelerations in both directions have been plotted for varying building heights.

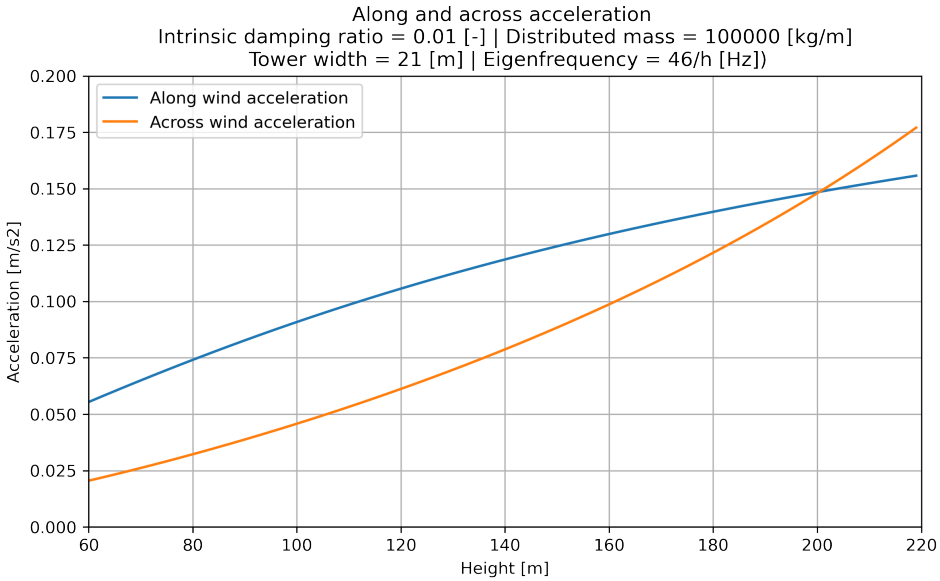

Figure 6.1: *Along-wind response versus across-wind response for dynamically sensitive buildings*

From this figure it can be determined that for medium high-rise buildings, the along-wind accelerations are clearly governing, while for higher high-rise the across-wind becomes governing. As discussed in Chapter 3 the across-wind will not be taken into account during this research. From this graph it can be concluded that neglecting the across-wind accelerations will not have too much influence on the results for buildings within the building scope, with a maximum of 150 meters. To be on the safe side regarding the maximum slenderness for the across-wind calculations, in the remaining part of this report a maximum height of 130 meters will be applied.

6.3 Dynamic parameters

In this section the influence of the dynamic parameters are investigated.

6.3.1 Building mass

Figure 6.2 visualises the effect of the building mass on the across-wind dynamic behaviour. The building mass is visualised by the distributed mass is in kg/m. As is described earlier in Chapter 4 all mass that contributes to the motion of the structure has to be considered in dynamic calculations, not only the structural mass. It can be observed that a negative relationship exists between the mass and along-wind accelerations: The higher the mass, the lower the along-wind acceleration. This means that very lightweight structures are more prone to wind-induced vibrations than heavy structures. This has to do with the differences in inertia. Regarding the dynamic response, a heavy concrete structure will response favourable in terms of acceleration compared to a slender steel structure or even a timber structure.

As mentioned in section 4.4, it is beneficial to reduce the storey height of a tower from a cost perspective. In addition, from the negative relationship between mass and accelerations, it can be understood that limiting the storey height of a building is beneficial for the dynamic behaviour as well. This is due to that fact that the floors of a building are the main contribution to the building mass. For buildings with a relatively low storey height, the distributed mass will thus be larger. Hence, the value of the accelerations for a building with a relatively low storey height will be less, compared to the same building with a larger storey height.

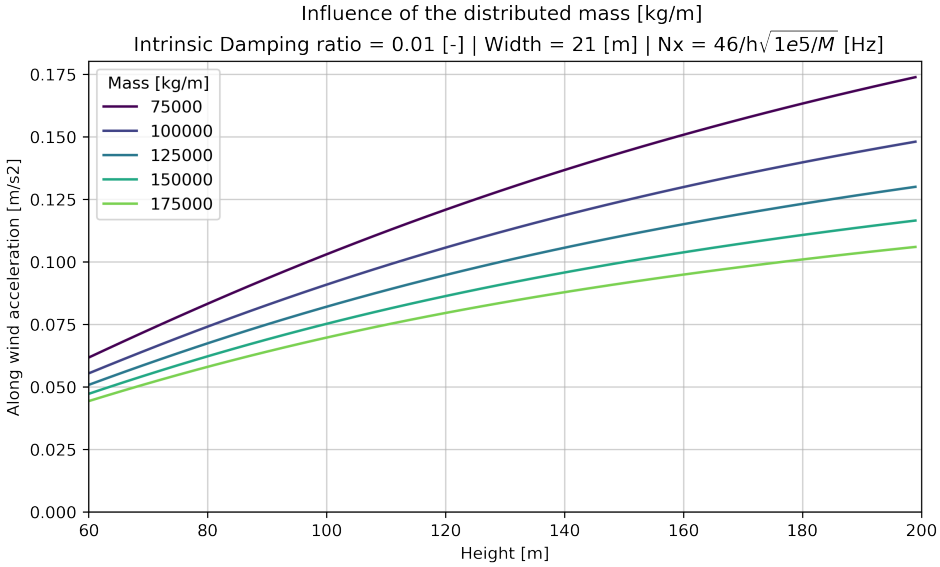

Figure 6.2: *Influence of the mass on the along-wind acceleration for varying height and eigenfrequency*

6.3.2 Stiffness and eigenfrequency

As described in Chapter 4 the (first modal) eigenfrequency of a structure plays an important role in the dynamic behaviour of a structure. The eigenfrequency depends on the height, mass, and stiffness of the structure. A different eigenfrequency results in different dynamic behaviour. From section 4.2.1 it is known that a positive relationship exists between the eigenfrequency and the stiffness: an increase in stiffness, results in an increase in the eigenfrequency. Therefore, the effect of the eigenfrequency has been investigated together with the stiffness, by varying the deflection limits. For this parameter study, the approximation of the eigenfrequency, 46/height, been altered to include the dependence on the stiffness. The deflection limit of 1/500 is considered as the starting point, for which 46/h holds. The fundamental eigenfrequency depends on the square root of the stiffness, see Equation 4.4. An increase of the stiffness to a deflection limit of 1/1000 hence results in an increase in the eigenfrequency with a factor $\sqrt{2}$. The effect of an increased in stiffness is visualised in Figure 6.3.

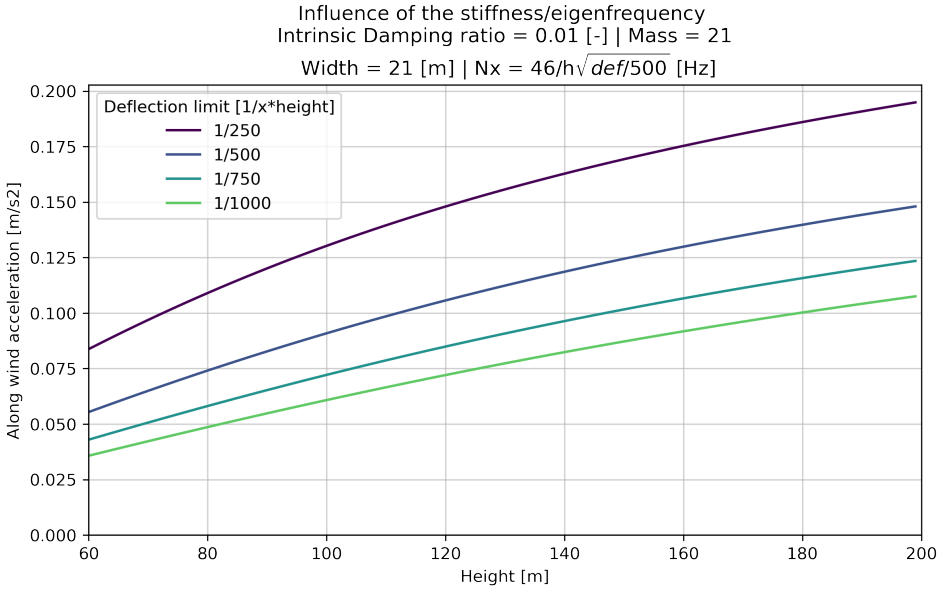

Figure 6.3: *Influence of the damping ratio on the along-wind accelerations for a varying height and eigenfrequency*

From this figure, a negative relationship can be observed:the higher the stiffness/eigenfrequency of a building, the lower the along-wind accelerations. A decrease in eigenfrequency is thus unfavourable for the dynamic behaviour of a structure. This is in line with the expectations from Figure 3.4, in which the frequencies of tall buildings were compared with the wind spectrum. Buildings with a relatively low stiffness can hence be considered as dynamically sensitive, which means that they are more prone to excessive acceleration .

6.3.3 Damping ratio

The influence of the damping ratio on the building response is investigated in Figure 6.4, by investigating the dynamic response for a range of damping ratios between 0.5% (0.005 [-]) and 5% (0.05 [-]). These ratios corresponds, respectively, to low intrinsic damping and a feasible amount of supplemental damping (Smith & Willford 2007).

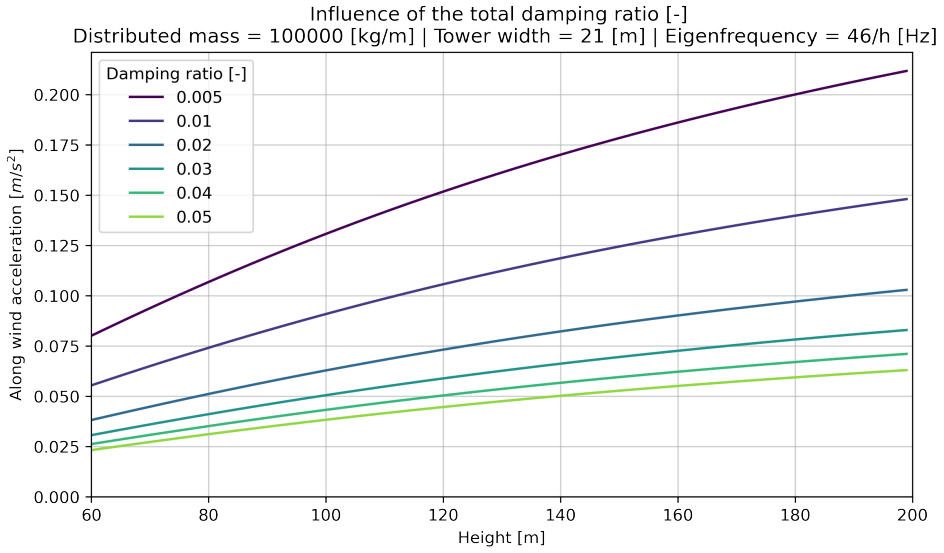

Figure 6.4: *Influence of the damping ratio on the along-wind accelerations for a varying height and eigenfrequency*

From Figure 6.4 it can be concluded that increasing the damping ratio reduces the maximum accelerations in the structure, as expected. Moreover, this graph clearly proofs that especially the first few percentages of an increase in the damping ratio are of importance. The increase of the damping ratio from a relatively low level is far more effective than increasing a damping ratio that is already relatively high. For a building of 120 meters, an increase in the damping ratio from 0.01 to 0.02 reduces the accelerations with 30%, while an increase from 0.04 to 0.05 only reduces the accelerations by 11%. From this it can be concluded that only a small increase in the damping ratio is already very effective, it is not very efficient to increase the damping ratio to values higher than 5%.

Moreover, it can be observed that the default assumed intrinsic damping ratio of 0.01 already has a significant effect on the along-wind accelerations, compared to a lower damping ratio of 0.005. With the uncertainties in design from Chapter 4 and 5 in mind, this is an important observation. From the large difference in response for the damping ratio of 0.005 and 0.01, it can be concluded that an overestimation of the intrinsic damping ratio can have significant effects on the actual dynamic building response.
As is described in chapter 4 the intrinsic damping ratio is a difficult parameter to determine. Moreover, the intrinsic damping ratios as advised in building codes are not necessarily conservative (Smith & Willford 2007). Caution on the determination of the damping ratio is hence advised, since an overestimation of the intrinsic damping ratio can have significant effects on the expected dynamic behaviour. From this point of view, the application of supplemental dampers can be beneficial. By installing dampers, the damping ratio can be determined with more certainty. In this way, the uncertainties in the building design are decreased. In addition, as mentioned, the scatter in the dynamic response is less for higher damping ratios. This means that an overestimation of the damping ratio has less impact on the response for higher damping ratios than for lower damping ratios. Therefore, by applying supplemental dampers, less conservatism is required during design, which can result in material and cost savings.

6.3.4 Building height

In the previous paragraphs, the dynamic parameters were plotted against an increasing building height. From these graphs, the relation between the maximum acceleration and the building height can be determined as well. From Equation it can be understand that an increase in building height results in a decrease in the eigenfrequency. From the relations in Figure 6.3 it can thus be concluded that a taller building becomes more sensitive to wind-induced accelerations. This is visible in the different graphs from Figure 6.2, 6.3, and 6.4.

However, it must be noted that these results should be interpreted with care, since the relation between height and accelerations is quite complex. This is because the building properties like mass and stiffness also depend on the height. Due to this dependence, opposite effects can occur by an increase of the height. For example: A taller building requires more structural mass, see Figure 4.3, which will have a favourable effect on the dynamic response.

6.4 Conclusions

- For building heights up to 150 meters and a floor plan of 21 x 21 meters, the risk of across-wind induced problems are relatively small. Therefore the scope of the research is limited to buildings with a height of 130 meter, to be on the safe side.
- An increase of mass results in a reduction of the dynamic response and in a reduction of the eigenfrequency.
- An increase of stiffness results in reduction of the dynamic response and in an increase of the eigenfrequency.
- An increase of height results in a reduction of the eigenfrequency. The relation with the dynamic response is complex, as a building's height influences the other dynamic properties. In general an increase in height will result in an increase of the dynamic response, but this not always the case.
- Only a small increase in the damping ratio is already very effective, it is not very efficient to increase the damping ratio to values higher than 5%.

Chapter 7

Set-up of the variant study model

To investigate the dynamic relations for different building properties and the relations between the different governing design factors, a variant study is performed. The objective of this variant study is to investigate the dynamic behaviour of all kinds of building variants. In this way it is possible to define ranges of parameters for which the application of supplemental damping could provide opportunities.

In this Chapter a Grasshopper model for the variant study is described. The definition of the case study building is described in Section 7.1. The results of this variant study are presented in Chapter 8. The definition of the Grasshopper model is described in Section 7.2. Relevant assumptions are explained in Section 7.3.

7.1 Definition of the building variants

With the results of the previous chapter, Chapter 6 and conclusions from the literature research, it is known which types of buildings can be considered as dynamically sensitive: low-damped, lightweight and flexible towers. These insights are applied in this section to define the properties for the case study building. The case study building should represent a dynamically sensitive building. This building has to represent a realistic building, which should be able to comply with all design criteria: strength, deflections, and accelerations. The design considerations for the variant study building are described in the following paragraphs.

7.1.1 Dimensions

The scope of this thesis is limited to residential buildings. To ensure that the model represents a feasible design, the building dimensions are based on the structure of the original Baantoren. It is assumed that the Baantoren floor plan results in an economical distribution of apartments that fulfills the additional requirements from section 4.4, like the day-light regulations. The dimensions of the floor plan are defined as 21m x 21m, see Figure 7.1b. The floor plan is symmetric to minimize the torsional acceleration effects, as explained in section 3.3.3.

The height of the building variants are varied between 60 meters and 130 meters. This results in slenderness ratios varying between 1/3 and 1/6. The storey height is set to 3.33 meters. This results in realistic building variants with heights that are a multiple of 10 meters. In an actual design, the storey height could be reduced slightly, up to a minimum of around 3.0 meters, see Appendix F.

The original design of the Baantoren contains one small core of only 7m x 7m. In the Baantoren design the core dimensions are governed by the function (elevators, staircases, apartment entrances, etc.), rather than by structural requirements. This implies that this building variant with a core of 7m x 7m, represents the variant with minimum core dimensions and hence the highest rentable floor ratio, since no additional useless core space is required from a structural perspective. In general structural cores can be larger in size, but as this report is about slender buildings, with an optimal use of floor area, the application of a minimum

core size in the model is considered desirable and interesting. To reduce the model complexity, the core dimensions are considered constant for all building heights.

7.1.2 Structural material

In Chapter 6 it is concluded that lightweight buildings are in general more sensitive to dynamic behaviour. Therefore, the choice of the structural material is an important factor in the dynamic behaviour of a building. In this variant study, steel is applied as the structural material. The application of steel results in a lightweight structure, which is interesting from a dynamic point of view. Moreover, designing more lightweight buildings by applying steel instead of concrete can be beneficial for the foundation design and construction time. Some considerations for the choice of structural material have been discussed in section 4.3. Timber could also have been an interesting material for this case study, but this would have increased the complexity of the research and the variant study. In general, the results of the performed variant study can be interpreted for concrete and timber as well, in a qualitative manner.

7.1.3 Stability system

Different stability systems have been discussed in chapter 4 and in Appendix A. From the described systems, a braced frame structure, an outrigger structure, a tube structure, and a megaframe structure could all be efficiently applied as stability systems for the considered slender steel building variants.

Although the tube structure system can be considered as a very efficient stability system, it is not ideal for the design of residential buildings due to the relatively closed facade. The same issue occurs with the large diagonals of a megaframe structure. Moreover, the design of a megaframe highly depends on the specific design requirement. It is hence not convenient to apply such a system in this parametric variable study.

Therefore, in this variant study, a braced frame structure is applied as the stability system, as defined in Figure 7.1. The facade of a braced core system is relatively open, which is an advantage for residential towers. In addition, this system is not very much dependent on specific design conditions. It is hence convenient to apply this systems in this more general oriented variant study. Moreover the braced core structure can be easily combined with an outrigger structure. This is beneficial for the higher range of building heights in this variant study. In these higher height ranges, an outrigger is applied to create an efficient stability system.

7.1.4 Loads and load factor

The following loads have been taken into account: Facade mass, Permanent floor loads, variable floor loads, structural mass, the second-order effect, and lateral wind loads.
The considered case study building is located in Dutch wind zone II (Rotterdam) in an urban area. The building is designed as a consequence class 3 building. Therefore, a permanent load factor of 1.32 and a variable load factor of 1.65 are applied.

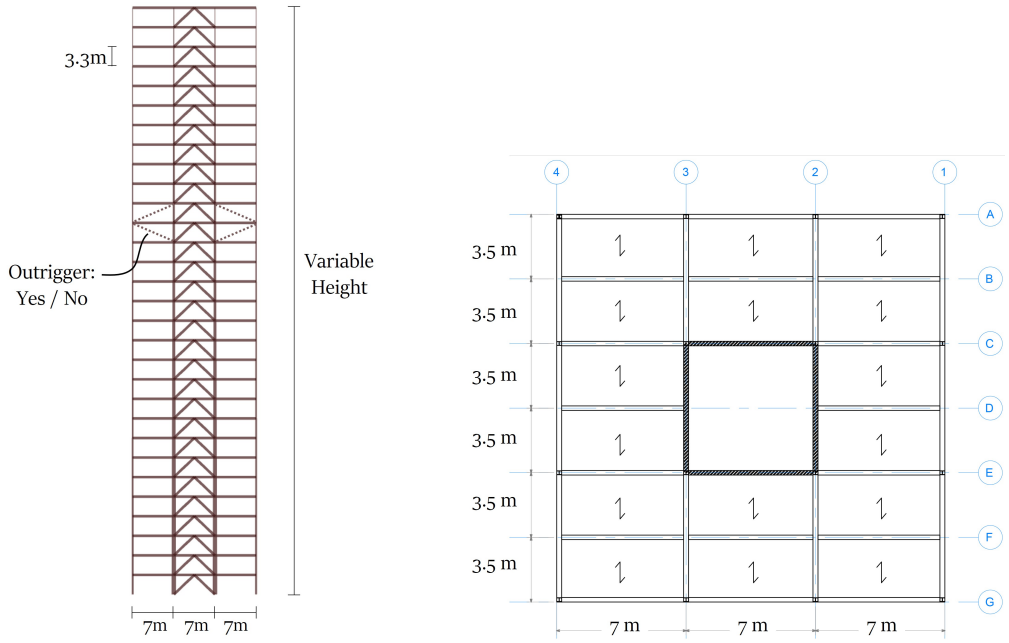

(a) *Stability system* (b) *Floor plan*

Figure 7.1: *Overview of the model geometry*

7.2 Definition of the Grasshopper model

The goal of the variant study is to investigate the dynamic behaviour of all kinds of building variants. As these variants can not all be modeled by hand, a parametric building model is developed to test all these building variants.

The parametric environment 'Grasshopper', a subprogram of Rhino 3D, has been used to generate a 2D parametric model. This parametric model has to contain the following components:

- Definition of the structural geometry, as defined in paragraph 7.1.3
- Definition of the horizontal and vertical design loads, as defined in paragraph 7.1.4.
- Generation of a realistic structure based on the ULS and SLS criteria, as defined in Chapter 2.
- Determination of the dynamic building properties and accelerations, as defined in Chapter 4.
- Automatic generation and calculations of the building variants, outputted in a readable data file.

The general workflow is described in Figure 7.2. In this model the Karamaba finite element tool is used to define the governing loads, calculate the dynamical building properties, and to generate realistic structural design options. In addition the Colibri plug-in has been used to automatically run the variant study. The output of this study is stored in a CSV output file. The data from this file is post-processed in Python by making use of the Pandas and Matplotlib libraries. In the following sections the model will be explaind in more detail, the Grasshopper will be on the Grasshopper model.

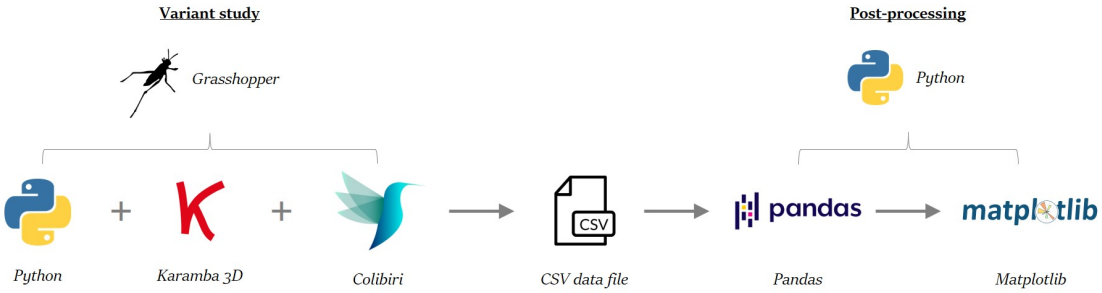

Figure 7.2: *Grasshopper model workflow*

7.2.1 Conceptual overview

An overview of the conceptual Grasshopper model is described in Figure 7.3. This figure illustrates the general set-up of the model in a schematic way. The three main parts will be discussed shortly in the following paragraphs: model generation, variant calculations, and model output.

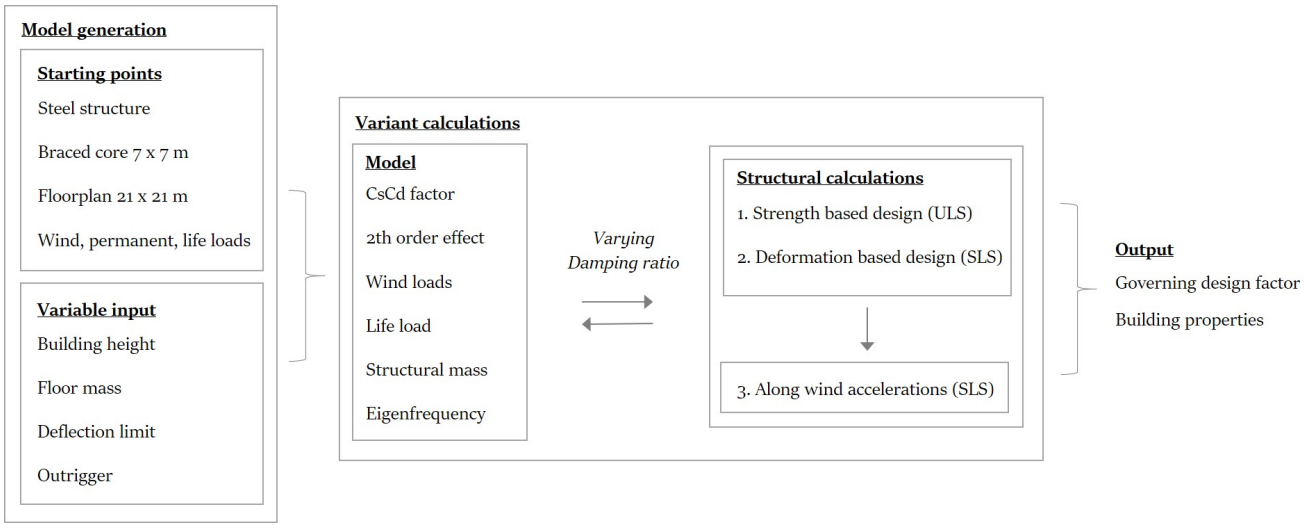

Figure 7.3: *Conceptual overview of the Grasshopper model*

7.2.1.1 Model generation

First, the parametric model and geometry of the case study building are generated. Therefore, the model requires both permanent input and variable input. The permanent input is defined by the case study building geometry (section 7.1.3) and the Eurocode design loads. The variable input describes the different building variants and can be considered as the basis of the variant study. The following properties are varied and studied during the analysis:

- Building height: 60 m - 130 m
- Floor mass: 300 kg/m^2 - 1000 kg/m^2
- Deflection limit: 1/200 - 1/800 of the building height
- Outrigger at 60% of the height: yes/no
- Damping ratio: 0.01 (intrinsic) - 0.05 (supplemental)

The floor mass represents a variation of the building mass. The Deflection limit represents a variation of the building stiffness.

7.2.1.2 Variant calculations

First, the gathered input is used to determine and calculate the design loads and several building properties like the self-weight and the eigenfrequency of a building variant. In this part the dynamic CsCd factor, the second order effect and the load factors are determined. Together with the generated geometry from paragraph 7.2.1.1, this data is used as input for the main calculations.

The core of the model is the part in which the structural properties of each variant are calculated. For these computations, the Grasshopper Karamba finite element plug-in is used, as illustrated in the workflow of Figure 7.2. With this tool, the determined geometry and loads are converted into a parametric finite element model. For this research, it is important that both structural system based on ULS and SLS are investigated, to determine which design criteria is governing. Since more than 6500 building variants have to be generated, it is not possible to determine the structural design properties of each variant separately by hand. Therefore, this process is automated with the Karamba structural opitimisation tool.

Karamba structural optimisation tool

The karamba optimisation tool contains an option that is able to automatically generate realistic and efficient structural systems for predefined input geometry and load cases. The defined structural geometry and load cases, as described in section 7.1, are used as input for this model. Figure 7.4 describes the workflow of this structural generation tool. This workflow is explained in the following paragraphs.

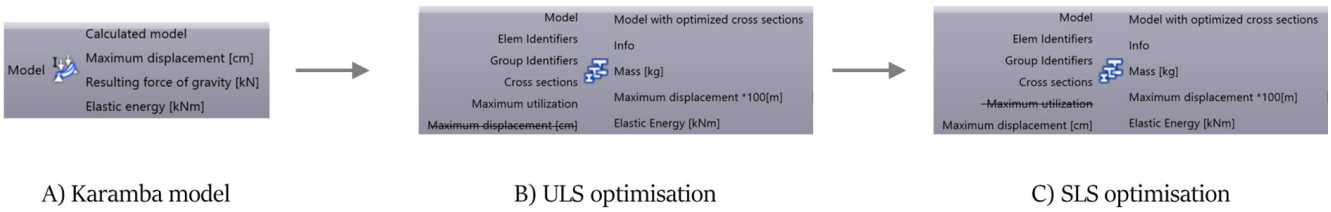

A) Karamba model B) ULS optimisation C) SLS optimisation

Figure 7.4: *Karamba optimisation workflow*

A) First, the defined geometry and the relevant load cases are converted to a finite element model.

B) Second, a design based on the strength requirements is generated. Therefore, an ULS optimisation run is performed. This optimisation run tries to find the minimum required steel members for the ULS load cases, in such a way that all the strength requirements are fulfilled. The output of this optimisation is a structure in which all element stresses are within the design limits, this structure hence fulfils the ULS requirements. The ULS stresses are determined for several load cases: wind from the left side, wind from the right side. Both have been calculated with and without including the vertical column loads. The steel members are chosen in such a way that the stress limits are fulfilled for all these load cases.
The maximum unity check in the ULS model is set to 0.80 instead of 1.0. This is necessary as not all structural aspects are modelled explicitly, like buckling. In this way some margin is included. This gives the model some redundancy, see Chapter D.

C) The output structure of the ULS optimisation fulfils the strength requirements, but does not necessarily fulfill the deflection limits yet. Therefore, in this last step a design based on the deformation requirements

is generated. These deformation limits are part of the research, and are defined as one of the varying input parameters. The steel column members of the ULS design are altered until the deformation requirements are met. In this structural optimisation process only the steel columns are included. The braces and outrigger members are defined prior to the optimisation process and are considered as constant cross sections. If for a certain variant the ULS design turns out to fulfill the deflection limits, this means that this variant is governed by the strength criteria. In this case the SLS optimisation step is skipped.

With this Karamaba optimisation tool, for each building variant a structural system that fulfills the design requirements is developed based on strength and deflections. From this analysis it can be determined which of the design criteria is governing. In addition, for all these variants, dynamic analyses are performed. The first eigenfrequency, modal shape and modal mass are determined by the Karamba 'Natural vibrations' tool. Moreover, the maximum along-wind accelerations are determined for each variant with the help of a developed python script, based on the Eurocode procedure, see Appendix E.

As mentioned, the total damping ratio of the building variants is varied as well. For each calculated building variant, with a certain damping ratio, the calculated accelerations can be compared to the maximum allowed accelerations. With this knowledge, it is possible to determine the minimum required total damping ratio that is needed to fulfill the acceleration requirements. In the end, with this Grasshopper model it can be determined which of the three main design criteria: strength, deflection, and damping is governing for each of the building variants.

7.2.1.3 Model output

As explained, the Grasshopper model is able to calculate a large number of building variants. The actual variant study is performed by the Colibri plug-in that is able to automatically run all building variants. All the output data from this analysis is stored in a CSV data file. Table 7.1 summarises the input and output parameters. This data is post-processed in Chapter 7 with the help of a Python script. This Python script is developed to analyse and interpret the generated results, as explained in the workflow of Figure 7.2.

Table 7.1: *Input and output parameters of the Grasshopper model*

Varying input parameter	**Output parameter result**
Amount of floors, Height	Governing design situation
Floor system mass	ULS structural mass
Damping ratio	SLS structural mass
Floor system mass	Total building mass
Outrigger yes/no	Maximum deformation
	Deformation unity check
	Inter storey drift
	Top floor acceleration
	Acceleration Unity check
	Maximum cross section
	Fundamental modal shape
	Fundamental modal eigenfrequency
	Fundamental modal mass
	CsCd factor ULS
	CsCd factor SLS
	Second-order effect factor ULS
	Second-order effect factor SLS

7.2.2 Detailed model overview

An overview of the full Grasshopper model is shown in Figure 7.5. To allow for a better understanding of the model, the components with a common function are grouped and labeled. The function of each component is described shortly in this paragraph. The model and its assumptions are described in more detail in Appendix D.

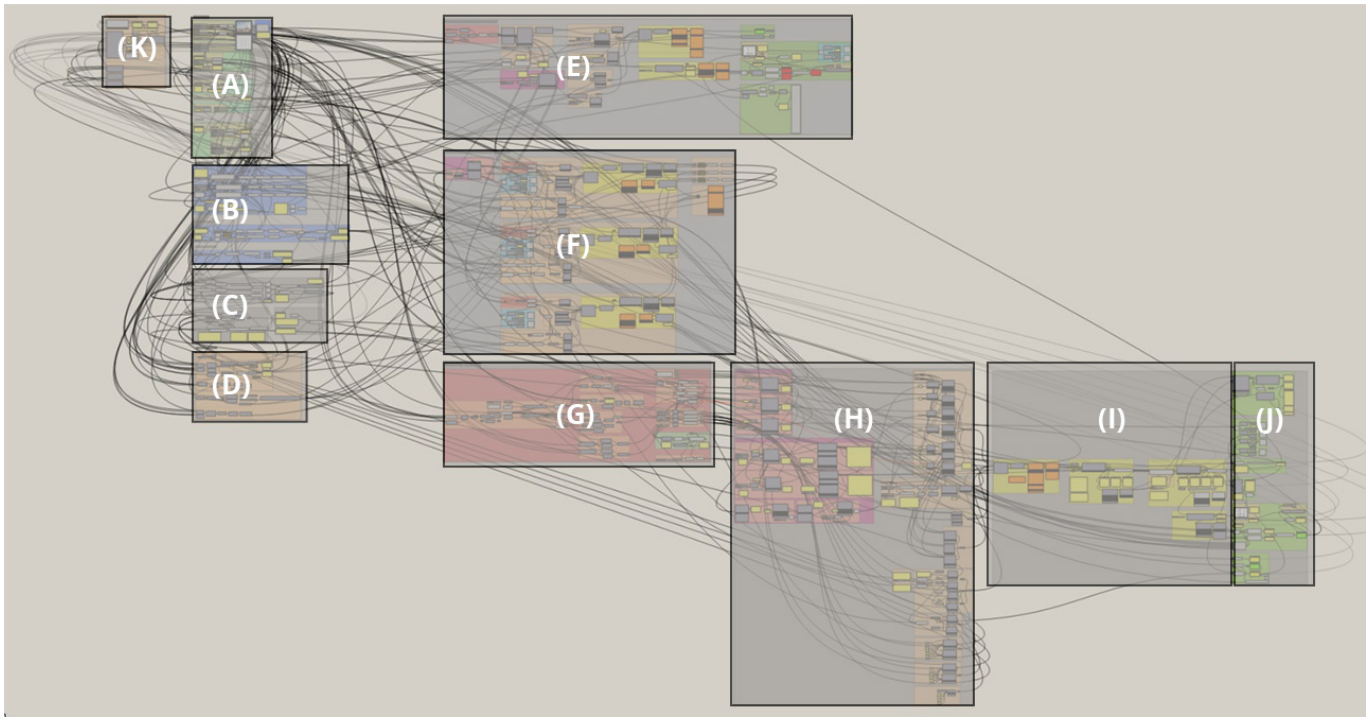

Figure 7.5: *Grasshopper model overview*

The following components are part of the Grasshopper model. Each label corresponds to a group from Figure 7.5.

A. Define model geometry.

B. Define input parameters of each variant.

C. Define and determine the design loads (ULS and SLS).

D. Visualisation of the model.

E. Simple beam model to estimate the eigenfrequency, as required for the CsCd calculation.

F. Karamba column cross section definition.

G. Full building model geometry definition.

H. Karamba finite element model definition.

I. Karamba Finite element calculations, as defined in section 7.2.1.2. ULS and SLS variants.

J. Calculation of the maximum accelerations and other output.

K. Colibri variant study iterator.

7.3 Main model assumptions and points of interest

This section describes the most important assumptions inherited in the Grasshopper model.

7.3.1 Along-wind accelerations

The maximum acceleration is determined by a Python script that calculates the along-wind acceleration. Eurocode Procedure 2 as described in appendix C is applied to calculate the maximum 1 year acceleration, as described in 4. The Python script is attached in Appendix E.

The calculated acceleration only takes into the contribution of the along-wind acceleration. The across wind and torsional accelerations are neglected to reduce complexity. As explained in Chapter 3.3.2 it is difficult to model across-wind effects in an accurate manner, therefore wind tunnel research would be needed. Including the torsional accelerations would require a 3D model to determine the 3D torsion effect, which would disproportionately increase the models complexity. It is expected that the exclusion of these types of accelerations is an acceptable assumption, since the case study building geometry has been defined in such a way that it is not very sensitive to across-wind and torsional responses, see Section 7.1. Since the calculated accelerations only represent the along-wind responses, the determined accelerations will be an underestimation of the actual accelerations.

7.3.2 Damping ratio

The damping ratio as included in the analyses represents the full damping ratio, as described in Chapter 4.2.4. This full damping ratio is composed of the intrinsic damping (δ_s), aerodynamic damping (δ_a), and the supplementary damping (δ_d). It is assumed that the intrinsic damping ratio and the aerodynamic damping ratio together generate a damping ratio of 0.010, which is present as initial damping ratio for all building variants. For building variants with higher damping ratios than 0.01, the difference has to be generated by the application of supplemental dampers. It is expected that the initial damping ratio of 0.01 would prove to be conservative for most towers, based on research (Eurocode 2005*b*) and (Gomez 2019), see Chapter 4.2.4.

7.3.3 CsCd factor

The structural factor CsCd factor takes into account the dynamic amplification factor for the equivalent static wind loads, as described in Chapter 3. The ULS and SLS lateral wind loads are both multiplied by this factor, to take into account the fluctuating wind response. As explained in Chapter 5, the ULS and SLS CsCd factor do not necessarily have to be of the same value, as the contribution of a TMD may only be taken into account for the SLS factor.

A complicating factor in the inclusion of the CsCd factor in the Grasshopper model is the fact that the computation of this factor requires an iterative calculation. The value of the factor namely depends on the eigenfrequency, which depends on the mass and stiffness of the structure. These properties, in return, depends on the CsCd factor, because this factor partly determines the design loads. To limit the computation time it is not possible to use a fully iterative model. It is therefore necessary to make realistic assumptions for the eigenfrequency, before the CsCd factor can be calculated. For this purpose, a simple Euler beam model has been modeled in the Grasshopper model, section E in Figure 7.5. This beam model inherits a close assumption of the building mass and stiffness, based on the allowed deflection limit. This estimated eigenfrequency of the beam model is subsequently applied in the calculation of the actual CsCd factor. In this way, a computationally heavy iterative calculation is prevented, which saves time.

7.3.4 Second-order effect

Contributions from the second-order effect can have an impact on the loads of high-rise buildings. Especially for flexible buildings, with relative high top displacements, the impact of the second order effect can be significant. Normally, this factor can be assumed being 1.2 in the preliminary design. However, as this variant study also investigates buildings with very large deformations, like 1/200, a more precise calculation of the second order effect has to be included. The second order effect is taken into account by an amplification factor, based on the Eurocode procedure for steel structures. This includes contributions from variable and initial deflections. Just as the CsCd factor, the second order effect is an iterative factor, the same beam model is used to simplify these calculations.

7.3.5 Foundation

The influence of the foundation on the maximum accelerations and deflections is significant. However, it is very complex to accurately parameterize the foundation of a high-rise tower. A lot of different factors play a role in the design of a high-rise foundations. First of all the soil profile is highly variable, even for close distanced locations. Moreover, the building mass, the building height, the foundation pile types, and the possible need for tension piles heavily influence the foundation design. Due to all these uncertainties it would be hard to develop a parametric script for the foundation of this variant study. Moreover, Taking all these different aspects into account to define a parametric foundation would heavily increase the amount of parameters for the overall model, which would increases the model complexity. As a consequence, insight in the overall results could get lost by parametrizing the foundation, which would have a negative effect on the interpretation of the results in this research.
Therefore, it is decided to model the foundation as being clamped. On the one hand, this exclusion of the foundation will result in an overestimation of the eigenfrequency and hence in an underestimation of the accelerations. On the other hand, if the foundation would be considered as a rotation spring, the generated building variants would require more mass and stiffness, to fulfill the defined deflection limits, this would

reduce the accelerations. Further research is advised to investigate the effects of the soil structure interaction on the dynamic behaviour.

7.3.6 Mass determination

As explained in Chapter 4, to determine the dynamic behaviour of a building, it is necessary to determine the total mass of the building: the dynamic mass. This mass consists of two components: building mass (floor, facade, structure) and a contribution of the life load. To calculate the dynamic mass, all the masses without safety factors have been applied, as the acceleration criteria are a SLS requirement.
Regarding dynamic behaviour, it would be unconservative the take into account the full life load mass, since a high mass is beneficial to reduce accelerations, see Chapter 6. Therefore, not the full mass as induced by the life load may be considered. In general 10% to 20% of the quasi permanent load is taken into account for the calculation of residential floor vibrations (European Commission. Joint Research Centre. Institute for the Protection and the Security of the Citizen 2009). Therefore, in this Grasshopper model an average value of 15% of the life loads has been considered as part of the dynamic mass. To account for other unknown masses (elevators, sprinker installations, etc.) the total mass has been increased by 5%.

7.3.7 Buckling

Buckling phenomena reduce the maximum allowed compression forces in structural beams and columns. The determination of the buckling properties, especially the buckling lengths, of steel members is considered as too detailed for this general variant study. In the considered variants column buckling is not expected to be a very significant factor, as the maximum storey height is only 3.3 meters. Therefore, it is considered acceptable to ignore the buckling behaviour in this Grasshopper model. Nevertheless, to add some redundancy in the model, the maximum unity check regarding stresses has been reduced to 0.80.

7.3.8 Applied cross sections

All the elements in the braced frame model are hinged connections, which implies that the model functions as a truss. No bending moments will thus occur in the beam elements. Moreover, as mentioned, the effects of buckling are not taken into account the model.
This simplification allows for a cross section optimisation on normal forces only, in which each member should only be able to handle the occurring tensions and compression stresses. Whether or not a member can handle a certain force, solely depends on the cross sectional area of the element in this case. Therefore, in the Grasshopper model no regular steel profiles have to be implemented, the definition of just the required structural area of an element is enough. This approach makes sense, as for tall towers custom made steel profiles are no exception. Therefore, the assumption in which only cross sectional area is used as a variable, comes in handy as it excludes the cross sectional profile as a variable.

7.3.9 Outrigger

For the variants in which an outrigger is applied, this outrigger is installed at 60% of the building height, see Figure 7.1. This location has been determined based on literature (Ham & Terwel 2017) and by a trial-and-error analysis of different outrigger heights. The applied outrigger spans two floors in height, see Figure 7.1.

7.3.10 Floors

The floor slabs of the variants are not explicitly modeled. Their contribution on the behaviour of the variants is taken into account by the parameter of the floor mass. The floor mass is varied in a range between 300 kg/m2 and 1000 kg/m2. This range respectively corresponds to the values of a lightweight CLT floor and to a heavy concrete floor. This is shown in Appendix F.

Chapter 8

Results: Governing design criteria

With the Grasshopper model as defined in Chapter 7, different building variants have been modelled and varied. With the data from this analysis the dynamic behaviour can be determined, for each building variant in the scope of this research. For each of these more than 6500 building variants it can be determined which of the design criteria is governing (strength, deflections, accelerations) and which building thus would benefit from additional damping.

As the data set of the analysis is large, it is important to visualise the data in a clear way. For this purpose, governing-design-criteria charts have been generated. These charts visualise the relations between the different dynamic parameters, show which of the design criteria is governing, and visualise the required target damping ratios. With this information it is possible to investigate for which combinations of building parameters, the application of supplemental dampers can provide opportunities. Furthermore, it can be determined how much damping is required to mitigate the wind-induced motions.

In the following sections these generated governing-design charts will be used to investigate and interpret the dynamic behaviour of different types of buildings. Firstly the concept of the governing-design-criteria charts will be explained in Section 8.1. In the reaming part of this chapter interesting results are discussed and opportunities for supplemental dampers are defined.

8.1 Introduction to the Governing-design-criteria charts

The purpose of the generated Governing-design-criteria charts is to visualise which of the three main design criteria: strength, deflection, and acceleration, is governing for a certain combination of relevant building parameters. The varied parameters are: floor mass, deflection limit, building height, and the stability system. As the design space of the variant study is a 4D space, in every chart some parameters are kept constant to allow for a 2D visualisation.

An example of a governing-design-criteria chart is added in Figure 8.1. In this figure the building height is fixed at 100 meter and a braced core system without outrigger is applied. The influence of the floor mass and the deflection limits on the governing design criteria is studied. The variation of the floor mass and the deflection limit can respectively be considered as a variation of the building mass and the building stiffness. In the next section, the legend of this chart is explained.

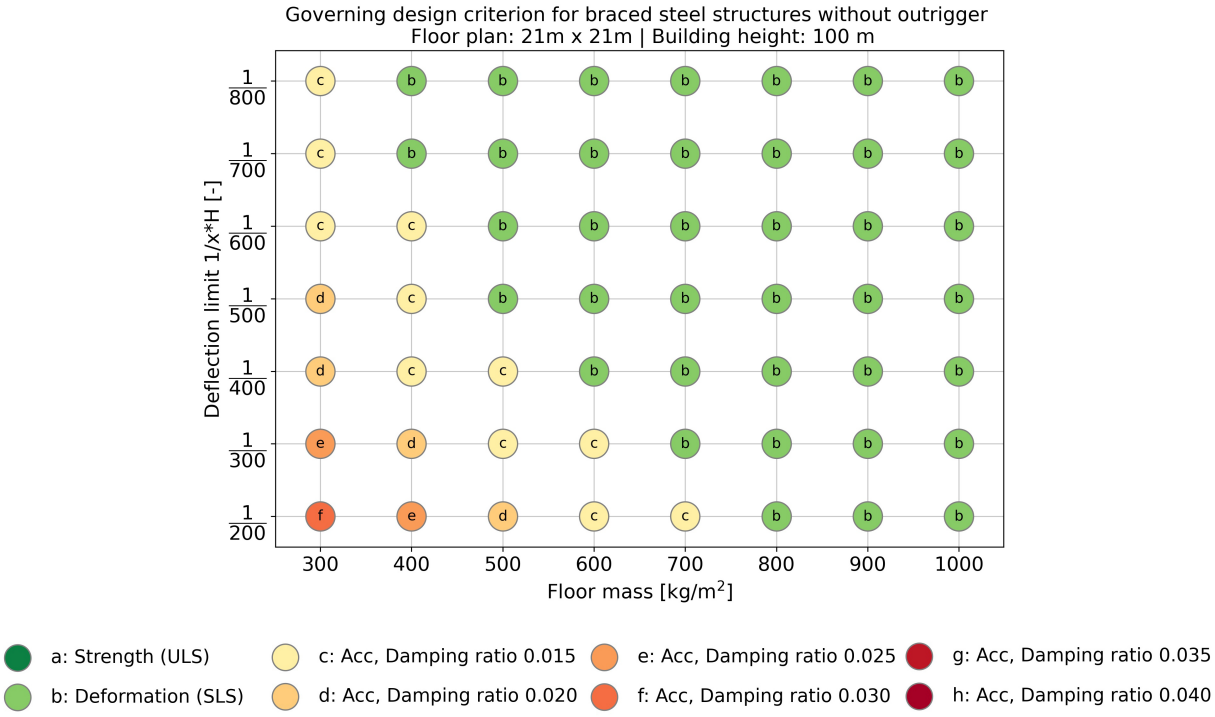

Figure 8.1: *Overview of the governing-design-criteria for buildings with a height of 100 meter.*

8.1.1 Explanation of the governing-design-criteria charts

Throughout this chapter, different governing-design-criteria graphs will be discussed. These graphs visualise the relations between strength governed, deformation governed, or acceleration governed design situations, as introduced in Chapter 2. These terms are described in the legends of the graphs. Because these terms are essential for the understanding of the concept of the governing-design-criteria charts, they are shortly introduced here:

- **Strength governing:** If the building design is governed by strength criteria this means that all the material in the building design is required to create a save building. Such a tower is designed to withstand the ultimate limit state load cases. The deflection and the comfort requirements are in the case of strength governed design automatically fulfilled: the strength-based design inherits already enough stiffness and inertia to meet these requirements and hence overrules the other requirements. For variants in which the strength is governing, the actual deflections are thus smaller than the deflection requirements, as presented on the y-axis of the chart.

- **Deformations governing:** If the building design is governed by the deformation criteria, this means that the lateral stiffness is the limiting factor in the structural design. This means the ULS design, based on strength, requires additional material to meet the deflection criteria as well. The final design thus must be stiffer than would be strictly necessary from a safety point of view.

- **Accelerations governing:** The last possibility is that the structural design is governed by the acceleration comfort criteria. If that is the case, the design based on strength or deflections criteria requires additional measures to limit the maximum accelerations, like an increase of mass, stiffness or damping.

To obtain the governing-design graphs, first the strength and deformation governed designs were determined for each variant, as described in Chapter 7. Subsequently, the maximum accelerations were determined for these building variants, based on the Eurocode calculation procedure and an intrinsic damping ratio of 1.0%. The total minimum required amount of damping ratio is visualised by the color of the scatter plot dots. If the required minimum damping ratio is higher than 1% this means that the initial damping ratio must be increased, which means that supplementary damping is required. For the other cases, in which strength and deformations are governing, the intrinsic damping ratio is enough to limit the building accelerations. If according to Figure 8.1 a variant requires a damping ratio of 0.030, this hence means that the acceleration limits are only met for this variant if a total damping ratio (inherited + aerodynamic + supplementary) of minimally 3.0% is reached.

8.1.2 Application of the governing-design-criteria charts

The governing-design charts, like Figure 8.1, are not only useful to investigate the relations between the different dynamic design parameters. They can be used by structural engineers in an early design phase of the structural design of a high-rise building. The charts offer insights into the governing design criteria and help to visualise the effects of possible design strategies. In this way, the impact of design choices can be easily understood. The application of the charts is explained in this section with two possible design examples, these are visualised in Figure 8.2. In addition, the total building mass and structural mass are visualised in Figure 8.3.

(a) **Design with a damper, Figure 8.2a:** The circled dot represents a designed building configuration that turns out to be sensitive to high accelerations. From the figure different design strategies can be extracted, which are represented by the arrows. Firstly, it can be observed that by the application of supplemental dampers it is possible to realise the design. A target damping ratio of 0.02 would reduce the accelerations to an acceptable level. Secondly, if the application of supplemental dampers is not desired, accelerations can also be reduced by adjusting the building configuration. An increase of mass and/or stiffness can ensure that the design meets the acceleration requirements. The benefits of the different strategies have to be considered for each case individually. The impact of these design choices on the material use and building mass can be understand from Figure 8.3.

(b) **Adjusting the building configuration, Figure 8.2b:** In this example case two building variants are shown. It can be observed that both configurations are governed by deformations, accelerations turn out not to be an issue. In addition, from this governing-design-chart it can be observed that there exists some redundancy in the design. The floor mass and stiffness can be decreased to some extent without introducing dynamic issues. This information can help engineers to make informed design decisions and identify design opportunities.

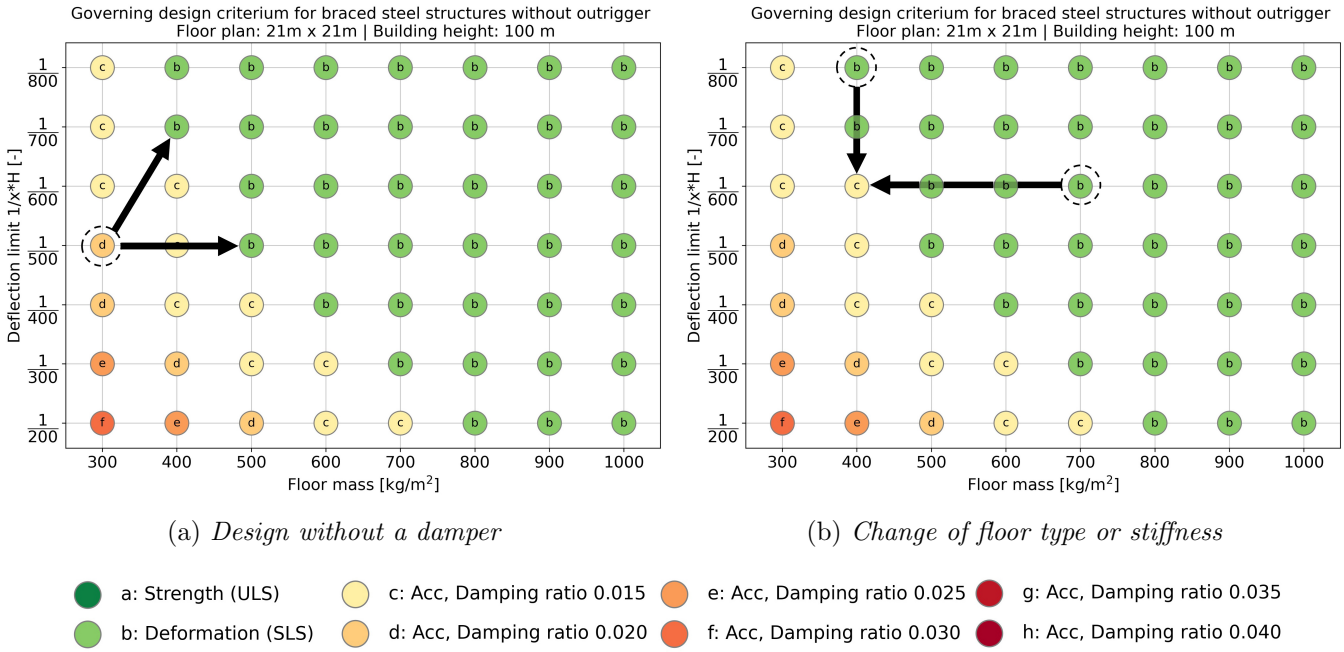

(a) *Design without a damper* (b) *Change of floor type or stiffness*

Figure 8.2: *Application of the governing-design-criteria for different building heights and deflection limits*

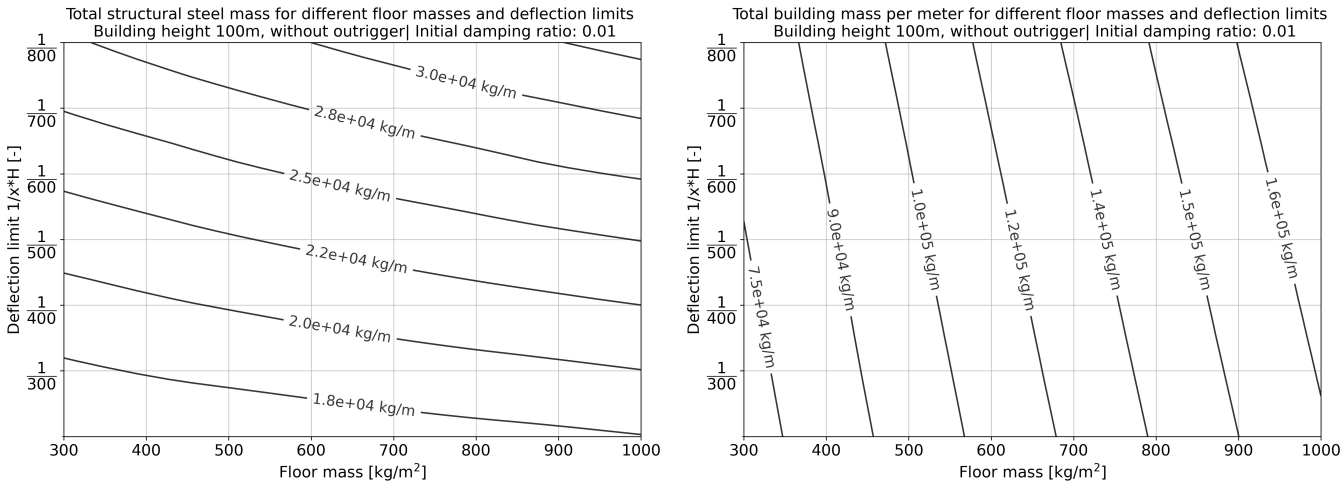

(a) *Total structural steel mass* (b) *Total building mass*

Figure 8.3: *Mass distribution for building configurations of 100 meter*

8.2 Governing design-criteria-charts for a constant height

In this section, governing-design charts with a fixed building height are discussed. It makes sense to use the building height as a starting point, as in general the building height is determined in an early design phase by the client and architect. The floor mass and the deflection limit can be influenced by the structural engineer and are thus of interest for the design charts. In this section, the focus is on buildings with a height of 100 meters, see again Figure 8.1. The governing-design charts for buildings with different other heights are attached in Appendix G.

8.2.1 Insights in the dynamic parameters

From Figure 8.1 the same relations as already have been discussed earlier in Chapter 6 become clear: for lightweight, flexible building variants the acceleration requirements become governing in the structural design. This can be observed in the lower left corner of Figure 8.1.

To determine and understand the relations between the dynamic behaviour and the building properties, it is of importance to obtain insight into the relevant dynamic parameters that influence the wind-induced building behaviour: the first eigenfrequency and the total building mass. Insight in these parameters will help to interpreter the governing-design-criteria graph from the previous paragraph, Figure 8.1. The distribution of the total building mass and the resulting eigenfrequencies are illustrated for different building variants in Figure 8.4a. The relations between these different parameters, as illustrated in Figure 8.4a determine to a large extend the resulting along-wind accelerations. These accelerations are visualised in Figure 8.4b. The unity check of 1.0 represents the boundary for which the Dutch comfort requirements are just met. This unity check is visualised by the dashed line in Figure 8.4b as a reference. The variants on the left side of this line do not fulfill the acceleration requirements, which means that the accelerations are too high.

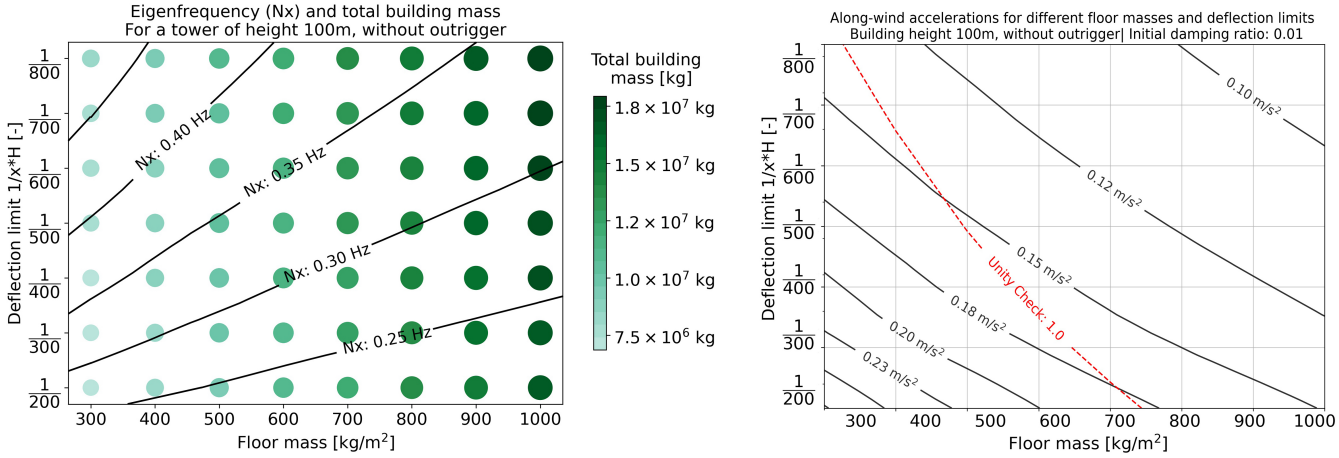

(a) *Dynamic parameters*

(b) *along-wind accelerations*

Figure 8.4: *a): Eigenfrequency Nx and total building mass. b): Resulting along-wind accelerations. For different floor masses and deflection limits for a tower of 100m. The size of the dots is linearly related to the total building mass.*

An interesting thing that can be observed from Figure 8.4a is the relationship between the deflection limit, the floor mass and the eigenfrequency. The same relations as from Chapter 6 can be observed: The higher the mass, the lower the eigenfrequency. and the stricter the deflection limit, the higher the eigenfrequency. The eigenfrequency appears to have a linear relationship with the mass and stiffness.
From Subfigure 8.4b the influence of the parameters mass, stiffness, and eigenfrequency on the along-wind accelerations can be determined. From the contour lines it is clearly observable that the highest acceleration occurs for building variants with a combination of a lenient deflection limit and light-weight floors. With the assumptions in this research, accelerations become governing for buildings with a deflection limit lower than 1/600 and a floor mass lower than 600 kg/m^2. For stiff and heavy buildings, the accelerations are relatively low and do not play a role in the design. An increase of the floor mass, or an increase of the stiffness both turn out to be effective measures in the reduction of the maximum acceleration.

An interesting part of Subfigure 8.4 is the line that represents the unity of 1.0. It is clear that the unity check is not directly related to one of the contour lines, since the unity check line intersects the different contour lines. This behaviour can be explained by the fact that the acceleration requirements depend on the structural eigenfrequency: the lower the eigenfrequency, the stricter the comfort requirements, as explained in chapter 2.

This concept can be illustrated by taking a closer look at two building variants in Figure 8.4. Building variant 1 represents a building with a floor mass of 400 kg/m2 and a deflection limit of 1/600. Building variant 2 represents a building with a floor mass of 800 kg/m2 and a deflection limit of 1/300. From the contour lines in Figure 8.4b it can be observed that both variants will experience the same along-wind acceleration of around 0.15 $m/s2$. Nevertheless, for building variant 1 this acceleration exceeds the comfort requirements, while variant 2 meets the requirements. This difference is caused by the difference in eigenfrequency for both variants, which can be determined from Figure 8.4a.

8.2.2 Influence of the building height

In the previous paragraphs Figure 8.1, the governing-design-factor chart for a building with a fixed height of 100 meters, was discussed. It is interesting to understand how the dynamic relations change for variants with different building heights. The governing-design-criteria in relation to the different building heights will be discussed in this section by having a look at the extreme values of this variant study: 60 meter and 130 meter. The governing-design-criteria graphs for all considered building heights (60, 70, 80, 90, 100, 110, 120, 130 meter) can be found in Appendix G. Figure 8.5 shows the governing-design-factor charts for a building height of 60 meters and 130 meters. In the next paragraphs, an analysis on the transitions between the acceleration governed zone, the deflection governed zone and the strength governed zone will be provided.

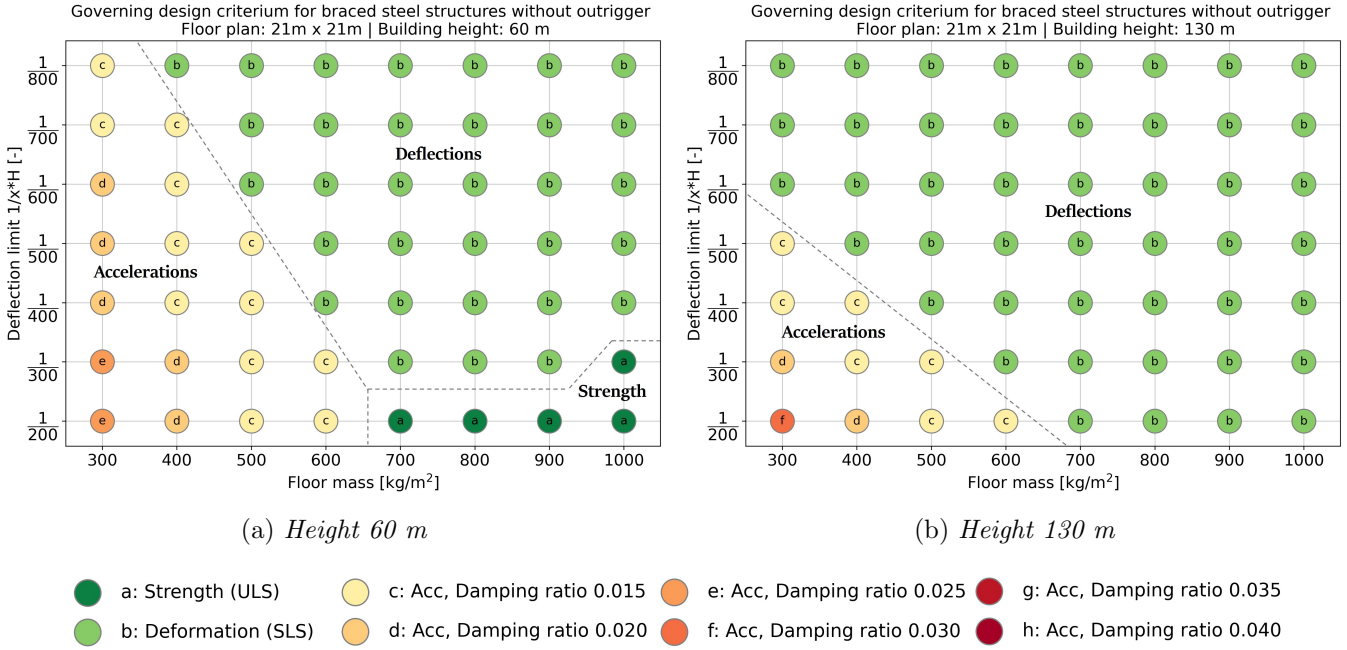

(a) *Height 60 m*

(b) *Height 130 m*

Figure 8.5: *Governing-design-criteria for a height of 60 meter and 130 meter.*

8.2.2.1 Deformation and acceleration governed zone

A few interesting things can be observed from the charts in Figure 8.5. A first general conclusion is the that the overall relation for different building heights in general remains the same: lightweight, flexible buildings require some additional damping, since the accelerations become governing. The overall behaviour does not change.

Now a more detailed look is taken to the buildings to buildings with different heights, a shift of the transistion results in some interesting observations. The imaginary transition line from deformation-governed design to accelerations-governed designs moves upward and downwards relative to the left corner for different building heights. This shift has been visualised in Figure 8.6. With an increase in building height to 130 meters, the acceleration-governed zone becomes smaller. For a decrease in building height to 60 meters, the acceleration-governed zone becomes larger. This observation may feel counter-intuitive, but is explained in section 8.2.2.3.

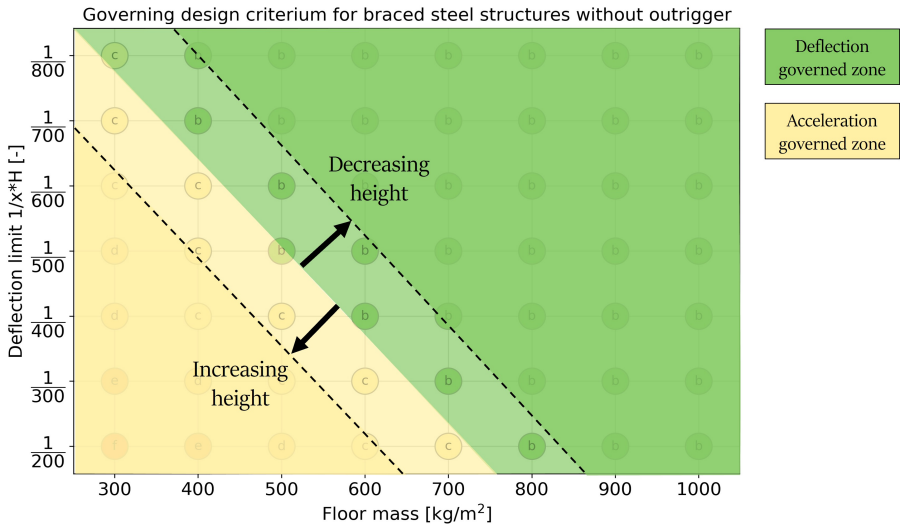

Figure 8.6: *Shift of the deformation-governed and acceleration-governed zones for a change in building height.*

8.2.2.2 Strength governed zone

In Figure 8.5a a strength governed zone is present. In this zone the strength design is the governing design criterion. Such a zone occurs for buildings with a relativity small height. For smaller buildings, lateral deflections play a less significant role in the design than for taller buildings. This is due to the fact that deflections are related to the height with a power of 4 (Hoenderkamp 2011). Therefore, for smaller buildings the strength requirements can be governing, while for tall buildings the deflection requirements are often governing.

An interesting point in Figure 8.5a is the fact that for higher floor masses, the strength design seems to become governing over the stiffness design. Compare for example, the building variants with a floor mass of 700 and 1000 kg/m^2, with a deflection limit of 1/300. For the former, the deformations are governing, while for the latter, the strength criterion is governing. This difference may seem counter-intuitive, as a higher floor mass should not directly influence the design of the stability system. The explanation of this difference in these governing-design criteria is two-fold: First of all, for higher floor loads, the vertical columns need to be stronger, because the normal forces in these columns increase. Due to this effect, the strength-governed

stability system will be stiffer for buildings with greater floor masses, which means that the chance increases that the ULS design meets the deformation requirements. Second, this effect can be explained by the inclusion of the second order effect in the model, which is an ULS factor. Since the vertical resulting force becomes larger, due to the higher floor loads for higher floor masses, the second-order factor is increased. As a result, the strength-based design can become governing.

8.2.2.3 In detail analysis of the influence of the height on governing design criteria

The observation that the acceleration-governed zone in Figure 8.6 becomes smaller for higher buildings, as described in section 8.2.2.1, may feel counter-intuitive. This apparent simple observation is the result of a complex interplay between different parameters that influence the result: mass, eigenfrequency, stability system and height. In general it holds that the higher a building, the lower the eigenfrequency, see Figure 8.7b. As described in Chapter 6, a lower eigenfrequency is unfavourable regarding the along-wind dynamic response. In addition, the acceleration limits also play a role in this response, since the acceleration requirements in turn depend on the eigenfrequency. For higher buildings, with a lower eigenfrequency, the acceleration requirements are less strict. This can be observed from the unity-check line in Figure 8.7a and in Figure 2.5. This partly explains the relations from Figure 8.6.

Moreover, it can be stated that the higher a building, the greater the total distributed building mass. This higher building mass helps to reduce the wind-induced dynamic response for the tallest types of buildings, see Figure 8.7a and 8.7c. The increase of mass is partly caused by the fact that the mass from the floors is increased, as there are simply more floor slabs. Next to that, it is also caused by the additional required structural mass that is needed to create a higher tower. For a higher building, more steel is required to keep the deformation within the limits than for a smaller tower, see Figure 4.3 (Hoenderkamp 2011).

However, it must be noted that the relations from Figure 8.6 are affected by the assumption that the across wind plays no role in the applied model. It can be stated that the higher the slenderness ratio, the greater the contribution of vortex shedding to the dynamic response will be. This effect becomes governing for tall towers. Therefore, for higher buildings the relations from Figure 8.6 will change. It is however expected that for the relatively small heights as investigated in this report, the influence of across winds will not be very significant, see Chapter 6.

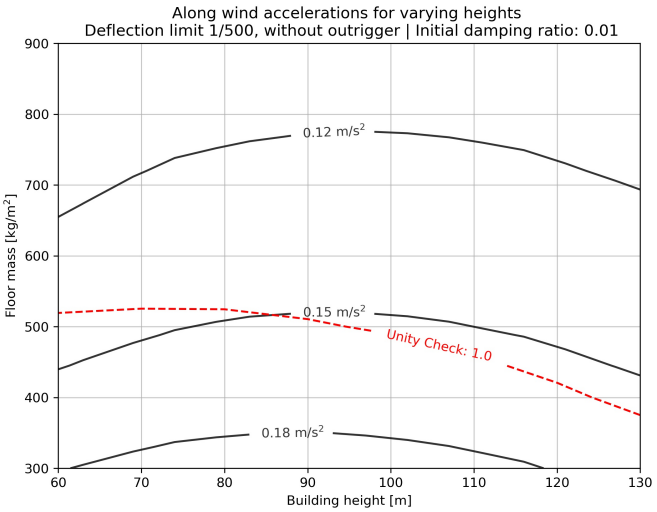

(a) *Along-wind accelerations [m/s^2]*

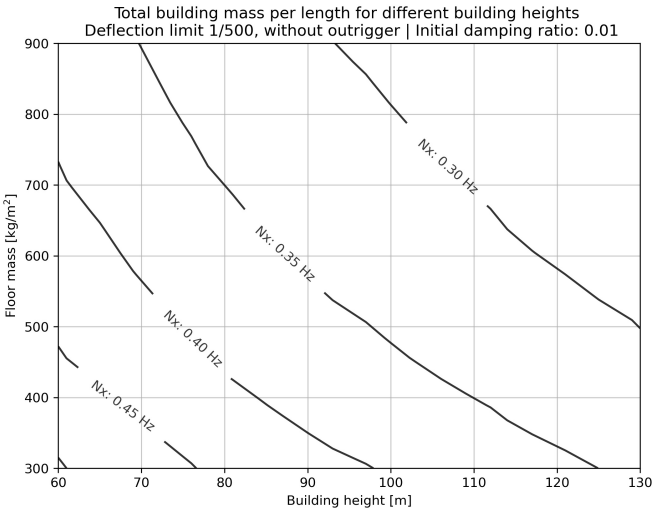

(b) *Eigenfrequency [Hz]*

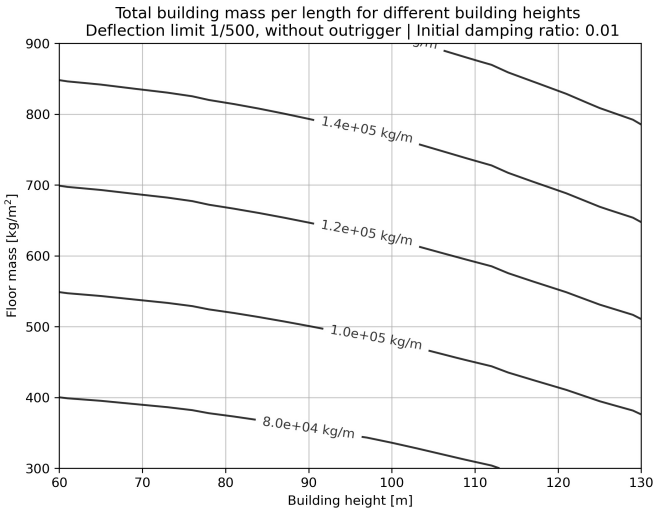

(c) *Building mass [kg/m]*

Figure 8.7: *Interplay between height, mass and the eigenfrequency.*

8.2.3 Influence of the stability system

Another factor that plays a role in the dynamic behaviour of high-rise buildings is the type of stability system. The effect of the stability system has been investigated by including an optional outrigger in the model. This outrigger is located at 60% of the building height, see Appendix D. The outrigger can be turned on and off, in this way, the dynamic response can be determined for a system with and without outrigger. The results for a building of 100 meters are visualised in Figure 8.8.

An interesting point that can be observed from Figure 8.8b is that for very flexible building variants (deflection limit 1/200) including an outrigger, strength becomes the governing design criterion. These variants can be observed in the strength governed zone. The existence of this zone makes sense as an outrigger increases the stiffness of a building, building variants that are governed by strength therefore automatically inherit more stiffness.

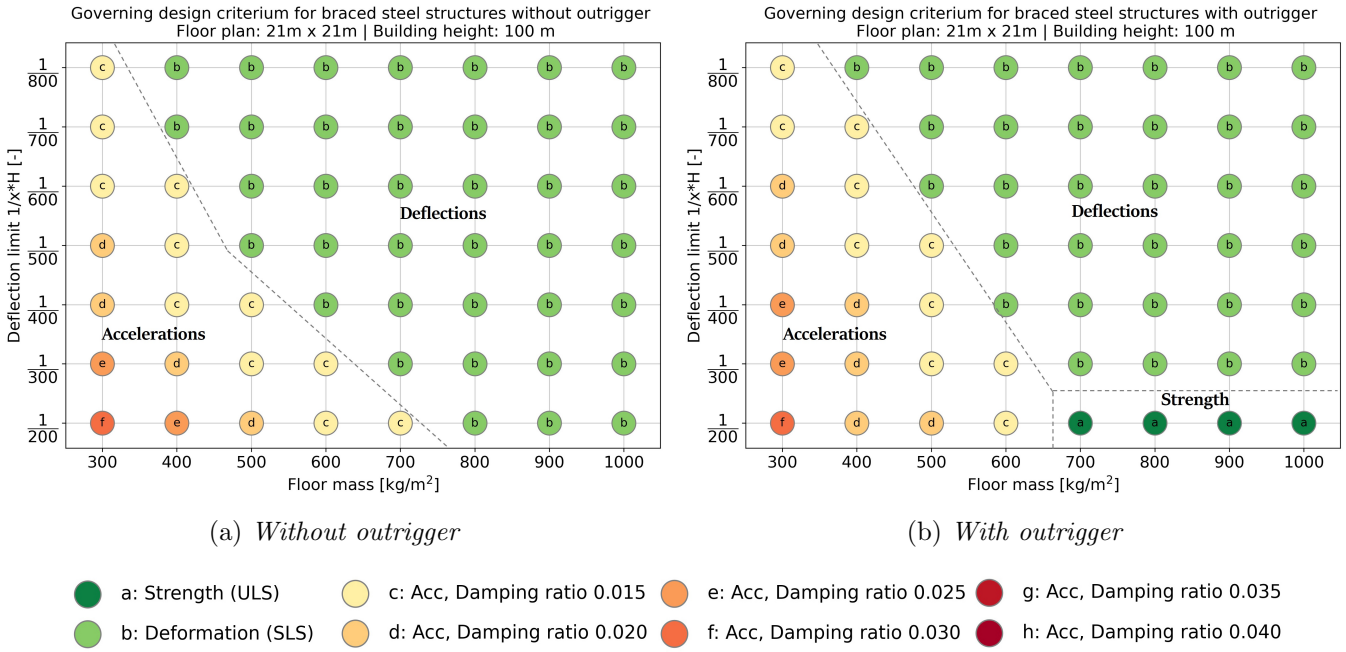

(a) *Without outrigger* (b) *With outrigger*

Figure 8.8: *Governing-design-criteria for systems with and without an outrigger*

Moreover, from Figure 8.8 it can be observed that the acceleration governed zone becomes larger for building variants in which an outrigger is included. This observations can be explained with Chapter 4 and Appendix A. The application of an outrigger increases the structural efficiency of a building, by activating the outer columns in resisting the wind loads. Therefore, less structural material is required to comply with the deflection requirements, than for the same building without an outrigger. This means that the total amount of structural steel is reduced. On the one hand, this reduction is beneficial. On the other hand, the dynamically sensitivity is increased for more lightweight buildings. In general it can be stated that for more efficient stability systems, building variants become more prone to wind-induced vibrations, if the same deflection limits are applied, this has been visualised in Figure 8.9.

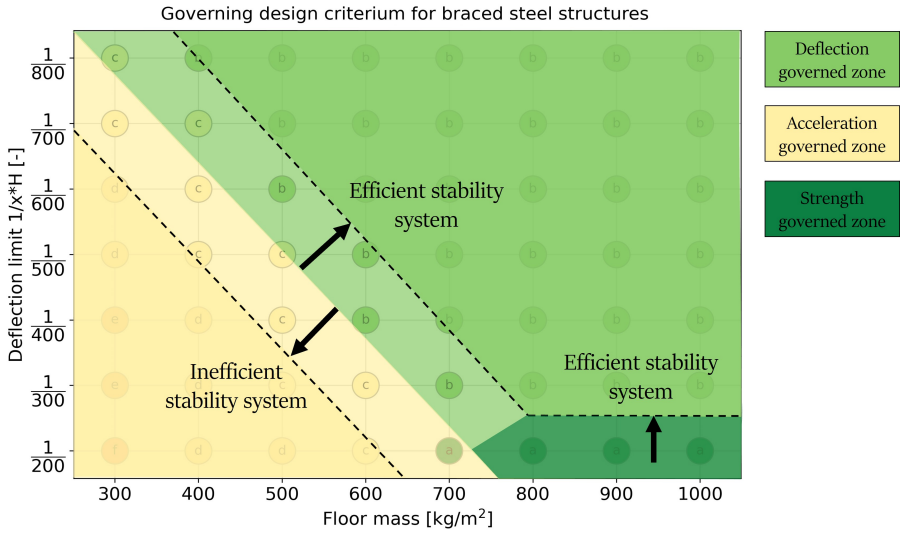

Figure 8.9: *Influence of the type of stability system on the distribution of the governing design criteria.*

8.2.3.1 Explanation of the results

These results may seem to suggest that the application of an outrigger is not an efficient design solution for dynamically sensitive buildings, however this is not the case. This is explained with the help of Figure 8.10. Figure 8.10a shows a building variant of interest, without an outrigger. The marked design is governed by deflections. Figure 8.10b shows the same building variant, with an outrigger. In the latter situation, the design is governed by accelerations, therefore additional design measures need to be taken. This may not seem like an efficient solution. Two options arise: 1) increase the building stiffness, 2) apply supplemental dampers. For option 1, it turns out that even though the stiffness has to be increased, the mass of this solution is still reduced compared to the variant without an outrigger. In the end, the design including outrigger turns out to be more efficient than the design without outrigger. Although, the change of accelerations to be governing increases, this drawback can be compensated by 'freely' increasing the stiffness.

The structural mass of the variants that include an outrigger, is generally around 25% lower. The material is thus used in a more clever and efficient way, which results in material savings. The apparent drawback of the higher required stiffness is compensated fully by these mass savings. From this, it can be concluded that if governing-design-charts for different stability systems are compared, the underlying building parameters always should be kept in mind, as the starting points of the different charts are simply different.

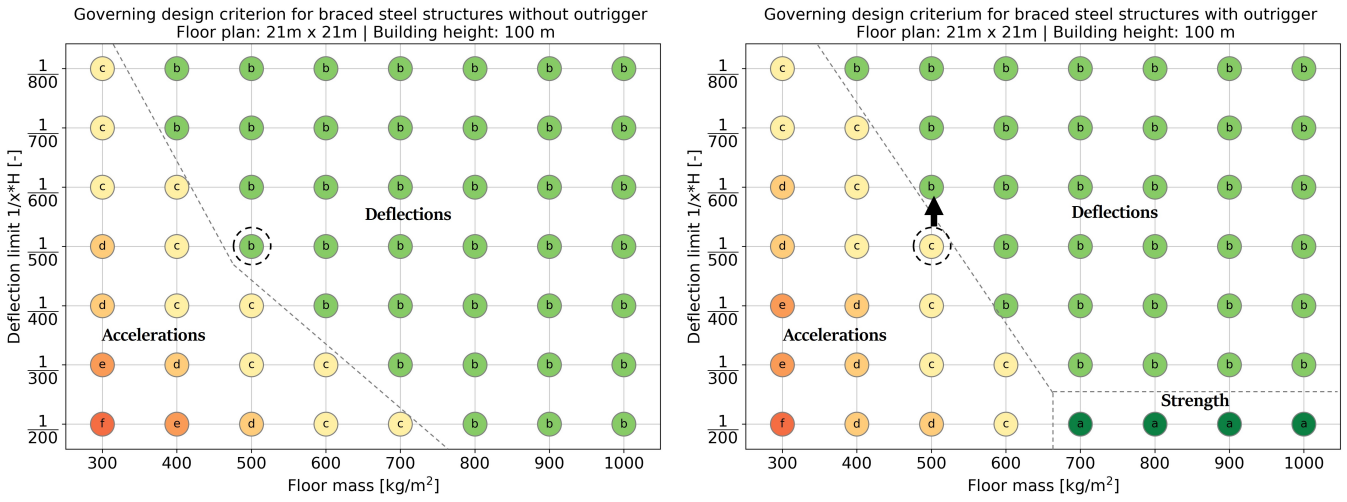

(a) *Without outrigger* (b) *With outrigger*

Figure 8.10: *Explanation of the outrigger influence*

8.3 Governing design-criteria-charts for a constant mass

Different design aspects have been presented so far, but all these charts used a constant building height as starting point. It can be helpful to change the perspective of the analysis and analyse the same data from a different point of view, to increase the understanding in the dynamic relationships. Therefore, in this section the governing design-criteria graphs will be presented for non-constant building heights, but for a fixed floor mass. This allows for an analysis of the deflection requirements versus the building height behaviour.

8.3.1 Buildings with a high floor mass

First a building configuration with a relatively heavy floor mass is visualised. A floor mass of 800 kg/m^2 is considered, which could represent a heavy concrete floor of 30 centimeters thick. Figure 8.11 shows the governing-design-criteria for such structures, with and without outrigger.

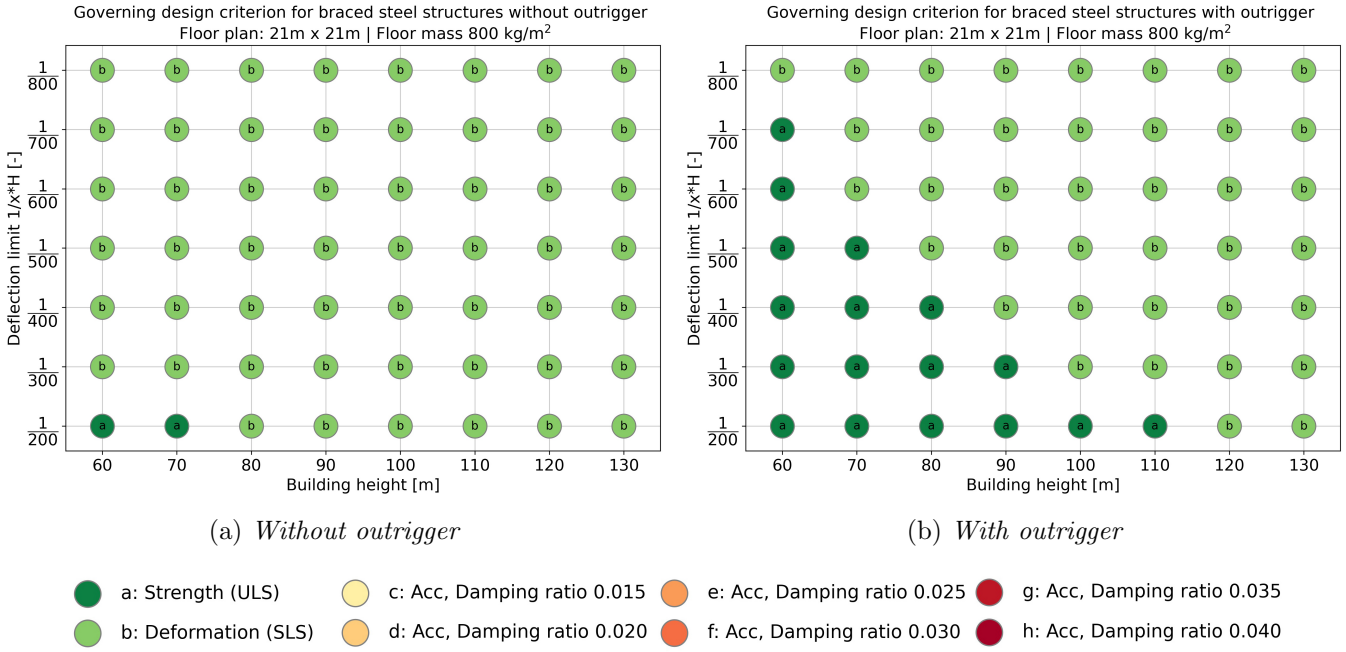

(a) *Without outrigger* (b) *With outrigger*

Figure 8.11: *Governing-design-criteria for towers with a heavy floor system of 800 kg/m^2. Building height versus deflection limits, for a system with and without an outrigger.*

As mentioned in Chapter 4 the mass of the floor slabs is the main contribution to a building's total mass. A tower with a concrete floor of 800 kg/m^2, hence can be considered as a heavy tower. From Figure 8.11 it becomes clear that for such a tower, wind-induced along-wind accelerations do not play a role in the design: for all possible height-stiffness configurations with a floor mass of 800 kg/m^2, the designs are governed by strength or deflections. It can be concluded that accelerations will not be governing for heavy towers.

Some other interesting conclusions can be drawn from the two subfigures of Figure 8.11. Due to the fact that acceleration design is not governing for this type of relatively heavy towers, these Figures visualise a kind of clean situation in which the distinction between deformation-governed design and strength-governed design can be observed clearly. Knowledge on the relations for these types of towers is very interesting as these relatively heavy towers in fact represent the nowadays Dutch high-rise situation.
Again, it can be observed that for a more efficient stability system, namely the one with outrigger, strength-design becomes governing in more building design configurations, see Figure 8.11b.
Overall, it can be observed that the smaller the building height, the bigger the chance that the design is governed by strength requirements, rather than by deflection requirements. This is due to the fact that for smaller buildings the wind force and wind moments are reduced, which means that the deformations are smaller. Moreover, from Figure 8.11 it can be concluded that the strength requirements turn out to be only governing for relatively flexible buildings. This makes sense, as the more lenient the deflection limits, the bigger the chance that the ULS design already complies with the deflection limits.

8.3.2 Buildings with a low floor mass

Regarding the opportunities for supplementary damping it is more interesting to take a look at building variants with a lower floor mass, since these buildings are more sensitive to wind induced vibrations, see Chapter 6. Two types of towers will be considered: 1) A tower with a floor mass of 300 kg/m^2, which could represent a lightweight CLT floor, 2) A tower with a floor mass of 500 kg/m^2, which represents a steel-concrete floor type. See Appendix F for a derivation of the typical floor weights. Both floor types are compared in Figure 8.12.

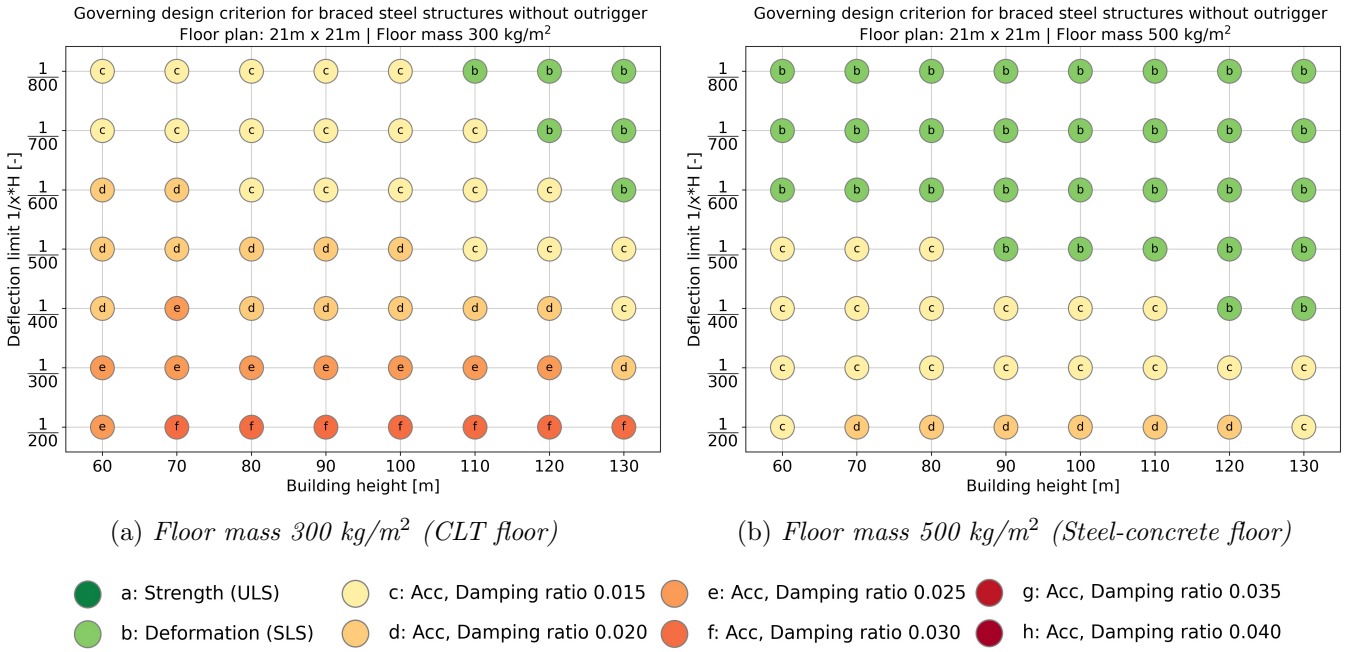

(a) *Floor mass 300 kg/m^2 (CLT floor)* (b) *Floor mass 500 kg/m^2 (Steel-concrete floor)*

Figure 8.12: *Governing-design-criteria for with lightweight floor systems of 300 and 500 kg/m^2, without outrigger.*

From this Figure the effects of a reduction in Floor mass becomes very clear. First of all, the difference between the heavy concrete floor from Figure 8.11 and the lightweight floor variants from Figure 8.12 is clearly observable: accelerations only become an issue for buildings with lightweight floors.
Moreover, it can be observed that for the 500 kg/m^2 variant, the acceleration requirements are only governing for relatively lenient deflection limits. These types of buildings are not very dynamically sensitive, as long as standard deflection limits (1/500) are applied. However, if it is decided to allow higher deformations in a performance-based approach, designers should be aware of the possible dynamic implications.

In contrast, for the lightest types of floor masses of around 300 kg/m^2, most building variants are governed by the acceleration limits. This means that a design choice for, for example CLT floors requires appropriate design measures to prevent excessive accelerations. Figure 8.12a demonstrates that a total damping ratio of maximum 0.030 would be enough to prevent most of these problems. These values of damping ratios can be achieved by the application of just a single (bi-directional) Tuned mass damper, as is described in Chapter 9.

In general from Figure 8.12a it can be concluded that the construction of relatively lightweight and flexible towers is only feasible if supplementary damping is applied. The application of supplementary dampers thus offers an opportunity to create more lightweight buildings, for example in timber. However, it must be noted that other design aspects, like fire safety and sound insulation, as introduced in Section 4.4, can play

a role as well. These aspects can turn out to be the governing design aspects, regarding the application of lightweight floors.

8.3.3 Relation height and accelerations

From Figure 8.12 it can be observed that for smaller buildings, the accelerations are the governing design requirement more often. This relation is the same as the relation observed in Section 8.2.2. The underlying concepts regarding the building mass and the frequency-dependent acceleration requirements were explained in Section 8.2.2.3.

8.4 Required amount of damping

The governing-design charts can be used to define the order of magnitude of the required amount of damping for high-rise buildings. The amount of total damping ratio that has to be reached by the application of a supplemental damper is called the target damping ratio. From Figure 8.1 it can be observed that for buildings with a height of 100 meters, the maximum target damping ratio is equal to 0.030. This result is in line with the parameter study from Chapter 6, as visualised in Figure 6.3. Such a damping ratio can be considered as a relatively low supplemental damping ratio, which can be obtained relatively easy by the application of a tuned mass damper, as is further elaborated on in Chapter 9.

8.4.1 Effect of an increasing damping ratio

It has been shown in Chapter 6, that the mitigating effect of an absolute increase in the damping ratio on the occurring accelerations gradually decreases. Figure 6.4 demonstrates that a small amount of supplementary damping can already be very effective in reducing the accelerations. This behaviour can also be observed with the data from the analysed Grasshopper model. For a building with a constant floor mass of 500 kg/m^2 and a constant deflection limit of 1/500 the effect of an increasing damping ratio has been visualised in Figure 8.13. The contours in this figure represent the accelerations for different building heights. It can be observed that the absolute reduction in acceleration becomes smaller for higher damping ratios. In line with, it can be concluded that the effectiveness of an increase in damping ratio gradually decreases for higher damping ratios, see Chapter 6.

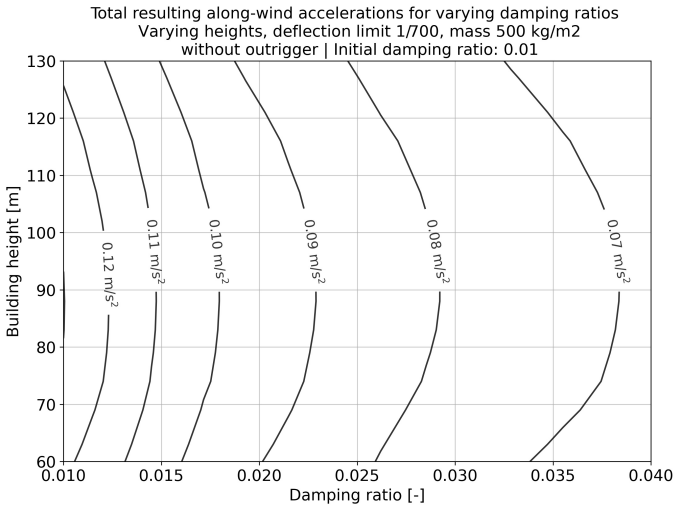

Figure 8.13: *Total along-wind accelerations for an increasing damping ratio*

8.5 Influence of acceleration limits on the governing design criteria

In the previous chapters, the different design criteria: strength, deformations and accelerations, design have been covered. As discussed in Chapter 2, fundamental differences exist between those concepts. Design based on strength requirements is about safety, which in fact can be considered as a clear binary concept: a structure may not collapse. Design based on accelerations requirements is more ambiguous, as it is about comfort: exceeding these limits does not result in any real danger, only in discomfort for the inhabitants (Burton et al. 2015). This is discussed in more detail in Chapter 2.

As acceleration levels do not influence the safety of a building, the accelerations requirements in building codes are not as stringent as the strength requirements. Building codes like the Eurocode do describe peak acceleration limits for a one year repetition time. If these requirements are fulfilled the building meets the minimal quality standards. As described in Chapter2 the correctness of the Dutch acceleration requirements from the Dutch design code can be argued. Moreover, a building client could decide to strive for a higher comfort level. This can be important, since for the higher floors, which are the most expensive floors, will face the highest accelerations.

Therefore, it is of interest to investigate the influence of the acceleration requirements on the governing-design-criteria charts from this chapter. As an example a reduction of the Dutch acceleration requirements by 20% is investigated in this section. This means that the maximum unity regarding accelerations check would be decreased to 0.80. The limit thus shifts from 1.0 to 0.80. Figure 8.14, again for a building of 100 meters, visualises both the original unity check of 1.0 and the reduced requirement with a unity check of 0.80. It can be observed that the zone for which the accelerations are governing, underneath the line of unity check 0.80, increases significantly with this new adjusted limit.

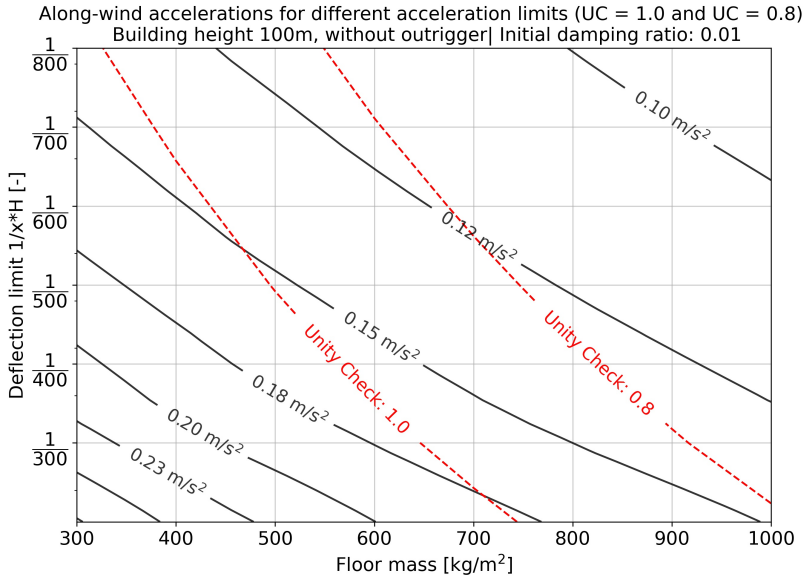

Figure 8.14: *Accelerations for a 100 meter tall building: Default acceleration limit (unity check 1.0) and the more strict limit (unity check 0.80).*

Figure 8.15 shows the governing-design-criteria charts for the default Eurocode acceleration requirements and the adjust, 80 %, acceleration limit, as introduced in Figure 8.14. From Figure 8.15 it becomes clear

that for stricter requirements. the acceleration governed zone increases significantly. Moreover, the minimum required damping ratios are increased, which means that heavier dampers are required to comply with the acceleration requirements. From these charts it can be concluded that the influence of the acceleration requirements on the results as presented in this chapter is significant. Moreover, it can be concluded that the application of supplementary damping can be useful to increase the building comfort.

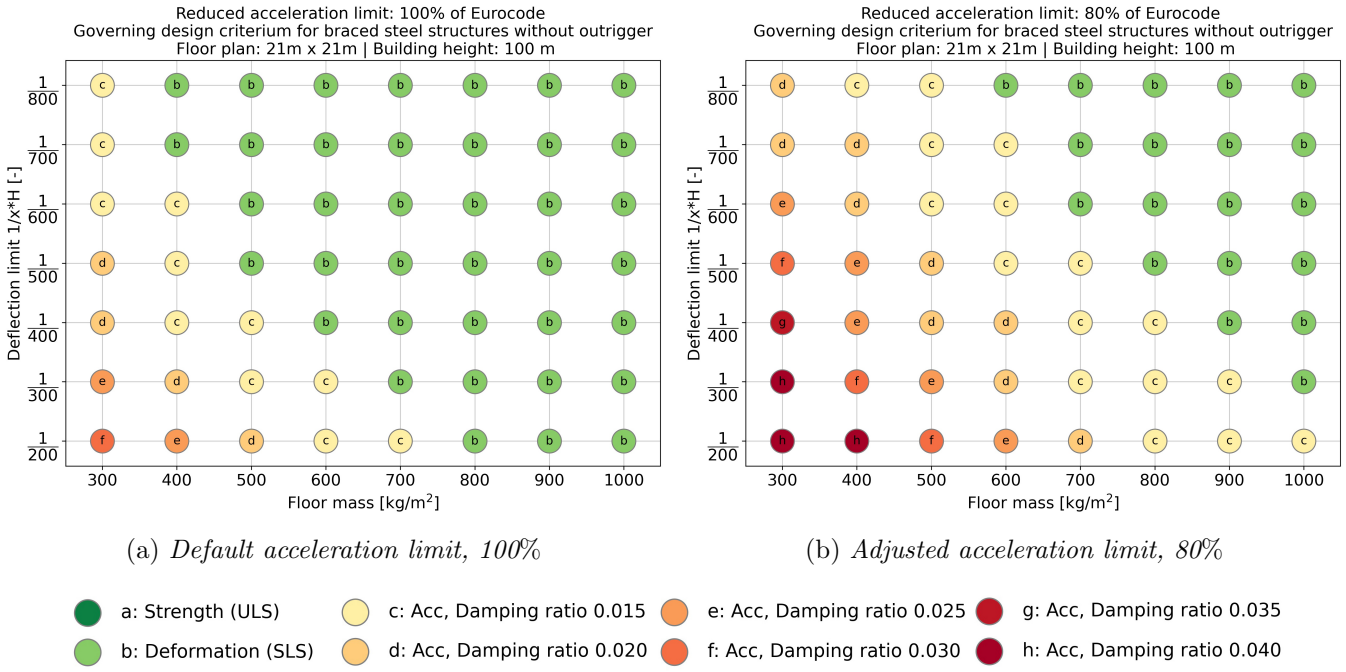

(a) *Default acceleration limit, 100%*

(b) *Adjusted acceleration limit, 80%*

Figure 8.15: *governing-design-criteria for different acceleration limits.*

Regarding the governing-design-criteria it is important to note that adjusting the acceleration requirements is fundamentally different from adjusting the structural parameters like height, mass, or stiffness. Adjusting these parameters changes the building properties and hence affects the dynamic building response. Adjusting the acceleration requirements is different in the sense that it only affects the interpretation of the occurring accelerations, rather than that it affects the actual dynamic response.

8.6 4D plots

Appendix H presents the results in a 3 dimensional space. These charts can not be used to obtain individual results, but they can provide insights into the general relations.

8.7 Effects of supplementary damping on wind-induced deflections

In the previous paragraphs the focus was mainly on the dynamic accelerations and how these accelerations could be reduced by the application of (supplementary) damping. It is also interesting to take a closer look at wind-induced deflections. As explained in Chapter 3 the wind-induced response of a building is the result of a static and a dynamic contribution. In the Eurocode the dynamic contribution to the building deflection is taken into account by multiplying the static wind load with a dynamic amplification factor. This dynamic

amplification factor is called the Cd factor, which is included in the CsCd factor.

The CsCd factor takes into account the wind-induced resonance response. The CsCd factor is directly dependent on the damping ratio, see Appendix C. If the total damping ratio is increased by making use of supplementary damping, the CsCd factor may be reduced. In this way the contribution of the wind-induced dynamic deflections to the overall deflection is reduced. However, such a reduction in the CsCd factor by applying supplementary damper may not be applied for the ULS design situations. As described in Chapter 5, the structural integrity of a building may not rely on tuned mass dampers because of safety reasons. This demand does not hold for SLS design situations in which the deformations are governing. Supplementary dampers may thus not be used to reduce the CsCd factor in ULS load cases, but they can be used to reduce the CsCd factor in SLS load cases.

From the previously discussed governing-design-factor plots, like Figure 8.11, it can be observed that for tall buildings the deflection limits (SLS) are in general governing over the strength requirements (ULS). In these cases the observation as described in the previous paragraph can be actually very useful. If the SLS design is governing, it determines the amount of required structural material in a building. Reducing the wind loads in the SLS design by applying additional damping will thus result in a reduction of the structural mass. The application of a damper can be beneficial if the reduction in structural material, compared to the inclusion of a TMD, is large enough too save cost and reduce the climate impact.

Figure 8.16a shows the effect of an increasing total damping ratio on the value of the CsCd factor for a building with a height of 100 meter, a floor mass of 800 kg/m2 and various deflection limits.

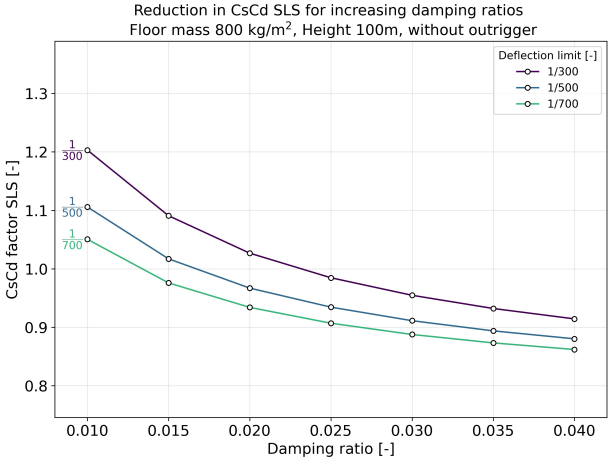

(a) *Absolute reduction in CsCd*

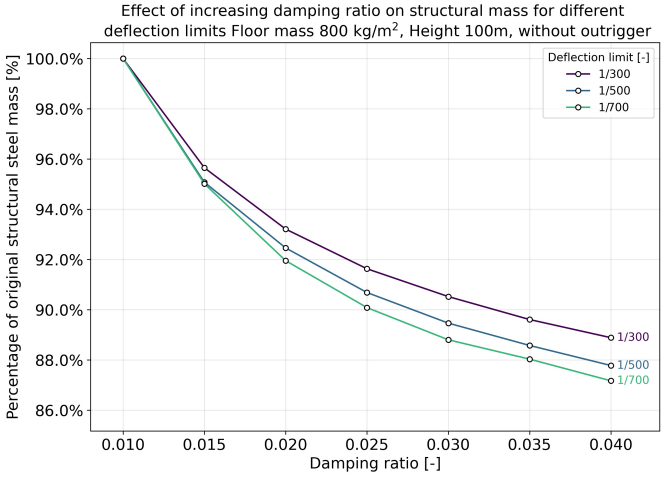

(b) *Percentage reduction in structrual mass*

Figure 8.16: *The effect of an increasing total damping ratio (by supplemental damping) on the value of the CsCd factor and on the total structural building mass.*

From Figure 8.11a it can be observed that for this building variant the deflection limit (SLS) is indeed governing over the ULS design. The applied reduction in the SLS CsCd factor thus results in a direct reduction of the governing wind loads. Which results in a reduction of the required structural mass for this building variants. This is visualised in Figure 8.16b. It can be observed that an increase in the total damping ratio up to 0.040 can reduce the structural mass by over 10%. In this way the application of supplementary dampers

increases the building comfort regarding accelerations, but also directly reduces the amount of required material. The possible reduction in CsCd factor works best for buildings that are already quite dynamically sensitive. From the data of other building variants it follows that an increase in damping ratio approximately results in the same percentage reduction of the CsCd factor for building variants with different heights

8.8 Conclusions

The main conclusion from this chapter can be defined as follows:

- For steel buildings with a lightweight floor system around 300 kg/m^2 and a regular top deflection limit of 1/800, dampers may provide an opportunity.
- For steel buildings with a relatively lightweight floor system, around 500 kg/m^2 and a reduced top deflection limit $\leq$ 1/500, dampers may provide an opportunity.
- For new types of lightweight and flexible structures that are barely feasible nowadays, dampers may provide an opportunity.
- For typically Dutch high-rise buildings with regular stiffness requirements and concrete floors, most designs are governed by the deflection criteria.
- Target damping ratios in the order of 2% to 4% are generally enough to reduce accelerations to an acceptable level.
- By the application of supplemental damping, the CsCd structural factor may be reduced up to 15% in SLS load cases.

Moreover, relations between the relevant dynamic parameters are defined:

- The higher the floor mass, the smaller the chance that accelerations are the governing design criterion.
- The stricter the deflection limits, the smaller the chance that accelerations are the governing design criterion.
- The higher the efficiency of a stability system, the larger the chance on wind-induced dynamic problems. The mass of these systems is generally lower. Moreover, strength can become governing for buildings with an efficient stability system.
- The stricter the acceleration limits and the higher the comfort requirements, the larger the chance on wind-induced dynamic problems.

Part III

The application of tuned mass dampers

Chapter 9

Practical design aspects of a TMD

In the previous chapters of this thesis, the effects of the application of supplementary damping have been investigated in a theoretical manner. To simulate additional damping, the overall structural damping ratio was simply increased in the Eurocode design formulas. In this chapter, the practical implications of the application of supplementary damping are investigated. The different relevant design aspects are described in Section 9.1. Section 9.2 provides a workflow for the design of a tuned mass damper.

9.1 TMD design parameters

Different design considerations play a role in the functioning and effectiveness of a TMD. The functioning of a tuned mass damper is determined by the interplay of four design parameters: the TMD mass (m_d), the TMD stiffness (k_d) and the TMD damping constant (c_d) and the TMD location. The optimal combination of these parameters differs per design case and depends on the design requirements. Furthermore, other practical design considerations like cost, maintenance, installation, etc. play a role as well. The design considerations regarding the TMD parameters are explained and discussed in this section.

9.1.1 Equivalent damping ratio

The first step in designing a tuned mass damper is to determine the minimum desired damping ratio for the structure, the target damping ratio. For this purpose, the acceleration response for a structure without damper has to be determined first. Then the required damping ratio to comply with the acceleration requirements can be determined. In this report, the governing-design-criteria charts, as presented in Chapter 7, are used to determine the target damping ratio. These charts visualise the minimum required damping ratio for different building variants, which can be used as the starting point for the TMD design.

By the application of a TMD, the maximum accelerations in a building are reduced. In contrast to viscous dampers, the application of a TMD does in itself does not result in an explicit increase of the damping ratio, as explained in Chapter 5. Nevertheless, the effect of a TMD on the structural motion is similar. Therefore, it is possible to compare the mitigating effects of a TMD on a structure, with the effects of a theoretical increase in the damping ratio. The theoretical damping ratio for which the dynamic response is similar to the behaviour including TMD, is referred to as the TMD's equivalent damping ratio ζ_e.

The TMD damping ratio should be equivalent to the target damping ratio. The equivalent damping ratio (for a simplified TMD system) can be calculated by Equation 9.1(Connor 2003). Optimal values for ω_d and ζ_d are assumed in the derivation of these equations, as described in Equation 9.4 and 9.7).

$$\zeta_e = \frac{1}{2 \cdot H_{opt}} \tag{9.1}$$

$$H_{opt} = \frac{1+\mu}{\sqrt{0.5\mu}} \tag{9.2}$$

9.1.2 Mass of a TMD

An important design factor in the design of a tuned mass damper is the mass ratio of the TMD mass to the modal mass, referred to as μ. The higher the mass ratio, the higher the equivalent damping ratio. By applying Equation 9.1 the required TMD mass ratio μ to generate the required target damping ratio can be determined. this information the TMD mass ratio can be estimated from Figure 9.1 (Connor 2003). From this chart it can be determined which mass ratio (μ) is needed to obtain a certain equivalent damping ratio (ζ_e). Different intrinsic damping ratios ζ_i can be used as starting point. In this report ζ_i is assumed to be 0.01.

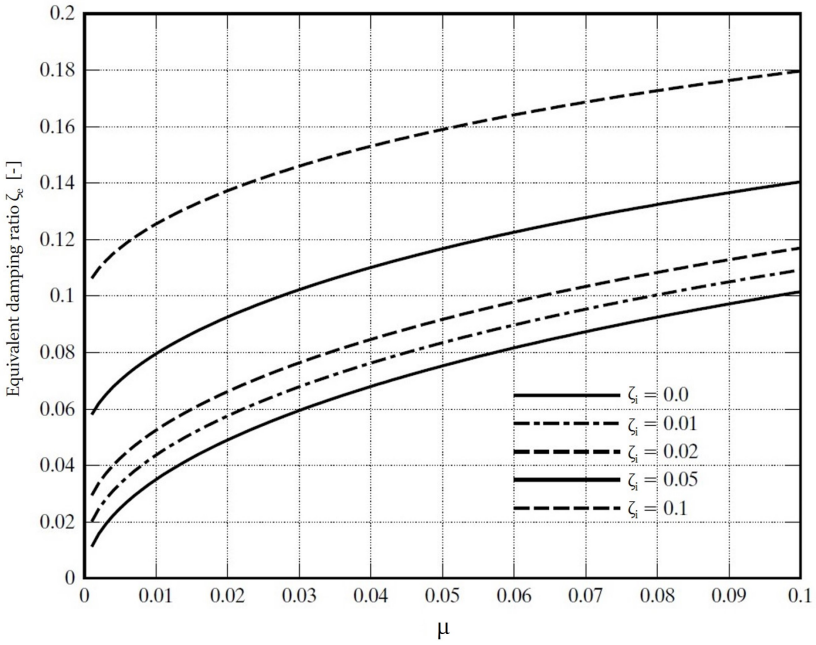

Figure 9.1: *Resulting equivalent damping ratio for different TMD mass ratios (μ). Various intrinsic building damping ratios (ζ_i) are presented. Adopted from: (Connor 2003)*

It can be understood that the practical values of the TMD mass are limited. If the TMD mass is (too) high, this will affect the design of the structural system. Furthermore, the efficiency of the TMD generally decreases with an increasing mass ratio.

9.1.3 Relative motions of a TMD

Another design parameter for the design of a tuned mass damper is the relative displacement of the TMD. Normally, the available space for a TMD in a building is limited, for example by physical boundaries. Hence, the TMD displacements can not be too large. The displacement ratio of a TMD describes the ratio of the TMD displacement to the fluctuating building displacement. Normally, this ratio is in the order of magnitude of 10. This means that the TMD motion is 10 times higher than the fluctuating wind component. Figure 9.2 visualises the TMD displacement ratio for different mass ratios. The higher the mass ratio, the lower the relative TMD motions. The maximum allowed displacement ratio provides an important boundary condition for the design of the TMD.

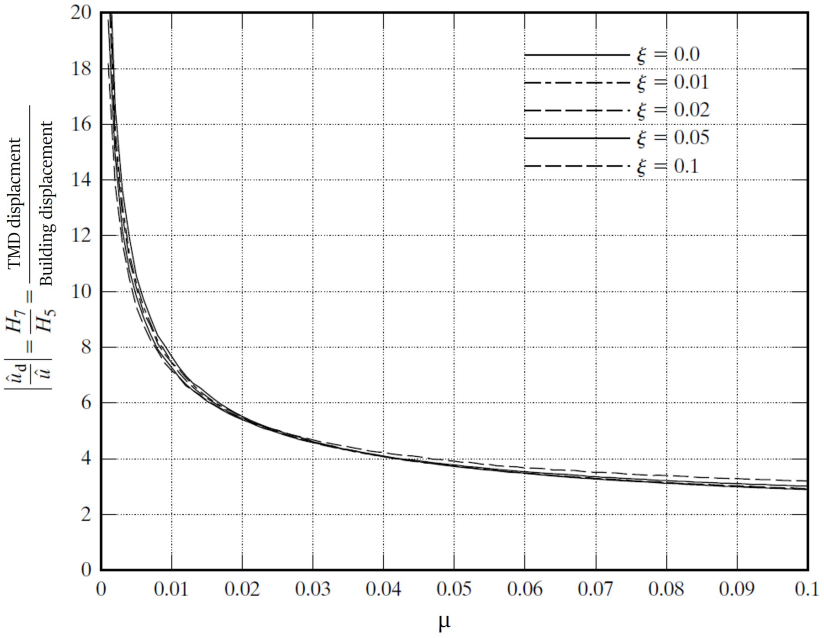

Figure 9.2: *TMD displacement ratio versus the TMD mass ratio. Adopted from: (Connor 2003)*

9.1.4 Stiffness and eigenfrequency of a TMD

A TMD is connected by springs to the main structure. The properties of these springs determine the eigenfrequency ω_d of the TMD, together with the TMD mass m_d. The eigenfrequency of a TMD is determined by Equation 9.3 (Krenk 2005).

$$\omega_d{}^2 = \frac{k_d}{m_d} \tag{9.3}$$

The eigenfrequency of the TMD is essential in the functioning of the supplementary damping system. The frequency should be tuned to the governing eigenfrequency of the structure, otherwise the TMD is not effective. The mass and stiffness of the TMD should be designed in such a way that an optimal TMD frequency is obtained for the system. The optimal TMD frequency is not exactly equal to the fundamental frequency of the main structure, but deviates a bit. The (near) optimal value for the ω_d is described by (Tsai & Lin 1993) based on curve fitting. This equations takes into account the initial damping ratio ζ_d, which is assumed to be 0.01 in this report. For low initial damping ratios, Equation 9.5 can provide an accurate assumption of the near-optimal frequency (Connor 2003).

$$\frac{\omega_d|_{opt}}{\omega_1} = \left(\frac{\sqrt{1-0.5\cdot\mu}}{1+\mu} + \sqrt{1-2\zeta_i} - 1\right) - (2.375 - 1.034\sqrt{\mu} - 0.426\mu)\zeta_i\sqrt{\mu} - (3.730 - 6.903\sqrt{(\mu)} + 20.496\mu)\zeta_d{}^2\sqrt{\mu} \tag{9.4}$$

$$\frac{\omega_d|_{opt}}{\omega_1} = \frac{\sqrt{1-0.5\cdot\mu}}{1+\mu} \tag{9.5}$$

9.1.5 Damping ratio of the TMD damper

In a building that is damped by a TMD, the energy from the building motion is transferred to the mass of the TMD. No energy is dissipated during this transfer of energy. This means that the energy is still within the building system. To dissipate this energy, an actual damper, like a viscous damper, has to be connected to the TMD. Such a damper will convert the kinetic energy of the TMD mass into heat, which means that the energy is dissipated. Without such a damper, the energy within the TMD will sooner or later be transferred back to the main building structure, which can result in dynamic issues. This concept is also explained in Chapter 5. Moreover, the additional damper, as part of the TMD system, enlarges the operating range of the TMD: A broader range of frequencies is damped for such a system (Meinhardt 2021). This makes the TMD less sensitive to changes in the buildings fundamental frequency and other design uncertainties, as discussed in Section 5.3.

The damping ratio of a TMD can be determined from the TMD properties with Equation 9.6:

$$\zeta_d = \frac{c_d}{2\sqrt{k_d m_d}} \tag{9.6}$$

The value of the TMD damping ratio influences the functionality of the damper. Literature provides formulas to determine the (near) optimal value of the TMD damping ratio ζ_d, as described in Equation 9.7. This formula is again based on a curve fit (Tsai & Lin 1993). For cases in which the initial buildings damping ratio is relatively low, like for the assumed 0.01, Equation 9.8 can be used.

$$\zeta_d = \sqrt{\frac{3\mu}{8(1+\mu)(1-0.5\mu)}} + (0.151\zeta_i - 0.170{\zeta_i}^2) + (0.163\zeta_i + 4.980{\zeta_i}^2) \cdot \mu \tag{9.7}$$

$$\zeta_d|_{opt} = \sqrt{\frac{\mu(3-\sqrt{0.5\mu})}{8(1+\mu)(1-0.5\mu)}} \tag{9.8}$$

Deviations of this optimal damping ratio are possible, for example to reduce the maximum relative displacement of the TMD. An alteration of for example 15% could be helpful to comply with design requirements, while the effectiveness of the TMD is only slightly reduced (Meinhardt 2021).

9.1.6 Location

The height at which the TMD is installed also plays a role in the TMD effectiveness. It is most effective to install a TMD at the location with the highest modal deformations (Kwok & Samali 1995). For the fundamental mode shape, the maximum deformation occurs at the top of the building, which is therefore in general the optimal location to install a TMD from the perspective of effectiveness. However, regarding cost, installation at the top may not be always provide to most cost-efficient solution. This is because the top floor is often the most profitable floor of a tall building, applying a TMD at this floor may therefore be relatively costly. Figure 9.3 schematically shows possible TMD locations.

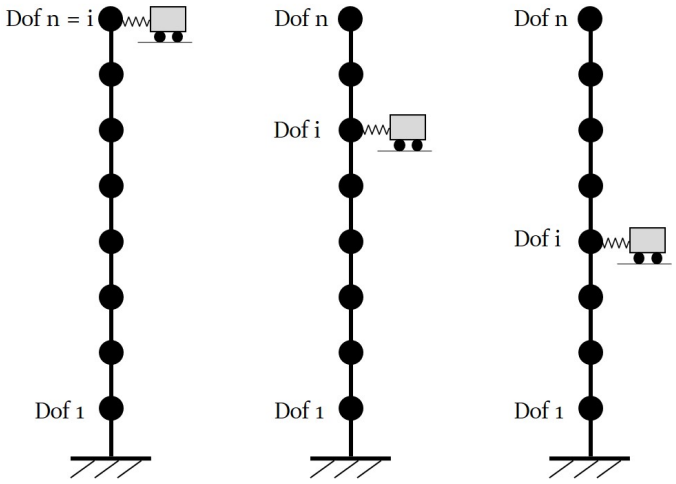

Figure 9.3: *Tuned mass damper installed at different locations, schematized overview*

9.1.7 Other practical design considerations

In addition to the main TMD parameters, other more practical factors play a role as well.

- The tuning range: as the real eigenfrequencies of buildings tend to deviate somewhat from the calculated design values or change over time, it is important to be able to alter the tuning frequency of a TMD. A TMD should allow for adjustments in the tuning range.
- Maintenance free design: As a tall building has a long life span, it is beneficial to reduce the maintenance needs of a TMD. Therefore, the amount of moving mechanical parts should be kept as low as possible. Keeping the maintenance needs low, saves money and increases the reliability.
- Installation: The application of a TMD has implications on the logistics during the construction phase of a building. If a modular TMD system is chosen, the spare parts can be transported to the top by the buck hoists instead of by tower cranes. This saves crane capacity and makes installation easier.

9.1.8 TMD Cost

The costs of the installation of a TMD are highly variable and depend on a lot of different design variables:

- Required effective damping ratio
- TMD mass, material cost
- TMD material: concrete, steel
- Location: effective location, or not.
- TMD size, space
- Type of damper: conventional TMD, pendulum TMD, Tuned liquid column dampers
- Amount of TMD's
- Installation method: modular system, crane capacity, weight

Due to these design aspects and uncertainties, it is difficult to determine the cost of TMD's in general. These factors have been discussed with a Damper manufacturer from Germany, named Gerb. As a general indication, it was told that light-weight (20.000 kg) dampers for intermediate Dutch high-rise cost in the order of €100,000 and €200,000. Large Dampers in skyscrapers of more than 300 meters in height, will cost around €1 to €2 million Euros (Meinhardt 2021).

9.2 TMD design strategy

In general, the design of a TMD is limited by different factors. First of all, the required effective damping ratio should be determined based on the output of a dynamic analysis, as shown in Chapter 7. With this value the minimum TMD mass can be determined from Figure 9.1. From this chosen TMD mass the (near) optimal values for the TMD damping ratio ζ_d and the TMD eigenfrequency ω_d can be determined. It is important that the design of the TMD results in a feasible and efficient design. On the one hand, the relative motions of the tuned mass damper must be limited, see Figure 9.2. On the other hand, the mass of the TMD may not be too high. The interplay of the different parameters results in the final TMD design.

The steps to design a dynamically sensitive building including a tuned mass damper are mentioned below. These steps are visualised schematically in Figure 9.4. This diagram is an extension of the flowchart from Figure 4.5. This time the focus is on the design of the tuned mass damper. Design options in which no TMD is applied are visualised by the dotted line and are only described concisely.
The design of a tuned mass damper consists of the following steps:

1. Design a tall building based on static design requirements. Determine the building stiffness, building mass, the fundamental eigenfrequency and the initial damping ratio.

2. Perform a dynamic analysis with an appropriate method and determine the maximum accelerations. Use for example: the building code procedures, fundamental dynamics including random vibrations or wind tunnel tests.

3. Compare the maximum accelerations to the governing acceleration limits and determine the minimum required damping ratio to comply with these acceleration requirements, the target damping ratio.

4. Define the TMD design limitations: maximum TMD mass and maximum allowed TMD motions.

5. The effective damping ratio, generated by the TMD, should at least be equal to the previously calculated target damping ratio. Determine the corresponding mass ratio μ from Figure 9.1.

6. Figure 9.2 can be used to check whetherthe determined TMD mass fulfills the requirements regarding the relative motions of the TMD.

7. Calculate the near optimal values for the TMD damping ratio and the TMD stiffness using Equation 9.4 and 9.7.

8. Verify the mitigating effect of the TMD on the dynamic response of the structure and compare this to the maximum allowed accelerations.

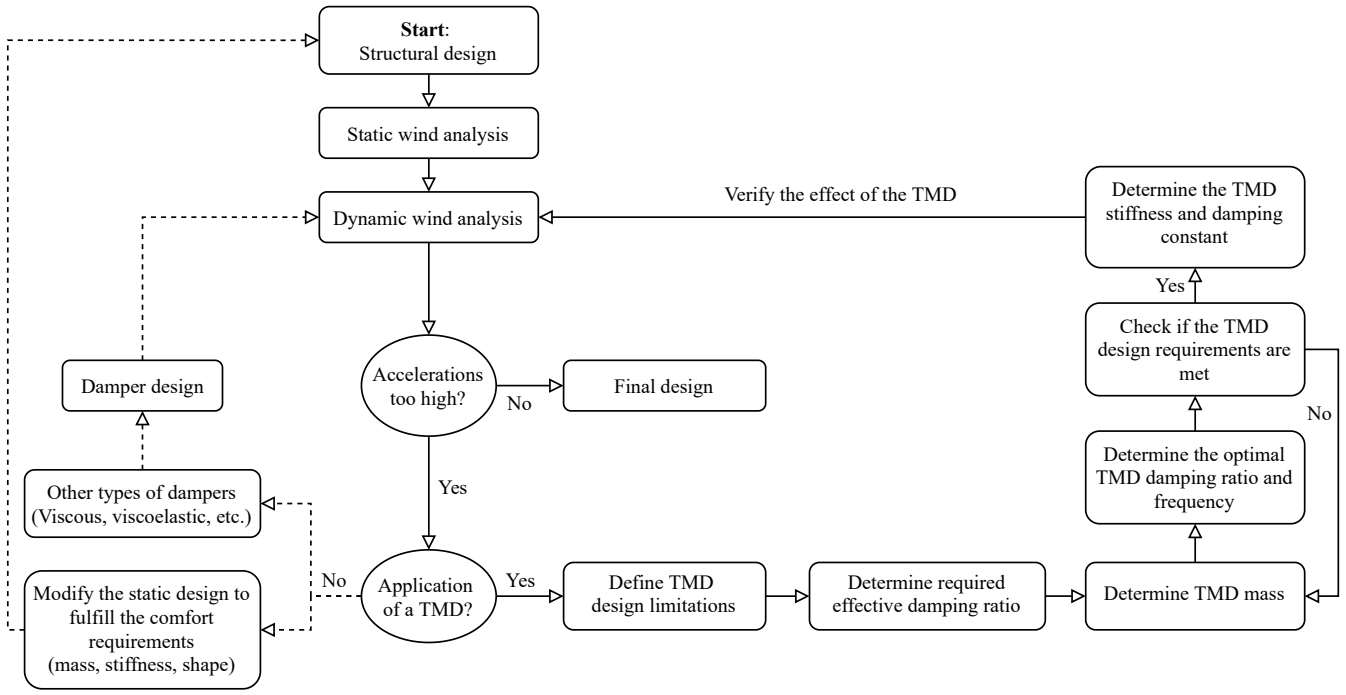

Figure 9.4: *Flowchart for the design for a building including a Tuned mass damper. The design options in which no TMD is applied are visualised by a dotted line.*

9.3 Conclusions

- The main parameters of a TMD are its mass, damping and stiffness. These factors together determine the damping behaviour.
- TMD's with a mass ratio around 1% can provide enough damping to reach a target damping of 4%.
- Practical aspects play a role in the design of a TMD.
- The cost of a TMD are highly dependent on the specific design requirements. For small high-rise buildings the cost will be a in the order of a (few) hundred thousand euros. For super tall buildings the damper can cost a few million euros.
- The workflow as described in Figure 9.4 can be used in the preliminary design phases of a TMD.

Chapter 10

Modelling the effects of a TMD

So far, the maximum along-wind accelerations have been calculated by making use of the procedures of the Eurocode. This procedure only offers the possibility to take supplementary damping into account in an implicit manner. Therefore, this method can only be used to determine the effects of dampers from which the contribution to the building's damping ratio is known. This is generally not the case. To determine the explicit effects of a TMD on the total damping ratio this Eurocode procedure thus can not be applied.

In these cases, the explicit modeling of the building including dampers is inevitable. Such a model must cover the fundamental wind-induced dynamic calculations. For this purpose, the theory of random vibrations is applied, as described in Chapter 3. In this chapter this theory has been applied to develop a model that is able to determine the effects of a TMD on a building. In this way, the dynamic response of the building variants from Chapter 7 can be determined analytically. Moreover, the effects of a TMD on the dynamic response of this building can be determined. In this script the properties of the TMD like mass, damping, stiffness and location can be varied and thus investigated.

In the first part of this chapter, Section 10.1, the equations of motions of a building including TMD are determined by a modal analysis. In Section 10.2 the wind velocity and load spectrum are defined. The application of the theory of random vibrations is covered in 10.3. The last section describes how these theories are applied in a Python script. This Python code is attached in Appendix N.

10.1 Equations of motions TMD system

To compute the effects of a TMD on the dynamic response of the different building variants from Chapter 7, the building has to be modeled as a multiple-degree-of-freedom-system, including a TMD. The schematized model of the tall building is illustrated in Figure 10.1. The considered n-storey tall building is represented by a 1D cantilever lumped mass system with n+1 discrete transitional degrees of freedom, in the x direction. In fact a tall building inherits an infinite amount of degrees of freedom, but very accurate results can be obtained by using a discrete model. Each discrete lumped mass represents the mass of one storey (M_i in Figure 10.1), including the floor mass, structural mass, facade mass, permanent loads, and reduced life loads. The lumped masses coincide with the floor's center of mass, which is located in the centre of the symmetric floor plan. In height, the DOFs are modeled at the floor levels, because the floor masses are in general the highest contributors to the total building mass (Alexander 2010). The TMD is explicitly modelled by an additional transitional DOF, connected to the i^{th} storey.

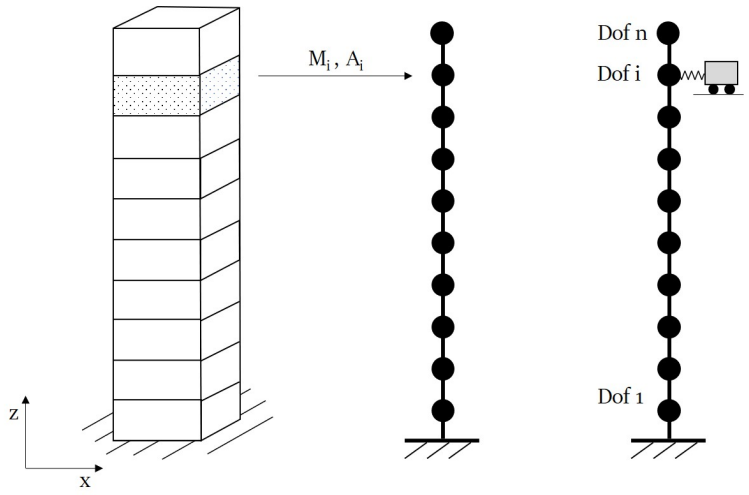

Figure 10.1: *Dynamic tower model of a slender tower with n storeys, including a TMD connected to floor i.*

10.1.1 Equations of motion

The equations of motion for this system can be described by Equation 10.1a and 10.1b (Lu & Chen 2011*a*). The derivation of this system is described in Appendix K and is also described by (Connor 2003).

$$[M]\ddot{\underline{u}} + [C]\dot{\underline{u}} + [K]\underline{u} = \underline{F} + \underline{E}(c_d\dot{v}_d + k_d v) \tag{10.1a}$$

$$m_d\ddot{v}_d + c_d\dot{v}_d + k_d v_d = -m_d\ddot{u}_i \tag{10.1b}$$

The two equations above define the system of Figure 10.1. Equation 10.1a defines the motion of the tall building, Equation 10.1b defines the equation of motion of the TMD. These equations are. $[M], [C], [K]$ respectively, represent the n x n mass, damping and stiffness matrices of the building. $\ddot{\underline{u}}, \dot{\underline{u}}, \underline{u}$ define the displacement, velocity and acceleration vector. The TMD is located at DOF number i, hence $\ddot{u}_i$ represents the acceleration of the TMD floor. $\underline{F}$ is a vector that contains the external forces on the structure. $\underline{E}$ is a vector of length n in which all components are equal to 0, except for the i^{th} component, which is equal to 1 and represents the location of the TMD. The relative displacement of the TMD is defined by the displacement of the damper minus the displacement of the TMD floor: $v_d = u_d - u_i$. The properties of the TMD are defined by: m_d as the TMD mass, c_d as the TMD damper's damping constant and k_d as the TMD stiffness, as visualised in Figure 10.2.

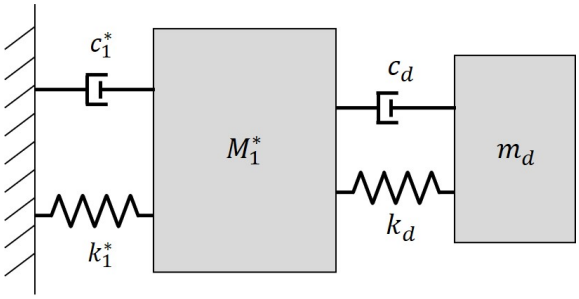

Figure 10.2: *Overview of 2DOF system: fundamental modal mass and TMD mass*

10.1.2 Modal analysis procedure

The response of a coupled multiple-degree-of-freedom system can not be determined in the same analytical manner as for a single-degree-of-freedom system, due to the coupling of equations. Performing a modal analysis is a standard procedure to analyse a multiple-degree-of-freedom-system. The purpose of such an analysis is to decouple a set of coupled equations of motion into orthogonal modes, which results in a set of uncoupled equations. These decoupled equations can be solved individually, which makes it possible to determine the responses in the same manner as for a simple single-degree-of-freedom-system. Together, the weighted individual modal responses determine the overall response of the system (Chopra 1995). Each mode has its own modal mass m^*, modal damping ratio ζ^* and modal eigenfrequency ω^*. The mode numbers are ranked by their modal frequency. The higher the modal frequency, the higher the mode number. The frequency of the first mode is called the fundamental frequency.

The approach to solve the system including TMD is as follows: A modal analysis will be performed on the equations of motion that represent the tall building from Equation 10.1. Only the first mode is taken into account in the subsequent dynamic response calculations, the other modes can be neglected (Lu & Chen 2011*a*). The contribution of the TMD is considered as an additional external force on the model. Together, the equation of motion of the first mode and the equation of motion of the TMD can be considered as a coupled two-degree-of-freedom-system, which can be mathematically solved in the frequency domain. A transfer function can be derived that relates the input force signal, to the output response. This transfer function can be used to determine the response to a random wind load by making use of the theory of random vibrations. The modal analysis procedure to obtain the Equations of motion of the system is explained in Appendix L.

10.1.3 Modal equations of motion

The modal analysis procedure, as described in Appendix L, can be applied to the equations of motion, as described in Equations 10.1a, that represent the building system. Only the first mode q_1 is considered. The resulting system that represents the first mode and the TMD displacement is presented in Equation 10.2. The resulting two-degree-of-freedom system is visualised in Figure 10.2. ${m_1}^*$, ${k_1}^*$, ${c_1}^*$ represent the first modal mass, stiffness and damping constant. The vector $\underline{q}$ represents the modal displacement, v_d represents

the relative displacement of the TMD.

$$m_1^* \underline{\ddot{q}}_1 + c_1^* \underline{\dot{q}}_1 + k_1^* \underline{q}_1 = \underline{\phi}_1^T \underline{F} + \underline{\phi}_1{}^T \underline{E} \cdot (c_d \dot{v}_d + k_d v) \tag{10.2a}$$

$$m_d \ddot{v}_d + c_d \dot{v}_d + k_d v_d = -m_d \cdot \underline{\phi}_{1,i} \ddot{q}_1 \tag{10.2b}$$

In Equation 10.2 the vector $\underline{E}$ represents an empty vector, except for the i^{th} component. This i^{th} component corresponds to the location of the TMD and is equal to 1. From this it follows that the multiplication as described in 10.2: $\underline{\phi}_1^T \cdot \underline{E}$ can be rewritten as $\underline{\phi}_{1,i}$, which represents the i^{th} component of the first modal eigenvector $\underline{\phi}_1$.

The 2DOF system from Equation 10.2 can be rewritten as the system of Equation 10.3 (Lu & Chen 2011*a*):

$$\begin{bmatrix} 1+\mu_1 {\phi_{1i}}^2 & \mu_1 \phi_{1i} \\ \phi_{1i} & 1 \end{bmatrix} \begin{bmatrix} \ddot{q}_1 \\ \ddot{v}_d \end{bmatrix} + \begin{bmatrix} 2\zeta_1 \omega_1 & 0 \\ 0 & 2\zeta_d \omega_d \end{bmatrix} \begin{bmatrix} \dot{q}_1 \\ \dot{v}_d \end{bmatrix} + \begin{bmatrix} {\omega_1}^2 & 0 \\ 0 & {\omega_d}^2 \end{bmatrix} \begin{bmatrix} q_1 \\ v_d \end{bmatrix} = \begin{bmatrix} \frac{F_1^*}{m_1^*} \\ 0 \end{bmatrix} \tag{10.3}$$

In which $\mu_1 = m_d/m_1^*$, represents the ratio between the modal mass and the TMD mass. The fundamental eigenfrequency of the structure is defined by $\omega_1 = \sqrt{k_1^*/m_1^*}$ and the first modal damping ratio is defined by $\zeta_1 = c_1^*/(2\sqrt{k_1^* m_1^*})$ in which the denominator represents the critical amount of damping. In the same way the TMD definitions are obtained: $\omega_d = \sqrt{k_d/m_d}$ and $\zeta_d = c_d/(2\sqrt{k_d m_d})$. F_1^* represents the modal force of the wind excitation.

10.1.4 Transfer function

The first modal force ${F_1}^*$ represents a summation of the weighted individual wind force components on each node. To obtain the first modal force, these force components are multiplied by the transpose of the first mode shape vector, as described in Equation 10.4.

$$F_1^* = \underline{\phi}_1^T \underline{F} = \sum_{r=1}^{n} \phi_{1,r} F_r = \phi_{1,1} F_1 + \phi_{1,2} F_2 + ... + \phi_{1,n} F_n \tag{10.4}$$

For wind excitation it is assumed that the force vector $\underline{F}$ can be considered as an harmonic function $\underline{F} = \underline{\hat{F}} \cdot e^{i\omega t}$. In which i represents the imaginary unit, ω represents the forcing frequency and $\underline{\hat{F}}$ represents the force amplitude. As the input force $\underline{F}$ is harmonic, the modal force ${F_1}^*$ from Equation 10.4 is harmonic as well. For this harmonic modal force component, the corresponding modal response q_1 will be harmonic too. Hence, the modal response can be considered as a multiple of the modal force value, which can be obtained by multiplying the modal force with a transfer function: $H_{transfer}$, as described in Equation 10.5.

$$q_1 = H_{transfer|q1} \cdot {F_1}^* = H_{transfer|q1} \cdot \left(\underline{\phi}_1^T \cdot \underline{\hat{F}} \cdot e^{i\omega t} \right) \tag{10.5}$$

This transfer function $H_{transfer|q1}$ directly relates a harmonic input force, in the frequency domain to the harmonic output response of the modal system. It can thus be used to compute the response of the system in the frequency domain. The value of the transfer function depends on the modal mass, modal stiffness, and modal damping constant.

The transfer function can be determined by solving the system of Equations 10.3. For this purpose the following substitutions are made: $F_1^* = \hat{F} \cdot e^{i\omega t}$ and $q_1 = H_{transfer|q1} \cdot \hat{F} \cdot e^{i\omega t}$. Maple is used to perform this derivation. The derivation is shown in appendix M. The same equation is found as described by (Lu & Chen 2011*b*), namely 10.6:

$$H_{transfer|q1}(\omega) = \frac{{\omega_d}^2 - \omega^2 + 2i\omega\zeta_d\omega_d}{D \cdot m_1^*} \tag{10.6}$$

In which D is:

$$D = \omega^4 - 2i\omega^3(\mu_1{\phi_{1i}}^2\zeta_d\omega_d + \zeta_1\omega_1) - \omega^2(\mu_1{\phi_{1i}}^2{\omega_d}^2 + {\omega_d}^2 + 4\zeta_1\zeta_d\omega_1\omega_d + {\omega_1}^2) + 2i\omega_1\omega_d\omega(\zeta_1\omega_d + \zeta_d\omega_1) + {\omega_1}^2{\omega_d}^2$$

10.1.5 Actual response

To obtain the actual structural response deformation response u of a certain node j, in the original coordinate system, the relation from Equation 10.7 can be applied:

$$u_j \approx \phi_{1,j} \cdot q_1 \tag{10.7}$$

This background of this relation is explained in Equation L.5. This equation in fact describes the reverse transformation, back from modal coordinates to the original coordinate system. To obtain this response, the modal response of Equation 10.5 is substituted in 10.7, this results in Equation 10.8:

$$u_j \approx \phi_{1,j} \cdot q_1 = \phi_{1,j} \cdot H_{transfer|q1} \left(\cdot \underline{\phi}_1^T \hat{\underline{F}} \cdot e^{i\omega t} \right) = H_{u_j} \cdot \underline{\phi}_1^T \hat{\underline{F}} \cdot e^{i\omega t} \tag{10.8}$$

In which H_{u_j} is defined as $\phi_{1,j} \cdot H_{transfer|q1}$. If all the force components are taken into account separately as described in Equation 10.4, this results in Equation 10.9. In which holds: $H_{u_j F_r} = H_{transfer|q1} \cdot \phi_{1,j} \cdot \phi_{1,r}$:

$$u_j \approx \sum_{r=1}^{n} H_{u_j} \cdot \phi_{1,r} F_r = \sum_{i=r}^{n} H_{u_j F_r} \cdot F_r \tag{10.9}$$

By combining Equation 10.8 and Equation 10.6 the equation for $H_{u_j F_r}$ can be derived. This result is applied in the function as presented in Equation 10.9:

$$H_{u_j F_r}(\omega) = \frac{\left({\omega_d}^2 - \omega_2 + 2i\omega\zeta_d\omega_d\right) \cdot \phi_{1,j} \cdot \phi_{1,r}}{D \cdot m_1^*} \tag{10.10}$$

This final function can be considered as the core of the developed Python script. It determines the wind-induced response of a certain node j in the original coordinate system. In this equation, the individual contributions of the modal force components to the final overall response are determined and summed together. The modal transformations are inherited in the final transfer function $H_{u_j F_r}$ by $\phi_{1,j}$ and $\phi_{1,r}$.

10.1.6 Determination of modal properties

In the previous section, the procedure to determine the structural response of the dynamic model is explained. To be able to perform these computations the modal properties need to be available. Otherwise, the values of the function $H_{u_j F_r}$ in Equation 10.9 can not be determined. To determine the modal prop-

erties, a structural model has to be created, from which the mass, stiffness and damping matrices can be derived. With these matrices, the Equations of motion can be determined. Subsequently, to perform a modal analysis, the eigenvector problem has to be solved for this structural model.

10.1.6.1 Modal properties

These modal properties can be derived in different manners. For relatively simple MDOF systems in which the equations of motion can be determined manually, a modal analysis can be performed by hand or with the help of mathematical software like Maple. For more complex structures, finite element software can be used to set up the modal analysis.

In this research, the modal properties have been derived by making use of the Karamba plug-in in Grasshopper, a tool based on the finite element method. For this purpose, the model as described in Chapter 7 is used. With the help of the Karamba FEA natural-vibrations-tool, a modal analysis is performed. From this analysis, the modal eigenfrequencies, the modal shape and the modal masses are determined. For all investigated building variants from Chapter 7, these modal properties are exported to a CSV data file, which can be imported by the developed Python model to perform the frequency response analysis.

The 2D model as created in Grasshopper is illustrated in Figure 10.3. The transfer of the first mode shape from Grasshopper to Python is shown.

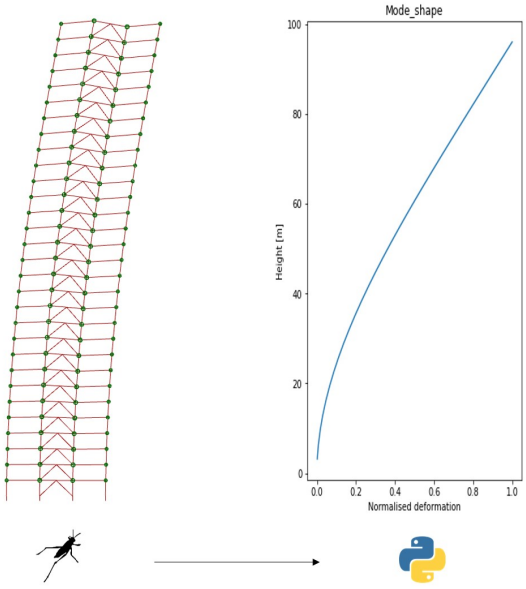

Figure 10.3: *Modal data transfered from Grasshopper to Python*

10.1.6.2 Modal mass

The total building mass in the model is distributed in two ways. The mass of the visualised red-colored beam elements of Figure 10.3 is represented directly by these beam elements. Karamba takes these masses into account by consistent mass matrices (Karamba 3D n.d.). For the dynamic analysis, the rotational degrees of freedom of the floor masses can be neglected. The rotational degrees of freedom are included in the static analysis and hence also in the stiffness matrix (Chopra 1995).

All other masses are represented by the lumped masses, the green colored dots in Figure 10.3. These lumped

masses are defined at the nodes and are assumed to have translational inertia only (Karamba 3D n.d.). Two types of contributions to the lumped masses can be distinguished. On the hand, these lumped masses take into account all the non-structural masses: the floor mass, facade mass, and a percentage of the life load. In addition, the lumped mass takes care of all the 3D in-plane structural elements that are not explicitly modeled in the 2D model from Figure 10.3. For structural static calculations, the 2D modelling of the 3D structure does not result into problems, as the 3D elements do not significantly contribute to the building's stiffness in the along wind direction. However, for dynamic calculations the full 3D building mass should be considered. This concept and the influence on the results are further explained in Appendix D.3.

The division of mass in The Grasshopper model is different compared to the mass division used in the Eurocode acceleration calculations. For the Eurocode calculations as used in this thesis, the mass is assumed equally distributed over the building height. In the Grasshopper model, the structural mass is distributed more in line with the real mass division: a higher percentage structural of structural is located on the bottom of the structure. This more realistic modeling will result in a lower modal mass, compared to the Eurocode accelerations. Therefore, it is expected that the calculated accelerations for the Python model will be a few percent higher than values calculated by the Eurocode procedure.

10.2 Modeling wind load in the frequency domain

This chapter explains how the wind load has been modeled in the frequency domain. The focus in this Chapter is on the mathematical calculation procedures and underlying concepts in the model. The relevant background knowledge about wind engineering is presented more in depth in Chapter 3. Chapter 9 covers the application of this model.

10.2.1 Wind spectrum analysis

As wind is a stochastic process, it has to be modelled with the theory of random vibrations, see Chapter 3. The approach to model wind loads with the theory of random vibrations consists of different steps. These steps combine the dynamic wind and structural properties and together determine the wind-induced response of a structure. The steps are are visualised in Figure 10.4. Steps 1, 2, and 3 determine the wind velocity around the structure and convert this to a load on the structure. The last two steps 4 and 5 represent the structural wind-induced dynamic response.

The following steps can be distinguished:

1. In this first subfigure of Figure 10.4 the wind velocity spectrum, based on the Solari wind spectrum is illustrated. The spectrum describes the distribution of the wind velocities amplitudes over the frequency range. In this spectrum the turbulence is described as a random function of space and time (Advisory Committee on Technical Recommendations for Construction 2008).

2. Subfigure 2 illustrates the aerodynamic admittance function. The aerodynamic admittance function is used to relate the incoming wind velocity spectrum to the wind pressure on a building surface (Zhou et al. n.d.). It describes how the building perceives the different wind fluctuations as a load.

3. Subfigure 3 describes the load spectrum. This resulting spectrum, is the result of the wind spectrum

and the aerodynamic admittance function. This spectrum describes the load amplitude for each frequency.

4. Subfigure 4 describes the mechanical admittance function. This is a function that represents the building's dynamic behaviour, based on its structural properties. It determines the structural response of a building to a harmonic load, with a certain frequency.

5. Subfigure 5 describes the response spectrum, this describes the structural behaviour for a certain building on which a load spectrum is applied. The response spectrum describes the structural effect for the specific wind load, that occurs with a certain frequency on the building.

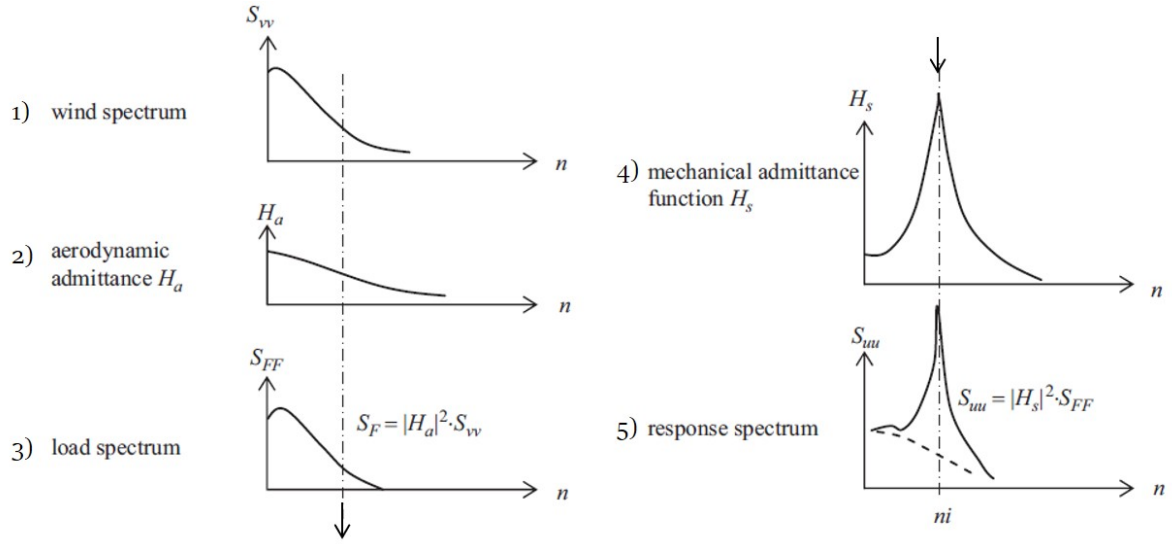

Figure 10.4: *Steps from a wind spectrum to a structural response spectrum. Adopted from (Steenbergen et al. 2012)*

The response spectrum describes both the wind-induced resonance response and the background response. The background response represents the quasi-static load effect, while the resonance response represents the dynamic load responses, see Figure 10.5. The background response mainly depends on the properties of the wind spectrum, while the resonant response is mainly determined by the structure's mechanical admittance function around the eigenfrequency. The structure's eigenfrequency can be recognized by the peak in the structural response in Figure 10.4.4.

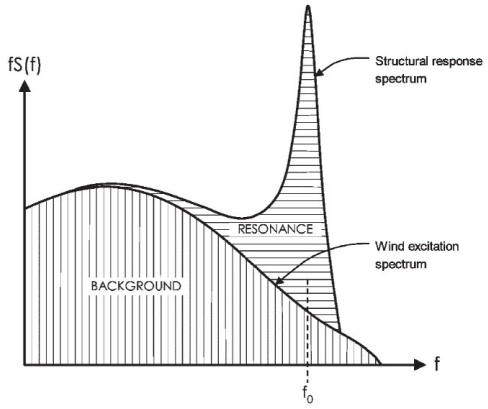

Figure 10.5: *Distribution of the background response and the resonance response. Adopted from (Boggs & Dragovich 2006)*

10.2.2 Modelling the wind profile

In this section the wind parameters and equations will be defined. The wind profile is location dependent. In this report it will be assumed that the considered structure is located in wind area II in the Netherlands. The input values of the different wind parameters are described in Appendix I.

A common method to determine the wind loads on a structure is by making use of a predefined wind spectrum, as explained in Section 3.2.1.2. This wind spectrum depends on the local circumstances, like the mean wind velocity and the turbulence length. Different wind velocity spectra are used in literature, for example the Davenport spectrum and the Von Karman spectrum. In the Eurocode the Solari wind spectrum is applied (Vrouwenvelder 2004), (Eurocode 2005*b*). The Solari velocity spectrum (Eurocode 2005*b*), is described in Equation 10.11.

$$S_u(\omega, z_i) = \frac{\sigma_v^2}{\omega} * \frac{6.8 * x(\omega, z_i)}{(1 + 10.2 * x(\omega, z_i))^{\frac{5}{3}}} \tag{10.11}$$

S_u represents the velocity spectrum, ω the angular frequency, z_i the building height at DOF i, and σ_v represents the standard deviation of the turbulence component. $x(\omega, z_i)$ is defined by Equation 10.12:

$$x(\omega, z_i) = \frac{\omega}{2\pi} * L_t * \left(\frac{z_i}{z_t}\right)^{\alpha} * \frac{1}{V_{ref}} \tag{10.12a}$$

$$\alpha = 0.67 + 0.05 * \ln(z_0) \tag{10.12b}$$

In which L_t describes the reference length scale, V_{ref} the reference velocity, and z_0 the roughness length.

The original spectrum depends on the frequency in hertz, while in this report the circular frequency ω is used. The conversion from f to ω is explained in Appendix J. The height dependence of the Solari wind velocity spectrum is visualised in Figure 10.6a. It is clearly observable that the intensity of the wind spectrum is highest for the lower frequency range, as is in line with the theory from Section 3.1.4.

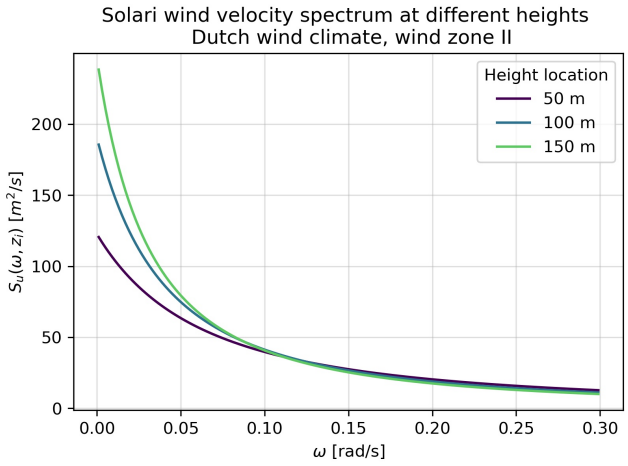

(a) *Solari wind velocity spectrum at* $z_i = 100m$

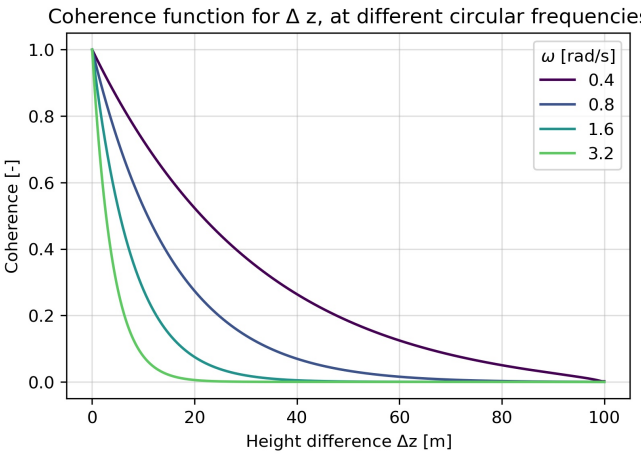

(b) *Coherence for different wind frequencies and height differences*

Figure 10.6: *Illustration of the wind spectrum and the coherence function*

The power spectrum of a fluctuating wind load spectrum S_{Fi} can be derived from the wind velocity spectrum by Equation 10.17 (Dyrbye & Hansen 1997) and (Kareem & Tamura 2013). This equation determines the wind load F_d based on Bernoulli's Equation, that converts the wind velocity to wind pressure. The reduced spatial correlation is taken into account by the aerodynamic admittance function χ, $V(z_i$ defines the velocity at DOF i.

$$S_{Fi}(\omega, z_i) = \frac{4 * F_d(z_i)^2}{V(z_i)^2} \cdot \chi^2 \cdot S_u(\omega, z_i) \tag{10.13}$$

The wind pressures are calculated from the incoming wind velocity by Bernoulli's Equation 10.14 as described in (Dyrbye & Hansen 1997).

$$F_d(z_i) = \frac{1}{2} \cdot \rho \cdot C_f \cdot A_i \cdot V(z_i)^2 \tag{10.14}$$

In which ρ is the air density, C_f a force coefficient and A_i the reference area of DOF i.
The SLS wind velocity profile $V(z_i)$ is described in the Eurocode (Eurocode 2005*b*) by Equation 10.15:

$$V(z_i) = V_{b_{sls}} \cdot k_r \cdot \ln\left(\frac{z_i}{z_0}\right) \tag{10.15}$$

For which the terrain factor k_r and the basic wind velocity $V_{b_{sls}}$ are described by Equation 10.16:

$$k_r = 0.19 \cdot \left(\frac{z_0}{0.05}\right)^{0.07} \tag{10.16a}$$

$$V_{b_{sls}} = V_{b_{uls}} \cdot c_{prob1} \tag{10.16b}$$

The fluctuating wind pressures on a building are caused by wind-gusts, that are a result of the incoming vortices in the wind flow. These vortices do have a dimension in space. The higher the frequency of a wind-gust the smaller this gust is in size. For a large building this means that when one side of the building is affected by a very strong wind gust, the other side will not necessarily be affected as well. These spatial

correlations needs to be included in the wind model, this is done by the aerodynamic admittance factor. In fact this factor compensates for the transformation from a 2d structure to a line-like structural model, as is described in Figure 10.1. An approximation for the aerodynamic admittance χ is described by (Kareem & Tamura 2013):

$$\chi^2 \approx \left[\frac{1}{1 + \frac{\omega\sqrt{A_i}}{\pi V(z_i)}^{\frac{4}{3}}} \right]^2 \tag{10.17}$$

This functions represent the aerodynamic admittance function for an area A_i. Where the relation with the vortex frequency and the wind velocity, is included by the wind frequency ω and the wind velocity V_{z_i}.

The effect of the wind-gust size is not only a factor of importance in the width direction of a building, but also over the height of a building. It can be imagined that the wind-gusts over the height contain a certain correlation: if the top of the tower is hit by a very heavy wind-gust, the second highest floor will simultaneously experience a heavy wind-gust while the bottom floor will barely experience this gust. This coherence can be described by the exponential decay function in Equation 10.18, as described in (Dyrbye & Hansen 1997) and (Ghorbani-Tanha et al. 2009). This coherence function is used to obtain the values of the cross-spectral density matrix.

$$Coh_{ij} = \exp\left(-\frac{|\omega| \cdot C_z \cdot |z_i - z_j|}{\pi \cdot |V_i - V_j|} \right) \tag{10.18}$$

A decay factor C_z of 11.5 is applied in the Eurocode (Dyrbye & Hansen 1997). V_i and V_j define the wind velocities at height i and j. This coherence function is plotted in Figure 10.6b for an increasing height difference. This height difference can represent the floor levels: storeys close to each other have a small height difference. A coherence of 1.0 represents full coherence. It can be observed that for bigger wind gusts, with a lower frequency, the coherence is higher than for small wind gusts.

10.3 Modelling of wind: random vibrations theory

This section covers the application of the theory of random vibrations.

10.3.1 Response spectrum

The functions as described in Section 10.1 are valid for multiple-degree-of-freedom-systems in which the load is described by a discrete To calculate the wind-induced response of the multiple-degree-of-freedom-systems the equations from Section 10.1 can be applied. To model wind loads, spectral load functions have to be used, rather than discrete force vectors. These load spectra describe the wind loads by a stationary Gaussian process, in which the load on each degree of freedom is the result of a random process. This random load is defined by a force spectrum, as described in Equation 10.17.

The response spectrum of a certain DOF j to the random wind load is defined according to Equation 10.19

(Vrouwenvelder 2004). This function describes the wind-induced response of a building.

$$S_{u_j u_j} = \sum_{p=1}^{n} \sum_{q=1}^{n} H_{u_j F_p} \cdot H^*_{u_j F_q} \cdot S_{F_p F_q} \tag{10.19}$$

Coherence is included by the cross spectral terms $S_{F_p F_q}$. By definition the terms in the spectral response function have to be squared. As the transfer function is a complex function, the complex conjugate of this function is required denoted by $H^*_{u_j F_p}$.

The cross-spectral terms $S_{F_p F_q}$ are defined by Equation 10.20 (Ghorbani-Tanha et al. 2009), (Dyrbye & Hansen 1997). The coherence function for the spatial correlation over the height is defined by the exponential decay function as described in (Ghorbani-Tanha et al. 2009) by Equation 10.18.

$$S_{F_p F_q} = \sqrt{S_{F_p} \cdot S_{F_q}} \cdot Coh_{ij} \tag{10.20}$$

From this equation it can be observed that the lower the spatial correlation of the wind loads, the lower the final wind-induced response will be.

This general concept can be applied to a system with or without a TMD. The general formulas do not change if a TMD is applied. The influence of the TMD is taken into account by the transfer functions $H_{u_j F_p}$. The transfer function for a system including a TMD is described in Equation 10.6.

10.3.2 Maximum along-wind accelerations

The wind loads that are applied on the building model are defined with the theory of random vibrations. The randomness of the load is addressed by statistical methods (Vrouwenvelder 2004). Due to this, it is not possible to determine fixed values for the maximum occurring wind loads. Instead, wind loads and wind-induced responses are characterised by a variance spectrum.

From the definition of the response spectrum it follows that the variance of the acceleration and deformation can be obtained by taking the integral of the response spectrum, see Equation 10.22 (Vrouwenvelder 2004), (Ghorbani-Tanha et al. 2009).

For the displacement:

$${\sigma_{u_i}}^2 = \int_0^{\omega} S_{u_i u_i}(\omega)\, d\omega \tag{10.21}$$

For the accelerations:

$${\sigma_{\ddot{u}_i}}^2 = \int_0^{\omega} \omega^4 * S_{u_i u_i}(\omega)\, d\omega \tag{10.22}$$

This calculated variance is a statistical parameter. With this data and statistical methods, the maximum peak acceleration for a certain return period can be determined. This maximum acceleration can then be checked to the building regulations.

To determine the value of the maximum acceleration, the value of the acceleration response variance $\sigma_{\ddot{u}_i}$ has to be multiplied by the peak factor as defined in the Eurocode. This peak factor defines the relation

between the variance and the probability that a certain threshold value is reached within a certain time interval. The maximum along-wind acceleration with a certain return period is defined by Equation 10.23:

$$\ddot{u}_i = k_p \cdot \sigma_{\ddot{u}_i} \tag{10.23}$$

The peak value k_p is defined by Equation 10.24 (Eurocode 2005b):

$$k_p = \sqrt{2 \ln \nu \cdot T} + \frac{0.6}{\sqrt{2 \ln \nu \cdot T}} \tag{10.24}$$

$$\nu = f_0 \cdot \sqrt{\frac{R^2}{B^2 + R^2}} \;\; ; \;\; \nu \geq 0.08Hz \tag{10.25}$$

In which T represents the averaging time for the mean wind velocity, which is 600 seconds in the Eurocode (Eurocode 2005b). Equation 10.25 defines the up-crossing frequency . The value depends on a combination of the fundamental eigenfrequency (f_0), the background response (B) and the resonance response (R). The minimum value of $= 0.08Hz$, corresponds to a minimum peak factor of $k_p = 3.0$.

It can be observed that ν depends on the resonance response. From this it can be understood that the resulting peak factor k_p is slightly affected by an increasing damping ratio, because the resonance response depends on the value of damping ratio, see Appendix C: The higher the damping ratio, the lower the resonance response. The actual peak factor will hence be slightly reduced for buildings with an increased damping ratio, which means that the actual accelerations are reduced as well.
To reduce the complexity of the calculation procedure, this relation is not taken into account in the model. For each building variant, the peak factor is set to the value as calculated for the intrinsic damping ratio of 0.01. This assumption will result in a small overestimation of the resulting acceleration for buildings with a TMD, of a few percent.

10.4 Python script

The modelling procedure as described in this section, has been modelled in a Python script. The developed Python code is attached in Appendix N, including comments.

This Python script determines the maximum 1 year along-wind accelerations for a building with a tuned mass damper. Based on the theory of random vibrations. This script can be used to investigate the mitigating effect of the application of a Tuned Mass Damper on the wind-induced response. Furthermore, the properties of the TMD can be adjusted in the script, which allows for a study of the TMD parameters: mass, stiffness, damping and location.

The workflow of the developed Python model is schematized in Figure 10.7. First, the modal properties that define the input data for the model are computed in the Grasshopper model from Chapter 7. This data is stored in a CSV file. The transfer function as described in Equation 10.6 is determined in Maple. With this data the respone of the system including TMD is determined. The Python libraries NumPy, and SymPy are used to model the random vibrations and perform the frequency response analysis. Matplotlib is used to visualise the data.

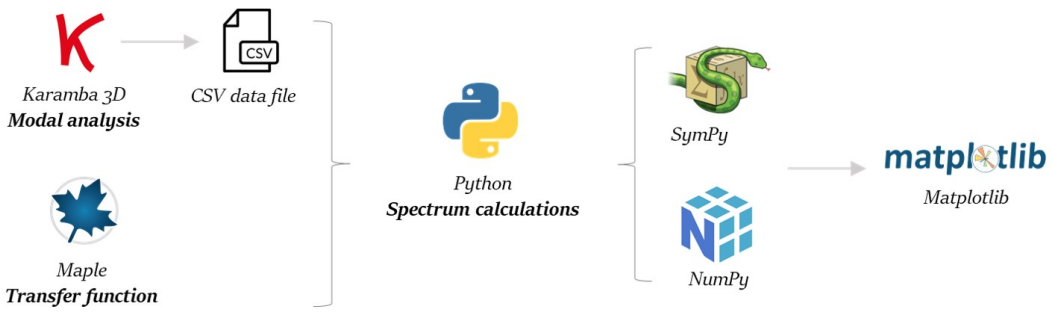

Figure 10.7: *Workflow of TMD design*

10.5 Discussion of the model

The theory behind the developed Python script has been compared to the theory behind the Eurocode acceleration procedure. The accelerations calculated with the script are consequently 10% higher. Taking into account the amount of simplifications, this is considered acceptable. The main differences between the two approaches are:

- The Eurocode procedure inherits assumptions for the mode shapes, only a fully parabolic and uniform mode shape can be applied. The modal masses are determined based on these assumptions, this is a simplification (Dyrbye & Hansen 1997). In contrast, the developed Python script takes into account the actual modal properties as derived from the Grasshopper model. This difference in mode shape appears to be the main reason for the deviations in the results.

- In the Eurocode a white noise spectrum simplification is applied. In the developed script the full wind spectrum is used (Vrouwenvelder 2004). For most cases, the white noise approximation will result in small underestimations of the actual accelerations.

- In the developed Python script, the aerodynamic admittance function has been simplified (Kareem & Tamura 2013). The approach as adopted in the Eurocode is more complex. Nevertheless, the final results seems to be barely influenced by these differences.

- Both the Eurocode and the developed script do not take into account the response of higher order mode shapes. In general, the fundamental mode determines more than 90% of the final response (Ellis & Bre 1980), which is considered acceptable.

- In the developed script, structural mass is lumped to the nearest floor levels. As the structure is heavier on the bottom floors, these floors will inherit more mass, while the top floors are lighter. The full mass is thus not equally distributed over the height. In contrast, in the simplified Eurocode approach, all mass is assumed to be equally distributed over the height. Therefore, more inertia is assumed at the top of the structure, which reduces the dynamic acceleration as bit.

10.6 Overview of the procedure

The overall concept of the dynamic modelling of a building with a tuned mass damper is illustrated in Figure 10.8. As the starting point of the model, a n+1 MDOF system is created that represents a n-storey tall

building, including a TMD. On this system acts a wind load spectrum, determined by the theory of random vibrations.

To determine the response of this system a modal analysis is performed. In this way the MDOF system is converted to a 2DOF system, that represents the first building mode and the TMD. The wind-induced response of this system can be determined by a transfer function. As a final step, the system is transfered back to it original coordinate system. In this way the response of a certain node can be determined.

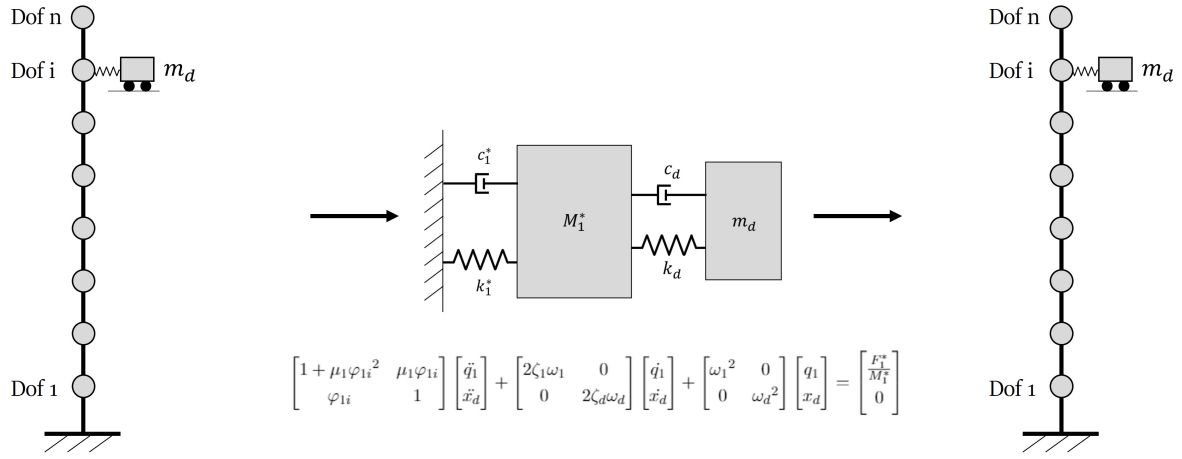

MDOF system:
-n storeys
-1 TMD

2 Dof system
-Mode q1
-1 TMD

MDOF system:
-n storeys
-1 TMD

$$[M]\underline{\ddot{u}} + [C]\underline{\dot{u}} + [K]\underline{u} = \underline{F} + \underline{E}(c_d\dot{v}_d + k_d v)$$

$$m_d\ddot{v}_d + c_d\dot{v}_d + k_d v_d = -m_d\ddot{u}_i$$

$$S_{u_j u_j} = \sum_{p=1}^{n}\sum_{q=1}^{n} H_{u_j F_p} \cdot H^*_{u_j F_q} \cdot S_{F_p F_q}$$

Figure 10.8: *Overview of the different transformations in the analysis*

Chapter 11

Results: TMD effects on a structure

The Python script, that is developed in Chapter 10, can be used to determine the dynamic response of a structure including a TMD. This script can thus be used to determine the mitigation effects of a TMD for each of the building variants from Chapter 7. In this way, it is possible to investigate the TMD parameters and to investigate how a certain target damping ratio can be achieved. In this Chapter case studies are performed on the effectiveness of a TMD. The first case study investigates the effects of a TMD on the accelerations in Section 11.1 . For this case study the developed Python script has been used to determine the response. In the last part of this Chapter, in Section 11.2, a case study is performed on the Baantoren, an actual designed dynamically sensitive building.

11.1 Case study: building variant A

A discussed throughout this report, building variants for which accelerations are governing may require supplemental damping. The governing-design-charts as discussed Chapter 7 can be used to select building variants for which a tuned mass damper could be an interesting option, since these charts include the required target damping ratio. The focus will be on buildings with a height of 100 meters without an outrigger, which corresponds to Figure 11.1. Other case studies have been performed as well which approximately generate the same results.

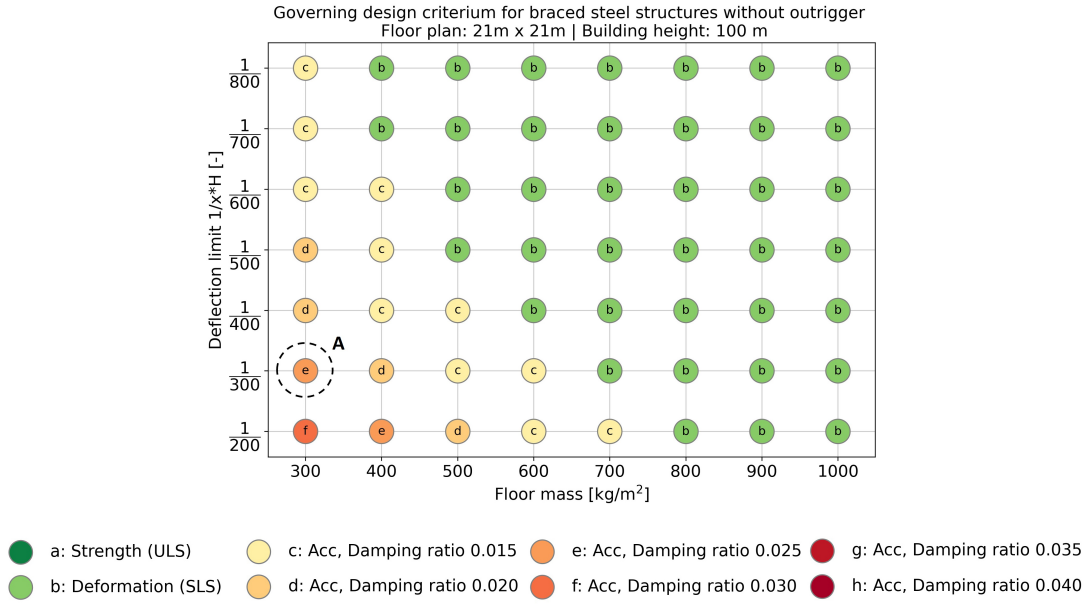

Figure 11.1: *The TMD case study, building A*

To investigate the possible advantages of a tuned mass damper, a building variant *A* has been selected, as visualised in Figure 11.1. This variant is chosen as it represents a very flexible and lightweight building variant, which means that a relatively high amount of supplementary damping is required. From Figure

11.1 it can be determined that the structural building design for variant A is governed by accelerations.For this variant the dynamic response including TMD is determined with the developed model from Chapter 10. The parameters of the TMD as described in 9 are varied to investigate the effect of TMD properties.

11.1.1 Approach

The flowchart from Figure 9.4 describes the different steps to determine the effect of a tuned mass damper. The required target damping ratio can be determined from Figure 11.1. For building A this damping ratio turns out to be 0.025. This target damping ratio can be used as a starting point for the design of a TMD. The expected required mass ratio can be determined with the help of Figure 9.1.

For this target damping ratio of 0.025 the minimum required mass ratio turns out to be 0.002. This means that the TMD mass should minimally be 0.2% of the first modal mass. For this analysis it is assumed that the intrinsic (modal) damping ratio for this variant ζ_d is equal to 0.01. In the Python model, the parameters for the TMD stiffness and TMD local damping ratio are determined based on the optimisation equations 9.4 and 9.7, as described in Chapter 9.

11.1.2 Model input

To determine the response of building A including TMD, the developed Python script is used. Table 11.1 presents the applied input values for the dynamic analysis. The dynamic building properties are extracted from the Grasshopper data as described in Section 10.1.6.

Table 11.1: *Dynamic parameters for case study variant A*

Parameter	**Value**
First eigenfrequency	0.32 [Hz] = 2.04 [rad/s]
First modal mass	1.57e6 [kg]
Total building mass	7.10e6 [kg]
Initial damping ratio	0.01 [-]
Required minimum damping ratio	0.025 [-]
Maximum allowed acceleration	0.16 [m/s^2]
Peak factor K_p (for $\zeta = 0.01$)	3.33 [-]
Amount of DOFS	30 [-]
Eurocode along-wind acceleration without TMD ζ=0.01	0.24 [m/s^2]

11.1.3 Response without TMD

This data is inputted in the TMD Python script to generate the acceleration response spectrum of building variant A. First the original response spectrum for the structure without a tuned mass damper is calculated and visualised in Figure 11.2.

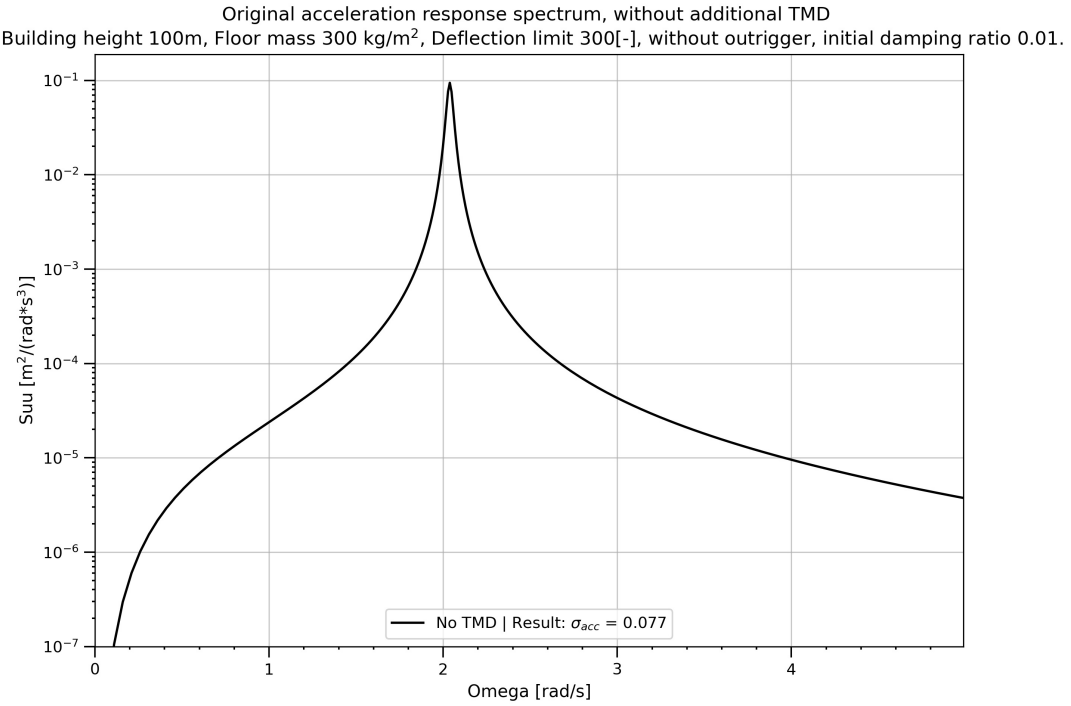

Figure 11.2: *Acceleration response spectrum for building variant A, without a TMD. The area below the chart represents the variance of the acceleration.*

This response spectrum clearly shows a resonance peak in the dynamic response around the first eigenfrequency. This peak is the main contributor to the intensity of the occurring accelerations. Therefore, to mitigate the dynamic response a TMD should damp this peak acceleration.

The area underneath the response spectrum of Figure 11.2 can be considered as the variance σ of the dynamic response, as described in Section 10.3.2. The square root of this integral of the spectrum represents the root mean square (RMS) value of the acceleration. This RMS is equal to the standard deviation σ of the acceleration, since the mean value of the fluctuating response is equal 0. The value of σ_{acc} is included in the legend of the chart and turns out to be equal to 0.077 m/s^2. The maximum acceleration for a return period of one year can subsequently be computed by multiplying the standard deviation with the peak factor, see Equation 11.1, based on the Theory of Section 10.3.2.

$$\text{Acceleration without TMD} = \sigma_{acc} * k_{peak} = 0.077 * 3.35 = 0.26 \text{ m/s}^2 \tag{11.1}$$

The acceleration for the variant without TMD turns out to be 0.26 m/s^2. which is somewhat higher than the calculated acceleration by the Grasshopper model of 0.24 m/s^2, see Table 11.1. As the computed acceleration in this model is somewhat higher than calculated by the Eurocode procedure, it is expected that the minimum required damping ratio should be somewhat higher as well in this model, this means that the damping ratio should be higher than 0.025. According to Figure 9.1 the mass ratio of the TMD thus will need to be higher than 0.2%.

11.1.4 Response with TMD

Figure 11.3 demonstrates the effect of TMD's with different masses on the acceleration response of building variant A. The mass ratio is varied between 0.002 and 0.02 and the TMD parameters (TMD eigenfrequency

ω_d and TMD damping ratio ζ_d) are determined by the near-optimal formulas from (Connor 2003) as described in Chapter 9. It can be observed that an increase in the mass ratio μ results in a decrease of the σ_{acc}. The accelerations are reduced with the same factor.

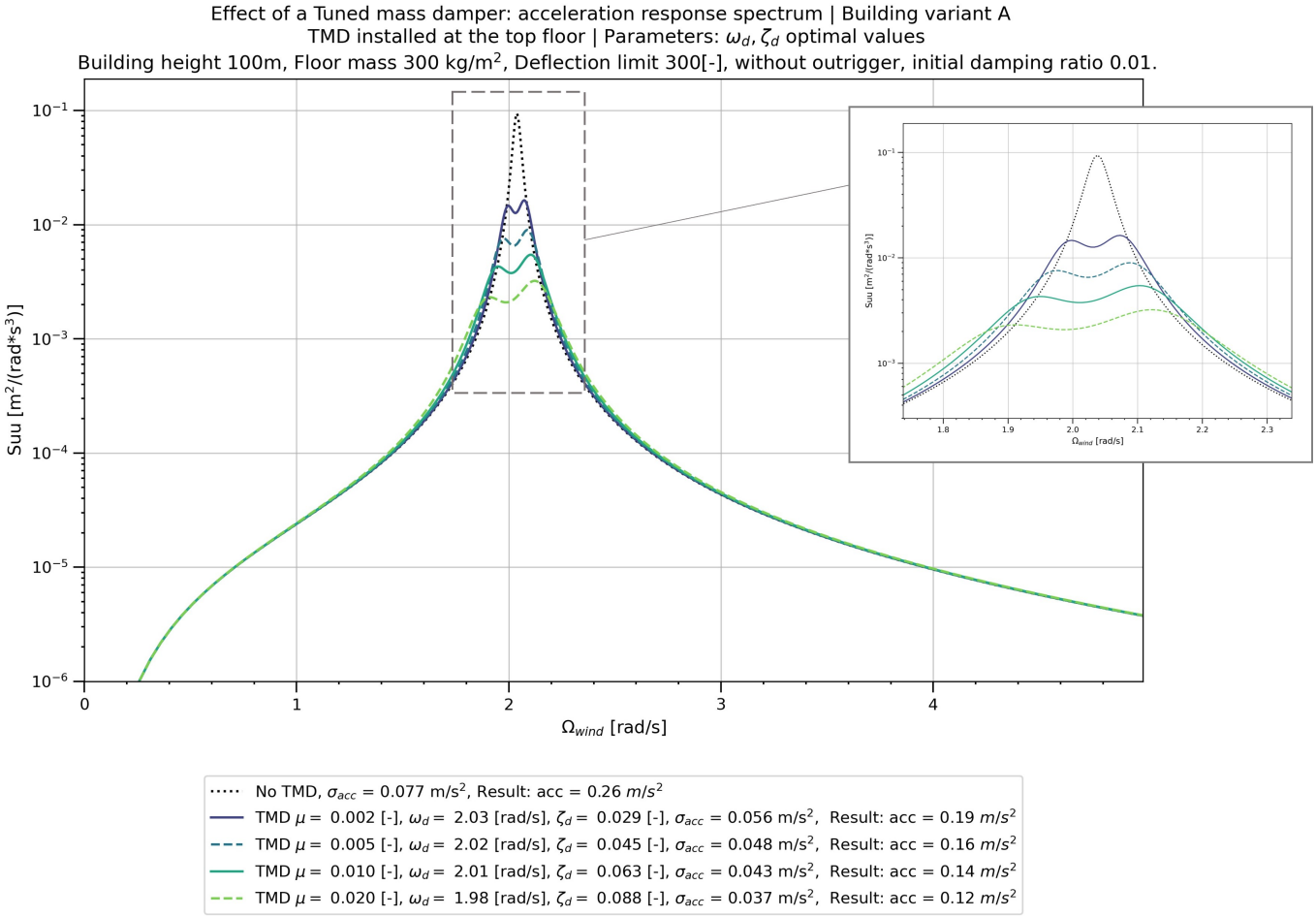

Figure 11.3: *Acceleration response spectra for building variant A including a TMD. The effect of different mass ratios (TMD mass / modal mass) is visualised.*

From the Figure it can be observed that the acceleration resonance response spectrum peak around the first eigenfrequency is reduced by the application of a TMD. It thus can be concluded that the application of a TMD is indeed effective in reducing the along wind acceleration response. This qualitative observation is supported by the quantitative resulting values of σ_{acc}. The higher the TMD mass ratio, the lower the σ_{acc}, hence the lower the occuring along-wind accelerations.

11.1.4.1 Acceleration limits for building variant A

The resulting accelerations for the different TMD's of variant A have been compared to the acceleration limits for the Dutch limit. Figure 11.4 shows this comparison.

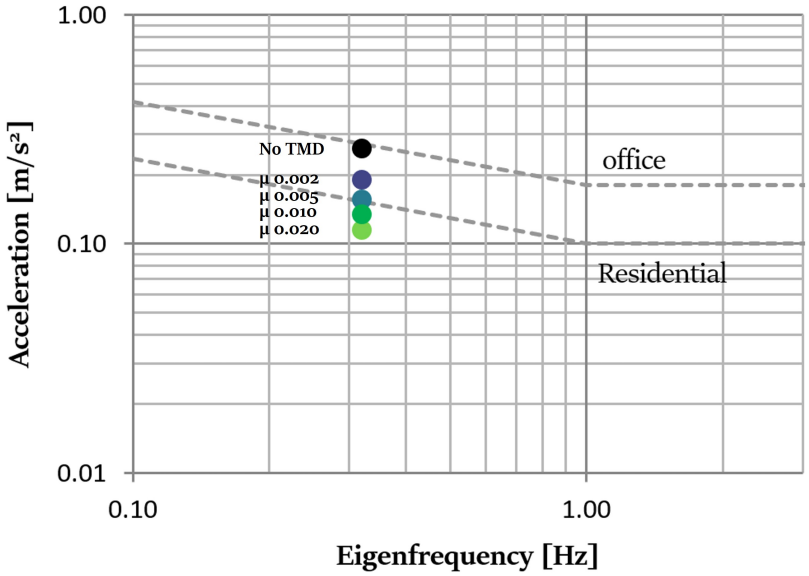

Figure 11.4: *Effect of a TMD for residential building variant A on the Dutch acceleration limits*

As described in Table 11.1 the maximum allowed acceleration for building variant A is 0.16 m/s^2. From the legend of Figure 11.3 it can be observed that a TMD with a mass ratio of 0.005 just fulfills this requirement. With this information the actual TMD mass can be determined. As expected by the tendency of the Python model to overestimate the along-wind accelerations, as described in Section 10.5, the required TMD mass is also somewhat higher than expected by Figure 9.1.

11.1.4.2 Final TMD design

The modal mass of building variant A is 1.57e6 kg, see Table 11.1. This means that the TMD would require a mass of approximately 8000 kg. The design properties of the TMD for the variant with $\mu = 0.005$ are listed in Table 11.2. c_d and k_d are determined with the equations from Equation 9.3 and 9.6.

Table 11.2: *TMD parameters for building variant A*

Parameter	**Value**
μ	0.005 [-]
ζ_e	0.035 [-]
m_d	7850 [kg]
k_d	0.80 [kN/m]
c_d	0.23 [kNs/m]

11.1.5 Alternative vibration mitigation possibilities

It is interesting to compare the structural implications for different wind mitigation strategies. As described in Chapter 7 three methods exist to overcome problems with excessive accelerations: 1) application of supplementary damping, 2) Increase of stiffness, 3) Increase of mass. For the considered building variant A, these methods have been visualised in Figure 11.5.
These different design techniques have implications for the structural design. For all 3 variants these building masses have been determined, see Table 11.3:

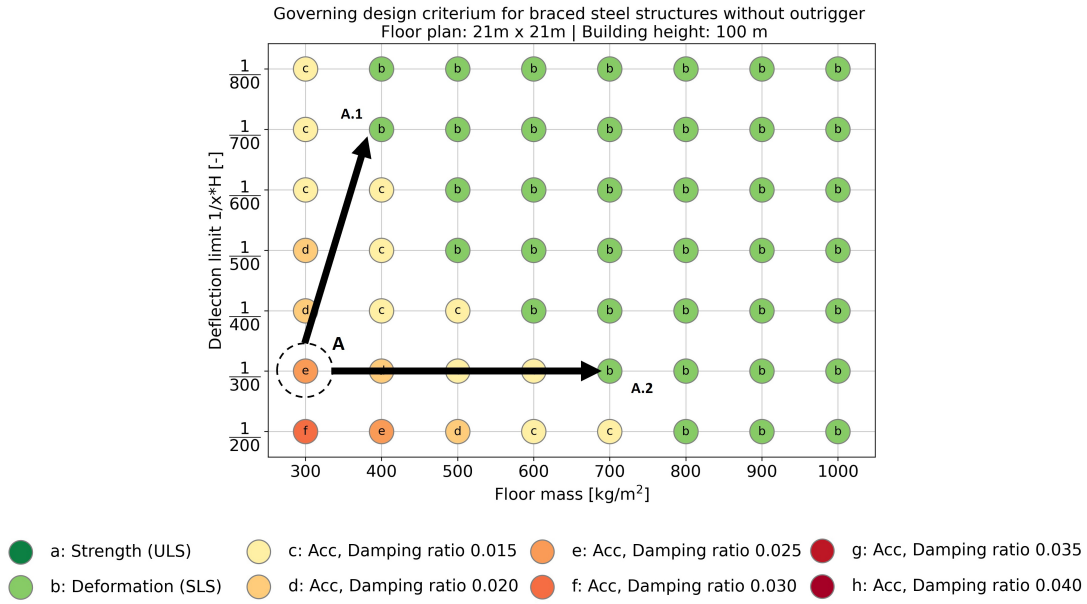

Figure 11.5: *Alternative possibilities to mitigate the wind-induced vibrations: increasing the stiffness or the floor mass*

Table 11.3: *Differences in mass for different wind-mitigation methods*

Mass	**Variant A: With TMD**	**Variant A.1: Increase of stiffness (1/700) mass (400 kg/m^2)**	**Variant A.2: Increase of floor mass (700kg/m2)**
Total structural steel [kg]	1.71e6	2.60e6	1.88e6
Total floor mass [kg]	3.96e6	5.29e6	9.26e6
TMD mass [kg]	1.50e4 (bi-directional)	-	-
Total mass [kg]	5.66e6	7.89e6	1.14e7

From Table 11.3 it can be determined that the variant with the TMD requires the least structural mass. This is beneficial regarding the climate impact and material usage. It is hence proven that the application of a supplementary damper may be beneficial.

On the other hand, it is important to notice that the interpretation of these results is more requires some nuance. Reduction of mass is not the only goal of a structural designer. Variant A.1 for example has a higher stiffness, and hence not only reduces accelerations, but also reduces the deformations. The deflection limit of 1/700 compared to 1/300 requires fewer additional design challenges. Variant A.2 inherits more mass in the floor system. This can be considered as a waste of material, but on the other hand, additional mass may be beneficial for the building climate, acoustics and fire safety requirements, as described in Chapter 4. The possibilities and opportunities of applying supplementary damping must therefore be weighted well and reconsidered for each design situation.

11.1.6 The effect of the TMD location

As explained in Chapter 9 the effectiveness of a TMD is influenced by the height on which the TMD is installed. In general the first mode is the governing mode for wind-induced accelerations. In these cases the top floor is the optimal TMD location. The Python script is used to study the quantitative effect of

different TMD locations. The previously discussed TMD with $\mu = 0.005$, $\omega_d = 2.02 rad/s$ and $\zeta_d = 0.045$ for building variant A is studied again. The mitigating effects of the TMD at 50m, 70m, 90m and 100m are investigated. This location study is visualised in Figure 11.6. The variant in which the TMD is installed at 100 meters represents the same design variant as that of Figure 11.3 with $\mu = 0.005$.

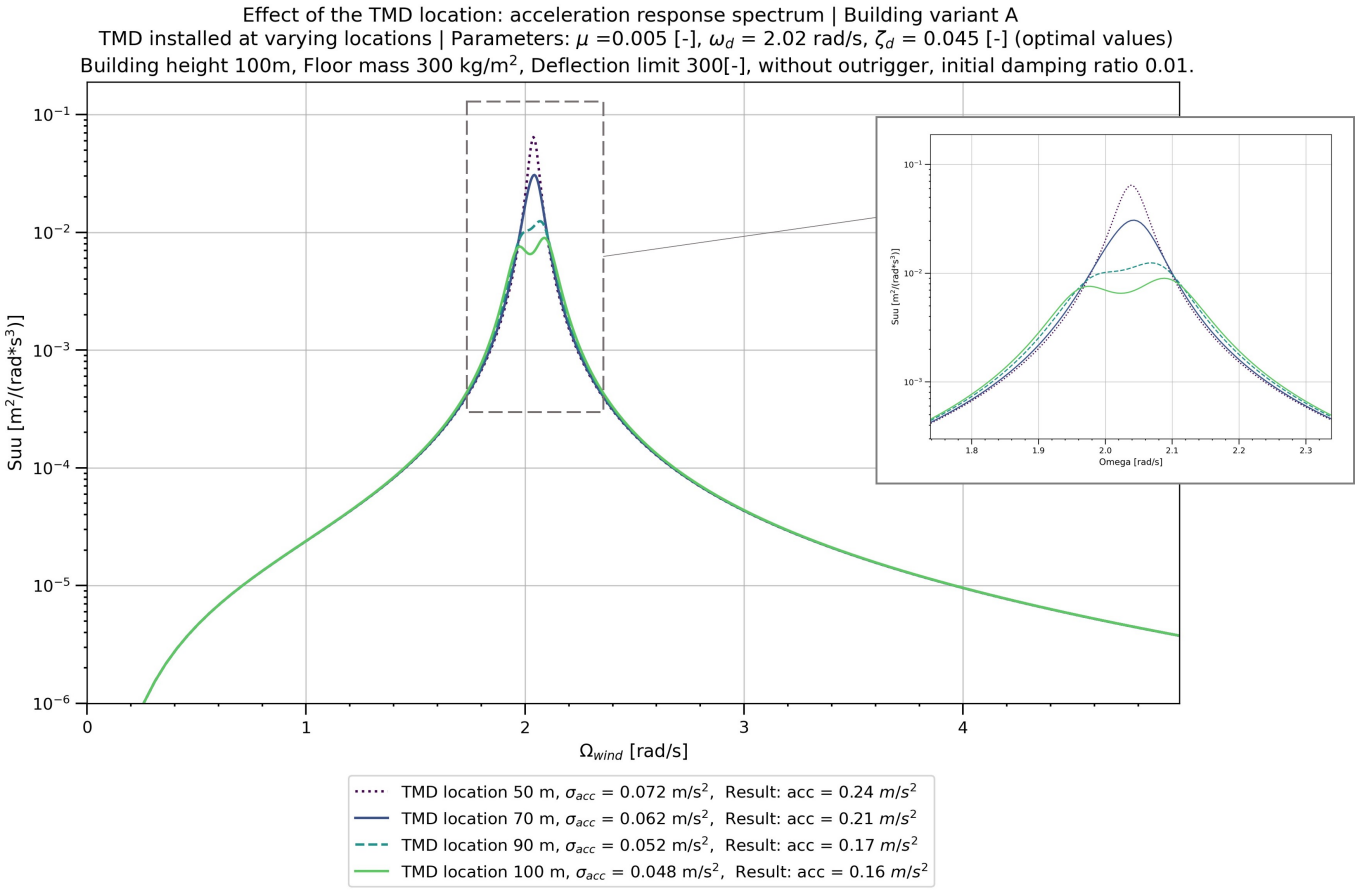

Figure 11.6: *The effect of the TMD location (in height) on the acceleration response spectra for building variant A.*

A schematized overview of the results is shown in Figure 11.7. It can be observed from Figure 11.6 that the resonance peak is damped less effectively for lower installation heights.

From the location analysis in Figure 11.7, it is clear that the positive effect of a TMD decreases if the TMD is installed at lower heights. If the effect of a TMD at the top of the tower is considered as an effectiveness of 100%, then a TMD installed at a height of 50 meters only has an effectiveness of 20%, see Figure 11.7. This means that a significantly bigger TMD is required to obtain the same final result, which is not efficient. On the other hand, if the TMD is installed at 90 meters it is still 90% effective for building variant A, see Figure 11.7. This option may be beneficial for the allocation of the penthouse for example. It is thus possible that the overall cost-efficiency of the TMD can increase. The reduction in TMD effectiveness could be considered acceptable in that case.

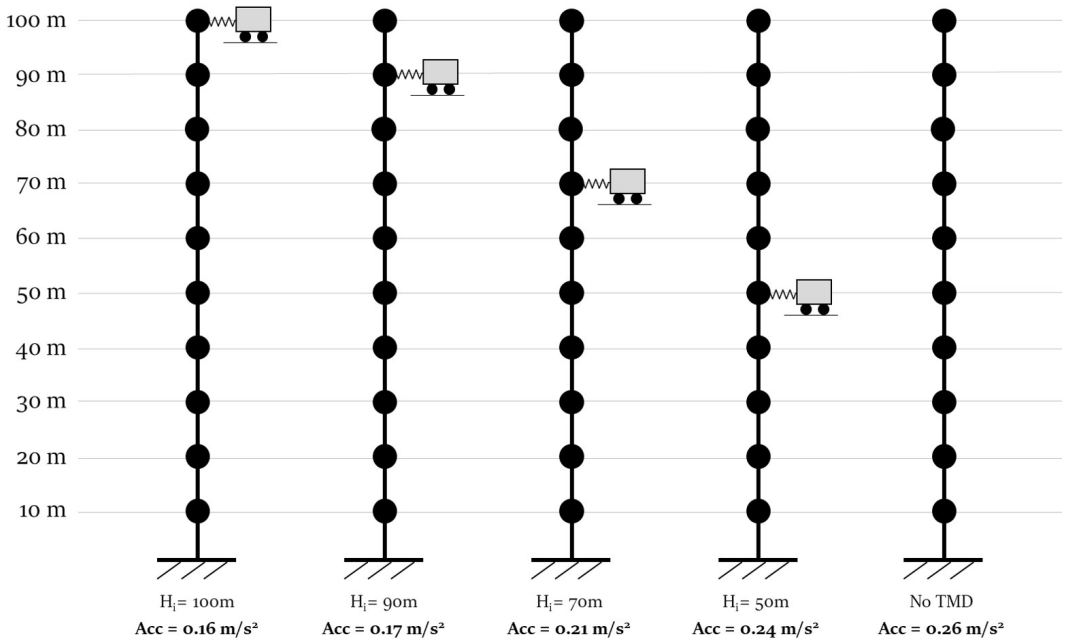

Figure 11.7: *The effect of the height location of a TMD on the maximum acceleration. TMD properties:* $\mu = 0.005$, $\omega_d = 2.02 rad/s$, $\zeta_d = 0.045$

It is clearly observable that the relationship between the effectiveness and the installation height of the TMD is nonlinear. This can be understood by taking a look at the variant's mode shape, see Figure 10.3. The effectiveness of the TMD can be traced back to the displacement of the TMD floor. The bigger the excitation of the floor on which the TMD is installed, the higher the TMD effectiveness. As the displacements of the fundamental mode shape are assumed to be parabolic, it can be understood that the relation between TMD location and effectiveness is also nonlinear. Moreover, the effect of an increase in damping ratio reduces with higher values of the effective damping ratio, this also influences the small deviations in effectiveness between installations at 100 meters and 90 meters.

11.2 Case study: Baantoren

In this section a case study to the application of a TMD in the Baantoren is presented. This case study provides an example of the possible beneficial effects of the application of a TMD. This example is meant to illustrate the order of magnitude of the possible befits regarding mass, cost, and material. The quantitative values of the benefits dependent highly on each specific design situation and building properties.

A Dutch building in which dynamic issues played a major role in the design is the Baantoren, see Figure 11.8. This 153 meter tall tower, with a floor plan of 21m x 21m, was planned to become the most slender high-rise tower of the Benelux with a slenderness ratio of 7 (Treels 2019*a*). The tower was designed as a concrete tube structure, with a concrete core of 7m x 7m and concrete floor slabs. Eventually, the design as covered in this case study was never built, but the tower still remains interesting for a case study.

Figure 11.8: *Render of the Baantoren. Adopted from The Powerhouse Company*

Table 11.4: *Parameters of the Baantoren*

Parameter	**Value**
Height	153 [m]
Floor plan	20 x 23 [m]
Fundamental eigenfrequency	0.21 [Hz]
Intrinsic damping ratio	0.01 [-]
Distributed mass	204000 [kg/m]
Fundamental modal mass	$8.13 \cdot 10^6$ [kg]

11.2.1 Dynamic mitigation strategy

During the design of the Baantoren, the building turned out to be dynamically sensitive. This dynamic sensitivity was mainly induced by the high slenderness ratio. Mass was not an issue regarding dynamic behaviour due to the applied concrete.

As described in this report three strategies exits to reduce the dynamic response: increase of mass, stiffness, or damping. In the Baantoren, it was decided to increase the building stiffness by applying 2% additional reinforcement over the first half of the building height. Moreover, additional H-profiles were included in the cast concrete of the bottom floors. The amount of extra steel mass is shown in Table 11.5. This additional reinforcement was not necessary to comply with the deformation and strength requirements, see Chapter 2. The cost of the additional steel is presented in Table 11.5 as well.
It can be investigated how much structural steel could have been saved by the application of a damper. For that purpose, the additional steel mass can be compared to the mass of a steel TMD.

Table 11.5: *Additional steel masses as applied in the original Baantoren*

Additional reinforcement	**Mass**	**Cost**
Reinforcement	$170 \cdot 10^3$kg	€332,000 (€2.00/kg)
HD profiles	$40 \cdot 10^3$ kg	€99,000 (€2.50/kg)
Total additional mass	$210 \cdot 10^3$ kg	€431,000

11.2.2 Application of a TMD

Based on the information from Chapter 9 and Case study A, it is assumed that a tuned mass damper in steel with a mass ratio of 0.5% would be enough to fulfill the requirements. Based on the modal mass from Table 11.4 this would require a TMD of approximately 40.000 kg. This mass can be compared to the amount of additional structural steel that could have been saved. This is visualised in Table 11.6.

The costs of a TMD are highly dependent on specific design factors, as described in Section 9.1.8. In this study the cost of the TMD are approximated to be €150,000 (Meinhardt 2021).

In addition, by saving structural steel, the climate impact of a building can also be reduced. The production of 1000 kg of structural steel, results in the emission of 480 kg of CO_2 (*Staal & CO2 | Bouwen met staal* n.d.).

Table 11.6: *Mass and Co2 savings by applying a TMD*

Additional reinforcement	**Mass**	**Cost**	**CO_2**
Additional steel savings	$210 \cdot 10^3$ kg	€430,000	$101 \cdot 10^3$kg tons
TMD	$-40 \cdot 10^3$ kg	-€150,000	$-19 \cdot 10^3$ kg
Total savings	$170 \cdot 10^3$ kg	€281,000	$81 \cdot 10^3$ kg

From this case study it turns out that the application of a TMD can indeed save material and cost. Approximately 170,000 kg of structural steel could have been saved by the application of a TMD in this case. This could save up to a few hundred thousand euro's. Furthermore, for the application of a TMD could have reduced the Co2 by more than 80,000 kg. This reduction in Co2 could be increased by applying a more sustainable TMD material, like water from sprinkler tanks. In addition, the higher the dynamical sensitivity of a building, the larger these benefits will become. Since the amount of required additional material to comply with the requirements would increase. It must be noted that the application of a TMD could also result in a loss of rentable space, this is not taken into account here.

11.3 Conclusions

- For the considered building the required target damping ratio can be achieved efficiently by tuned mass dampers with a mass ratio in the order of 0.5% to 1%.
- A TMD is the most effective installed at the upper floors of a structure. The mitigating effect drops fast if the TMD is installed at lower floor levels, and almost vanishes if the TMD is installed at half of the building height.
- It is shown that by applying a TMD in the Baantoren approximately 210,000 kg of steel, 170,000 euro, and 80 tons of CO_2 could have been saved.

Part IV

Discussion & conclusion

Chapter 12

Discussion

As this report covers a broad subject, it is inevitable to make some assumptions and simplifications. Throughout this report, these assumptions were made with the relevant background theory in mind to obtain a balanced set of assumptions. Nevertheless, the results will be influenced to some extent. This is not a problem, since the focus of this research was on the general dynamic behaviour of tall buildings, rather than finding individual solutions. The results should be considered with care and should not be directly applied to individual design cases.

This chapter discusses the simplifications and assumptions that are expected to have the largest impact on the obtained results. First, the relevant aspects and assumptions of the Grasshopper model are discussed. Second, the assumptions and simplifications on the tuned mass damper (TMD) Python script are discussed.

12.1 Variant study

As the variant study in this thesis covers more than 6500 configurations, it was important to reduce the computation time. The amount of detail in the Grasshopper model is a trade-off between this computational efficiency and the accuracy of the results. It is unavoidable that these assumptions influence the accuracy of the result. However, within the scope of this research, this loss of accuracy is acceptable.

12.1.1 Across-wind

It was not possible to model the effects of across-wind vibration. The model building properties were chosen in such a way that the effects of this simplification on the results are minimised, as explained in Chapter 7. It is expected that this simplification results in a small underestimation of the accelerations. Furthermore, due to this simplification, the results of this research are not directly applicable to buildings with a slenderness ratio larger than 7, since in these situations across-wind motions can become governing.

12.1.2 Torsional-wind

Torsional wind accelerations have not been taken into account, since these are highly influenced by the building geometry. The applied building model is considered as torsional insensitive. Therefore, the torsional effects are not expected to have a large impact on the results, because of the symmetric building shape. For buildings with an asymmetric shape or a large facade area, the results of this research should be interpreted with care, as explained in Chapter 3.

12.1.3 Surrounding environment

Buildings in the surrounding environment of a structure, in particular high-rise buildings, will affect the occurring wind loads. This can result in additional along-wind accelerations and vortex shedding. These effects are specific for individual buildings and have to be investigated by wind tunnel tests. Therefore, this effect could not be taken into account.

12.1.4 Structural material

The Grasshopper model geometry represents a steel structure. Throughout this thesis results are extrapolated to concrete and timber structures as well. This extrapolation is solely based on the values of the structural mass and stiffness. Other material properties, like the cracking of concrete, have not been taken into account.

12.1.5 Foundations

In the model the foundation was considered fully clamped, as is often done in the preliminary design phase. This simplification was necessary to reduce the complexity of the parametric variant study, as described in Chapter 7. Not taking into account, the rotational capacity of the foundation affects the dynamic properties. For example: the building stiffness, the eigenfrequency, and mode shape. The interplay of these parameters is complex. Therefore, the influence of this simplification is difficult to predict.

12.1.6 Model assumptions and simplifications

To reduce the computational complexity of the model, iterative factors such as the CsCd factor and the second-order factor have been simplified, as described in Chapter 7. The required structural mass could be overestimated due to these assumptions, which will slightly influence the results. To determine the CsCd factor, an estimation of the eigenfrequency, generated by a simplified model, has been applied. For the extreme cases, this results in an underestimation of the CsCd factor in the order of 5% to 10%.

The simplified value of the second-order effect is based on the target deflection, as defined by the deflection limit. This results in an overestimation of this effect for variants that are governed by strength. In the extreme cases (combination of: small height, lenient deflection limit, heavy floor mass) this overestimation can be as high as 15%.

12.1.7 Cross section optimisations

The cross-sectional optimisation algorithm of the Karamba optimisation tool ensures that all cross sections meet the ULS requirements, as explained in Chapter 7. It must be noted that the sizes of actual cross sections are bounded by physical limits. The physical feasibility of the size of the cross sections has not been taken into account in the model. In particular, very stiff and tall building configurations, may turn out not to be feasible in practice. In addition, buckling is not considered. This is not expected to be a problem due to the relatively small buckling lengths.

12.1.8 Damping

The initial damping ratio is assumed to be 1% (0.01) for all variants, as is standard in structural practice. This value includes a combination of the intrinsic component and to a lesser extend the aerodynamic damping component. In general, the initial damping ratio is difficult to determine and depends on different factors, as described in Chapter 5. This will influence the results of the governing-design-criteria charts to some extent. On the one hand, in some cases the intrinsic damping ratio will turn out to be higher than expected, supplementary damping may then not be necessary. On the other hand, these uncertainties in the value of the intrinsic damping ratio can be considered as a motivation for the implication of dampers to decrease design uncertainties, as explained in Chapter 1.

12.1.9 Acceleration calculations

The applied Eurocode acceleration procedure, procedure 2, only applies to the two extreme mode shapes, namely linear and parabolic. The observed mode shape from the Grasshopper model turns out to be an intermediate shape. In such cases, it is recommended to apply the parabolic mode shape (Steenbergen et al. 2012). This assumption results in an overestimation of the accelerations. The maximum observed difference between the uniform and parabolic mode shape of the accelerations was 30%. Since the occurring Grasshopper mode shapes are relatively close to the parabolic shape, the overestimations are expected to be smaller, in the order of 10%.

12.1.10 Acceleration limits

The Dutch limits have been applied throughout this report. As described in Chapter 2 some doubts occurred on the Dutch acceleration limits, these seem to be too lenient. This will influence the results. When stricter acceleration limits would be applied, like the ISO regulations, the application of dampers will become beneficial in more design situations.

12.1.11 Mass

The structural floor masses have been varied throughout this report. A reduction of the floor mass results in material savings. However, additional aspects such as sound insulation and fire safety are also affected by the mass, as discribed in Chapter 4. The drawbacks and benefits of a reduced floor mass should be considered carefully in every design case.

12.2 Tuned mass damper design

In Part III the practical aspects of a TMD have been investigated by a numerical analysis based on the theory of random vibrations. This analysis is a simplification of reality. The output as generated by the Grasshopper model has been used again as the input for this TMD analysis. Therefore, all assumptions and simplifications as described in Section 12.1 apply on this TMD analysis as well.

12.2.1 Verification of the results

The quantitative results of the analysis will be less accurate due to the fact that these values depend on a lot of different parameters, which are all based on assumptions, rather than wind tunnel tests.
The resulting generic TMD behaviour from the analysis is reliably modelled, for the following reasons. Firstly, the quantitative results have been compared with the Eurocode accelerations, as described in the next paragraph. Furthermore, the qualitative results of the analysis are close to theoretically expected results. Finally, the observed results are in line with international literature.

12.2.2 Assumptions Eurocode

The theory behind the developed Python script has been compared to the theory behind the Eurocode acceleration procedure. The accelerations calculated with the script are consequently 10% higher. Taking into account the amount of simplifications, this is considered acceptable. The main differences between the two approaches are:

- The Eurocode procedure inherits assumptions for the mode shapes, only a fully parabolic and uniform

mode shape can be applied. The modal masses are determined based on these assumptions, this is a simplification (Dyrbye & Hansen 1997). In contrast, the developed Python script takes into account the actual modal properties as derived from the Grasshopper model. This difference in mode shape appears to be the main reason for the deviations in the results.

- In the Eurocode a white noise spectrum simplification is applied. In the developed script the full wind spectrum is used (Vrouwenvelder 2004). For most cases, the white noise approximation will result in small underestimations of the actual accelerations.

- In the developed Python script, the aerodynamic admittance function has been simplified (Kareem & Tamura 2013). The approach as adopted in the Eurocode is more complex. Nevertheless, the final results seems to be barely influenced by these differences.

- Both the Eurocode and the developed script do not take into account the response of higher order mode shapes. In general, the fundamental mode determines more than 90% of the final response (Ellis & Bre 1980), which is considered acceptable.

- In the developed script, structural mass is lumped to the nearest floor levels. As the structure is heavier on the bottom floors, these floors will inherit more mass, while the top floors are lighter. The full mass is thus not equally distributed over the height. In contrast, in the simplified Eurocode approach, all mass is assumed to be equally distributed over the height. Therefore, more inertia is assumed at the top of the structure, which reduces the dynamic acceleration as bit.

12.2.3 Wind model

For this research, a wind model based on the theory of random vibrations has been used. This wind model is based on the theoretical Solari wind spectrum, as explained in Chapter 10. The theory of random vibrations and the application of wind spectra are approximate methods. Based on literature, it is believed that the results generated with theoretical wind spectra are reliable enough to fit the generic character of this research. To obtain more better insights in the wind velocity profile, wind tunnel tests have to be performed.

12.2.4 Practical TMD aspects

In this research, the TMD has been considered a theoretical device with a mass, stiffness, and damping ratio. These properties are important for the preliminary design of a TMD. However, for the final design, more practical aspects must be taken into account as well. Such as the type of TMD, the size of the TMD, tolerances, tuning range, material, etc.

12.2.5 Numerical analysis

The determination of the damper behaviour is determined by a Python script. This results in a numerical solution, rather than an analytical solution, which inevitably results in numerical errors. Parameters that influence those numerical errors, such as the step size of an integral, have been varied to ensure that these errors would not influence the results significantly. The step size has been chosen such that the results do not change for finer step sizes, for at least two decimal places. The applied Python script is attached in Annex N.

Chapter 13

Conclusion and recommendations

13.1 Answer to the main research question

Based on this research conclusions are drawn and recommendations are made. The main research question as defined in Section 1.3.1 can be answered:

In what way can supplementary damping be applied in Dutch, slender, tall buildings to efficiently meet the structural design requirements?

When taking into account the specific conditions and assumptions of the research, the answer to the main research question can be defined as follows:

The application of supplemental dampers proves to provide opportunities for buildings in a height range of 60 to 130 meters with the following properties:

- For steel buildings with a lightweight floor system around 300 kg/m^2 and a regular top deflection limit of 1/800.
- For steel buildings with a relatively lightweight floor system, around 500 kg/m^2 and a reduced top deflection limit $\leq$ 1/500.
- For new types of lightweight and flexible structures, such as timber high-rise buildings.

For these types of buildings a target damping ratio between 2% and 4% turns out to reduce most along-wind accelerations to an acceptable level.

This target damping ratio can be achieved efficiently by tuned mass dampers with a mass ratio in the order of 0.5% to 1% to the modal mass, installed at the upper floor levels of a building.

13.2 List of conclusions

When taking into account the specific conditions and assumptions in this research, the following subconclusions can be drawn, that together answer the main research question as defined in Section 13.1.

1. The application of supplementary damping will provide opportunities for the design of relatively lightweight and flexible (non-stiff) buildings. These buildings can be considered as dynamically sensitive. For these types of buildings, the application of supplemental dampers can be beneficial, since a target damping ratio between 2% and 4% turns out to reduce most along-wind accelerations to an acceptable level. From this research two design situations can be defined for which the application of dampers can be beneficial:

   (a) For the conventional types of high-rise buildings in which accelerations are governing. This turns out be the case for buildings with very lightweight floor systems of approximately 300 kg/m^2 (CLT floors) and a default deflection limit of around 1/800. Accelerations are governing as well for buildings with reduced deflection limits, $\leq 1/500$ in combination with a floor mass lower than 500 kg/m^2 (steel-composite floors).

   (b) For the design of new types of lightweight and flexible structures, like timber high-rise buildings. Such structures are barely feasible in the current situation.

2. Tuned mass dampers with a mass ratio in the order of 0.5% to 1.0% of the modal building mass, are effective in achieving the required target damping ratios. The application of a TMD is most effective when installed at the upper floor levels of a structure, the efficiency drops rapidly for a TMD installed at lower floor levels.

3. Three possible wind-induced acceleration mitigation strategies exist: an increase of mass, increase of stiffness, or an increase of the damping. The benefits of applying supplemental dampers compared to the other mitigation strategies depends highly on the particular design requirements. Therefore the benefits of the application of a TMD differs largely per design case. A case study on the 153 meter tall Baantoren was performed to provide an indication of the benefits. In this study it was shown that approximately 170,000 kg of additional reinforcement steel and 80 tons of CO_2 could have been saved by the application of a TMD, since the governing design criterion shifts from accelerations to deflection. This could result in cost savings in the order of a few hundred thousand euros. The benefits for dynamically more sensitive buildings will be even larger.

4. For typical Dutch high-rise buildings with regular stiffness requirements and concrete floors, most designs are governed by the deflection criteria. For these buildings, the application of supplemental dampers will not be very beneficial. However, some benefits can still be achieved by incorporating a reduced dynamic amplification factor that accounts for the mitigation of fluctuating wind loads. This could result in a reduction of the governing lateral wind loads by 15%. Whether this results in cost savings, differs per individual design case.

5. For safety and reliability reasons, the mitigating effects of tuned mass dampers may only be taken into consideration in the design of the serviceability limit state load cases. They can thus only be used to comply with the acceleration and deflection design criteria.

6. The Dutch acceleration requirements turn out to be relatively lenient, which may result in discomfort for building occupants. In the current Dutch high-rise buildings, accelerations will normally become as high as these extreme limits. However, for future dynamically sensitive buildings this could result into accelerations problems. When applying stricter acceleration criteria, that are more in line with internationally established regulations, the potential benefits of the application of supplemental dampers increases.

This research proves that the application of supplementary damping in Dutch high-rise can be beneficial for slender and lightweight structures. The application of tuned mass dampers creates new design opportunities regarding structural material savings, climate impact, foundation costs, occupant comfort,timber high-rise design, and design uncertainties. In conclusion, supplemental dampers are not a solution to all challenges in the design of structural high-rise buildings, but they can prove to be a valuable contribution to the toolbox of Dutch structural engineers.

13.3 Recommendations

From the performed research, recommendations can be made. These recommendations are mainly addressed to Dutch structural engineers, that deal with the design of dynamically sensitive high-rise buildings.

- It is concluded that the application of supplemental dampers, like tuned mass dampers, can provide opportunities for the design of Dutch high-rise buildings. Therefore, it is recommended to be alert for dynamically sensitive buildings, in which these opportunities may occur. For the design of dynamically sensitive structures the application of dampers should be considered just as seriously as the other mitigating options: the increase of mass or stiffness.

- For the design of dynamically sensitive structures and for the application of dampers, structural engineers should closely collaborate with experienced experts from wind engineering and damping engineering firms. The subject of wind dynamics is an extensive and complex subject and should be considered as a separate field of expertise, just as the fields of building physics and soil mechanics.

- Engineers in the Netherlands should be careful when they apply the Dutch acceleration regulations for the design of high-rise buildings. As discussed in Chapter 2 the extremes of the Dutch regulations seem to allow for too high accelerations, in comparison to international building codes and literature. In contrast to these international codes, proper literature backgrounds seem to be lacking for the Dutch acceleration regulations. In standard buildings this will not induce large problems, as the accelerations will simply not reach the extreme values of the limits. However, for future dynamically sensitive buildings, this could become an issue. Therefore, further research on the Dutch limits is recommended.

- Engineers are recommended to be careful with the interpretation of the calculated eigenfrequencies for their buildings. Nowadays, the eigenfrequency of a structure can be easily determined by finite element programs. However, structural engineers should be aware that these values are based on their own modelling input. These values can vary significantly from the real physical behaviour. It is therefore important to perform sensitivity analyses on the calculated eigenfrequencies, especially when a TMD will be applied. Equations like Equation F.2 from NEN1991-1-4, should only be applied to obtain rough estimates of the eigenfrequency. This equation is not suitable for the estimation of the eigenfrequency for dynamically sensitive structures.

13.4 Further research

As this report covers a broad topic, a lot of opportunities for new research arises. These topics are subdivided in two categories: new research topics and topics that focus on the a continuation of the current research. Firstly, the suggestions for new research topics are about separate subjects, with new main research questions that are not directly related to this current research. Secondly, the suggestions on the continuation of the research offer possibilities for an expansion of the scope of this report, to further develop the answer to the main research question.

13.4.1 Interesting new research topics

- Additional research on the (Dutch) comfort requirements would be insightful, and even important. Defining the tolerance limits to acceleration is an ongoing topic of international research (Kwok et al. 2015). Better understanding of this topic could result in savings and prevent wind-induced problems.
- Based on this research, the design of timber high-rise buildings in combination with the application of supplemental dampers appears to be a promising combination. Further research is necessary to quantify the opportunities and identify the challenges.
- Better approximation methods of the intrinsic damping ratio could reduce the dynamic design uncertainties, which could result in savings and prevent wind-induced problems. This is an ongoing topic of research by TNO (Gomez 2019).
- Research on performance-based deflection limits could result in a new, more efficient, approach to the design of tall buildings.

13.4.2 Continuation of the research

- The across-wind response can be governing for tall and slender buildings. It could be interesting to include these effects in the variant study. For example, by applying the Canadian building code.
- Taking into account the foundation effects in the Grasshopper model could be interesting and would allow for a better interpretation of the results.
- The mitigating effects of different types of dampers like viscous and viscoelastic dampers could be investigated. Moreover, active damping systems could be included in the research.
- Different types of stability systems could be included in the analysis, like a tube structure and a concrete core system. In addition, heights up to 250 meter could be investigated.
- The building shape has a large influence on the wind-induced response. Therefore, it would be interesting to include the building shape as an additional parameter in the variant study. For example, by CFD analyses or by wind tunnel tests.

- The effects of a TMD could be determined by a finite element analysis. This would allow for insight into the exact structural effects. Moreover, a finite element analysis would allow for the modelling of different types of dampers as well.

Bibliography

Abrahamsen, R. & As, M. L. (2016), 'Mjøstårnet – Construction of an 81 m tall timber building', p. 44.

Advisory Committee on Technical Recommendations for Construction (2008), *Guide for the assessment of wind actions and effects on structures.*

Alexander, N. (2010), *Seismic Analysis.*
URL: *https://www.amazon.com/Seismic-Analysis-2nd-Edition/dp/1445279703*

Aly, A. M. (2012), 'Proposed robust tuned mass damper for response mitigation in buildings exposed to multidirectional wind', p. 28.

An introduction to CFD: what, why and how (n.d.).
URL: *https://www.femto.nl/stories/what-is-cfd/*

Boggs, D. & Dragovich, J. (2006), 'The nature of wind loads and dynamic response', *Special Publication* **240**, 15–44.

Borgström, E. & Fröbel, J. (2019), *The CLT handbook.*

Burton, M. (2021), 'Perception and tolerance of accelerations'.

Burton, M., Kwok, K. C. S. & Abdelrazaq, A. (2015), 'Wind-induced motion of tall buildings: designing for occupant comfort.'.

Chopra, A. K. (1995), *Dynamics of Structures.*

Christopoulos, C. & Montgomery, M. (2013), 'Viscoelastic coupling dampers (VCDs) for enhanced wind and seismic performance of high-rise buildings montgomery', *Earthquake engineering &structural dynamics* (42).

Clough, R. & Penzien, Y. (1995), 'Dynamics of structures'.

Connor, J. J. (2003), *Introduction to Structural Motion Control.*

De Vries, P., Fennis, S. & Pasterkamp, S. (2013), *Veiligheid*, Bouwen met staal.

Dlubal (2019), 'Mode Shape'.
URL: *https://www.dlubal.com/en/solutions/online-services/glossary/000069*

Dyrbye, C. & Hansen, S. O. (1997), *Wind loads on structures.*
URL: *https://trid.trb.org/view/573276*

El-Khoury, O. & Adeli, H. (2013), 'Recent Advances on Vibration Control of Structures Under Dynamic Loading', *Archives of Computational Methods in Engineering* **20**(4), 353–360.
URL: *http://link.springer.com/10.1007/s11831-013-9088-2*

Ellis, B. & Bre (1980), 'An assessment of the accuracy of predicting the fundamental natural frequencies of buildings and the implications concerning the dynamic analysis of structures.', *Proceedings of the Institution of Civil Engineers* **69**(3), 763–776.
URL: *http://www.icevirtuallibrary.com/doi/10.1680/iicep.1980.2376*

Emil Simiu, D. Y. (2019), *Wind effects on structures: modern structural design for wind*, John Wiley Sons.

Eurocode (2005*a*), *Eurocode loads*.

Eurocode (2005*b*), *Eurocode wind*.

Eurocode (2011), *Eurocode steel*.

European Commission. Joint Research Centre. Institute for the Protection and the Security of the Citizen (2009), *Design of floor structures for human induced vibrations : background document in support to the implementation, harmonization and further development of the Eurocodes*, Publications Office, LU.
URL: *https://data.europa.eu/doi/10.2788/4640*

Feldmann, A., Huang, H., Chang, W.-S., Harris, R., Gräfe, M. & Hein, C. (2016), 'Dynamic properties of tall timber structures under wind-induced vibration', p. 11.

Geurts, C. & van Bentum (2015), 'Demping hoogbouw voorspeld'.

Ghorbani-Tanha, A. K., Noorzad, A. & Rahimian, M. (2009), 'Mitigation of wind-induced motion of Milad Tower by tuned mass damper', *The Structural Design of Tall and Special Buildings* **18**(4), 371–385.
URL: *http://doi.wiley.com/10.1002/tal.421*

Gomez, S. S. (2019), Energy flux method for identification of damping in high-rise buildings subject to wind, PhD thesis, TU Delft.

Gutierrez Soto, M. & Adeli, H. (2013), 'Tuned Mass Dampers', *Archives of Computational Methods in Engineering* **20**(4), 419–431.
URL: *http://link.springer.com/10.1007/s11831-013-9091-7*

Ham, P. & Terwel, K. C. (2017), 'Structural calculations of Highrise structures 170426'.

Hoenderkamp (2011), *Hoenderkamp_lateral_building_design.pdf*.

Kalkman, I. M., Bronkhorst, A. J., van Bentum, C. A., Geurts, C. P. W. & Blocken, B. (2013), 'Implicaties bij CFD', *Bouwen met Staal* **43**(234), 44.

Karamba 3D (n.d.), 'Natural Vibrations'.
URL: *https://manual.karamba3d.com/3-in-depth-component-reference/3.5-algorithms/3.5.7-natural-vibrations*

Kareem, A., Kijewski, T. & Tamura, Y. (1999), 'Mitigation of motions of tall buildings with specific examples of recent applications', *Wind and Structures* **2**(3), 201–251.
URL: *https://doi.org/10.12989/WAS.1999.2.3.201*

Kareem, A. & Tamura, Y. (2013), *Advanced Structural Wind Engineering kareem.pdf*.

Krenk, S. (2005), 'Frequency Analysis of the Tuned Mass Damper', *Journal of Applied Mechanics* **72**(6), 936–942.
URL: *https://asmedigitalcollection.asme.org/appliedmechanics/article/72/6/936/474156/Frequency-Analysis-of-the-Tuned-Mass-Damper*

Kwok, K. C. S., Burton, M. D. & Abdelrazaq, A. K. (2015), *Wind-Induced Motion of Tall Buildings - Designing for Habitability*.

Kwok, K. & Samali, B. (1995), 'Performance of tuned mass dampers under wind loads', *Engineering Structures* **17**(9), 655–667.
URL: *https://linkinghub.elsevier.com/retrieve/pii/0141029695000356*

Kwon, D. K. & Kareem, A. (2013), 'Comparative study of major international wind codes and standards for wind effects on tall buildings', *Engineering Structures* **51**, 23–35.

Lago, A., Trabucco, D. & Wood, A. (2019), *Damping Technologies for Tall buildings*, Elsevier.
URL: *https://linkinghub.elsevier.com/retrieve/pii/B9780128159637000087*

Lu, X. & Chen, J. (2011*a*), 'Mitigation of wind-induced response of shanghai center tower by tuned mass damper', *The Structural Design of Tall and Special Buildings* **20**(4), 435–452.

Lu, X. & Chen, J. (2011*b*), 'Parameter optimization and structural design of tuned mass damper for shanghai centre tower', *The Structural Design of Tall and Special Buildings* **20**(4), 453–471.
URL: *http://doi.wiley.com/10.1002/tal.649*

Meinhardt, D. C. (2021), 'Interview with representative from Gerb'.

Montgomery, M. (n.d.), Fork configuration dampers for enhanced dynamic performance of high-rise buildings, PhD thesis.

moon Kim Ki-pyo You Jang-youl You, Y. (2014), 'Across and along-wind responses of tall building'.

Nakamura, Y. (1993), 'Bluff-body aerodynamics and turbulence', *Journal of Wind Engineering and Industrial Aerodynamics* **49**(1-3), 65–78.
URL: *https://linkinghub.elsevier.com/retrieve/pii/016761059390006A*

Patil, V. & Jangid, R. S. (2011), 'Response of wind-excited benchmark building installed with dampers'.

Philippe, D. (2011), 'Considerations in the design of viscous dampers used to suppress wind-induced vibration in high-rise buildings', p. 5.

RDWI (n.d.), 'Supplementary damping systems', p. 2.

Robbemont, I. A. (2019), '4d dynamische analyse van hoogbouw', *Cement* (6—7), 48–54.

Rossmann, Dym & Bassman (n.d.), Supplemental material case study: natural frequencies of tall buildings, *in* 'Introduction to Engineering Mechanics'.

Rotterdam, G. (2019), 'Hoogbouwvisie 2019 Rotterdam'.

Smith, R. (2011), 'Deflection Limits in Tall Buildings—Are They Useful?', pp. 515–527.

Smith, R. J. & Willford, M. R. (2007), 'The damped outrigger concept for tall buildings', *The structural design of tall and special buildings* **16**(4), 501–517.

Smith, R. & Willford, M. (2008), 'Damping in tall buildings – uncertainties and solutions', *IABSE Congress Report* **17**(28), 66–67.
URL: *http://www.ingentaconnect.com/content/10.2749/222137908796225618*

Sockel, H., ed. (1994), *Wind-Excited Vibrations of Structures*, Springer Vienna, Vienna.
URL: *http://link.springer.com/10.1007/978-3-7091-2708-7*

Staal & CO2 | Bouwen met staal (n.d.).
URL: *https://www.bouwenmetstaal.nl/themas/duurzaam/staal-co2/*

Steenbergen, R., Vrouwenvelder, A. & Geurts, C. (2012), 'The use of eurocode en 1991-1-4 procedures 1 and 2 for building dynamics, a comparative study', *Journal of wind engineering and industrial aerodynamics* **107**, 299–306.

Strømmen, E. (2010), *Theory of bridge aerodynamics*, Springer Science & Business Media.

Sun, J. (2019), 'Research on vocal sounding based on spectrum image analysis', p. 11.

Tracy Kijewski, Fred Haan, A. K. (2000), 'Wind-induced vibrations'.

Treels, I. R. (2019*a*), 'Berekeningsmethoden dynamische responsies hoogbouw', *Cement* (6—7), 28–37.

Treels, R. (2019*b*), 'Excel-sheet dynamische windberekeningen'.

Tsai, H.-C. & Lin, G.-C. (1993), 'Optimum tuned-mass dampers for minimizing steady-state response of support-excited and damped systems', *Earthquake Engineering & Structural Dynamics* **22**(11), 957–973.
URL: *http://doi.wiley.com/10.1002/eqe.4290221104*

Vrouwenvelder, A. (2004), *Lecture notes random vibrations*.

Zhou, Y., Kareem, A. & Geurts, C. (n.d.), 'On the aerodynamic admittance functions of tall buildings'.

Appendices

Appendix A

Types of stability systems

This appendix describes the structural stability system as described in Chapter 4 in more detail. The different systems are illustrated in Figure A.1, which is similar to Figure 4.1:

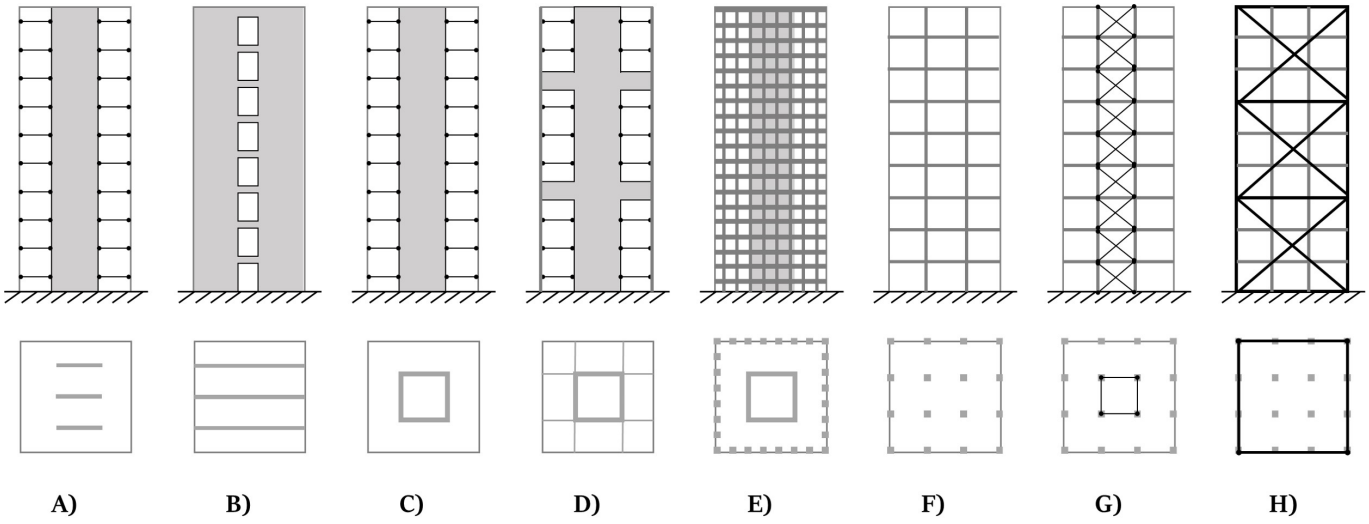

Figure A.1: *Most common types of stability systems*

A.1 Description of systems

A.1.1 Shear walls

Often in high-rise building concrete reinforced walls are used to provide stability, see Figure A.1 A. These walls, called shear walls, can provide horizontal stiffness by wall actions and guide the lateral forces through the structure to the foundations. Walls are often applied anyhow in a structure for example for elevator shafts, fire safety reasons or for the separation of housing units. It is therefore convenient to use these elements in the stability system, as this does not require additional elements. The major drawback of the use of shear walls as a stability system is that a certain amount of flexibility in the floor plan is reduced, the walls can not be removed to create a different floor plan lay-out. Reinforced concrete shear walls in tall buildings can economically be used in structures up to 35 stories (Hoenderkamp 2011).

A.1.2 Coupling walls and central core structure

Separate shear walls can also be coupled in such a way that they work together, this increases the overall shear wall stiffness. Coupling walls can be applied in two ways. The first option is to enlarge the length of a shear wall, by coupling separate walls by the use of coupling beams, see Figure A.1 B. These coupling beams must inherit enough shear strength to handle the large shear forces on these elements. The coupling of detached shear walls largely increases the strength and stiffness of the combination of the separate walls. In fact a coupled shear wall functions as a rigid frame structure with wide columns. Coupled wall structures

will allow building heights of up to 50 stories (Hoenderkamp 2011).

The second option is to couple the shear walls into a concrete core. A core system is in fact compromised of different concrete shear walls, connected in such a way that a tube shape is formed, see Figure A.1 C. This core is normally located in the center of the buildings floor plan to reduce eccentricities. Often, the inside of the stability core is used to locate the elevator shafts, staircases and MEP installations. In that way the lose of flexibility in the floor plan is only limited. Moreover these functions no not have to meet day-light requirements, which reduces the amount of openings that would effect the stability function of the core. An advantage of combining shear walls into a core is that the torsional stiffness is heavily increased compared to non-connected shear walls in different directions. Usually the core width does not exceed 15 meter to attain a feasible economic gross-netto floor-plan ratio, therefore core stability systems are not very feasible for very slender high-rise. As a rule of thumb the core-width is 1/10 of the building height, this implies that a single-core system can be efficiently used up to 150 meters (Ham & Terwel 2017).

A.1.3 Outrigger structure

If a single-core structure is not enough to provide enough horizontal stiffness, an outrigger structure can be used, see Figure A.1 D. An outrigger structure in fact is an extension of the central core type of structures extended with the so called outriggers. Outriggers rigidly connect the central core and the structures outer columns. In this way the outer columns get activated under lateral loading. Due to this activation normal forces are generated in these columns, that together create an opposing moment against the lateral wind-load, see Figure A.2. In this way the bending moment resistance is partly transferred from the core to the facade columns. This is highly effective due to the larger moment lever arm of the outer columns. As the shear stiffness of columns is very low, the shear forces will still be resisted mainly by the concrete core. The effectiveness of the outrigger system can be increased by the application of a belt structure. A belt structure is compromised of a truss structure in the buildings outer perimeter. This belt structure ensures that the forces from the outrigger walls are distributed equally over all the facade columns, so that all facade columns are activated. When necessary more than one outrigger can be applied in a building, the relative effectiveness of each outrigger will then drop (Ham & Terwel 2017).

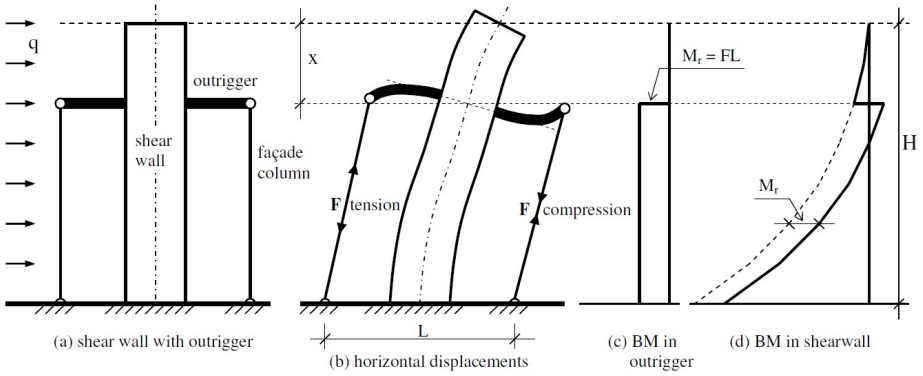

Figure A.2: *The concept of an outrigger structure. Adopted from: (Hoenderkamp 2011)*

A.1.4 Tube structure

A tube structure is applied when a lower order system is not able to generate enough stiffness. Where in a core system most material is applied in the center of the floor-plan, in a tube system this material is shifted to buildings outer perimeter. A tube system can be applied in steel and concrete. In this system columns are applied in the facade in a dense grid and function in fact as an increased core structure, see Figure 4.1 E. Due to the increased lever-arm this system is more efficient. However, a big disadvantage is that the material is applied in a dense grid around the facade, this reduces the amount of windows and daylight inside the structure. Moreover, the tube structures effectiveness is decreased due to the shear-lag effect (Hoenderkamp 2011).

A.1.5 Rigid frame and braced frame structure

A rigid frame is constructed out of columns and beams that are rigidly connected, see Figure A.1 F. Due to the moment resisting connections a rigid frame can take up horizontal loads, however this construction not very efficient for lateral loads. The structure will deform in two separate modes that together result in the overall behaviour: a bending mode and a shear mode, see Figure A.3. Both steel and concrete can be used. Rigid frame structures can be used in an economical efficient manner up to 25 stories (Hoenderkamp 2011). A rigid frame is often constructed out of steel, which results in a relative lightweight structure.

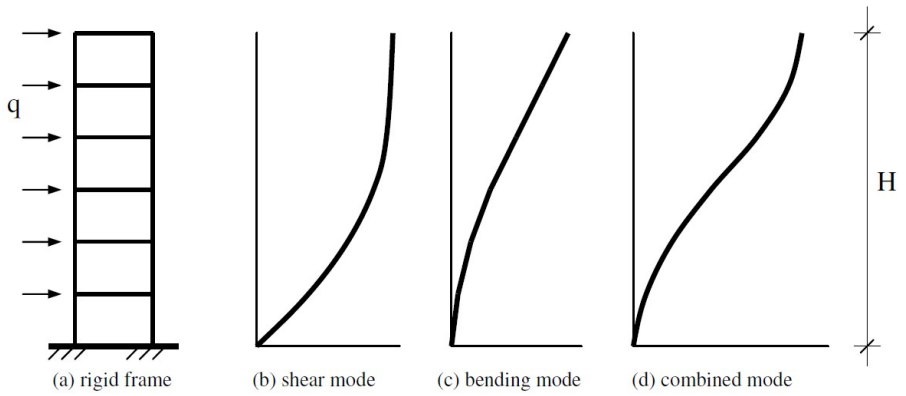

Figure A.3: *Shape modes of a rigid frame structure due to lateral loads. Adopted from: (Hoenderkamp 2011)*

Another frame type of structure that can be used for high-rise structures are braced frames. In contrast to a rigid frame, a braced frame is compromised of columns and beams that are hingedly connected. The lateral loads are resisted by diagonal braces located inside the construction, see Figure A.1 G. This force distribution of a braced frame is more efficient than a rigid frame as a braced frame takes up lateral loads by normal forces instead of bending moments. However the diagonal crosses inside the structure can create a barrier and reduces the flexibility of the floor-plan.

A.1.6 Mega structure

A megaframe structure is a stability system which is in fact the larger scale variant of a braced frame, see Figure A.1 H. In a megaframe the stability members are located at the buildings outer perimeter instead of inside the structure. These braced diagonals span multiple stories. The building can be perceived as a combination of a large frame structure and smaller infilled structures: the lateral loads on the inner structures are transferred to the mega structure which are then carried to the foundation. Some megaframe structures

can take up all the vertical loads as well. Megaframe structures allow for the highest types of buildings. Two megaframe properties make this stability system so effective. On the one hand, the resistance of lateral loads by normal forces through the diagonals instead of by bending moments and second the fact that stability members are located in the buildings outer perimeter, which results in a large moment lever arm. A big disadvantage of a megaframe is however that the diagonals are located in the facade. As these member sizes can get very large this has implications for the amount of daylight and the architectural appearance of a building.

Appendix B

Design considerations for different types of dampers

In this appendix the advantages and disadvantages are described for the dampers as covered in Chapter 5: tuned mass dampers (TMD), viscous fluid dampers, and viscoelastic dampers. All these types can be applied to reduce wind-induced motion. In this report the focus is on tuned mass dampers as they are relatively easy to install and to use.

B.1 Properties of tuned mass dampers

The concept of a TMD is described shortly in paragraph 5.2.1. Advantages and disadvantages of the use of a TMD are listed below:

Advantages

- The concept of a TMD is well understood and in general less complex to calculate than other supplementary damping systems. A TMD does not influence the structural properties of the main building, which means that the inclusion of a TMD does not require an iterative structural design procedure for the main building. The TMD system can hence be designed separately from the building, which simplifies the calculations.
- Even in a late design stage, it can be decided to include a TMD in design, again because the building properties are barely affected by the TMD. It could even be decided to install a TMD after the construction is finished, if accelerations turn out to be too high (Smith & Willford 2008).
- A TMD only has to be located at one single floor in the building and functions separately. Other damping systems are often distributed over the full structure and must be incorporated in the structural system.
- A TMD system can be tuned. If the actual building properties differ from the calculated properties, or change over time, the TMD can be tuned to ensure that the damper keeps operating effectively.
- In some cases, large masses that are anyhow present in a building on the higher floors, can be used as a secondary mass for the TMD. For example, a swimming pool or a sprinkler storage tank (Kareem et al. 1999).

Disadvantages

- A TMD is the most effective if it is located high in the structure. At this location the TMD takes up quite some space, partly because of the required amount of material, but also because space has to be reserved for the TMD motion. This means that valuable space at the top of the building, for example the penthouse, has to be used to locate the TMD (Smith & Willford 2007).
- A single TMD is only effective in a small range of frequencies close to the tuning frequency. As a result, the higher order modes of a structure remain undamped.

- A TMD consists of a large mass of around 1% of the building's modal mass, see Chapter 9. This weight results in additional forces in the structure, which must be taken into account in the design of the tower. This reduces possible material savings. If an existing mass is used as TMD, for example a sprinkler installation, this disadvantage is obviated.
- The efficiency of the TMD depends on how well the TMD is tuned to the fundamental modal frequency of a structure. If the calculation of the dynamic parameters during design was not accurate or if the dynamic properties change over time, the TMD can become 'detuned' (Montgomery n.d.). As a result the TMD will not function optimal. This does not have to be an big issue as the TMD can the TMD can be re-tuned during its lifetime (Smith & Willford 2007).

- As is explained in chapter 5.3.3 it is not recommended to rely on a TMD to fulfill the strength requirements, it can not be used to guarantee the structural integrity. This may be problematic if ULS design is governing.

B.2 Properties of viscous dampers

The concept of viscous dampers is described shortly in paragraph 5.2.2. Advantages and disadvantages of the use of viscous dampers are listed below:

Advantages

- Viscous dampers will provide damping for every type of motion that results in a relative velocity between the damper ends, independent of the frequency. Viscous dampers do not have to be tuned to a specific frequency (Lago et al. 2019).
- If distributed cleverly, viscous dampers can provide damping to all dynamic modes (Smith & Willford 2007).
- Viscous dampers can be located in combination with the structural system. In contrast to a TMD they do thus not take a lot of space (Smith & Willford 2007).
- As a viscous damper on its own does not provide additional stiffness, the modal properties of the system, like the eigenfrequency, do not change by the application of viscous dampers (Philippe 2011). This limits the complex iterative character of the design process.
- The amount of damping of a viscous damper is dependent on the relative velocity. Therefore, the resulting force is out of phase with the building motion. This allows for a reduction of the deformations, without increasing the stresses.
- Viscous dampers can be used to fulfill the ULS strength requirements, see paragraph 5.3.3. The silicone oil fluid used in viscous dampers is nontoxic, fire-resistant, and stable over time, it will not degrade. These are important factors for the applicability of this type of dampers (Philippe 2011).

Disadvantages

- As viscous damper undergoes a lot of loading cycles, therefore the dampers have to be maintained regularly, for example to prevent possible fluid leakages (Lago et al. 2019).
- Viscous dampers do not inherit significant amounts of stiffness. As a consequence, the structural members in which viscous dampers are applied can not be used to generate stiffness for the structures stability system.

- Viscous dampers can not easily be applied in later design phases as these dampers will influence the structural properties of the stability system, especially the stiffness and the force distribution, of a building will change by the application of viscous dampers.
- Viscous dampers are often applied in diagonal braces. These diagonal elements can reduce the flexibility of the floor plan lay-out.
- Tolerances regarding the installation of viscous dampers must be tight as only little movements in the connection can reduce the effectiveness of the dampers heavily.

B.3 Properties of viscoelastic dampers

The concept of viscous dampers is described shortly in paragraph 5.2.3. Advantages and disadvantages of the use of viscous dampers are listed below:

Advantages

- Contrary to viscous dampers, a viscoelastic damper inherits some stiffness. It can therefore be applied in the structural system without losing too much stiffness.
- A viscoelastic damper can be applied as a replacement of coupling beams in shear walls, in that manner they do not require additional structural space in the building (Christopoulos & Montgomery 2013).
- The long-term behaviour of a viscoelastic damper is strong. Only a limited amount of maintenance is required (Lago et al. 2019).

Disadvantages

- The damping properties of a viscoelastic damper are a function of the forcing frequency, the external temperature and the internal strain. For the target wind service level, these damper properties are in general stable. It is however, still needed to perform an upper and lower bound analysis validate the damping properties (Christopoulos & Montgomery 2013).
- The stiffness of a viscoelastic damper is different for static loads than for fluctuating dynamic loads. This makes the structural design tasks more complicated (Christopoulos & Montgomery 2013).
- The deformation capacity of a viscoelastic damper is relatively limited and can thus not be applied for buildings with too high deformations (Lago et al. 2019).

Appendix C

Dependencies of the damping ratio

As this thesis is about the opportunities of supplementary dampers, it is interesting to investigate how the different dynamic wind calculations from the Eurocode wind load norms, NEN-EN 1991-1-4, are influenced by the damping ratio. This allows for the identification of design opportunities and a better understanding of the different parameters. The dependencies have been investigated with the help of the dynamic calculation sheet by R. Treels (Treels 2019*b*) . These dependencies for both ULS and SLS are visualised in C.1.

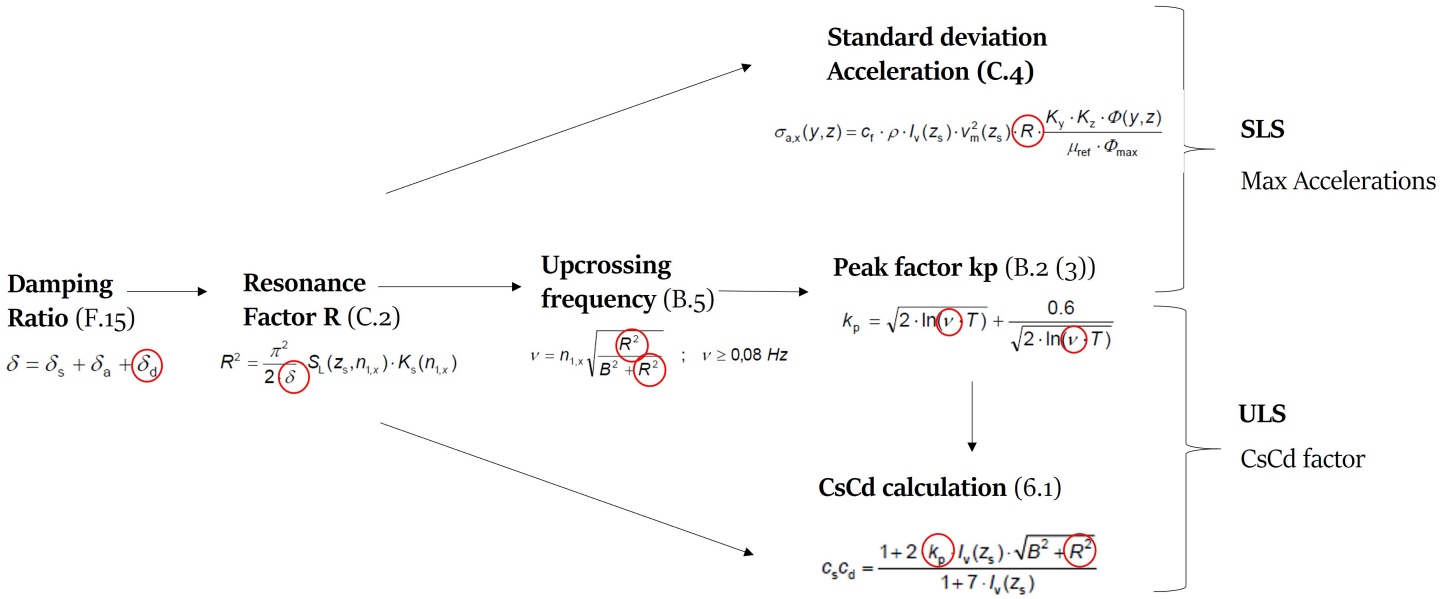

Figure C.1: *Eurocode 1991-1-4 factors that are dependent on the supplementary damping ratio in the wind calculations, for both ULS and SLS.*

Appendix D

Grasshopper model

This appendix covers some additional aspects of the Grasshopper model, that are not covered in the main body of this report.

D.1 Model description

Figure D.1 again represents the Grasshopper model. Some aspects are explained in this appendix.

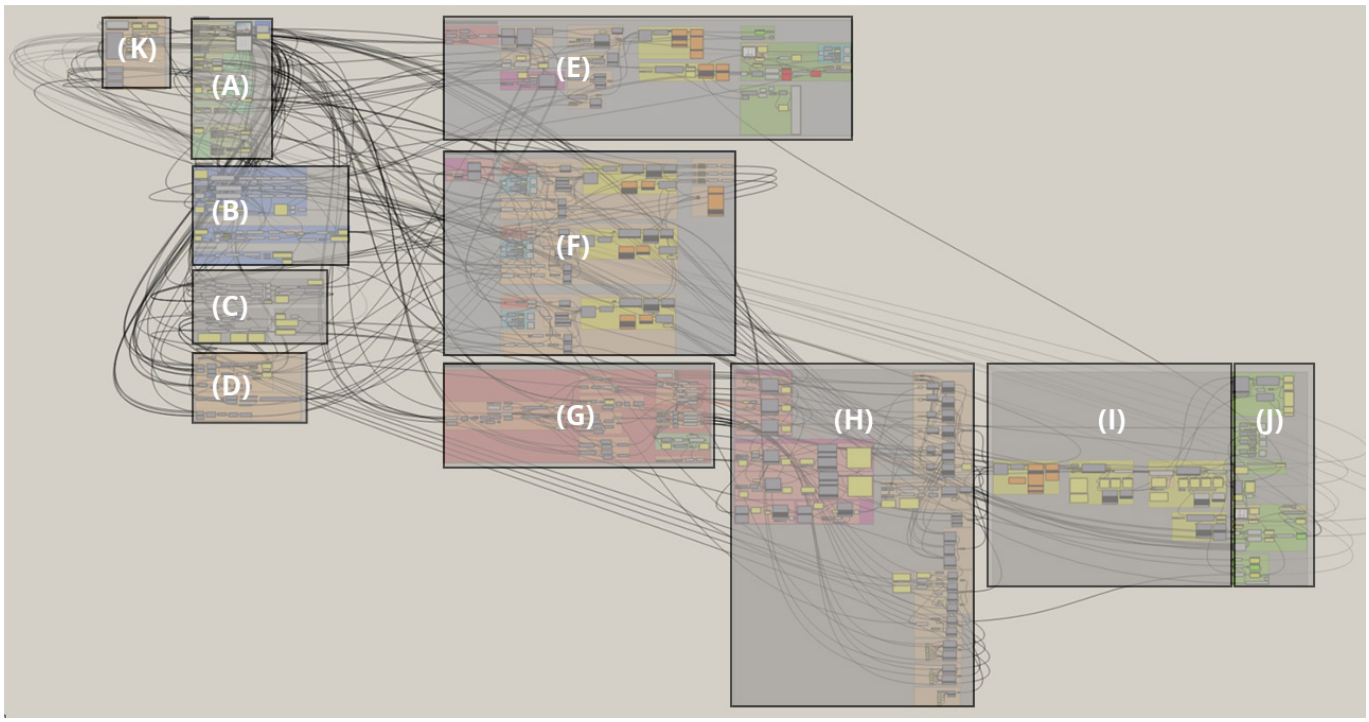

Figure D.1: *Grasshopper model overview*

A) Define model geometry

B) Define variant parameters

C) Define/determine design loads

D) Visualisation of the model

E) Simple beam model to estimate the eigenfrequency

F) Karamba column cross section determination

G) Geometry definition

H) Karamba finite element model definition

I) Karamba Finite element calculations (ULS, SLS optimisations and dynamic analysis):

J) Calculation of maximum accelerations, deflections, etc.

K) Colibri variant study itterator

D.1.1 (E) Simple dynamic beam model

Part E models the variant tower as a 1D beam element created with Karmaba 3d FEA elements. This model is used to determine a proper estimate of the CsCd factor. This is necessary as the CsCd factor is dependent on the eigenfrequency, which is unknown yet. The use of simple rule of thumbs like $Nx = \frac{46}{H}$ is not possible, as these rule of thumbs do not take into account the varying stiffness.

In section B of the Grasshopper model the maximum allowed deformation for a certain variant is defined. By assuming the structural material properties and the load on the beam element as described in the previous paragraphs, the required stiffness for this maximum allowed deformation can be calculated. To do so equation D.1 can be used, which is derived from the deformation of a cantilever beam.

$$I_{required} = \frac{q * L^4}{8 * E * w_{max}} \tag{D.1}$$

After this calculation the mass, stiffness, damping ratio and loads are known or estimated. This allows for the computation of the first eigenfrequency of the model by the Karamba Natural vibrations element. This natural frequency can be used to calculate a proper estimation of the CsCd factor for wind loading.

D.1.2 (F) Column mass determination

Part F is used to estimate the structural mass of the modeled tower. It is based on simple Karamba 1D beam elements that are subjected to vertical loads. The vertical loads from part (B) are transferred to equivalent column loads, based on the column division in the floor plan. These column loads are placed on the vertical beam element with the length of the tower. Karamba contains a cross section optimisation element, that iterates cross sections until all cross section unity checks are met. This component takes into account NEN-EN steel requirements like buckling. By using this component on the column beam elements the minimum structural columns can be defined and their mass can be determined. This mass can then easily be multiplied by the amount of edge and corner columns, resulting in the total required structural column weight. This result is shown in Figure D.2 for a specific variant.

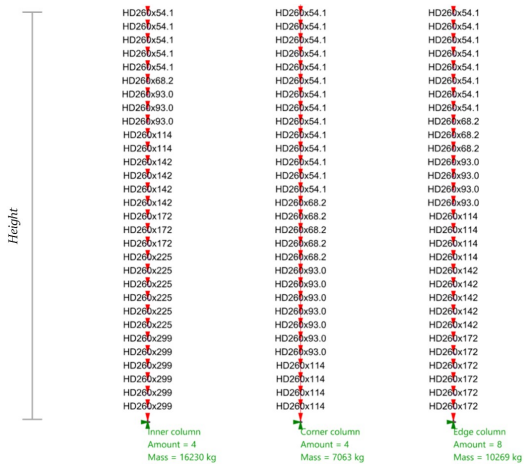

Figure D.2: *Column mass determination model*

D.1.3 (I) Cross section optimisation

This sections forms the most import part of the model. The Karamba finite element model is analysed with a first order analysis. After this an optimisation is executed with the help of the standard Karamba optimisation components. A simplified overview of this process is shown in Figure D.3.

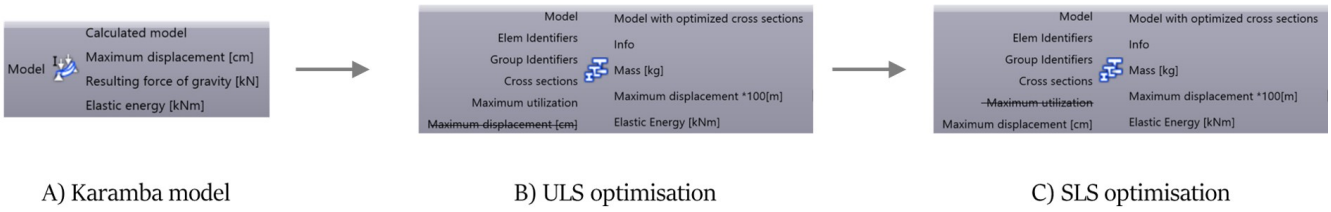

A) Karamba model B) ULS optimisation C) SLS optimisation

Figure D.3: *Optimisation workflow*

This optimisation first calculates the a minimal required amount of cross sections for strength (ULS) calculation based on three different load cases ((1) Wind left-side , (2) Wind right-side, (3) Vertical column loads). This optimisation returns profiles which just meet the strength requirements. The maximum unity check in the model is set to 0.80 instead of 1.0. This gives the model some margin. This is necessary as not all structural aspects are modelled explicitly. It allows for some backup for the case that for example buckling or higher second order effects than expected require additional strength.

When the optimised ULS structural system has been determined this variant is saved and the SLS optimisation step is performed on the ULS cross sections. This optimisation step does not try to optimise the unity check on strength, but tries to limit the maximum deformation. In section (A) of the model the maximum allowed deformation has been specified. If the stiffness requirement of a tower of 100 meters for example is 1/500*L, the maximum allowed deformation for the optimisation will be 0.20 meter.

The SLS optimisation tool does it's job, but is not considered as a very smart component. Additional material is not always located in a very effective manner. Especially for structures that have difficulties to full fill the stiffness requirements as is the case with for example very high, slender towers the algorithm tends to enlarge cross sections of beams elements that are not very influential for the overall result. Diagonal braces for example turn out to have only very little influence, but in the case of non-convergence of the algorithm very heavy profiles are proposed. Therefore it was decided to optimise only the core-columns and outrigger columns to be optimised with the SLS optimisation tool, this results in more realistic solutions, which are only a little bit less optimal.

D.1.4 q_p calculation

To define the wind profile on a high-rise building the Eurocode refers to a discrete profile as shown in Figure D.4, which is based on the peak velocity pressure coefficient (q_p). The discrete character of this load definition does not match very well with the parametric charachter of the Grasshopper model. Therefore a trendline formula for the q_p(h) wind-load has been calculated with excel to define the logarithmic wind-profile on the model. This formula calculates the correct q_p factor for each given height. This logarithmic wind-profile is converted to point loads on all the model nodes. This approach is considered sufficiently precise for the goal of this variant study.

The used wind formula is described in D.2 and produces the same value of q_p(h) for every building height.

$$q_p = 0.3927 * \ln(h) - 0.1622 \tag{D.2}$$

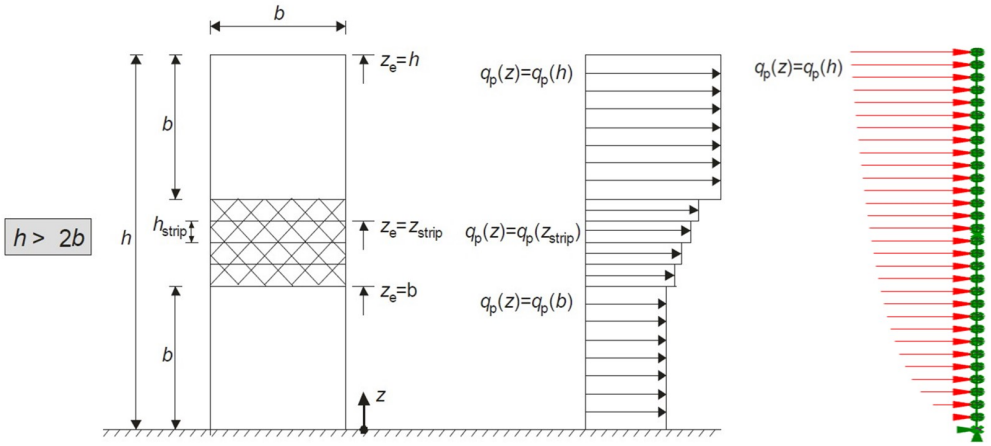

Figure D.4: *Eurocode wind-load (A) vs. Model wind load (B)*

D.2 Model assumptions

D.2.1 Effects of deformed geometry on the structure

Deformation of the structural geometry can result in additional loading, especially in the case of multi storey buildings, and therefore must be addressed. Two effects can be distinguished: Additional loading due to deformations caused by initial imperfections and additional loading due to the second order effect. It must be noted that the initial sway only has to be taken into account in ULS calculations. Both have been taken into account by the Grasshopper model.

Imperfections

The initial sway for a steel structure is calculated conform NEN-EN 1993-1-1 paragraph 5.3 (Eurocode 2011).
The initial rotation Φ can be calculated by Equation D.3.

$$\Phi = \Phi_0 \cdot \alpha_h \cdot \alpha_m = 0.0026\, rad \tag{D.3}$$

$$\Phi_0 = \frac{1}{200} = 0.005\, rad \tag{D.4a}$$

$$\alpha_h = \frac{2}{\sqrt{h}} > \frac{2}{3} \tag{D.4b}$$

$$\alpha_m = \sqrt{0.5(1 + \frac{1}{m})} = 0.79 \tag{D.4c}$$

In which h is equal to the building height. For the multistorey buildings as considered in this thesis, this means that α_h is always equal to $\frac{2}{3}$. The variable m represents the amount of columns in one row which is equal to 4 for the building as considered in this report.
The final initial imperfection can then be calculated by Equation D.5:

$$\Phi_0 = \frac{1}{200} = 0.005\, rad \tag{D.5a}$$

$$\alpha_h = \frac{2}{\sqrt{h}} > \frac{2}{3} \tag{D.5b}$$

$$\alpha_m = \sqrt{0.5(1 + \frac{1}{m})} = 0.79 \tag{D.5c}$$

Second order

The second order effect is also caused by the additional moment that is generated by vertical loads and the lever arm from the deformed structure. To to do so the vertical reaction forces are determined and applied at half of the structures height. The lever arm is a combination of the wind induced deformation and the imperfection effect on half the height.

The second order effect can be taken into account during design by a amplification factor. This factor is based on the ratio n which is equal to the ratio of the original moment caused by the wind load and the moment due to geometrical effects. The amplification factor is then determined by Equation D.6b.

$$\text{Amplification factor} = \frac{n}{n-1} \tag{D.6a}$$

$$n = \frac{M_{wind}}{M_{geometry}} \tag{D.6b}$$

The original moment on the structure is caused by the wind-load and can be calculated from the grasshopper model. The additional moments from the deformed structure and the initial imperfections are calculated as described above. A different second order factor for ULS and SLS is used. The wind-induced deformation is based on the SLS deflection limits and multiplied by the safety factor for wind to obtain the ULS value. Moreover the applied vertical load is smaller in SLS and the initial imperfection factor is neglected. Therefore the SLS second order factor is significantly smaller and in general almost equal to 1.0.

Points of attention: The deformation is equal to the ULS or SLS deformation (depending on the situation). If the ULS is governing, the second order effects results in an overestimation, as the deformation won't be reached in these cases.

D.3 Mass determination in Grasshopper

Not all masses in the Grasshopper model were automatically taken into account, due to the 2D representation. For static analyses, this is not problem, but for dynamic calculations the full mass is of importance.. This problem is schematized in Figure D.5, in which the elements that are automatically taken into account

are visualised in green, and the neglected masses are visualised in red. These neglected masses are added to the model manually.

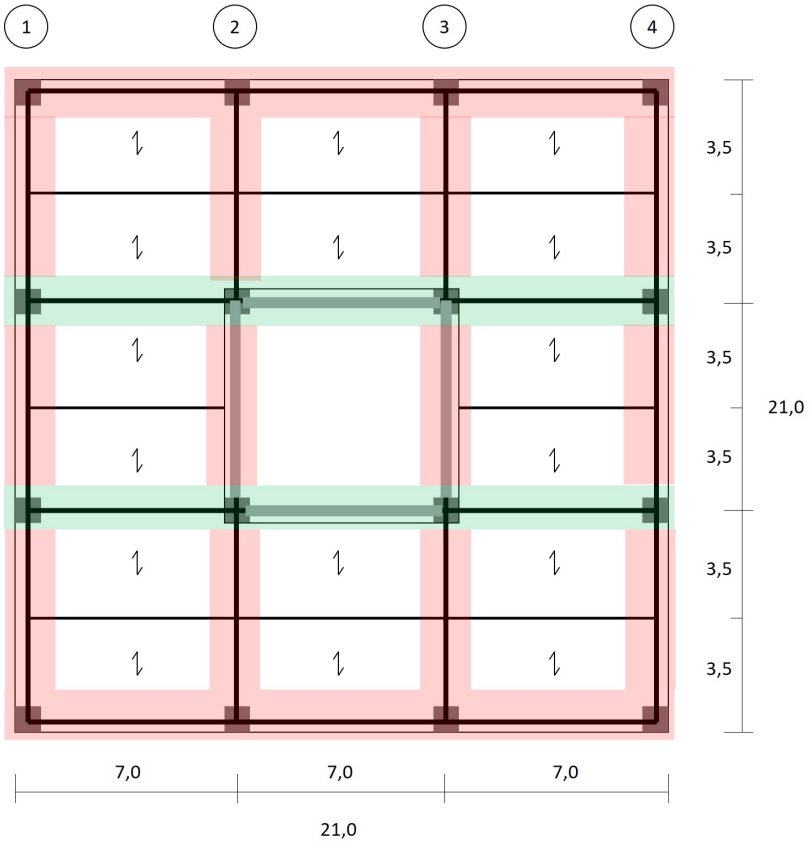

Figure D.5: *Structural mass that is not automatically considered in the conversion from a 3D model to a 2D model. Red: not taken into account in 2D, Green: Taken into account in 2D.*

Appendix E

Acceleration calculations

E.0.1 Along-wind acceleration Eurocode and CsCd factor

The following script has been used to determine the CsCd factor and the along-wind accelerations based on the Eurocode for different buildings. Based on Eurocode procedure 2 and chapter 6 (Eurocode 2005*b*).

```
#Determine CsCd value based on Eurocode procedure 2, annex C
#Tower_object is a class in which all the tower data like height, width, etc is stored
#NA = National annex

def CsCd_func(tower_object, Nx=Eigenfrequency):
    #PLEASE NOTE TO USE ULS VALUES AS CSCD IS A ULS VALUE
    height = tower_object.height() #[m]  #EC, referred to as 'h' in Eurocode
    width = tower_object.width() #[m] #EC, referred to as 'b' in Eurocode
    Z_interest = height
    Ztop = height #[m]

    Me = tower_object.mass_length() #[kg/m] distributed mass per height
    damping_log = tower_object.damping_log() #[-] #0.0628 #[log decrement of damping]

    #calculate turbulence factor
    #Use wind area II throughout all the calculations
    ##############################################

    Zs = 0.6 * Ztop #[m] Reference height, structural factor
    #Terrain category
    Z0 = 0.5 #[m] Terrain category III (NA)
    zmin = 7 #[m] (NA)
    zmax = 200 #[m] (NA) (maximum allowed)
    ##########################################################33

    vb_ULS = 27.0 # [m/s]= vbo=27 (II NA) * cdir = 1.0 (NA) * cseason = 1.0 (NA)

    #Return period
    K, n = 0.234, 0.5 #NA Table NB.2
    T = 50 #[year] #ULS as CsCd is an ULS factor
    p = 1-np.exp(-(1/T)) #return period

    cprop = ((1-K*np.log(-np.log(1-p)))/(1-K*np.log(-np.log(0.98))))**n #probability factor

    vb_ULS = cprop * vb_ULS #mean wind ULS

    ##############################################

    kl = 1.0 #standard value
    kr = 0.19*(Z0/0.05)**0.07 #(eq 4.5)

    stand_dev_turb = kr * vb_ULS * kl #(eq 4.6)
```

```
    ########################################


    Cr_zs = kr * np.log(Zs/Z0) #(z) |roughness factor — np.log = LN
    C0 = 1.0 #Orography factor
    Vm_zs  = vb_ULS*Cr_zs #(z) | [m/s] Characteristic mean wind velocity at height reference
     height SLS

    ##################################

    Iv_zs = stand_dev_turb / Vm_zs #(z) |

    ################
    alpha = 0.67 + 0.05*np.log(Z0)
    Zt = 200 #[m] #Turbulence scale
    Lt = 300 #[m] #Reference height top

    L_zs = Lt*(Zs/Zt)**(alpha) #B1(1) (z=Zs) turbulence scale at Zs, describes gust size

    ##################
    #Solari spectrum
    FL_zs = (Nx * L_zs)/ Vm_zs #dimensionless frequency
    SL_zs = (6.8*FL_zs) / (1+10.2*FL_zs)**(5/3) #Solari spectrum


    ###############
    #Mode properties

    Fie_y_z = Z_interest / height
    Fie_max = 1.0

    Gy = (1/2)
    Gz = (3/8)
    Ky = 1
    Kz = 1.5

    #Decay factors
    cy, cz = 11.5, 11.5 #EC page 102
    height = Ztop #[m] height of interst

    phi_y = (cy*width*Nx)/(Vm_zs)
    phi_z = (cz*height*Nx)/(Vm_zs)

    Ks = 1 / (1 + np.sqrt( (Gy*phi_y)**2 + (Gz*phi_z)**2 + ((2/math.pi)*Gy*phi_y*Gz*phi_z)
    **2 ))
    ################################################

    #Resonant response factor
    R_p2 = (math.pi**2 / (2*damping_log)) * SL_zs * Ks #dependent on: Zs, Nx
    R = np.sqrt(R_p2)

    #Background response factor
    B_p2 = (1)/(1+(3/2)*np.sqrt((width/L_zs)**2+(height/L_zs)**2+((width*height)/L_zs**2)
```

```
    **2))

    B = np.sqrt(B_p2)
    ##############################################

    u_ref = Me / width # [kg/m2] reference mass per area

    stand_dev_acc = Cf * rho_air * Iv_zs * Vm_zs**2 * R  * (Ky * Kz * Fie_y_z)/(u_ref *
    Fie_max)

    v = max(Nx*np.sqrt((R**2)/(B**2 + R**2)), 0.08) #[Hz] should be bigger than 0.08
    T = 600 #[s]
    Kp= max(np.sqrt(2*np.log(v*T))+(0.6/np.sqrt(2*np.log(v*T))), 3) #peak factor, minum
    should be 3.0


    CsCd = (1 + 2*Kp*Iv_zs* np.sqrt(B_p2 + R_p2))/(1 + 7*Iv_zs)
    acceleration_k = Kp*stand_dev_acc #[m/s2]

    return(CsCd, acceleration_k)
```

E.0.2 Across-wind acceleration Eurocode

The following script has been used to estimate the across-wind accelerations based on the Italian report (Advisory Committee on Technical Recommendations for Construction 2008).

```
#PLEASE NOTE THAT THIS RESULTS IN THE MINIMUM VALUES AS H/D SHOULD BE LOWER THAN 6!
#Across wind acceleration based on Italian report
#NA = National annex


def acceleration_across_func(tower_object, Ny=Eigenfrequency_y):
    #Building parameters
    height = tower_object.height() #[m]
    width = tower_object.width() #[m]
    depth = tower_object.depth() #[m]
    Z_interest = height
    Ztop = height #[m]\
    Me = tower_object.mass_length() #[kg/m]
    damping_ratio = tower_object.damping_ratio() #[kg/m]

    ######################################
    d_w = depth/width
    ######################################
    #calculate turbelence factor
    #Use wind area II throughout all the calculations
    ######################################

    Zs = 0.6 * Ztop #[m] Referentie hoogte bouwwerkfactor FIG 6.1

    #Terrain cattegory
    Z0 = 0.5 #[m] Terrain cattegory III (NB)
    zmin = 7 #[m] (NB)
```

```
    zmax = 200 #[m] (NB) (maximum allowed)
    ########################################

    vb_ULS = 27.0 # [m/s]= vbo=27 (II NB) * cdir = 1.0 (NB) * cseason = 1.0 (NB) #alleen maar ULS omdat het returnT =50year

    #Return period
    K, n = 0.234, 0.5 #NB Tabel NB.2
    T = 1 #[year]
    p = 1-np.exp(-(1/T))

    cprop = ((1-K*np.log(-np.log(1-p)))/(1-K*np.log(-np.log(0.98))))**n

    vb_SLS = cprop * vb_ULS

    ########################################

    kr = 0.19*(Z0/0.05)**0.07 #(eq 4.5)

    Cr_zs = kr * np.log(Zs/Z0) #(z) |roughness factor - np.log = LN
    C0 = 1.0 #Orography factor
    Vm_zs  = vb_ULS*Cr_zs #(z) | [m/s] Characteristic mean wind velocity at height reference height SLS

    ########################################

    C_L = 0.0082*(d_w)**3 - 0.071*(d_w)**2 + 0.22*(d_w)

    ########################################
    k1 = 0.85
    k2 = 0.02
    beta1 = ((d_w**4 + 2.3*d_w**2)/(2.4*d_w**4 - 9.2*d_w**3 + 18*d_w**2 + 9.5*d_w - 0.15)) + (0.12/d_w)
    beta2 = 0.28 * d_w**(-0.34)
    n1 = (0.12 / (1 + 0.38*d_w**2)**0.89) * (Vm_z/width)
    n2 = (0.56/d_w**0.85)*(Vm_z/width)

    S_L1 = (4*k1*(1+0.6*beta1)*beta1)/(np.pi) * (Ny/n1)**2 / ((1-(Ny/n1)**2)**2 + 4*beta1**2*(Ny/n1)**2)
    ###Note: als depth/widht > 3 then take into account S_L2 as well
    S_L2 = 0 #(4*k2*(1+0.6*beta2)*beta2)/(np.pi) * (Ny/n2)**2 / ((1-(Ny/n2)**2)**2 + 4*beta2**2*(Ny/n2)**2)
    S_L = S_L1 + S_L2

    ########################################

    R_L = np.sqrt((np.pi*S_L)/(4*damping_ratio))

    ########################################

    mode_z = (Z_interest / Ztop)

    ########################################
```

```
76
77      stand_dev_acc = ((0.5 * rho_air * Vm_z**2 * width )/(Me)) * (C_L * R_L * mode_z)
78      # :height is removed on purpose as this is already included in Me = kg/m
79
80      ######################################
81      T = 600 #[s]
82      G_L = Max(np.sqrt(2*np.log(Ny*T)) + (0.5572)/(np.sqrt(2*np.log(Ny*T))), 3)
83
84      acceleration_k = G_L*stand_dev_acc #[m/s2] #Across wind acceleration
85
86      ######################################
87
88      return(acceleration_k)
```

Appendix F

Floor systems

This appendix provides the calculation of the floor masses. Two floor systems have been calculated. A CLT floor and a steel-composite floor. Both floors are supported by steel beams. For the CLT floor additional mass has been incorporated regarding building physic requirements as sound and fire (Borgström & Fröbel 2019). The two systems have been designed on the edge, to investigate the dynamic behaviour of the most lightweight options. Heavier configurations of these floor types are possible in practice.

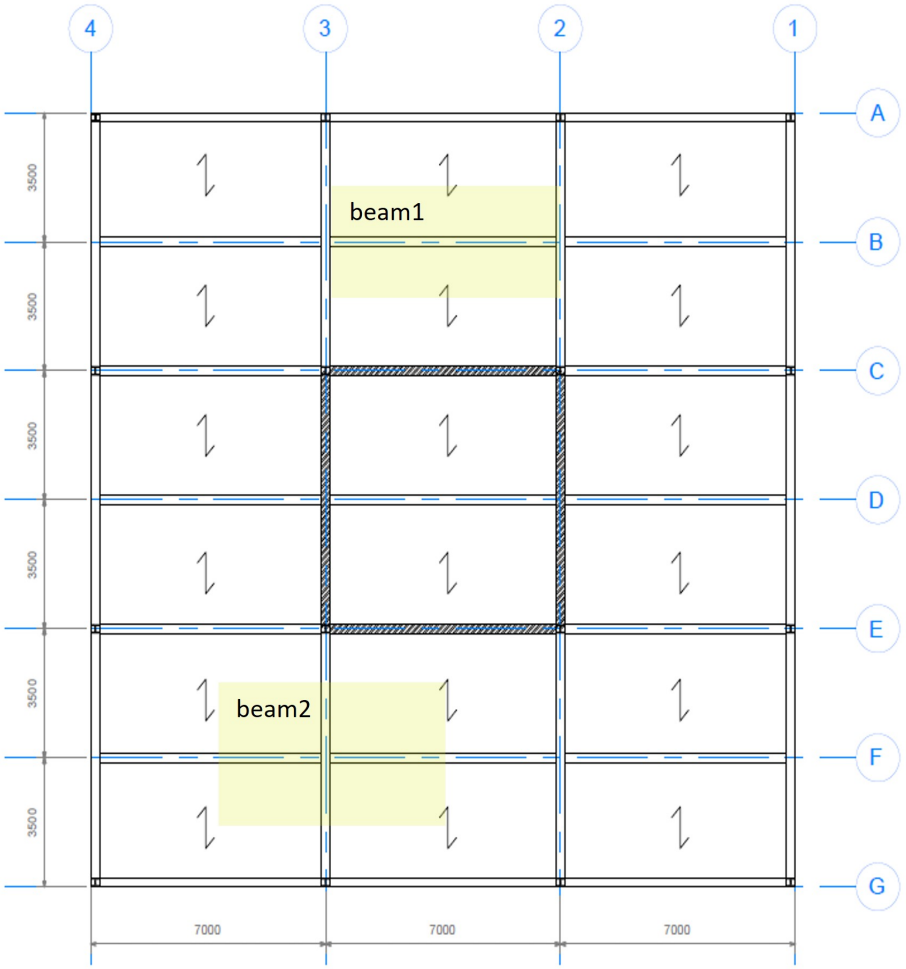

Figure F.1: *Load paths floor plan*

CLT fLoors

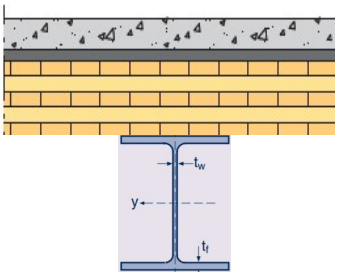

CLT Floor

CLT floor is based on insulations values

	Load	SLS	ULS		
var	lifeload floor	1.75	2.9	kN/m2	
var	partions	0.8	1.3	kN/m2	
CLT 139V - floor structure type 3: 307 kg/m2 (reduce clt thickness by 50 mm) --> 250 kg/m2					
per	self-weight CLT	0.75	0.99	kN/m2	(150 mm)
per	deck, aucostics	1.75	2.31	kN/m2	(rest)

Houd voor CLT 2 kN/m2 aan zodat ook aan eisen mbt geluid kan worden voldaan

Grid A,B,C,D

Beam1 **Grid B3-B2 On lettered gridlines a, b, c, d, e, f, g)**

kN/m = N/mm

	SLS	ULS		
Lineload (xb [m])	18.604988	27.2	kN/m	N/mm
	beam weight included			
Moment max		1.67E+08	Nmm	(kN/m * mm^2)
W_required		4.69E+05	mm3	
sigma		145	N/mm2	
Unity check		0.41	-	
I_required	1.19E+08	mm4		
deformation	18.56	mm		
Unicty check	0.795387962	-		

(bold = change for new profile)

Profile properties

Name	HEB260		
Mass	94.8	kg/m	0.929988 kN/m
Wy	1.15E+06	mm3	
height	260	mm	
I	1.49E+08	mm4	
E	210000	N/mm2	
smax	355	N/mm2	
width floor	3500	mm	3.5 m
length beam	7000	mm	7 m
max def	23	mm	

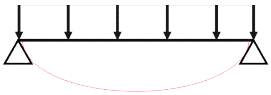

Grid 1,2,3,4

Beam2 **Grid 3E-3G (on numbered gridlines 1,2,3,4)**

*This beam is loaded by F from beam grid B3-B2 from two directions (reactionforce * Length)*

	SLS	ULS		
pointload	138.41	198.6	kN	(neem eigen gewicht
	1.38E+05	1.99E+05	N	aan als puntlast = conservatief)
	beam weight included in SLS			
Moment max		3.48E+08	Nmm	
Wrequired		9.79E+05	mm3	
sigma		207.1376299	N/mm2	
Unity check		0.583486281	-	
I_required	2.02E+08	mm4		
deformation	18.71	mm		
Unicty check	0.801919052	-		

Profile properties

Name	HEB300		
Mass	119	kg/m	1.16739 kN/m
Wy	1.68E+06	mm3	
Heigth	300		
I	2.52E+08	mm4	
E	210000	N/mm2	
smax	355	N/mm2	
width floorbeam	3500	mm	3.5 m
length beam	7000	mm	7 m
max def	23	mm	

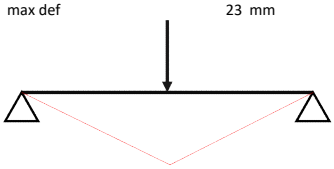

Mass sumation

Floor beams	grid A,B,C,D			
amount	7	-		
length	21	m		
total	147	m		
Weight	94.8	kg/m		
Total	**13936**	**kg**	31.60	kg/m2
Floor beams	grid 1,2,3,4			
amount	4	-		
length	21	m		
total	84	m		
Weight	119	kg/m		
Total	**9996**	**kg**	22.67	kg/m2
Floor slabs				
Area	441	m2		
permanent (sls)	2.5	kN/m2	254.8	kg/m2
Variable (sls)	2.55	kN/m2		
variable * Psi	1.02	kN/m2	104.0	kg/m2
Sum	358.8	kg/m2		
Total	**158239**	**kg**		
Sum beam A, beams 1, floor slabs				
Total	**182170**	**Kg/floor**		
including lifeload	413	kg/m2		

Structural mass	**309**	**kg/m2**

Steel-concrete floors

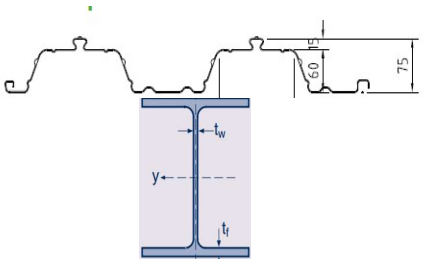

Concrete steel deck floor

ComFlor 75 - 150 mm | 1.2 mm | stempel			mass	267	kg/m2
	Load	**SLS**	**ULS**		
var	lifeload floor	1.75	2.9	kN/m2	
var	partions	0.8	1.3	kN/m2	
CLT 139V					
per	self-weight	2.62	3.46	kN/m2	
per	deck + acoustics	1.57	2.07	kN/m2	(7 cm concrete deck + 0.2 insulation -2000 kg/m2)

Grid A,B,C,D

Beam1 **Grid B3-B2 On lettered gridlines a, b, c, d, e, f, g)**

kN/m = N/mm

(bold = change for new profile)

	SLS	**ULS**		
Lineload	24.616095	35.1	kN/m	N/mm
beam weight included				
Moment max		2.15E+08	Nmm	(kN/m * mm^2)
W_required		6.06E+05	mm3	
sigma		156	N/mm2	
Unity check		0.44	-	
I_required	1.57E+08	mm4		
deformation	19.02	mm		
Unicty check	0.815281429	-		

Profile properties

Name	HEB280			
Mass	105	kg/m	1.03005	kN/m
Wy	1.38E+06	mm3		
height	280	mm		
I	1.93E+08	mm4		
E	210000	N/mm2		
smax	355	N/mm2	3.5	m
width	3500	mm	7	m
length	7000	mm		
max def	23	m		

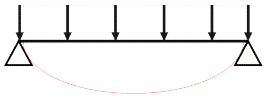

Grid 1,2,3,4

Beam2 **Grid 3E-3G (on numbered gridlines 1,2,3,4)**

This beam is loaded by F from beam grid B3-B2 from two directions

	SLS	**ULS**		
pointload	184.40	257.8	kN	
	1.84E+05	2.58E+05	N	
beam weight included in SLS				
Moment max		4.51E+08	Nmm	
Wrequired		1.27E+06	mm3	
sigma		209.001451	N/mm2	
Unity check		0.58873648	-	
I_required	2.69E+08	mm4		
deformation	20.04	mm		
Unicty check	0.859001144	-		

Profile properties

Name	HEM260			
Mass	176	kg/m	1.72656	kN/m
Wy	2.16E+06	mm3		
Heigth	290	mm		
I	3.13E+08	mm4		
E	210000	N/mm2		
smax	355	N/mm2		
width	3500	mm	3.5	m
length	7000	mm	7	m
max def	23.33	m		

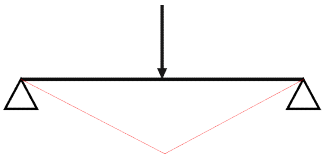

Mass sumation

Floor beams	grid A,B,C,D			
amount	7	-		
length	21	m		
total	147	m		
Weight	105	kg/m		
Total	**15435**	**kg**	35.00	kg/m2
Floor beams	grid 1,2,3,4			
amount	4	-		
length	21	m		
total	84	m		
Weight	176	kg/m		
Total	**14784**	**kg**	33.52	kg/m2
Floor slabs				
Area	441	m2		
permanent (sls)	4.18887	kN/m2	427.0	kg/m2
Variable (sls)	2.55	kN/m2		
variable * Psi	1.02	kN/m2	104.0	kg/m2
Sum	531.0	kg/m2		
Total	**234160**	**kg**		
Sum beam A, beams 1, floor slabs				
Total	**264379**	**Kg/floor**		
	599	kg/m2		

Structural mass	**496**	**kg/m2**

Appendix G

Governing design criteria

This appendix presents the governing-design-criteria for all the possible building heights, with and without outrigger.

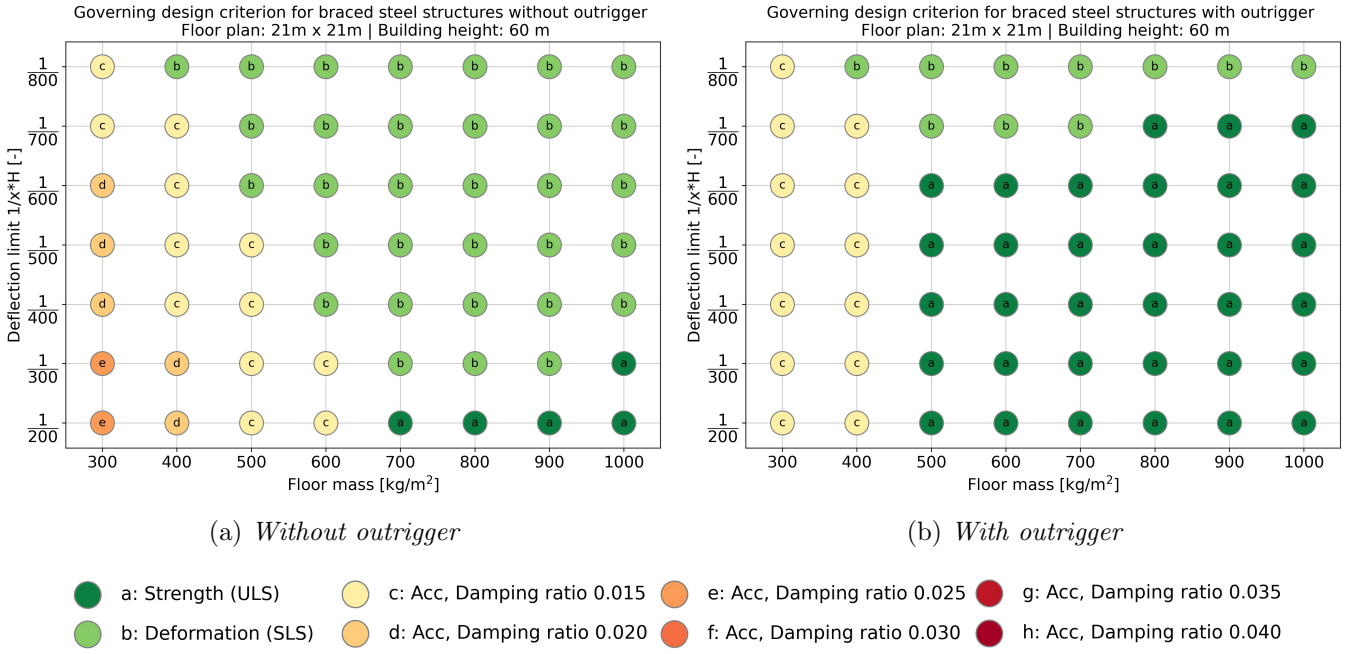

(a) *Without outrigger*

(b) *With outrigger*

Figure G.1: *Overview of the governing design factors for towers with a height of 60 meters*

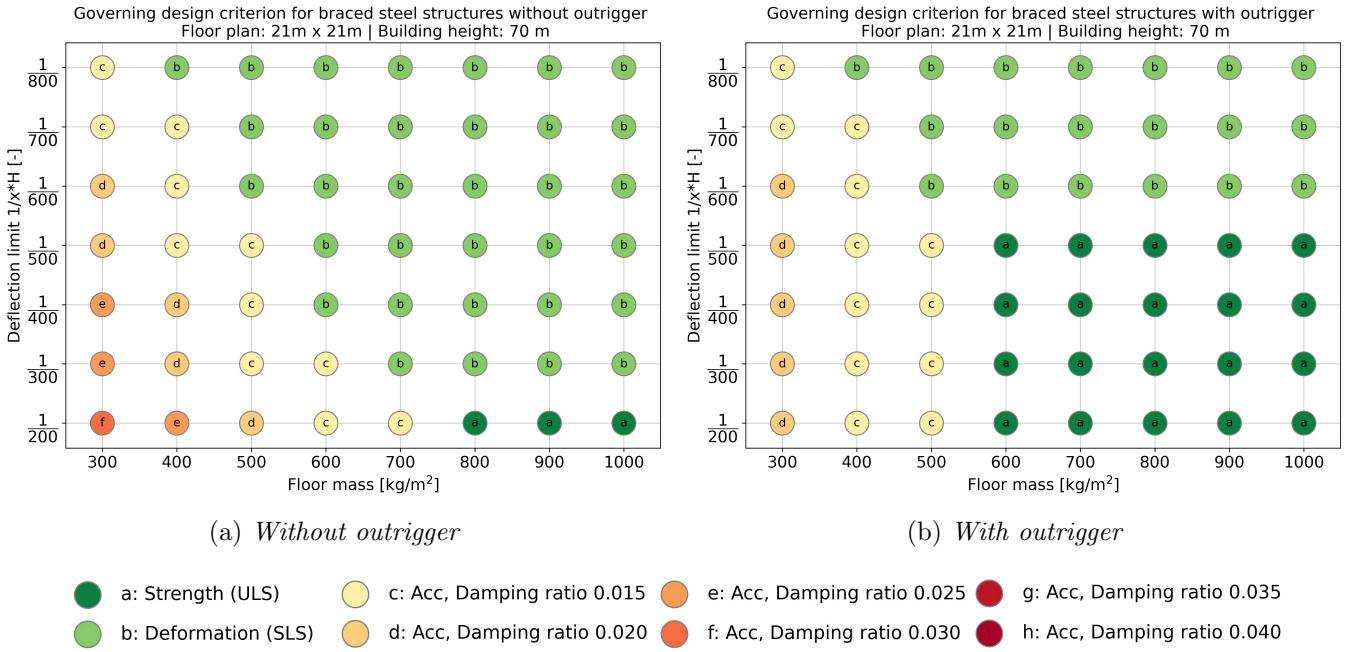

(a) *Without outrigger* (b) *With outrigger*

Figure G.2: *Overview of the governing design factors for towers with a height of 70 meters*

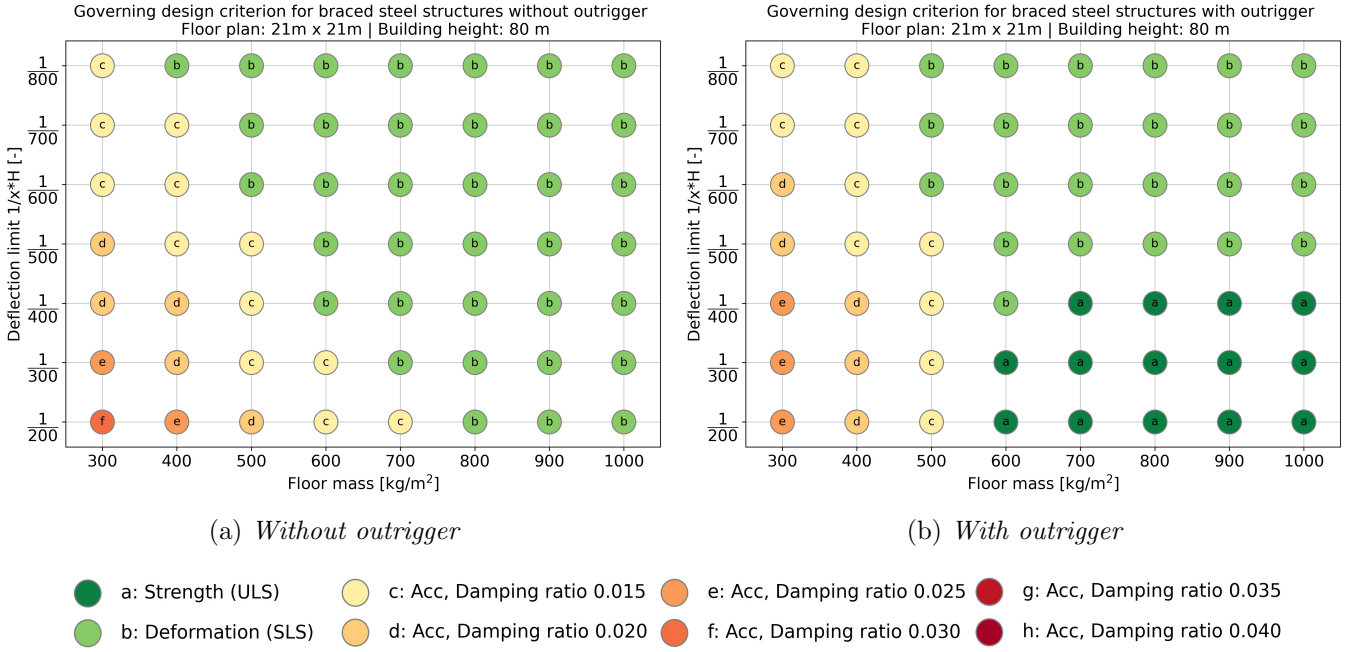

(a) *Without outrigger* (b) *With outrigger*

Figure G.3: *Overview of the governing design factors for towers with a height of 80 meters*

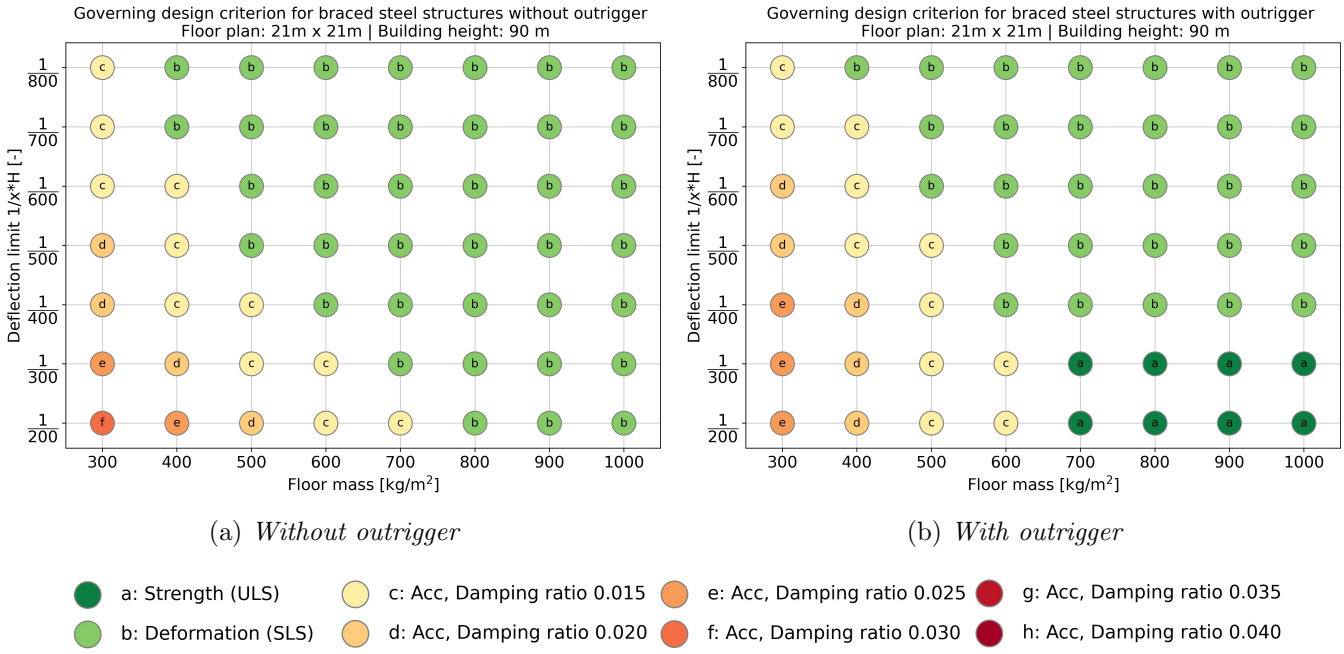

(a) *Without outrigger* (b) *With outrigger*

Figure G.4: *Overview of the governing design factors for towers with a height of 90 meters*

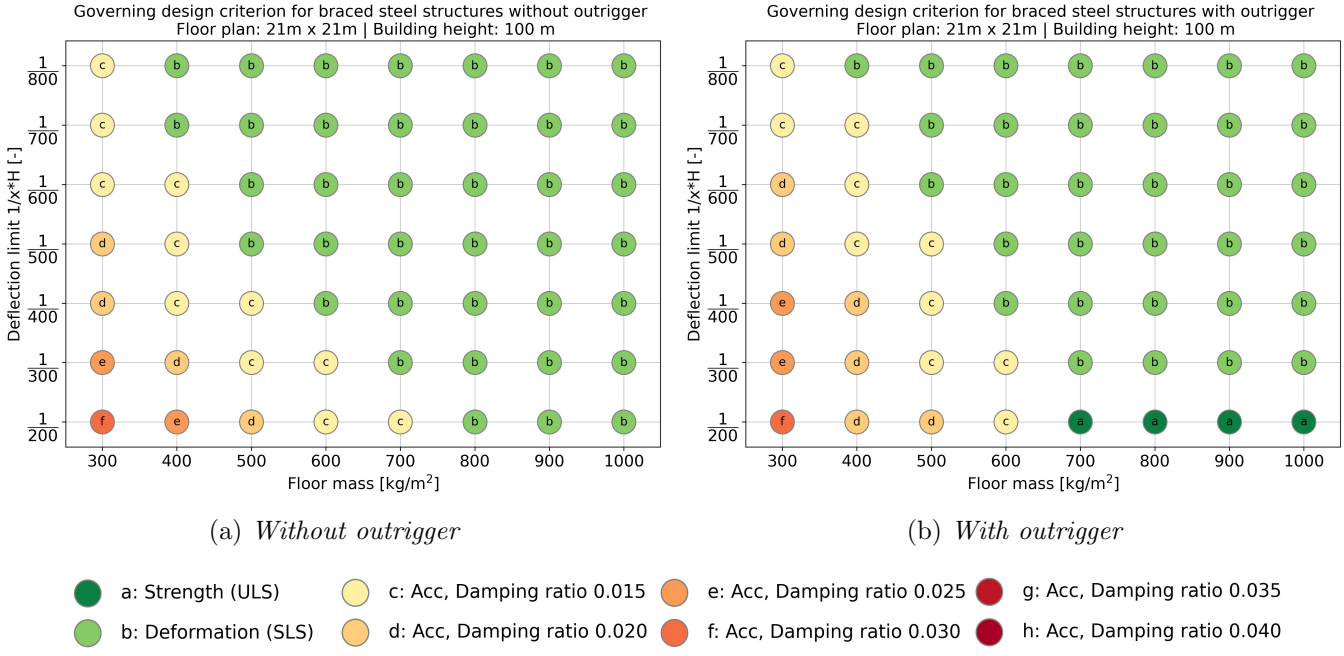

(a) *Without outrigger* (b) *With outrigger*

Figure G.5: *Overview of the governing design factors for towers with a height of 100 meters*

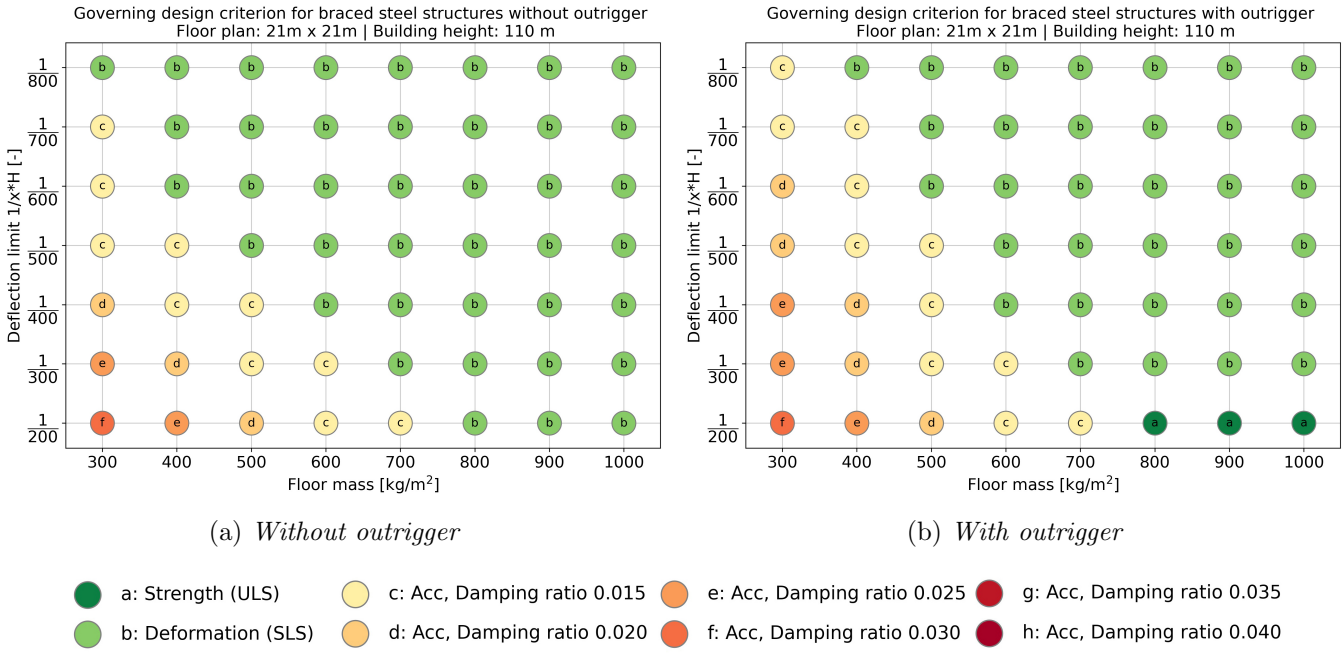

(a) *Without outrigger* (b) *With outrigger*

Figure G.6: *Overview of the governing design factors for towers with a height of 110 meters*

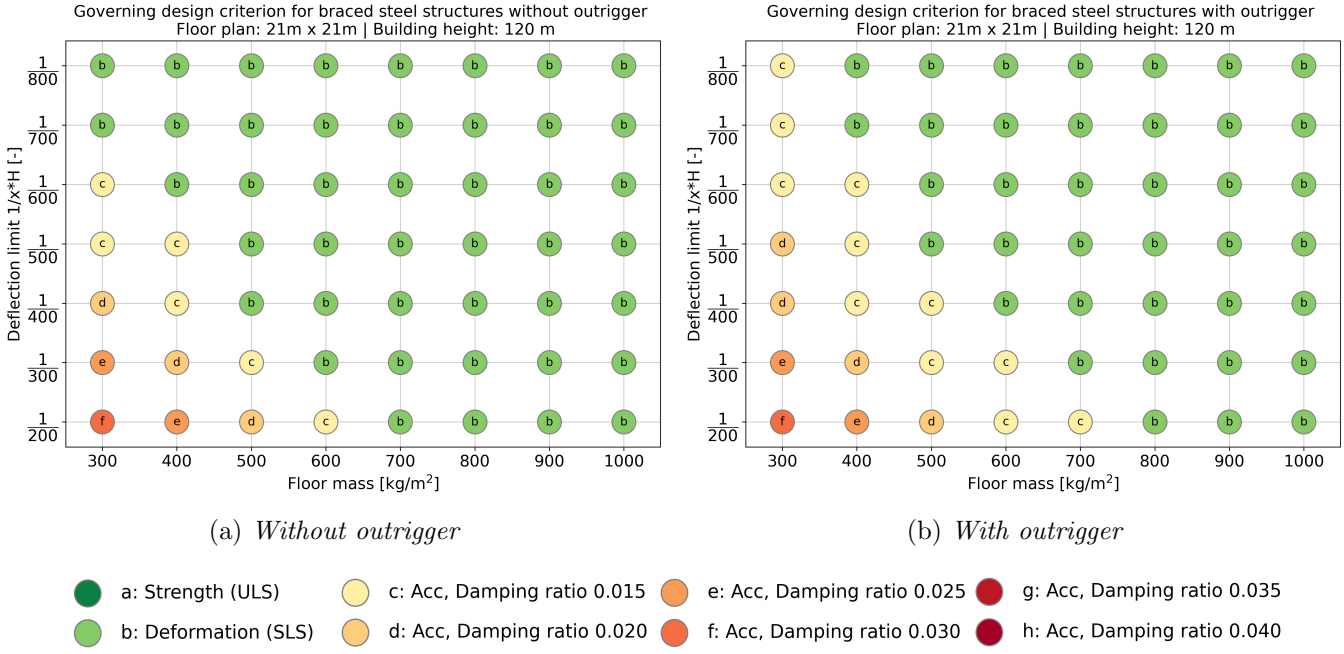

(a) *Without outrigger* (b) *With outrigger*

Figure G.7: *Overview of the governing design factors for towers with a height of 120 meters*

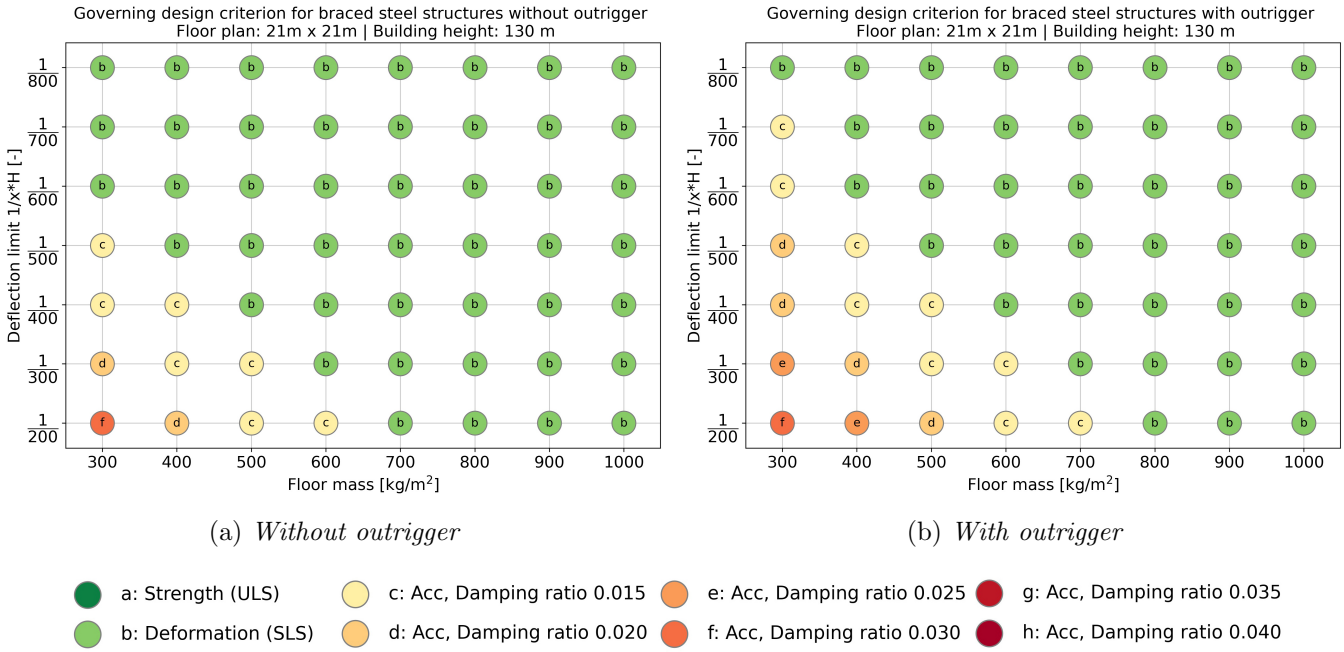

(a) *Without outrigger*

(b) *With outrigger*

Figure G.8: *Overview of the governing design factors for towers with a height of 130 meters*

Appendix H

4D distributions governing design criteria

This appendix visualises the variant study data in 4D.

The effect of all the building variants can be visualised in different ways. So far, all the graphs were presented in 2D. To finalise this Chapter about governing-design-criteria, some 4D plots will be presented in which the building height, deflection limits and floor masses are varied all together in one graph. These plots are only meant to demonstrate the general distribution of the acceleration governed zone for different values of the mass, height and stiffness. They are not used for the determination of the individual results. To increase the understanding of the 4D plot design space, first a 3D plot including all tested building configurations is shown. Each dot in Figure H.1 represents one of the modelled building configurations with a specific mass, stiffness and height. This plot does not provide any useful information, it is only included in this report to visualise the variant study space.

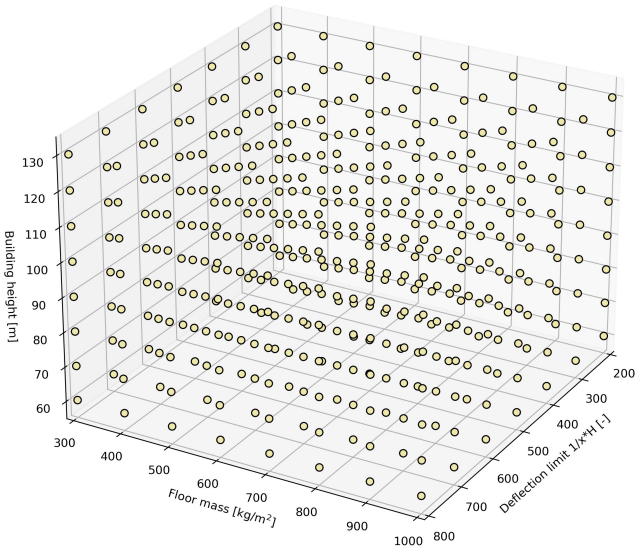

Figure H.1: *3D visualisation of the full variant study. Each dot corresponds to an analysed building variant.*

The outcomes of the variant study can be visualised in 4 dimensions: floor mass, deflection limit, building height and the required minimum damping ratio. Only variants for which the acceleration design is governing are visualised. The deflection-governed and strength-governed variants are not included in this plot. Subfigure H.2a demonstrates the 4D distribution for all building variants without an outrigger, subfigure H.2b presents the results for all the variants with an outrigger. The colored dots represent the values of the building variants for which the acceleration design is governing. Each dot represents a specific building variant for which supplementary damping is required to fulfill the acceleration limits. The color of these dots represents the required total damping ratio. For all the building variants from Figure H.1 for which no dot is shown in Figure H.2, accelerations are not governing.

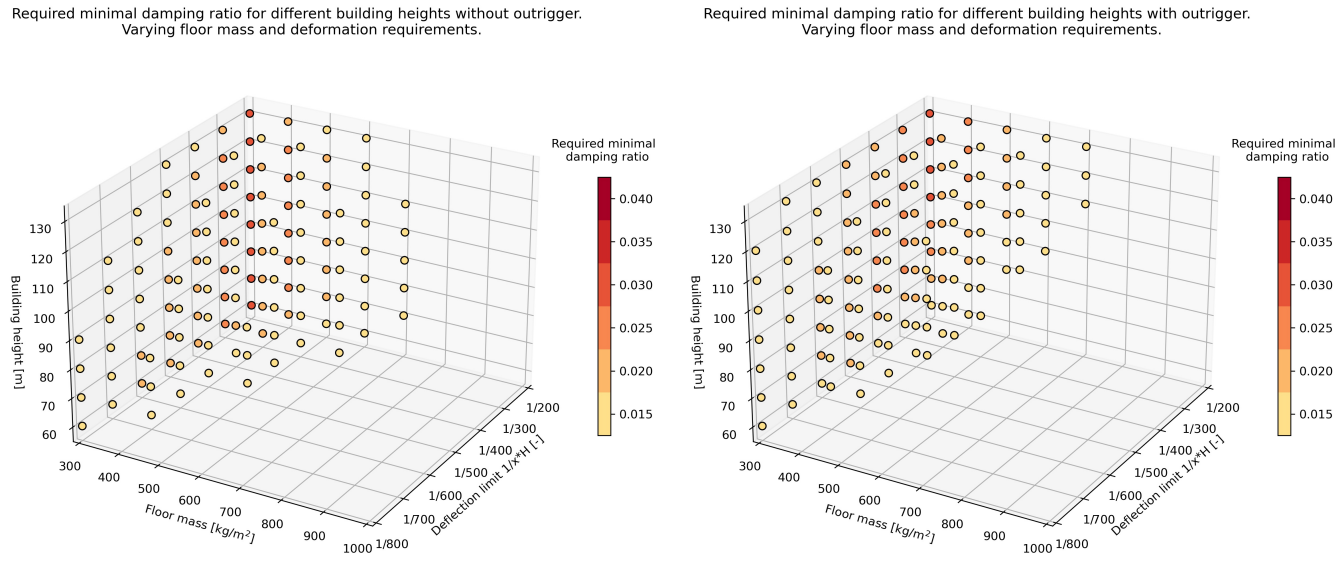

(a) *Without outrigger*

(b) *With outrigger*

Figure H.2: *3D visualisations of the acceleration governed zone for buildings with a varying height, floor mass and deflection limits*

From these Figures the general relation between mass, stiffness, height and damping ratio can be observed again: acceleration design gets governing for relatively flexible and relatively lightweight buildings. The building height also plays a role.

In general, a higher building height results in less favourable dynamic behaviour, as the eigenfrequency is negatively correlated with height. On the other hand, the higher the building, the more difficult it becomes to meet the deflection limits. Especially for buildings with a very strict deflection limit, a significant amount of structural steel is required to limit the maximum deflections, as has been pointed out in paragraph 8.2.2. This additional structural mass is beneficial in reducing the accelerations. This interaction between the negative effects of building height and the positive effects of increasing stiffness highly influences the 3D distribution. This may be noticed in the upper left corner of Figure H.2a: high and stiff buildings are less sensitive to wind-induced accelerations than somewhat smaller buildings.
Figure H.2b shows the same variables as the previous graph without outrigger, but in this case the variants do include an outrigger. The buildings still should fulfill the same requirements, but the relation between the stiffness and the total mass will change. This effects the required amount of total damping in two ways:

First, if an outrigger is included less mass is required to fulfill the deflection limits. The favourable dynamic effect of an increasing mass, for an increasing deflection limit is therefore less strong. Second, due to the outrigger, the building variants behave stiffer. As a consequence for relatively lenient deflection limits the strength based (ULS) design becomes governing over the acceleration and deflection design.

Appendix I

Applied wind parameters

The following wind parameters have been applied in the Python TMD model.

Parameter	**Value**
ρ	1.25
Wind region	II, Netherlands
Z_{ref}	$0.6 \cdot Height$
Z_0	0.5 m
$V_{b_u ls}$	27 m/s
Repetition time SLS	1 year
$V_{b_s ls}$	19.5 m/s
$V_{z_{ref}}$	$V_{b_{sls}} \cdot Cr_{z_{ref}}$
k_l	1.0
C_0	1.0
σ_v	$kr_r \cdot k_l \cdot V_{b_s ls}$
$I_{v_r ef}$	σ_u / z_{ref}
Return period	1 year
C_z	11.5
C_d	1.5
Width	21 m
Height	variable
Storey height	3.2 m
Initial damping ratio first mode	0.01

Table I.1: *Input parameters python script: retrieved from (Eurocode 2005*b*) and (Dyrbye & Hansen 1997)*

Appendix J

Spectrum calculations

This appendix explains the spectral conversion from a frequency in Hertz to a the angular frequency, as used throughout this report.

J.1 Solari spectrum f $\rightarrow \omega$

Equation J.1 shows the conversion of a spectrum from the angular frequency (rad/s) to the standard frequency (Hz). It's not enough to simply replace the frequency f by the circular frequency ω (Vrouwenvelder 2004), (Strømmen 2010).

$$S(f) = 2\pi S(\omega = 2\pi f) \tag{J.1}$$

The original spectrum is described by Equation J.2 :

$$S_u(f, z_i) = \frac{\sigma_v^2}{f} * \frac{6.8 * x(f, z_i)}{(1 + 10.2 * x(f, z_i))^{\frac{5}{3}}} \tag{J.2}$$

In which x(f) is defined by Equation J.3.

$$x(f, z_i) = f * L_t * (\frac{z}{z_t})^{\alpha} * \frac{1}{V_{ref}} \tag{J.3a}$$

$$\alpha = 0.67 + 0.05 * \ln(z_0) \tag{J.3b}$$

The conversion from f to ω leads to the following equations as described in the main report:

$$S_u(\omega, z_i) = \frac{\sigma_v^2}{\omega} * \frac{6.8 * x(\omega, z_i)}{(1 + 10.2 * x(\omega, z_i))^{\frac{5}{3}}} \tag{J.4}$$

In which $x(\omega, z_i)$ is defined by Equation J.5:

$$x(\omega, z_i) = \frac{\omega}{2\pi} * L_t * \left(\frac{z_i}{z_t}\right)^{\alpha} * \frac{1}{V_{ref}} \tag{J.5a}$$

$$\alpha = 0.67 + 0.05 * \ln(z_0) \tag{J.5b}$$

Appendix K

Derivation of the equations of motions a of TMD

In this appendix, the equations of motion for the system including TMD as described in Equation 10.1 in Chapter 10 are derived.

K.1 Equations of motion TMD

The equations are derived for a TMD installed at the i^{th} storey, considered as a 2 degree-of-freedom system. The effects of the neighbouring storeys on the i^{th} storey are assumed to be covered by c_i and k_i. For this derivation, the displacement method is used. Newtons second law: $F_{res} = m \cdot \ddot{u}$ is applied to obtain the equations of motion. The considered 2DOF system is visualised in Figure K.2.

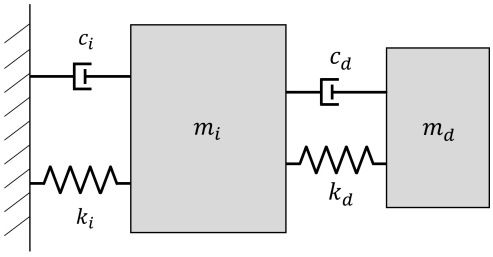

Figure K.1: *Dynamic model overview*

K.1.1 Step 1

Figure K.2 shows the situation in which both masses are not displaced yet.

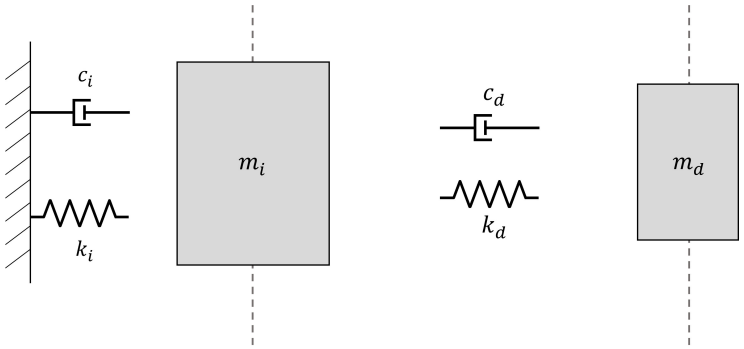

Figure K.2: *Dynamic model overview*

K.1.2 Step 2

In this first step, the floor mass of storey i is displaced due to a force F_i. The resulting forces due to this displacement on both the mass of the storey and on the TMD are visualised in Figure K.3.

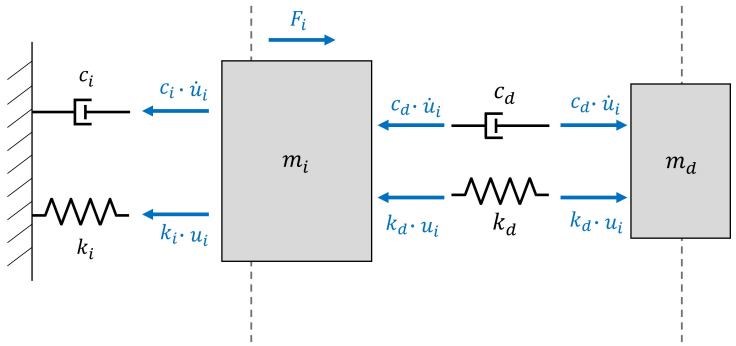

Figure K.3: *Dynamic model overview*

K.1.3 Step 3

In this first step, the floor mass of the TMD m_d is displaced. The resulting forces due to this displacement on both the mass of the storey and on the TMD are visualised in Figure K.3.
K.4.

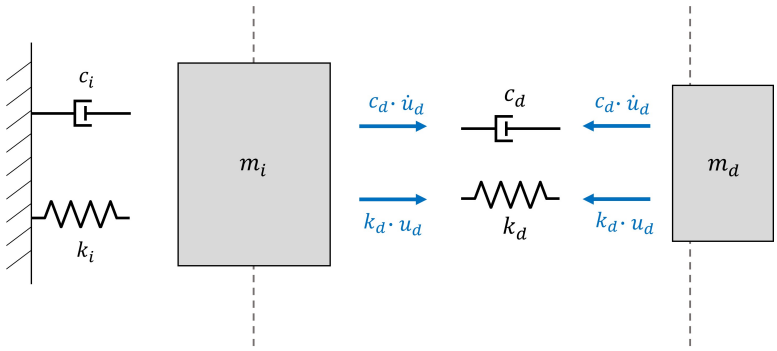

Figure K.4: *Dynamic model overview*

K.1.4 Step 4

In this last step, the resulting forces on the total system are determined. Therefore, the resulting forces on the different masses are summed and combined. From Newton's second law, Equation K.1a and K.1b can be obtained.

$$m_i\ddot{u}_i = F_i - c_i\dot{u}_i - k_iu_i - c_d\dot{u}_i - k_d\dot{u}_i + c_d\dot{u}_d + k_d\dot{u}_d \tag{K.1a}$$

$$m_d\ddot{u}_d = c_d\dot{u}_i + k_du_i - c_d\dot{u}_d - k_du_d \tag{K.1b}$$

If the absolute TMD displacement u_d is replaced by the relative displacement $x = u_d - u_i$ the following equations can be obtained. These equations are of similar shape as Equations 10.1 in Chapter 10.

$$m_i\ddot{u}_i + c_i\dot{u}_i + k_iu_i = F_i + c_d\dot{x} + k_dx \tag{K.2a}$$

$$m_d\ddot{x} + c_d\dot{x} + k_dx = -m_d\ddot{u}_i \tag{K.2b}$$

In Equation 10.1 the vector E represents are null vector in which only the i^{th} is equal to 1. The equations of the other storeys and their effect on the i^{th} storey is taken into account by the matrices M, K and C of In Equation 10.1.

Appendix L

Theory of modal analysis

This appendix conceptually explains the modal analysis as performed in Section 10.1.1, to obtain the equations of motion of the MDOF system including TMD.

L.0.1 Concept of the modal analysis

The MDOF system representing the tall building without TMD, Equation 10.1a, can be schematized as Equation L.1. This system is coupled.

$$[M]\underline{\ddot{u}} + [C]\underline{\dot{u}} + [K]\underline{u} = \underline{F} \tag{L.1}$$

These equations can be uncoupled by performing a modal analysis in which the system is transformed to n orthogonal modes: $\underline{\phi_1}$,$\underline{\phi_2}$, ..., $\underline{\phi_n}$, . These modes are combined in a n x n matrix $[\phi]$ in which each column represents a mode vector. Each mode vectors represent is equal to an eigenvector of the system. Hence the matrix $[\phi]$ is the eigenmatrix of the system. The corresponding eigenvalues ω_n^2 represent the modal eigenfrequencies for each mode (Chopra 1995). The first mode represents the fundamental mode.

The original displacement vector $\underline{u}$ can be defined as a summation of all the modal contributions, see Equation L.2. $[\phi]$ represents the Eigenmatrix and $\underline{q}(t)$ represents the modal displacement vector. In the remaining part of this report, the dependency of q(t) on time will not be explicitly mentioned anymore.

$$\underline{u}(t) = [\phi] \cdot \underline{q}(t) = [\underline{\phi_1}, \underline{\phi_2}, ..., \underline{\phi_n}] \cdot \underline{q}(t) \tag{L.2}$$

From this equation it follows that the displacement u_1 of the first degree of freedom can be calculated according to Equation L.3. The displacement of, for example the first DOF is thus dependent on the contributions of all the modal equations.

$$u_1 = \sum_{c=1}^{n} \underline{\phi}_{c,1} \cdot q_c = \phi_{1,1}q_1 + \phi_{2,1}q_2 + ... + \phi_{n,1}q_n \tag{L.3}$$

In the case of wind-induced vibrations and acceleration, the previously described procedure can be simplified. As described in Chapter 3 frequencies of the wind spectrum are relatively low compared to the eigenfrequencies of tall buildings. As a result the contribution of the first mode (lowest eigenfrequency) may account for 90% of the overall motion. Therefore, to determine the along wind accelerations, only the fundamental mode has to be considered (Ellis & Bre 1980) (Lu & Chen 2011*a*). Hence the response of the n^{th} DOF displacement can then be calculated by only taking into account the first mode. This simplifies the procedure as described in the previous paragraphs.

In this case Equation L.2 can be simplified to Equation L.4, in which only the first mode is considered:

$$\underline{u} \approx \underline{\phi_1} \cdot q_1(t) \tag{L.4}$$

From this equation it can be understood that the displacement of a certain DOF in the original coordinate system can be determined with only the equation of motion of the first mode . If the mode shape ϕ_1 and the first modal displacement function are known, the total response $\underline{u}$ can be determined. The displacement of the upper node, node n, can for example be calculated by Equation L.5, compare this one to Equation L.3.

$$u_n \approx \phi_{1,n} \cdot q_1 \tag{L.5}$$

This means that the displacement of dof 1 can be calculated by multiplying the corresponding modal deformation of mode 1 by the modal displacement function q.

L.0.2 Response

To analyse the system as described in Equation L.1, the system should be uncoupled. Therefore, the mass, stiffness and damping matrices have to be transferred to diagonal matrices. To diagonalise these matrices and hence uncouple the system of equations, the system has to be pre-multiplied by the modal matrix $[\phi]^T$. In addition, the displacement vector $\underline{u}$ in Equation L.1 has to be substituted with Equation L.2.

$$[\phi]^T[M][\phi]\underline{\ddot{q}} + [\phi]^T[C][\phi]\underline{\dot{q}} + [\phi]^T[K][\phi]\underline{q} = [\phi]^T\underline{F} \tag{L.6}$$

The multiplication by $[\phi]_T$ and $[\phi]$ results in the desired diagonal modal matrices which are notated by $[M^*]$, $[C^*]$, $[K^*]$, see Equation L.7. $\underline{F}^*$ represents the modal force.

$$[M^*]\underline{\ddot{q}} + [C^*]\underline{\dot{q}} + [K^*]\underline{q} = \underline{F}^* \tag{L.7}$$

In general it can not be assumed that the modal damping matrix is diagonal, which would mean that the equations can not be uncoupled. However, as mentioned in the previous paragraph, only the first mode has to be considered for wind induced motions. It is assumed that the modal damping value of the first mode is known. With this value as a starting point, Rayleigh damping can be used, which results in a diagonal modal damping matrix. This finally results in a set of uncoupled equations. For the proof, the reader is referred to the book by Chopra (Chopra 1995).

Since only the fundamental mode is considered in this analysis, the system of modal equations as described in Equation L.1 can be reduced. Except for mode 1, all other equations can be neglected.The equation of motion of mode 1 is formulated in Equation L.8.

$$\underline{\phi}_1^T[M]\underline{\phi}_1\ddot{q_1} + \underline{\phi}_1^T[C]\underline{\phi}_1\dot{q_1} + \underline{\phi}_1^T[K]\underline{\phi}_1 q_1 = \underline{\phi}_1^T\underline{F} \tag{L.8}$$

In which $\underline{\phi}_1$ is the first modal eigenvector. This Equation can also be rewritten in the style of Equation L.7. In which m_1^*, k_1^*, c_1^* and F_1^* respectively represents the first modal mass, first modal stiffness, first modal

damping constant and first modal force.

$$m_1^* \ddot{q}_1 + c_1^* \dot{q}_1 + k_1^* q_1 = F_1^* \tag{L.9}$$

Appendix M

Derivation of the transfer function

In this appendix, the transfer function as described in Equation 10.6 is derived with Maple.

```
> restart;
> with(linalg) :
```

Manually solve equation 9 and 10 from X. Lu and J. Chen as described in the main report.

```
> Matrix1 := Matrix([[1 + μ1·ϕ1i^2, μ1·ϕ1i], [ϕ1i, 1]])
```

$$Matrix1 := \begin{bmatrix} \mu_1 \phi_{1i}^2 + 1 & \mu_1 \phi_{1i} \\ \phi_{1i} & 1 \end{bmatrix} \tag{1}$$

```
> Vector1 := Vector([q1.., v1..])
```

$$Vector1 := \begin{bmatrix} q1_{..} \\ v1_{..} \end{bmatrix} \tag{2}$$

```
> Matrix2 := Matrix([[2·Zeta1·ω1, 0], [0, 2·Zetad·ωd]])
```

$$Matrix2 := \begin{bmatrix} 2\zeta_1 \omega_1 & 0 \\ 0 & 2\zeta_d \omega_d \end{bmatrix} \tag{3}$$

```
> Vector2 := Vector([q1., v1.])
```

$$Vector2 := \begin{bmatrix} q1_{.} \\ v1_{.} \end{bmatrix} \tag{4}$$

```
> Matrix3 := Matrix([[ω1^2, 0], [0, ωd^2]])
```

$$Matrix3 := \begin{bmatrix} \omega_1^2 & 0 \\ 0 & \omega_d^2 \end{bmatrix} \tag{5}$$

```
> Vector3 := Vector([q1, v1])
```

$$Vector3 := \begin{bmatrix} q1 \\ v1 \end{bmatrix} \tag{6}$$

```
> VectorF := Vector([F1, 0])
```

$$VectorF := \begin{bmatrix} F1 \\ 0 \end{bmatrix} \tag{7}$$

Define F and q and v

```
> F1 := exp(I·omega·t)/M_star
```

$$F1 := \frac{e^{I\omega t}}{M\_star} \tag{8}$$

```
> v1 := Hv·exp(I·omega·t); v1. := diff(v1, t$1); v1.. := diff(v1, t$2)
```

$$v1 := H_v e^{I\omega t}$$

$$v1_{\cdot} := I H_v \omega e^{I\omega t}$$

$$v1_{\cdot\cdot} := -H_v \omega^2 e^{I\omega t} \quad (9)$$

> $q1 := H_q \cdot \exp(I \cdot \text{omega} \cdot t) : q1_{\cdot} := diff(q1, t\$1) : q1_{\cdot\cdot} := diff(q1, t\$2) :$

> $Function\_matrix := simplify(Matrix1 \bullet Vector1 + Matrix2 \bullet Vector2 + Matrix3 \bullet Vector3)$

$$Function\_matrix := \begin{bmatrix} \left(\left(-H_q \mu_1 \phi_{1i}^2 - \mu_1 \phi_{1i} H_v - H_q \right) \omega^2 + 2 I \zeta_1 \omega_1 H_q \omega + \omega_1^2 H_q \right) e^{I\omega t} \\ \left(\left(-\phi_{1i} H_q - H_v \right) \omega^2 + 2 I \zeta_d \omega_d H_v \omega + \omega_d^2 H_v \right) e^{I\omega t} \end{bmatrix} \quad (10)$$

>

>

>

First solve equation 2 to obtain Hv and express it in Hq

> $eq2 := Function\_matrix[2] = VectorF[2]$

$$eq2 := \left(\left(-\phi_{1i} H_q - H_v \right) \omega^2 + 2 I \zeta_d \omega_d H_v \omega + \omega_d^2 H_v \right) e^{I\omega t} = 0 \quad (11)$$

> $H_v := solve(eq2, H_v)$

$$H_v := \frac{\phi_{1i} H_q \omega^2}{2 I \zeta_d \omega \omega_d - \omega^2 + \omega_d^2} \quad (12)$$

> H_v

$$\frac{\phi_{1i} H_q \omega^2}{2 I \zeta_d \omega \omega_d - \omega^2 + \omega_d^2} \quad (13)$$

Then solve eq1 with Hv expressed in Hq

> $eq1 := Function\_matrix[1] = VectorF[1]$

$$eq1 := \left(\left(-H_q \mu_1 \phi_{1i}^2 - \frac{\phi_{1i}^2 H_q \omega^2 \mu_1}{2 I \zeta_d \omega \omega_d - \omega^2 + \omega_d^2} - H_q \right) \omega^2 + 2 I \zeta_1 \omega_1 H_q \omega + \omega_1^2 H_q \right) e^{I\omega t} = \frac{e^{I\omega t}}{M\_star} \quad (14)$$

This finaly results in the transfer function Hq

> $H_q := solve(eq1, H_q)$

$$H_q := -\left(2 I \zeta_d \omega \omega_d - \omega^2 + \omega_d^2 \right) \Big/ \left(M\_star \left(2 I \zeta_d \mu_1 \omega^3 \phi_{1i}^2 \omega_d + 4 \zeta_1 \zeta_d \omega^2 \omega_1 \omega_d + \mu_1 \omega^2 \phi_{1i}^2 \omega_d^2 + 2 I \zeta_1 \omega^3 \omega_1 - 2 I \zeta_1 \omega \omega_1 \omega_d^2 + 2 I \zeta_d \omega^3 \omega_d - 2 I \zeta_d \omega \omega_1^2 \omega_d - \omega^4 + \omega^2 \omega_1^2 + \omega^2 \omega_d^2 - \omega_1^2 \omega_d^2 \right) \right) \quad (15)$$

>

Appendix N

Python script wind model

This appendix describes the developed Python TMD model as described in Chapter 10.

N.0.1 Import libraries

```
import numpy as np
import matplotlib.pyplot as plt
import scipy
from scipy.linalg import eigh
import sympy as sy
from sympy import *
import csv
from csv import writer
import pandas as pd
from pandas import read_csv
pd.set_option('display.max_columns', None)
from matplotlib.ticker import (MultipleLocator, AutoMinorLocator)
from datetime import datetime
import matplotlib.cm as cm # matplotlib's color map library
```

N.1 Define building of interest

N.1.1 Read Grasshopper model data into the script

```
def load_data_func():
code = 'Eurocode'
error_filter = 'no'

#open csv file as a dataframe
data_sheet = pd.read_csv('C:\\Users\\...\\data.csv',  delimiter=',')

#Change the column names to more better understandable names
data_sheet.rename(columns={'in:Number_of_floors':'Number_of_floors',
                        'in:Damping_ratio':'Damping_ratio',
                        'in:Floor_mass_[kg/m2]':'Floor_mass',
                        'out:maximum_SLS_deformation_m':'maximum_SLS_deformation',
                        'out:building_height[m]':'Building_height',
                        ....
                        ....
                        ....
                        'out:Mode_shape':'Mode_shape',
                        'out:Info':'Info',
                        'out:ULS_2th_order':'ULS_2th_order',
                        'out:SLS_2th_order':'SLS_2th_order',
                        'img':'Image'
```

```
                        }, inplace=True)
    return data_sheet

data_sheet = load_data_func()
```

N.1.2 Select data from building variant of interest

```
    #Select the building variant of interest for which the response including TMD should be
    caclulated
    height_var = 100 #building height in meters
    mass_var = 400 #floor mass in kg/m2
    EI_var = 500 #deflection limit 1/x
    damp_var = 0.01 #initial damping ratio, for the first mode
    outrigger_var = 'without outrigger' #select building variant without outrigger
    outrigger_dict = {'without outrigger':False, 'with outrigger':True}

    df = data_sheet
    #Select the building variant of interest from the data frame, building_variant
    represents the data row of interest
    building_variant = df[(df['Building_height']==height_var) & (df['Floor_mass']==mass_var)
    & (df['Maximum_allowed_deformation']==EI_var) & (df['Outrigger_on']==outrigger_dict.get
    (outrigger_var))& (df['Damping_ratio']==damp_var)]

    display(building_variant)
```

N.1.3 Store the modal information of the building variant of interest

```
    #Height and storey height
    Building_height = building_variant.iloc[0]['Building_height']
    Storey_height = building_variant.iloc[0]['Storey_height']
    modal_info =  building_variant.iloc[0]['Info'] #Obtain short string with information of
    building variant, for naming of Figures

    #Mode shape
    #For convenience in Python scripting, the first mode is considered as mode 0
    #transfer the grasshopper string to a python list containing the mode shape per DOF
    Mode0_information = building_variant.iloc[0]['Mode_shape']
    Mode0_information = list(Mode0_information.split("_")) #unpack the mode string from
    grasshopper to obtain the mode shape
    Mode0_information=Mode0_information[:-1] #get rid of empty last value, only contains: ''
    Mode0_string_to_list = []
    for item in Mode0_information:
        Mode0_string_to_list.append(abs(float(item)))
    Mode0_string_to_list.pop(0) #remove the first 0.0 item from the mode as this is not
    really a DOF
    Mode0 = Mode0_string_to_list #Store the mode shape of the first mode

    #List of dofs
    Dof_list = np.arange(0, len(Mode0),1)
    Amount_of_dofs = len(Dof_list)

```

```
    #Determine the eigenfrequency
    f = building_variant.iloc[0]['Nx'] #[Hz]
    omega0 = f*2*np.pi #[rad/s] angular frequency
    #print('f [hz]',f)

    #Modal mass
    M_star0 = building_variant.iloc[0]['Modal_mass']

    #Assume damping ratio of first mode is equal to the intial damping ratio
    Cdamp_0 = damp_var #damping ratio

    #Only take into account the first mode
    Mode_list = [0] #mode 0 refers to the fundamental mode
```

N.1.4 Create list with storey heights

```
    # List with heights, both row and columns
    # Zi_list = list with storey heights, required for coherence matrix
    Z_i_list = []
    for level in range(1,Amount_of_storeys+1):
        Z_i_list.append(round(Storey_height*level,2))
    Z_j_list = Z_i_list
```

N.2 Define TMD damping properties for analysis

N.2.1 Define optimal value for omega (frequency TMD) and zeta (damping ratio TM)

```
#Function to define the near optimal TMD frequency and Damping frequency, based on mass ratio and eigenfrequency of the building
def optimal_tmd_parameters_func(mu_0, omega_0):
    #Defined in book Introduction to Structural Motion Control, by Connor,  page 261 - 4.105
    #TMD frequency
    omega_tmd_opt = omega_0*( (np.sqrt(1-0.5*mu_0)/(1+mu_0) + np.sqrt(1-2*Cdamp_0**2) - 1) -(2.375 - 1.034*np.sqrt(mu_0) - 0.426*(mu_0))*Cdamp_0*np.sqrt(mu_0) -(3.730 - 16.903*np.sqrt(mu_0) + 20.496*mu_0)*Cdamp_0**2*np.sqrt(mu_0))
    #TMD damping ratio
    zeta_tmd_opt = np.sqrt((3*mu_0) / (8*(1+mu_0)*(1-0.5*mu_0))) + (0.151*Cdamp_0 - 0.170*Cdamp_0**2) + (0.163*Cdamp_0 + 4.980*Cdamp_0**2)*mu_0
    return omega_tmd_opt, zeta_tmd_opt
```

N.2.2 Define TMD properties

```
    #Mode properties
    #Please be aware that the first mode in fact is mode 0 in this convention
    first_mode = 0
    Mode_matrix = np.array([Mode0])
    omega_0 = omega0 # sy.Symbol('omega_1') #First mode omega
    Mass0 = M_star0 #modal mass

```

```
    ##########################################

    TMD_location_dof_nr_i = Dof_list[-1] #Define TMD location
    phi_0i =  Mode0[TMD_location_dof_nr_i] #TMD location
    mu_0 = 0.02 #Mass ratio

    #Define the optimal values of the frequency and damping ratio with the defined function
    omega_tmd_opt, zeta_tmd_opt = optimal_tmd_parameters_func(mu_0, omega_0)
    omega_tmd = omega_tmd_opt
    Cdamp_tmd = zeta_tmd_opt
```

N.3 Wind properties

N.3.1 Define wind parameters

```
    #NA = National Annex

    #Building properties
    Width = 21 #[m]
    Amount_of_storeys = Amount_of_dofs #[-]
    Height = Amount_of_dofs*Storey_height #[m] Total building height
    A_i = Storey_height*Width #Facade area corresponding to one DOF

    ##########################################

    #Wind properties
    rho = 1.25 #[kg/m3] Air density
    C_di = 1.5 #[-] Wind drag factor (windward + leeward)
    C_z = 11.5 #[-] Decay constants, from EC and Hansen
    L_t = 300 [m] #Turbulence length

    ##########################################
    Z_top = Height #[m]
    Z_ref = 0.6 * Z_top #[m] Reference height for determining the structural factor, in EC defined as Zs
    Z0 = 0.5 #[m] Roughness, Terrain cattegory III (NA)
    zmin = 7 #[m] minimum height (NA)
    zmax = 200 #[m] maximum height (NA)
    ##########################################

    #Return period and mean wind velocity
    K, n = 0.234, 0.5 #National annex (NA); Table NB.2
    T = 1 #[year] #accelerations = 1 year return period
    p = 1-np.exp(-(1/T)) #annual probability of exceedence
    cprop = ((1-K*np.log(-np.log(1-p)))/(1-K*np.log(-np.log(0.98))))**n #probability factor

    vb_ULS = 27.0 # [m/s] fundamental value of the basic wind velocity | v_bo=27 (II NA), cdir = 1.0 (NA), cseason = 1.0 (EC NA eq 4.1)
    vb_SLS = cprop * vb_ULS #fundamental value of the basic wind velocity for 1 year return period

```

```
    ##########################################

    # Calculate sigma_v (required for the spectrum)
    #Sometimes U* is used in equations, sigma_v = 2.5 x U*
    kI = 1.0 #Turbulence factor
    kr = 0.19*(Z0/0.05)**0.07 #Terrain factor (EC eq 4.5)

    stand_dev_turb = kr * vb_SLS * kI #Standard deviation fluctuating windspeed (EC eq 4.6)
    sigma_v = stand_dev_turb #Standard deviation fluctuating windspeed

    ##########################################

    Cr_zref = kr * np.log(Z_ref/Z0) #roughness factor at height z_ref #np.log = LN
    C0 = 1.0 #Orography factor
    U_zref  = vb_SLS*Cr_zref #[m/s] The mean wind velocity vm(z_ref) at a height z_ref

    ##########################################

    #Turbulence
    Iv_zs = sigma_v / U_zref #Turbulence intensity
    ##########################################
```

N.3.2 Define the fluctuating wind load spectrum

These equations are based on the theory of Section 10.2

```
#Define wind parameters and spectrum, as defined in Chapter wind model defenition

#Solari velocity spectrum S_ui
def su_i_solari_func(omega,Z_i):
    x_spec_solari = x_spec_solari_func(omega, Z_i) #Define x
    s_ui=(sigma_v**2 / omega) *(( 6.8 * x_spec_solari)/ ((1+10.2*x_spec_solari)**(5/3)))
    return (s_ui)

#Solari spectrum part x
def x_spec_solari_func(omega, z_i):
    Z_t = 200 #Reference height
    alpha = 0.67+0.05*np.log(Z0)
    L_solari = L_t*(z_i/Z_t)**(alpha)
    x_spec_solari = (omega/(2*np.pi) )*((L_solari)/ (U_zref)) #Divide by 2pi to account
for f-->omega
    return x_spec_solari

#Wind speed to force #Bernoulli
def Fd_func(Z_i):
    Uz_i = Uz_i_func(Z_i)
    Fd = (0.5 * rho * C_di * A_i * Uz_i**2 ) #Volgens mij is dit in [N]
    return Fd

#Aerodynamic admitance #kareem
def Aerodynamic_admittance(omega, Z_i):
    Uz_i = Uz_i_func(Z_i) #wind velocity
    X_2 = (1 / (1+ ((omega*np.sqrt(A_i))/(Uz_i*np.pi))**(4/3)))**2 #with f = omega/2PI
```

```
        return X_2

    #Eurocode wind velocity U at height Z_i
    def Uz_i_func(Z_i):
        Cr_zi = kr* np.log(Z_i/Z0) #Roughness factor at height Zi
        Uz_i  = max(vb_SLS*Cr_zi,0) #[m/s] SLS mean wind velocity at height zi
        return Uz_i

    #Wind load spectrum
    def Sf_i_func(Z_i, omega):
        Fd = Fd_func(Z_i)
        Uz_i = Uz_i_func(Z_i)
        X_2 = Aerodynamic_admittance(omega, Z_i)
        Su_i = su_i_solari_func(omega,Z_i)
        Sf_i = ((4 * Fd**2)/(Uz_i**2)) * X_2 *  Su_i
        return Sf_i

    #Coherence at height i
    def Coh_ij_func(Z_i, Z_j, omega):
        Uz_i = Uz_i_func(Z_i)
        Uz_j = Uz_i_func(Z_j)
        Coh_ij = np.exp(- (abs(omega) * C_z * abs(Z_i-Z_j) )/ (np.pi * (Uz_i + Uz_j) ) )
        return Coh_ij
```

N.4 Random vibration response

N.4.1 Create coherence matrix

See Equation 10.18

```
    #The coherence matrix is dependent on the input omega, so for each omega a new coherence
     matrix must be set-up
    #Each value ij corresponds with the coherence for certain freq and delta z; this is used
     for cross spectrum density matrix
    #Define the coherence for each relation Zi and Zj,
    def Coh_matrix_func(omega):
        Coh_matrix = np.ones([Amount_of_dofs, Amount_of_dofs])
        for i in Dof_list:
            for j in Dof_list:
                Z_i = Z_i_list[i]
                Z_j = Z_j_list[j]
                coh_ij = Coh_ij_func(Z_i, Z_j, omega)
                Coh_matrix[i,j] = coh_ij
        return Coh_matrix
```

N.4.2 Define Sfpfq matrix

See Equation 10.20

```
    def Sff_omega_matrix_func(omega):
        Sff_omega_matrix = np.ones([Amount_of_dofs, Amount_of_dofs])
```

```
        Coh_matrix = Coh_matrix_func(omega)
        for i in Dof_list:
            for j in Dof_list:
                Z_i = Z_i_list[i]
                Z_j = Z_j_list[j]

                Sf_i = Sf_i_func(Z_i, omega)
                Sf_j = Sf_i_func(Z_j, omega)
                Coh_ij = Coh_matrix[i,j]

                Sff_omega_matrix[i,j] = np.sqrt(Sf_i*Sf_j)*Coh_ij
        return Sff_omega_matrix
```

N.4.3 Transfer function, including modal transformations

See 10.10. Based on modal transformations and Transfer function 10.6.

```
def H_uj_fi_TMD_func(j,i, omega_force): #omega_force = force frequency [rad/sec]

    HujFi = 0 #initial value before summation

    #Define transfer function H_transfer for the system including TMD, including complex
    numbers
    #J=complex number (i)
    Hq0_top = (-2J*omega_force*Cdamp_tmd*omega_tmd + omega_force**2 - omega_tmd**2)

    Hq0_bottom = -omega_force**4 + (mu_0*Cdamp_tmd*omega_tmd*phi_0i**2 + Cdamp_tmd*omega_tmd
    + Cdamp_0*omega_0)*(2J*omega_force**3) +( mu_0*(phi_0i**2)*(omega_tmd**2) + (omega_tmd
    **2) + 4*Cdamp_0*Cdamp_tmd*omega_0*omega_tmd + (omega_0**2))*(omega_force**2)          -(2
    J*omega_force)*(Cdamp_0*omega_0*(omega_tmd**2) + Cdamp_tmd*omega_tmd*(omega_0**2))\ -((
    omega_0**2)*(omega_tmd**2))

    Hq0 = Hq0_top / (Hq0_bottom * Mass0) #Full transfer function

    #Calculate mode contribution to HujFi, take into account the modal transformation
    contribution as explained in Chapter
    for k in Mode_list:
        u_k =  Mode_matrix[k]
        HujFi_k = ( u_k[j]*u_k[i] ) * Hq0
        HujFi = HujFi + HujFi_k #Sum all the mode contributions #= formula 4.31 Random
    vibrations lecture notes
    return HujFi
```

N.5 Response spectrum

N.5.1 Determine the individual response spectrum contributions

See equation 10.10. Store all possible responses

```
#Define the H_uj_fi and the H_uj_fi* (conjugte) values for all possible combinations of I and J to create the summation
#Store these values in a seperate dictionary to sum the response later

def H_dict_func():
    H_uj_fi_dict = {}
    H_uj_fi_conjugate_dict = {}
    OMEGA = sy.Symbol('OMEGA')  #Define omega as a symbal variable, which can be defined later


    for i in Dof_list:
        for j in Dof_list:
            H_uj_fi_dict['H_u{0}_f{1}'.format(j, i)]= H_uj_fi_TMD_func(j,i, OMEGA)
            H_uj_fi_conjugate_dict['H_u{0}_f{1}_conjugate'.format(j, i)]= sy.conjugate(H_uj_fi_TMD_func(j,i, OMEGA))
    return H_uj_fi_dict,H_uj_fi_conjugate_dict

H_uj_fi_dict,H_uj_fi_conjugate_dict = H_dict_func()
```

N.5.2 Displacement response spectrum function

Define the response spectrum. 10.19

```
#Determine response spectrum
#Obtain response for dof i, dof j; normally i=j to obtain respons Su1u1 for example
#i = dof, j = dof; So su1u1 = response dof 1
#omega = frequency of force component

def S_ui_uj_response_func(i, j, omega):
    S_ui_uj = 0 #start value

    S_fi_fj_matrix = Sff_omega_matrix_func(omega) #obtain force contribution
    for p in Dof_list: #Loop over all possible combinations to sum the response
        for q in Dof_list:
            H_ui_fp = H_uj_fi_dict.get('H_u{0}_f{1}'.format(i, p))
            H_uj_fq_star = H_uj_fi_conjugate_dict.get('H_u{0}_f{1}_conjugate'.format(j, q))
            S_fp_fq = S_fi_fj_matrix[p,q]
            contribution = H_ui_fp * H_uj_fq_star * S_fp_fq #Displacement response spectrum
            S_ui_uj = S_ui_uj + contribution #Summation of all components
    return S_ui_uj
```

N.5.3 Acceleration response spectrum

```
#Determine the acceleration response spectrum
#Obtain response for dof i, dof j; normally i=j to obtain respons Su1u1 for example

```

```
def S_ui_uj_acceleration_response_func(i, j, omega):
    S_ui_uj = 0 #Start value

    S_fi_fj_matrix = Sff_omega_matrix_func(omega)
    for p in Dof_list:
        for q in Dof_list:
            H_ui_fp = H_uj_fi_dict.get('H_u{0}_f{1}'.format(i, p))
            H_uj_fq_star = H_uj_fi_conjugate_dict.get('H_u{0}_f{1}_conjugate'.format(j, q))
            S_fp_fq = S_fi_fj_matrix[p,q]
            contribution = omega**4 * H_ui_fp * H_uj_fq_star * S_fp_fq #Acceleration
    response spectrum
            S_ui_uj = S_ui_uj + contribution #Summation of all components
    return S_ui_uj
```

N.6 Generate spectrum plots

N.6.1 Displacement response graph

```
#Function used in the generation of the response graph. Obtain the acceleration spectrum
    response graph for the top DOF
def Get_Su_acceleration_response_func(omega_list):
    #Obtain the repsons function S_u_u
    top_dof = Dof_list[-1] #Check response for the upper DOF
    su_top_value_list = [] #Start

    for sub_omega in omega_list:
        su_top_function = S_ui_uj_acceleration_response_func(top_dof,top_dof,sub_omega) #use
     top dof to get Suiui
        item = su_top_function.subs(OMEGA,sub_omega)
        su_top_value_list.append(complex(item))
    return(omega_list, su_top_value_list)
```

N.6.2 Displacement TMD plot

This function generates data lists that are plotted as the displacement response spectra as visualised in this report.

```
def TMD_plot_displacement_func(mu_0_value,Cdamp_tmd_value ,omega_tmd_value,
    TMD_location_dof_nr_i_value)
    #Set up the parameters as global to ensure that you do not need to put the parameters
    again in every function, use it as a reset
    global mu_0, Cdamp_tmd, omega_tmd, phi_0i

    #Set the parameters
    mu_0, Cdamp_tmd, omega_tmd, phi_0i = mu_0_value, Cdamp_tmd_value, omega_tmd_value, Mode0
    [TMD_location_dof_nr_i_value] #-1 = top
    ###############################################################

    #Fill the H_uj_fi and conjugate dictionary
    #Set global so that all functions make use of these updated dictionairies
```

```
    global H_uj_fi_dict, H_uj_fi_conjugate_dict
    H_uj_fi_dict,H_uj_fi_conjugate_dict = H_dict_func()

    #Set the omega_list to define the graph x-axis
    omega_list = np.arange(0.01,omega0+2, 0.01)
    #Obtain Su response by looping over all possible omega:
    omega_list, su_top_value_list = Get_Su_displacemnt_response_func(omega_list)

    return omega_list, su_top_value_list
```

N.6.3 Acceleration response graph

```
#Function used in the generation of the response graph. Obtain the acceleration spectrum
    response graph for the top DOF
def Get_Su_acceleration_response_func(omega_list):
    #Obtain the repsons function S_u_u
    top_dof = Dof_list[-1] #Check response for the upper DOF
    su_top_value_list = [] #Start

    for sub_omega in omega_list:
        su_top_function = S_ui_uj_acceleration_response_func(top_dof,top_dof,sub_omega) #use
     top dof to get Suiui
        item = su_top_function.subs(OMEGA,sub_omega)
        su_top_value_list.append(complex(item))
    return(omega_list, su_top_value_list)
```

N.6.4 Acceleration TMD plot

This function generates data lists that are plotted as the acceleration response spectra as visualised in this report. The quality of the data could be manually adapted for different zones in the graph to ensure that the numerical errors were reduced, while the computation time was limited.

```
def TMD_plot_acceleration_func(mu_0_value,Cdamp_tmd_value ,omega_tmd_value,
    TMD_location_dof_nr_i_value): #mu_0 = Mass_tmd/M0* ; i = TMD_location ; Cdamp_tmd =
    viscous damper TMD; omega_tmd = eigenfreq TMD
    #Set up the parameters as global to ensure that you do not need to put the parameters
    again in every function, use it as a reset
    global mu_0, Cdamp_tmd, omega_tmd, phi_0i

    #Set the parameters
    mu_0, Cdamp_tmd, omega_tmd, phi_0i = mu_0_value, Cdamp_tmd_value, omega_tmd_value, Mode0
    [TMD_location_dof_nr_i_value] #-1 = top
    ###############################################################
    #Fill the H_uj_fi and conjugate dictionary
    #Set global so that all functions make use of these updated dictionairies
    global H_uj_fi_dict, H_uj_fi_conjugate_dict
    H_uj_fi_dict,H_uj_fi_conjugate_dict = H_dict_func()

    #Define different quality's of data for the visualisation of the respons
    #Around the resonance peak, the step size is taken smaller, as the graph is steeper here

```

```
    if quality == 'fine':
        delta = 0.005
    else:
        delta = 0.01

    #The different parts of the omega_list are defined, based on the quality of the data and
     pasted together
    #Different step sizes have been used throughout the generation of the graph, this is an
    example
    omega_list1 = list(np.arange(0.01,omega0-0.7, 0.05))
    omega_list2 = list(np.arange(omega0-0.7,omega0+0.7, delta)) #around peak value
    omega_list3 = list(np.arange(omega0+0.7,omega0+3, 0.05))
    omega_list = np.concatenate((omega_list1,omega_list2,omega_list3))

    #Obtain Su response by looping over all possible omega:
    omega_list, su_top_value_list = Get_Su_acceleration_response_func(omega_list)

    return omega_list, su_top_value_list
```